UNIVERSITE BRETAGNE SCIENCES LOIRE POUR L'INGENIEUR

Oniris
École Nationale Vétérinaire, Agroalimentaire et de l'Alimentation
Nantes Atlantique
Santé et alimentation au cœur de la vie

THESE DE DOCTORAT DE

ONIRIS
DELIVREE CONJOINTEMENT AVEC
L'UNIVERSITE DE NANTES
COMUE UNIVERSITE BRETAGNE LOIRE
ECOLE DOCTORALE N° 602
Sciences pour l'Ingénieur
Spécialité : Génie des Procédés

Par

Piyush Kumar JHA

"Étude de l'effet des radiations électromagnétiques pendant la congélation sur la structure de glace et la qualité des tissus des fruits et légumes"

or

"Study on the effect of electromagnetic radiations during freezing on ice structure and quality of fruit and vegetable tissues"

Thèse présentée et soutenue à Oniris, le 9 Novembre 2018
Unité de recherche : GEPEA-UMR CNRS 6144

Rapporteurs avant soutenance :

Fernanda FONSECA, Directrice de Recherche, AGROPARISTECH, INRA, Grignon
Dominique CHEVALIER-LUCIA, Professeur, Université de Montpellier

Composition du Jury :

Examinateurs : Catherine RENARD, Directrice de Recherche, INRA Paris
Manabu WATANABE, Maitre de conférences, TUMST Japan
Epameinondas XANTHAKIS, Chercheur Senior-Chef de Projet, RISE Sweden

Dir. de thèse : Alain LE BAIL, Professeur, Oniris Nantes

Invité(s) Vanessa JURY, Maitre de Conférences, Oniris Nantes

ACKNOWLEDGEMENT

"Arise! Awake! and stop not until the goal is reached"
Swami Vivekananda

First and foremost, I am grateful to the God for the good health and wellbeing that were necessary to complete this book. Heart filled with growing love, I thank my family members as without their moral support and blessings this day would have never come in my life. Their advice and encouragement are what allowed me to carry this project to completion.

I express my profound gratitude and regards to my thesis director Prof. Dr. Alain Le-bail who provided me with an opportunity to work under him. I deeply appreciate his exemplary guidance, monitoring and persistent encouragement in every phase of the project work. The blessing, help and guidance given by him time to time shall carry me a long way in the journey of life on which I am about to embark.

I acknowledge my heartfelt thanks to my co-supervisor Dr. Vanessa Jury**,** for her constant inspiration and perspicacious consults to complete my research work effectively and within the given time.

I will be always grateful to Dr. K. Alagusundaram (DDG, ICAR) for his sustained guidance, constructive suggestions, encouragement, kindness and moral support.

I take immense pleasure in devoting my thanks to Dr. Epameinondas Xanthakis for his key contribution to the field of microwave assisted freezing technology, which laid the foundation for this current project work. Besides, I thank him for helping me out with paper writing and providing me with technical assistance.

I am very much grateful to Sylvie Chevallier for sharing her knowledge on microscopy and image analysis. I would like to take this opportunity to thank Luc Guihard, Christophe Couëdel and Delphine Queveau for their valuable help during the period of study. I sincerely thank Anne Rousseau-Doré and Christina Péréon for their helping nature and taking care of my administrative related work.

A special thanks to Kevin Vidot (INRA, Nantes) for helping me with CLSM imaging. His expertise in this field made the analysis smooth and trouble-free. I thank Xavier Falourd

(INRA, Nantes) for helping me out with NMR tests. I also thank Romain Mallet (Univ-Angers) for cryo-SEM imaging.

I would also render my special Guru Raj for assisting me during the experimentations.

I will be failing with my responsibility if I don't acknowledge the help rendered by PhD students, Masters intern and all staffs from the laboratory during my PhD work.

I wholeheartedly thank Pays de la Loire region and FREEZEWAVE European project (FP7-ERA-Net SUSFOOD) for funding this thesis work. My sincere thanks to Mccain foods company for supplying me potatoes for my project.

Lastly, I would again thank my family members, my mother Mrs. Sunita Kumari Jha, my father Prof. Dr. Indu Shekhar Jha who not only provided me financial, moral, and all other helps but also assisted me with paper and thesis writing. I am also grateful to my elder brother and sister for their love, support, and guidance throughout my course of study.

TABLE OF CONTENT

Nomenclature

Symbol	Description	Units
c	Dry matter concentration	g of dry matter/g of sample
D	Mass diffusivity	m^2/s
D10, D50 and D90	Intercepts for 10%, 50% and 90% of the cumulative pore size distributions	[m]
E	Electric field	[V/m]
f	Frequency	[Hz]
ΔG_n	Gibbs free energy	[J]
H	Height	[m]
ΔH_f	Enthalpy of fusion	[J/g]
I	Electric current	[A]
k	Boltzmann constant	[J/K]
K_l	Electrical conductivity of intact samples in low frequency range (1–5 kHz)	S/m
K_l'	Electrical conductivity of treated (freeze-thawed) samples in low frequency range (1–5 kHz)	S/m
K_h	Electrical conductivity of intact samples in high frequency range (3–50 MHz)	S/m
K_h'	Electrical conductivity of treated (freeze-thawed) samples in high frequency range (3–50 MHz)	S/m
M	Molarity	mol/L
P	Permanent polarization	$[C/m^2]$
p	Pressure	[Pa]
p_0	Disintegration index	-
r	Radius of the nuclei	[m]
t	Time	[s]
t_{PEF}	Time of PEF treatment	[s]
T	Temperature	[K]
T_{IFP}	Initial freezing temperature	[K]
T_m	Initial freezing temperature as a function of concentration	[K]
T'_m	Temperature at which maximum cryoconcentration is reached	[K]
T'_g	Glass transition temperature	[K]
T_1	Spin-lattice or longitudinal relaxation time	[s]
T_2	Spin-spin or transverse relaxation time	[s]
TSS	Total soluble solids	°Brix
ΔT	Degree of supercooling	[K]
V	Voltage	[V]
ε'	Dielectric constant	[F/m]
ε''	Dielectric loss factor	[F/m]
d_P	Penetration depth	[m]
λ	Wavelength	[m]
σ	Surface tension	$[J/m^2]$
τ	Time constant	[s]
ρ	Mass density	$[kg/m^3]$
$\emptyset$	Diameter	[m]

Abbreviations

AMF	Alternating magnetic field
AMFs	Alternating magnetic fields
DC-V	DC voltage
CAEMF	Crystallisation assisted by electromagnetic field
CAT	Catalase
CLSM	Confocal laser scanning microscopy
CMAF	Constant power microwave assisted freezing
CWP	Cell wall polysaccharides
Cryo-SEM/C-SEM	Cryo-scanning electron microscopy
C1	Plasma membrane capacitance
C2	Vacuole membrane (tonoplast) capacitance
DMI	Directly measured impedance
EF	Electric field
EF	Electric fields
ELFFs	Extremely low-frequency fields
EM	Electron microscopy
EMFs	Electromagnetic fields
ESEM	Environmental scanning electron microscopy
FDA Index	Freeze damage assessment index
IFP	Initial freeing point temperature
IIF	International Institute of Refrigeration
ILT	Inverse Laplace transformation
KSC	Kramer shear cell
LOX	Lipoxygenase
MAF	Microwave assisted freezing
MF	Magnetic field
MFs	Magnetic fields
MRI	Magnetic resonance imaging
MW	Microwave
MWs	Microwaves
NMR	Nuclear magnetic resonance
PDCO	Primal–dual interior method for convex objectives
PEF	Pulsed electric field
PMAF	Pulsed power microwave assisted freezing condition
PMAFs	Pulsed power microwave assisted freezing conditions
POD	Peroxidase
PPO	Polyphenoloxidase
RF	Radio frequency
RF-CF	Radio frequency assisted cryogenic freezing
ROI	Region of interest
R1	Plasma membrane resistance
R2	Vacuole membrane (tonoplast) resistance
R3	Cytoplasmic resistance surrounding the vacuole in the direction of current
R4	Cytoplasmic resistance in vacuole direction
R5	Resistance of the vacuole interior
R6	Resistance of the extracellular compartment
SEF	Static electric field
SEFs	Static electric fields
SEM	Scanning electron microscopy
TEM	Transmission electron microscopy
TPA	Texture profile analysis

TTT	Time-temperature-tolerance
WSP	Water-soluble pectin fraction
XMT	X-ray micro-computed tomography
h	Hours
min	Minutes
2-D	Two-dimension
3-D	Three-dimension

LIST OF FIGURES

LIST OF TABLES

INTRODUCTION

Freezing is an efficient method of food preservation. It is a process, which transforms free water available in the food products to ice, resulting in a reduction of water activity in the food matrix. The immobilization of free water inhibits the microbial growth and slows down enzymatic and chemical degradation reactions causing deterioration of food products at a slower rate. However, it can also induce irreversible damages at the cellular level, which then degrade the overall quality of the frozen food products.

The extent of freeze damage caused to the food products on thawing is linked, for the most, to the size of ice crystals, and which in turn is related to freezing speed being used. Freeze damage is also linked to the cryoconcentration effect; the solutes that are present in the cells are undergoing a cryoconcentration effect resulting from the progressive formation of ice. The remaining aqueous phase turns to become more and more concentrated; this concentrated solution is causing denaturation to the proteins and other organized biopolymers (i.e. cellulose based systems for fruits and vegetables), which in turn degrade their mechanical properties and by the way the overall texture of the tissue.

Freezing processes are often qualified as fast or slow on a more or less subjective base. A freezing rate is sometimes proposed, either based on the kinetics of temperature drop over a given temperature interval (in °C/min usually), or again based on the time needed to freeze a given dimension of the product undergoing freezing (in cm/h usually). At slow freezing rate, intracellular waters move to the extracellular domains (from inside of the cell) and thus would result in bigger size ice crystals and also in a higher cell dehydration. In fact, the formation of larger ice crystals and the highly dehydrated cell would cause a higher destruction of cellular structure (highly punctured cell membrane, collapsed cell structure and separated cellular). As an outcome, the leakage of the fluid from the cell will be higher and a product having water-soaked appearance and mushy texture will be obtained. A slow freezing rate will also result in a prolonged exposition of the tissue to the concentrated solution resulting of the cryoconcentration effect. On contrary, rapid freezing (high freezing rate) favors the genesis of fine ice crystals distributed uniformly within the product, thus reducing the dislocation of water (leading to lower shrinkage). The result is lesser cell destruction and better quality preservations. However, rapid freezing rates have two main disadvantages: (i) rapid freezing process consumes a higher amount of energy hence increases the operating cost and (ii) use of extremely high freezing rates, particular in the case of cryogenic freezing, may lead to crack

development in the samples and yield unexpectedly a poor quality final product. The last important parameter that may be responsible for quality losses of frozen foods is the storage conditions; time-temperature parameters, as well as temperature fluctuations, are mainly responsible for the quality loss.

Even though the freezing technology is optimal in terms of blocking most or all microbial and enzymatic degradation that occur for fresh foods, it is a great challenge for the frozen food industry to minimize the freeze damage by achieving small ice crystals with a minimum expenditure of energy. Several innovative freezing processes have been developed lately taking into consideration the energy saving and/or quality preservations to a larger extent upon thawing. Among these technologies, the use of electromagnetic waves (EW) assisted freezing has proven to be a promising technology due to their capability to refine ice crystals and to impart lesser freeze damage. It has been reported that radio frequency (RF) assisted freezing doesn't affect the freezing time, while microwave (MW) assisted freezing slightly increases the freezing time. Indeed, MW represents some energy dissipation (more than RF) and optimization must be carried out to reduce MW energy while improving efficiently the microstructure of frozen tissues. The influence of electromagnetic radiation on water was reported to result from the electrical rather than the magnetic impact. It is because, electric fields are more efficient in changing the conformation of water network due to the intrinsic electric dipole moment of the water molecule, while much stronger magnetic fields are required in order to exert the same force. It is hypothesized that the torque exerted by an alternating electric field component of electromagnetic radiation can destabilize the equilibrium state of water clusters (during ice crystals formation), and thus can interfere with both ice nucleation and kinetics of crystal growth leading to the formation of small size ice crystals.

Frozen fruits and vegetables are the next-gen product in the global frozen food market. Besides, frozen fruits and vegetables are much more affected by the freezing process than other foods like meat. Thus, in order to produce frozen fruits and vegetables of highest quality, three things are of utmost importance

(i) Better understanding of the nature and mechanism of freeze damage.
(ii) Methods (both qualitative and quantitative) estimating freeze damage accurately and cost-effectively.
(iii) Development of new freezing methods capable of reducing the freeze damage.

Following a previous study by Xanthakis et al. (2014b), who showed that MAF (MW assisted Freezing) was capable of reducing the size of ice crystals (pork loin application), a collaborative European H2020 project named "FREEZEWAVE" (SUSFOOD ERA-NET project) was started in 2015 to in-depth study the effects of microwave assisted freezing (MAF) on the food matrix. This project has 4 partners; ONIRIS (France) who is project's coordinator, RISE (Sweden), TTZ (Germany) and SAIREM company (France). At ONIRIS, MAF of the model system (tylose gel) and some specific horticulture product (apple and potato), as well as modelling of MAF process, are being carried out. MAF of meat and fish matrix are being studied at RISE (Sweden) and TTZ (Germany). SAIREM (France) have designed the microwaves emitter (solid state generator) for this project. To the best of our knowledge, this technology has been used, for the first time within FREEZEWAVE, for the freezing of fruits and vegetable matrix. Apart from MAF, the effects of several conventional methods on the quality of fresh fruits and vegetables were also explored at ONIRIS under this PhD work.

This PhD work was initiated with 3 main objectives

(i) To better understand the impact of freezing on the cohesion and damage in fruits vegetables.
(ii) To develop techniques capable of accessing the freeze damage of horticulture product (mainly fruits and vegetables) at various level (cellular to organ level).
(iii) To optimize microwave assisted freezing process from the product quality point of view.

To reach these objectives, a strategic work plan has been established with the following key milestones:

(i) To develop a MAF prototype equipment able to freeze a sufficient amount of samples to carry out assessment of freeze damage with a substantial statistical significance.
(ii) To develop a set of techniques that can permit to assess freeze damage at different scale and to benchmark these techniques.
(iii) To perform and optimize MAF of apple and potato, the two models fruit and vegetable chosen for this study.

This manuscript presents an overview of the work that has been carried out during my PhD project.

In the first chapter, a state of the art is first proposed; crystallization assisted by electromagnetic field (CAEMF) will first be introduced, followed by a description of past studies related to the assessment of freeze damage in fruits and vegetables.

The second chapter presents the materials and methods that have been used, covering both process aspects and techniques to assess freeze damage.

The third chapter is pooling the main results obtained during the project on apple and potato.

The last part of the PhD proposes a resume of the work that has been done and addresses some outlooks on possible future investigation of this highly innovative process.

The writing of the PhD manuscript is endorsed by several research articles that have been for the most already published or being under submission-review status. A “lean writing style” has been adopted for this manuscript to (i) avoid the duplication of detailed information contained in published papers and (ii) facilitate the reading by relating the key outcomes.

I. REVIEW OF LITERATURE

In this chapter, a state of the art is first proposed; crystallization assisted by electromagnetic field (CAEMF) will first be introduced, followed by a description of past studies related to the assessment of freeze damage in fruits and vegetables.

I.1 Freezing

I.1.1 Basics of food freezing process

Food freezing is an important and largely used process. Apart from drying, it is the most efficient mean to extend the shelf life of food. Freezing has been used for centuries in cold regions and cold seasons as a method for preserving food. Freezing stops or slows down the growth of most microbial species. Freezing prevents microorganism growth by turning liquid water of the food into ice and making this water not available for microorganism growth. This results in a longer preservation and a great reduction of decomposition of the food.

The main component of most frozen food products is water and understanding the freezing process of the water contained in food is a key element to understand the freezing process of the food itself. The phase diagram is a good representation of the physical phenomenon that occurs during the freezing of food and of water. A standard phase diagram of a food is presented below Figure 1.

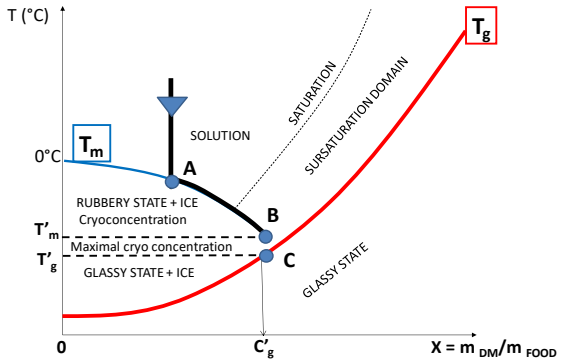

Figure 1: Phases diagram of a food. For a given dry matter content, the evolution of concentration and temperature of the aqueous phase is drawn with first ice crystal formed in A, maximal cryoconcentration in B and glass transition in C.

The different phases presented on the diagram in Figure 1 show the temperature as a function of the concentration or titer of the aqueous phase of the food (mass of dry matter per total mass). On the blue curve, T_m represents the evolution of the initial freezing temperature as a function

of concentration; this curves starts at 0 °C for a zero titer, corresponding to pure water, which is known to freeze at 0 °C. The red curve corresponds to the glass transition frontier. Two key temperatures are identified, namely T'_m and T'_g. T'_m corresponds to the temperature for which the maximum amount of ice that can freeze in a given matrix is reached; it is usually called the maximum cryoconcentration temperature. T'_g corresponds to the glassy state transition temperature, for which the material in which the ice crystals are embedded will turn from a rubbery state to a glassy state, corresponding to a highly stable condition with a highly reduced mobility of the molecules contained in this material. The concentration C'_g is in principle the same for T'_m and T'_g, and T'_g is usually a few degrees below T'_m. The location of these points is specific to each matrix.

The evolution of a given food undergoing freezing is proposed in the black line trace. At point A, the first crystals of ice appear; it may happen that a departure of equilibrium occurs, resulting in a supercooled state. In such case, the temperature drops below the expected IFP (initial freeing point temperature) without any ice formation, until a certain point at which a rupture of supercooling happens (sudden rapid return to the equilibrium curve) and a given amount of ice is formed. From point A to point B, a phenomenon of cryoconcentration occurs; the formation of the ice crystals causes the residual solution to increase in titer and its freezing temperature to drop. At point B, the maximum cryoconcentration is reached at temperature T'_m. Below this temperature, it is no longer possible to crystallize more water. If the food is cooled beyond its maximum cryoconcentration point, it will reach the point C corresponding to the glass transition temperature T'_g. The temperature T'_m is often in the range of − 30 °C to − 40 °C and therefore the temperature is lower than the reference frozen storage temperature of − 18 °C. At this temperature, which is above T'm, the freezable water will not be fully frozen for most foods.

The function describing the evolution of the fraction of freezable water effectively frozen as a function of temperature (assuming an initial freezing temperature of − 1 °C) and an end-of-freezing temperature T'_m of − 40 °C is shown in Figure 2. The calculation has been done according to Le-Bail et al. (2008) based on Fikiin (1998) and Fikiin (1999). It shows that 96.9% of the freezable water is frozen at − 18 °C. The International Institute of Refrigeration (IIR, 1986) considers that a food is "frozen" if (a) 80% of the freezable water is frozen, or (b) below the temperature of − 10 °C. In the case shown in Figure 2, the temperature at which 80% of freezable water froze corresponds to − 4.6 °C. The most restrictive value, that is to say the lowest value, must be considered. The maximum crystallization zone, on which the quality of

a deep-frozen food is set, in particular in terms of the size of the ice crystals, is therefore within this range covering the gap between the initial freezing temperature and T'_m.

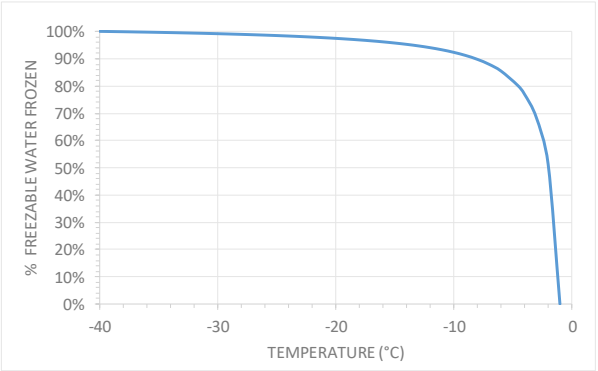

Figure 2: Graph showing the evolution of the fraction of freezable water frozen as a function of the temperature assuming an initial freezing temperature of $T_{IFP} = -1$ °C and an end of freezing temperature of $T'_m = -40$ °C.

The control of ice crystal size appears as a key point to minimize freeze damage. Slow freezing speeds yield larger ice crystals and increase the damage to the food products. On the contrary, rapid freezing rates form smaller ice crystals within the product structure and impart minimal damage to the cellular structure (Otero et al., 2000; Orlowska et al., 2009; Singh & Heldman, 2009; Sadot et al., 2017). However, rapid freezing processes are energy-demanding. It is thus, a great challenge for the food industry to achieve small homogenously distributed ice crystal size with a minimum energy investment. Several technologies have been identified to improve the quality of frozen foods such as pressure shift freezing (Koch et al., 1996; Le-Bail et al., 2002), ultrasound (Sun & Li, 2003), vacuum impregnation freezing (Li et al., 2018) etc. In recent times, the use of electric and magnetic (static/DC and alternating/AC) and electromagnetic fields to support freezing has bloomed. Several review papers and book chapters have appeared lately demonstrating the positive impact of these techniques on the freezing process and frozen product quality. This section focuses not only on the fundamental mechanisms underlying ice nucleation under electric and magnetic, and electromagnetic field but also on their application in food freezing.

I.1.2 Mechanism of crystallization

Crystallization involves three stages, namely supercooling, nucleation, and crystal growth (Woo & Mujumdar, 2010). In the first stage, the specimen (i.e. water or aqueous solution for freezing) is cooled down at a certain cooling rate below the initial solidification point. Due to rapid cooling, the sensible heat is removed; this causes the specimen to surpass its phase change

temperature and reach into a supercooled state. The negative difference in temperature, when compared to the solidification point, denotes the degree of supercooling (ΔT). At a particular ΔT, the second stage begins, i.e. nucleation or the formation of a minuscule crystalline lattice structure in the solution. The second stage occurs instantaneously, and it is accompanied by a sudden increase in temperature known as the release of latent heat of crystallization. After the initial nucleation is achieved, crystallization proceeds into the next stage, which corresponds to a subsequent growth of the existing nuclei plus secondary nucleation until the final temperature imposed by the ambience is reached. All these stages of crystallization are responsible for the final crystalline structure.

Note: "Secondary nucleation" is the nucleation, which occurs, irrespectively of its mechanism, only because of the presence of crystals of the material being crystallized. When no crystals are present, no secondary nucleation occurs.

I.1.3 Heat and mass transfer mechanism during food freezing

Food freezing is a typical thermodynamic process involving heat and mass transfer. When the cellular matrix cooled below its freezing point, the ice crystals are first formed in the extracellular space, while the intracellular space remains in the supercooled state primarily due to the fact that the cellular membranes impede the heat transfer during the freezing process. The supercooled water in the cells has a higher chemical potential than the partially frozen phase in the extracellular space. As a result of this difference, water migrates from the inner of the cell to the extracellular domain and freezes externally. This particular physical event depends on the rate of freezing rates. In the case, the cooling rate imparted by the freezing condition is relatively slow, the cell is able to lose water rapidly enough to concentrate the intracellular solutes sufficiently to eliminate supercooling. As an outcome, the cells shrink and do not freeze intracellularly. On the contrary, if the cell is cooled too rapidly, it is not able to lose water fast enough to maintain equilibrium (maintain chemical potential), hence becomes increasingly supercooled and eventually freezes intracellularly (Mazur, 1977, 1984; Gao & Critser, 2000).

I.1.4 Freezing assisted by electric fields

Electric field assisted freezing can be divided into two main categories such as under the application of static electric field (SEF) and alternating electric field (AEF). One of the difficulties that appear when compiling literature is that the authors used different ways to determine the value of the electric field. Most of the time they divided the voltage by the

distance between electrodes, which is the first approach. More precise determinations have been proposed by some authors based on modelling of electric field lines while taking into account the dielectric properties of the different materials installed between the electrodes (Havet et al., 2009).

Dufour seems to be the first scientist who studied crystallization assisted by static electric field (CA-SEF) of supercooled water (Dufour, 1861). Since then, SEF assisted freezing has been investigated at a laboratory scale in both model and more recently in real food systems. SEF application during freezing affects both freezing process parameters (all stages of the freezing process) and quality attributes of food products. For example, when compared to no field condition, the application of SEF during the freezing process promotes nucleation at a higher temperature, reduces the induction time, provokes the nucleation and lastly elongates the phase transition time. With respect to product quality, SEF assisted freezing process reduces the size of ice crystals in the product, lessens cell destruction, decreases the protein denaturation, minimizes the drip loss, and better conserves the texture compared to freezing under no electric field condition (Dalvi-isfahan, Hamdami, & Le-bail, 2017; Dalvi-Isfahan, Hamdami, & Le-Bail, 2016; Dalvi-Isfahan, Hamdami, & Le-Bail, 2018; Jha, Sadot, et al., 2017; Jha, Xanthakis, Jury, Havet, & Le-Bail, 2018; Jha, Xanthakis, Jury, & Le-Bail, 2017; Jia et al., 2017; Orlowska, Havet, & Le-Bail, 2009; Wei, Xiaobin, Hong, & Chuanxiang, 2008; Xanthakis, Havet, Chevallier, Abadie, & Le-Bail, 2013).

The major explanations proposed in the literature are:

- SEF can modify the free energy barrier for phase transition (ΔG_n) and consequently influence the nucleation process. More precisely, SEF tends to reduce the critical radius which in turn decreases the Gibbs free energy of the system and consequently increases the nucleation rate (Figure 3 and Figure 4) (Kashchiev, 1972; Marand et al., 1988; Saban et al., 2002; Orlowska et al., 2009; Stan et al., 2011; Yuryev & Wood-Adams, 2012; Orlowska et al., 2014; Xanthakis et al., 2014a; Mok et al., 2015; Jha et al., 2017a, b; Jha et al., 2018b).

- SEF aligns the water dipole from random directions to the direction of the electric field vector. This polarisation phenomenon makes the hydrogen bond between the water molecules stronger in the direction of the electric field. As a result, water clusters structure can be reordered, which in turn may aid in the nucleation process (Vegiri & Schevkunov, 2001; Shevkunov & Vegiri, 2002; Vegiri, 2004; Sun et al., 2006; Wei et al., 2008).

- The formation of electric double layer at water–dielectric interface was ascribed as one of the factors that enhanced the nucleation rate during SEF assisted freezing of water droplets (Zhang et al., 2016).

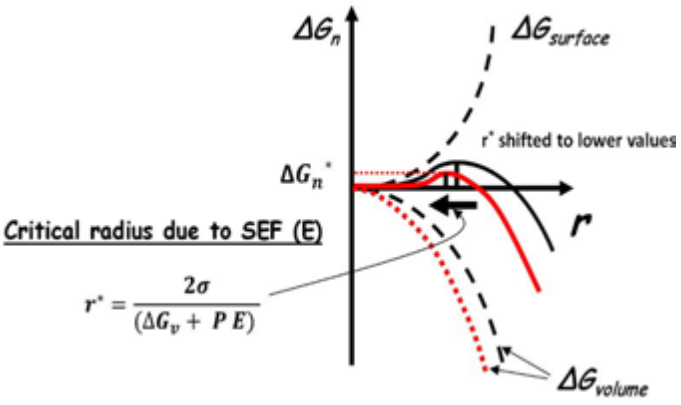

Figure 3: Pictorial representation of decrease in critical radius and free energy (red curves) by the application of static electric field (SEF) during freezing. On applying SEF, the critical radius (r^*) for ice nucleation shifts to a lower value (Jha et al., 2017a). E is the electric field, σ is the surface tension, ΔG_v is the free energy change of the transformation per unit volume, P is the permanent polarization, ΔG_n is the Gibbs free energy, $\Delta G_{(s)}$ is the surface free energy, $\Delta G_{(V)}$ is the volume free energy, ΔG_n^* is the critical Gibbs free energy, r is the radius of ice nuclei.

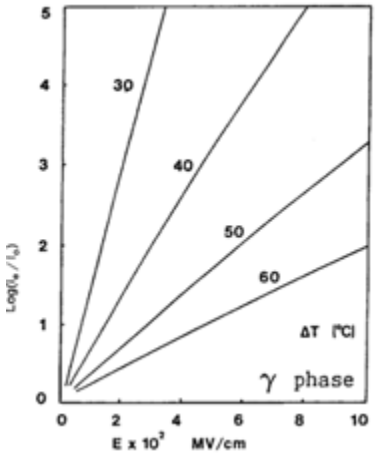

Figure 4: Plot of the ratio of field (I_e) to non-field (I_o) nucleation rates as a function of electric field strength at various degrees of supercooling (ΔT) for crystallization in a polar phase (γ phase) (Marand et al., 1988).

- Surface theory: Regarding the surface theory, in the case of freezing of an aqueous solution containing a solute, Pruppacher et al. (1968) and also Fletcher (1970) explained that a semi-liquid layer is present around an ice crystal under formation. Within this semi-liquid layer, ions are moving towards the mother solution, whereas H_3O^+ and OH^- ions are travelling towards the pure ice crystal. A voltage difference of up to 10 V generating a tiny current in the range of 10^{-7} A has been proposed by Fletcher (Fletcher, 1970) (Figure 5). Applying an external electric field may interfere with these charge motion. Since SEF is directional, it is likely that crystals growth may be rather favoured in selected facets of the crystals under formation.

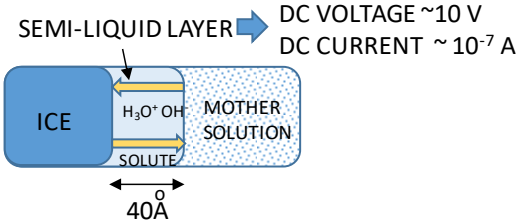

Figure 5: Scheme of the semi-liquid layer surrounding ice crystals under formation within an aqueous solution (Fletcher, 1970). A tiny voltage difference is present within this layer and is linked to mass diffusion of chemical species (solute) and ions travelling within this layer. Imposing an external voltage and static charges may affect ice crystallization process (Fletcher, 1970).

At present, it is difficult to say the exact strength of the electric field that is required to influence the crystallization process of water to ice. However, based on simulation and experimental studies, it seems that the electric field between 10^3 to 10^{10} V/m is required to assist the crystallization process of water. It has to be noted here that the use of electric field having strength $>10^7$ V/m may lead to a dielectric breakdown of the system, thus promoting current flow and ohmic heating of the system.

As a conclusion, SEF assisted freezing technology appears as an efficient way to control the nucleation during freezing and during any process based on crystallization. But, the use of high voltage (in several kV to generate electric field) in the humid environment may raise some safety concerns such as risk of electrical shock, or again ozone formation which is an irritant gas. A proper electrical insulation would mitigate the electric shock risk, whereas proper design of the electrodes set up and of the voltage level should prevent the apparition of ozone.

Fewer studies have been conducted on freezing assisted by alternating electric field than compared to SEF assisted freezing. These studies are focused mainly on freezing of aqueous solutions and a few on water. Similar to SEF, alternating electric field (AEF) can interfere with all the stage of crystallization i.e. supercooling, ice crystal nucleation in the supercooled water and its subsequent growth. The effect of AEF on crystallization process depends on the frequency and intensity of AEF applied to the system. The degree of supercooling, pure ice crystal size, crystallization fraction of pure ice and freezing time while freezing a salty solution (for e.g. 0.9% NaCl or K_2MnO_4 water) decrease with increase in frequency and reach a minimum at a particular frequency. Further increase in frequency increase the above-mentioned freezing parameters (i.e. supercooling, pure ice crystal size, etc.) (Sun, Xu, Zhang, et al., 2006; Sun, Xu, Sun, et al., 2006; Sun & Li, 2010; Ma et al., 2013). The strength of AEF also plays an important role, it was observed that application of AEF of 15 kV (60 Hz) elevated the nucleation temperature up to 8 ℃ compared to no field condition (− 2 ℃ observed under AEF condition against − 10 ℃ for field-free case) (Salt, 1961). AEF (up to $(1.6 \pm 0.4) \times 10^5$ V/m and 3-100 kHz) use during freezing affect the homogeneous nucleation by a factor less than 1.5 (Stan et al., 2011). The strength of AEF also impact the grain size and crystallization fraction of pure ice while freezing of 0.9% NaCl solution: the size and crystallization fraction of pure size have a proportional relationship with the strength of AEF (Ma et al., 2013).

As of now, no peer-reviewed article is available in the literature on freezing of real food matrix using AEF assisted freezing technology. However, a few patents claim better food preservations using AEF assisted freezing and/refrigeration (Owada, 2007; Kim et al., 2013a).

It is hypothesized that the torque exerted by an AEF can destabilize the equilibrium state of water clusters, and thus can interfere with both ice nucleation and kinetics of crystal growth (Hanyu, 1992; Jackson et al., 1997; Sun, Xu et al., 2006; Woo & Mujumdar, 2010). Another hypothesis states that the vibration and collision induced by the AEF could produce thinner solid-liquid boundaries and decrease heat transfer resistance, similar to acoustic stress (Mok et al., 2015; Hu et al., 2013).

For more information on electric field assisted freezing, please refer Jha et al. (2017a, b, 2018b).

I.1.5 Freezing assisted by magnetic fields

Among all the innovative freezing technologies discussed in this chapter, only magnetic field assisted freezing technology has been commercialized. ABI Co., Ltd. (Chiba, Japan) sells it by the name 'CAS (Cell Alive System) freezer'. The manufacturer claims that the weak alternating magnetic fields (AMFs) applied by these devices are capable of producing numerous small size ice crystals in the food product and preserving the quality of food product to a greater extent after thawing. It has been proposed in the patents that the AMFs application will delay the formation of ice crystals, increase the supercooling and enhance the heat transfer. As a consequence, most of the ice crystals form at the same time resulting in the genesis of numerous ice crystals (Owada & Kurita, 2001; Owada, 2007; Owada & Saito, 2010). However, these theories lack scientific backing. The research studies conducted on magnetic field assisted freezing of food product have yielded a mixed set of results. Some reported that magnetic field assisted freezing preserved the quality of food products better than conventional methods (Kim et al., 2013b, c; Choi et al., 2015), while some concluded no positive effect of magnetic fields application (Suzuki et al., 2011; Otero, Pérez-Mateos, Rodríguez, & Sanz, 2017; Purnell, James, & James, 2017). At this point in time, many doubts exist about real effects of magnetic fields on freezing and the science behind the potential mechanisms involved. Thus, extensive research is required in this domain to reach a decisive conclusion (confirm or reject the efficacy of magnetic fields in improving the quality of the frozen product). For more information on magnetic field assisted freezing, please refer Jha et al. (2017b).

I.1.6 Freezing assisted by electromagnetic fields

Concerning the electromagnetic effects on water, Xanthakis et al. (2014a) reported that the presence of electromagnetic fields (EMFs) tends to reorient the water molecules and some hydrogen bonds of the network may be broken. The influence of electromagnetic radiation on water was reported to result from the electrical rather than the magnetic impact. The electric fields are more efficient in changing the conformation of water network due to the intrinsic electric dipole moment of water molecule, while much stronger magnetic fields are required in order to exert the same force. Furthermore, Xanthakis et al. (2014a) suggested that lower frequency microwaves (central frequency 2450 MHz) (MW) or radio frequency (RF) radiation and even extremely low-frequency fields (ELFFs) (3 Hz–300 Hz) have significant and lasting effects on liquid water (Figure 6). There are claims that water shows memory effects on electromagnetic radiation due to the long lifetime that these effects seem to have. Although several studies have been conducted regarding the impact of electromagnetic fields on liquid water, just a few experimental and computer modelling studies have been carried out concerning the application of such fields during the phase change of water (Xanthakis et al., 2014b; Xanthakis and Valdramidis, 2017; Barba et al., 2017; Sadot et al., 2017).

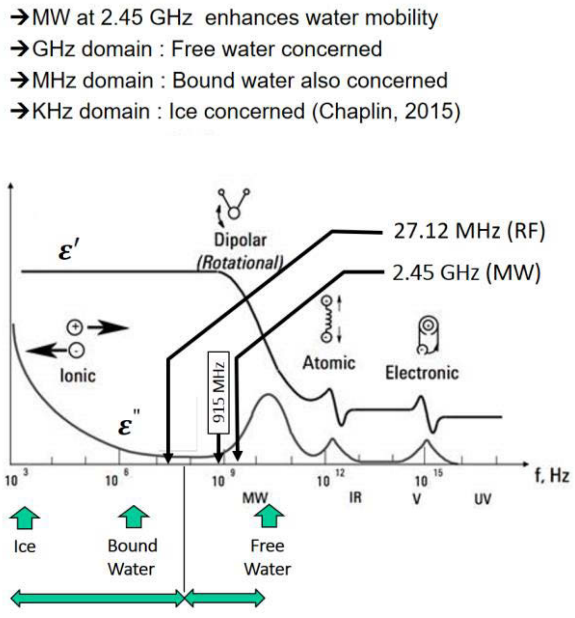

Heat dissipation during electromagnetic radiations exposure depends on dissipation factor value (or loss tangent or tan (δ)) Eq. (1). Smaller tan (δ) values means lower amount of heat generated in the product. With respect to electromagnetic radiations, microwave of 2.45 GHz would cause higher heat generation than microwave of 915 MHz or radiofrequency of 27.12 MHz.

$$\tan(\delta) = \varepsilon''/\varepsilon' \quad (1)$$

Another, important parameter related to electromagnetic radiation assisted processing is the penetration depth. The depth of penetration determines the relative ability of the product to attenuate electromagnetic energy. From Eq. (2), it can be understood that for product of similar dielectric constant loss tangent, penetration depth is higher at a lower frequency.

$$d_P = \frac{\lambda}{2\pi}\left(\frac{2}{\varepsilon'\left[(1+tan^2\delta)^{1/2}-1\right]}\right)^{1/2} \quad (2)$$

Figure 6: Miscellaneous information on the relative impact of selected frequencies of electromagnetic radiations on water. ε' is the dielectric constant (F/m), ε'' is the dielectric loss factor (F/m), d_P is the penetration depth (m), λ is the wavelength (m). Abbreviations used in this figure: MW = microwave; RF = radiofrequency. Adapted from Deshmukh et al. (2017).

Concerning the experimental studies, the use of electromagnetic waves (EW) during freezing has proven to reduce the size of ice crystals in the food product. To date, only three approaches related to the application of EW during freezing have been investigated. One is the use of microwaves (MW) as a pre-treatment prior to freezing (Hanyu et al., 1992), the second one is the constant EW energy application throughout a cryo-freezing process (Jackson et al., 1997), and the last one is the part time application of EW (in forms of pulses) during the freezing process (Anese et al., 2012; Xanthakis et al., 2014b).

Hanyu et al. (1992) studied the final impact of MW application on biological matrices prior to freezing. They pre-treated the sample by applying MW (2.45 GHz and 500 W) for 50 ms prior to freezing. The researchers reported that MW irradiation followed by freezing produced smaller ice crystals in the frozen items with a good repeatability. Moreover, the zone of good freezing extended to a greater depth into the microwaves irradiated sample (squid retina, rat liver and heart muscle) compared to the control sample (Figure 7). The zone of good freezing can be referred as the area where there is no sign of detectable ice-crystal damage. In other words, MW irradiated sample had a larger ice-free (vitrified) region compared to untreated sample. Jackson et al. (1997) reported that the continuous application of MW (2.45 GHz and 1000 W) during attempted vitrification of ethylene glycol solution (cryo-protectant) caused a significant reduction in ice formation (Figure 8). Moreover, the effect of MW irradiation on ice formation depended on the molarity of the glycol solution. For example, at a fixed microwave power and frequency the reduction in ice formation was maximal at 3.5-4 M and minimal at 3.0 M (lowest concentration been used) and 5.5 M (highest concentration been investigated).

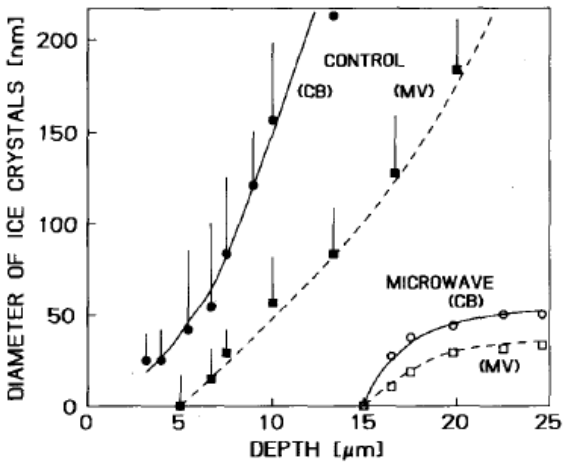

Figure 7: Graph showing a clear reduction of the size of ice crystals in a living tissue exposed to freezing under MW irradiation (2.45 GHz). The sample was a squid retina. CB = cell bodies and MV = microvilli (Hanyu et al., 1992).

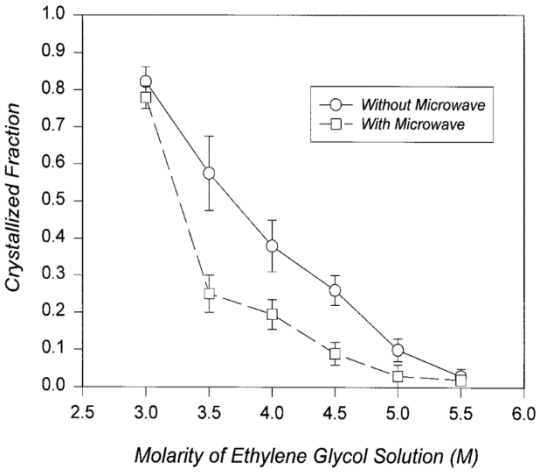

Figure 8: Fraction of samples which crystallized into visible ice plotted as a function of the molar concentration of ethylene glycol for MAF (2.45 GHz) and no MAF conditions (Jackson et al., 1997).

Recently, a different approach of MAF was applied for first time in a real food system by Xanthakis et al. (2014b). Freezing of pork samples under different microwave power levels (40 %, 50% and 60%) was performed (Figure 9 and Figure 10). In this study, a prototype equipment was built in order to be able to freeze a food sample inside a tailored modified domestic microwave oven. The power levels in common domestic microwave ovens are in general an average power level adjusted by electronic duty cycling supervision. Hence, during duty cycling, the power that is delivered by the magnetron is alternating from full power to null power (ON/OFF); such operating mode can be referred as an application of pulsed MW energy. Their results revealed that at 60% microwave power level, the average ice crystal size and the degree of supercooling decreased by 62% and 92% when compared to the conventionally frozen sample. The degree of supercooling and the ice crystal size are influenced by the level of the emitted power since at the low power level of 40% the degree of supercooling and the ice crystal size were greater than the ones observed at 60% of power level. Moreover, they found that freezing rate decreased and overall freezing time increased with the increasing power level of microwaves due to the heat generated by MW (Figure 11 and Figure 12). A peculiar observation made by them was that limited temperature oscillation happened at both stages of nucleation and crystal growth during MAF process (Figure 12). According to Xanthakis et al. (2014b), this limited oscillation of the temperature during the genesis of the ice nuclei and crystal growth might have caused instantaneous melting and regeneration of ice crystals, which in turn prohibited the crystal growth and led to an increase in the number of smaller ice crystals.

Overall, their study provide quantitative data regarding the ice crystal size and the impact of MW radiation during freezing of meat microstructure and highlight the need to be further investigate and the potentials of this technology to be applied for the production of frozen food with improved quality.

A model to describe MAF has been proposed by Sadot et al. (2017). The simulations performed with COMSOL Multiphysics showed a complex behaviour of electric field distribution and generated heat due to the phase change. In fact, because dielectric and thermophysical properties are very different in frozen and fresh state, penetration depth and local heat generation evolved dramatically during unidirectional freezing. In their study microwaves reached the product at the same surface that the cooling fluid. It showed that due to the increase in penetration depth in frozen phase, a hot spot and a local maximum of electric field, was following the freezing front advance. Their method seems to be appropriate to study the impact of microwave irradiation on the phase change. Furthermore, the aforementioned study figured out that a complex behaviour of reflection at air/product interfaces and resonance within the product occurred during MAF process.

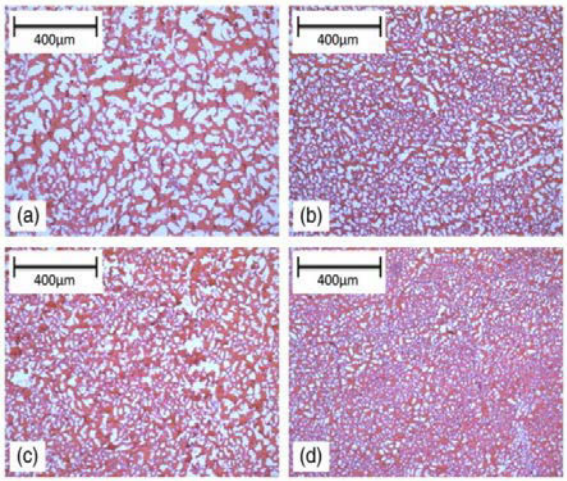

Figure 9: Reduction of the size of ice crystals in pork loin exposed to MW (2.45 GHz) during freezing (Xanthakis et al., 2014b). (a) control freezing, (b), (c), (d) increasing MW power irradiation i.e. 40 %, 50% and 60% power levels.

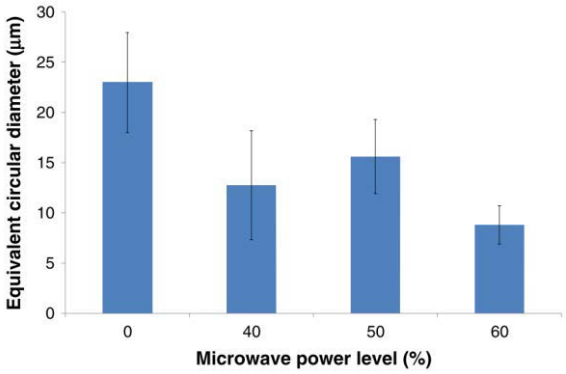

Figure 10: Mean equivalent circular diameter (EqD) of ice crystal voids under different levels of microwave power radiation (Xanthakis et al., 2014b).

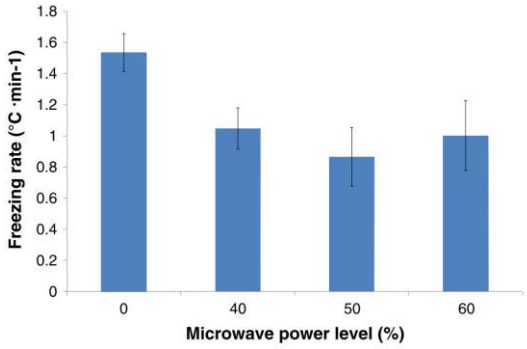

Figure 11: Freezing rate at control conditions Vs. at different microwaves power levels during freezing (Xanthakis et al., 2014b).

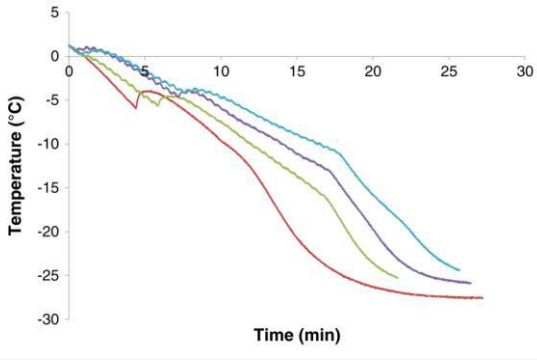

Figure 12: Freezing curves obtained during control conditions and under different power levels of microwave radiation (40% — green curve, 50% — purple curve, 60% — blue curve) (Xanthakis et al., 2014b).

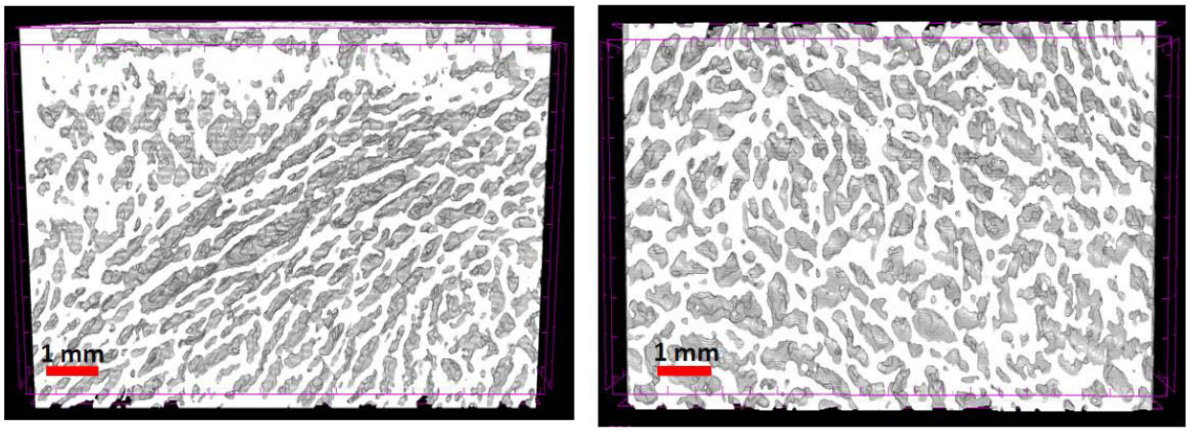

(a) (b)

Figure 13: Microstructure of potato after freezing under (a) control condition and (b) constant MW condition (Jha et al., 2018a).

Most recently, it was observed that MAF processes generated smaller size ice crystals in food matrix (i.e. potato, fish and pork meat matrix) (Jha et al., 2018a; Xanthakis, et al., 2018). In comparison to the control condition, the application of MWs during freezing significantly reduced the D90 value of ice crystal size in the potato sample (up to 32% reduction was observed at constant MW (294 W/kg) freezing condition) (Figure 13). The results obtained for fish showed that the application of constant MW (15 W/kg) power during freezing led to the elimination of the intracellular crystals. In the case of pork meat, pulsed MAF condition (882 W/kg with 8 s pulse width and 8 s pulse gap or average power of 441 W/kg) gave the best result regarding the ice crystal size where the average size was ca. 20% lower than that of the conventionally frozen samples (Figure 14). However, it was also found that freezing under MAF conditions slightly increased the freezing time. Indeed, MW represents some energy

dissipation and optimization must be carried out to reduce MW energy while improving efficiently the microstructure of frozen tissues.

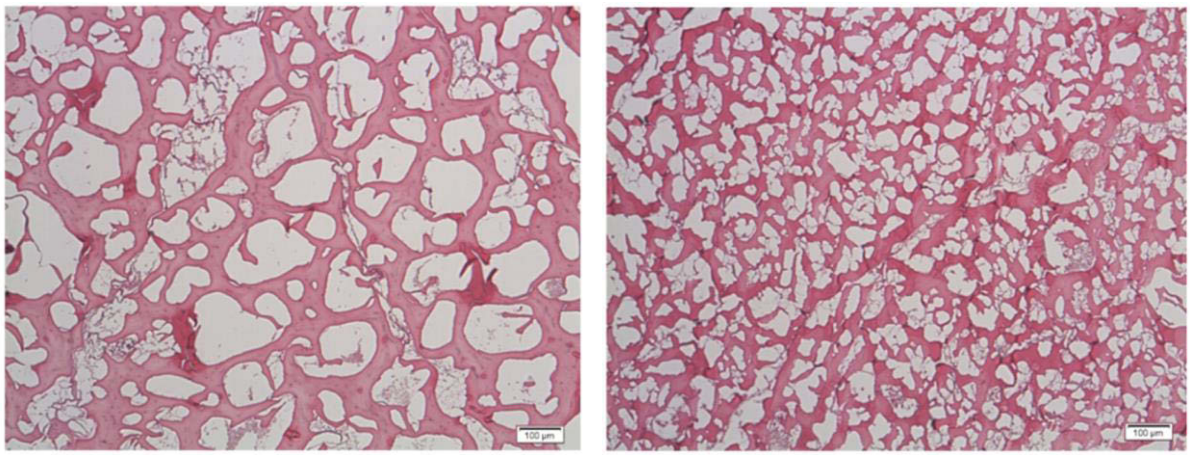

(a) (b)

Figure 14: Representative micrograph images of frozen pork tenderloin transversal cuts under (a) conventional and (b) pulsed MAF freezing conditions (Xanthakis, et al., 2018).

Anese et al. (2012) explored the freezing assisted by radio frequency (RF-27.12 MHz). In their study, they compared RF assisted cryogenic freezing (RF-CF) with other freezing methods, such as: cryogenic freezing and air blast freezing. They found that the application of low voltage RF pulses during cryo-freezing of pork sample produced better microstructure compared to other two freezing methods (Figure 15). The product frozen in air blast freezer had ice crystals mostly in the intercellular domain. As an outcome, the cell damage increased and drip loss increased (Figure 16). While the product frozen by cryogenic freezing method and RF-CF method had ice crystal formation in both extracellular and intracellular domains. The ice crystals formed under RF-CF seemed to be greater number of smaller ice crystals in the intracellular domain than compared to cryogenic method but unfortunately this study was not supported by quantitative image analysis. Moreover, they found that the cryo-frozen meat cubes had large surface fractures in the direction of meat fibres contributing higher drip loss in the thawed sample. While RF-CF sample had lower drip loss compared to other conditions (Figure 16). Furthermore, they found that the firmness of fresh meat (control) (40.5 $\pm$ 5.8 N) was not significantly different from that of the RF-CF sample (40.8 $\pm$ 1.0 N). In contrary, air blast and cryogenic frozen meat sample showed significantly higher firmness value (47.6 $\pm$ 1.2 N and 58.4 $\pm$ 11.6 N) compared to control and RF-CF sample.

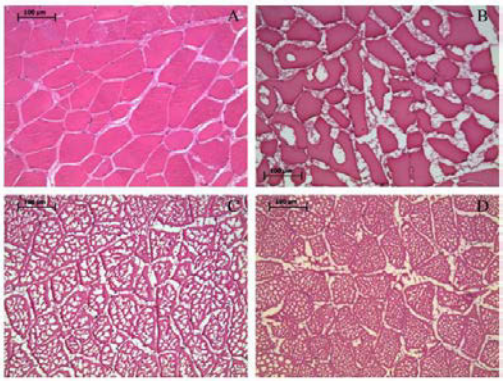

Figure 15: Reduction of the size of ice crystals in pork loin exposed to RF waves (27.12 MHz) during freezing (Anese et al., 2012). A (fresh), B (air blast freezing), C (cryogenic freezing), D (RF-CF).

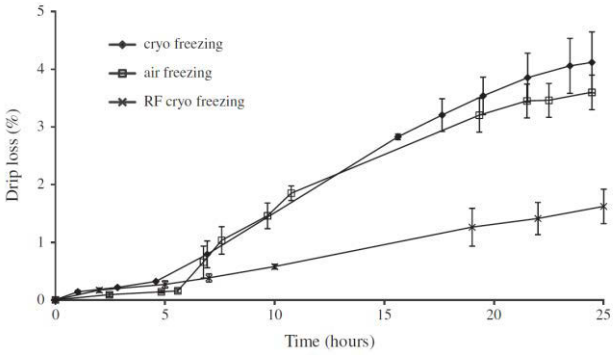

Figure 16: Drip loss of thawed meat cubes previously frozen under different conditions (Anese et al., 2012).

Most recently, Hafezparast-Moadab et al. (2018) performed radio frequency (27.12 MHz) assisted air blast freezing ($-30(\pm 2)$ °C and airspeed of 2 m/s) of fish. In their study, they investigated the impact of three radio frequency (RF) pulse patterns and three electrode gaps (2, 3 and 4 cm) on the freezing curve and quality characteristics of rainbow trout (*Oncorhynchus mykiss*) fish fillet. The RF pulse patterns studied by them were (i) RF–10–20: RF pulses of 10 s on and 20 s off, (ii) RF–20–20: RF pulses of 20 s on and 20 s off and (iii) RF–30–20: RF pulses of 30 s on and 20 s off. The results reveal that the freezing curves shape and the freezing rate values were the same for RF conditions and control condition (no RF application) (Figure 17). With respect to the impact of RF assisted freezing process on the quality characteristics of fish, it was observed that RF assisted frozen fish had finer ice crystals (up to 75% smaller) (Figure 18), lesser damage to the structure, lower drip loss, and superior texture (close to fresh sample) than sample frozen in the absence of RF. The electrode gap was found as factor that determined the final size of ice crystals in the fish matrix; the size of ice crystals decreased upon narrowing the gap between the electrodes (Figure 18).

The underlining mechanism behind freezing assisted by electromagnetic radiation (ER) is still unknown, but a few findings and assumptions have been put forward by some research groups. These are: (i) Anese et al. (2012) claimed that the application of ER causes depression in the freezing point and thereby produces more nucleation sites, however, time-temperature detail obtained by Hafezparast-Moadab et al. (2018) during RF freezing of fish observed no depression in freezing time (Figure 17); (ii) the torque exerted by ER displaces the water molecules from their equilibrium relationships in the ice cluster resulting in break-down of existing ice crystals. The disintegrated ice crystals may act as nucleation site and promote the

secondary nucleation, thus, causing ice crystal size reduction (Hanyu et al., 1992; Jackson et al., 1997; Anese et al., 2012; Xanthakis et al., 2014a, b; Dalvi-Isfahan et al., 2016; Cheng et al., 2017); (iii) ER may decrease the ice crystal growth rate and consequently increase the number of ice crystals (Jackson et al., 1997); and (iv) Xanthakis et al. (2014b) reported that the temperature oscillation (caused by the on-off duty ratio of the commercial domestic oven (for low power emission)) during genesis of the ice nuclei and crystal growth might have reduced the growth rate of ice crystals, thus leading to the formation of small size ice crystals.

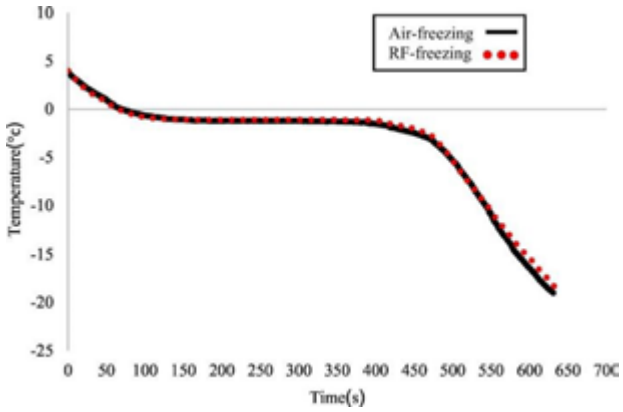

Figure 17: Freezing curves obtained during control and RF assisted freezing of fish (Hafezparast-Moadab et al., 2018).

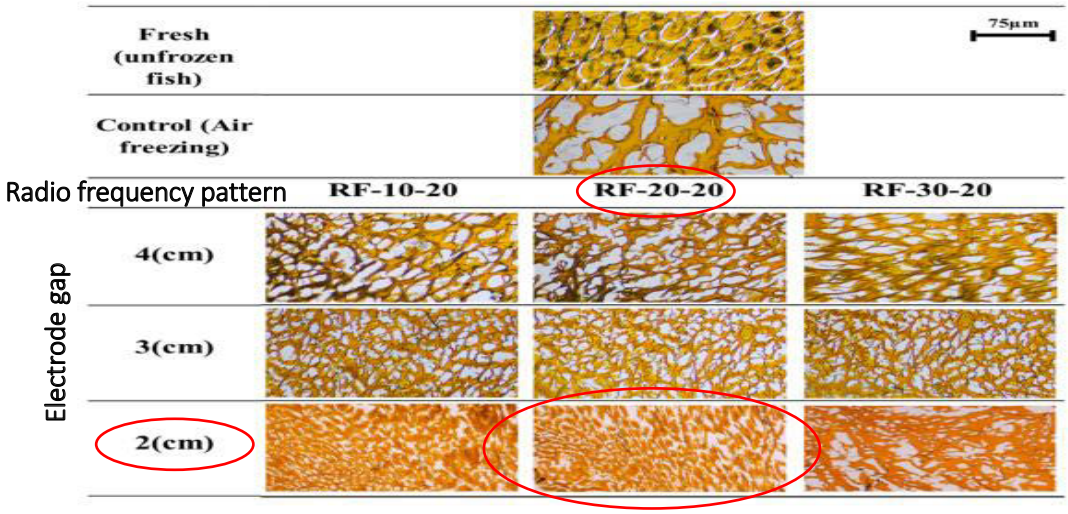

Figure 18: Microstructure of fish fillets frozen by different RF conditions (3 pulse pattern and 3 pulse spacing) as compared to the fresh and control samples. The encircled combination of electrode gap (2 cm) and RF pattern (RF–20–20) resulted in 75% decreases in the ice crystals size compared to control freezing condition (Hafezparast-Moadab et al., 2018).

➔**Intermediate conclusions:**

This state of the art showed that not so many (around 6) studies are available on MAF, and even, within this number are some studies related to non-food material. It appears therefore, quite obvious that further scientific investigations are needed to better understand how MW may affect freezing process and also to assess through a scientific approach the possible improvements that MAF may have in terms of mitigation of freeze damage.

To address these lacunae, further analysis on freezing under electromagnetic radiation considering MW range (2450 MHz) will be envisaged in this project, aiming at (i) confirming the outcomes proposed in the literature from the quality point of view and (ii) establishing more precisely the specifications needed for the MAF process. Regarding the later point, Xanthakis et al. (2014b) have proposed two assumptions to explain the positive effect of MW in terms of reduction of the size of ice crystals; these were (i) possible effect of MW to disrupt/fractionate the ice crystals under formation and (ii) possible effect of temperature oscillation caused by the on-off duty ratio of the commercial domestic oven that was used (for low power emission). Within this project, we intend to investigate these assumptions and eventually optimize the operating condition in particular for temperature oscillation case.

I.2 Assessment of freeze damage in fruits and vegetables

I.2.1 Introduction

Fruits and vegetables are considered as living entities even after harvesting as they continue to respire and perform various metabolic processes at a cellular level (Sharma, Thakur, & Maiti, 2016). Respiration is a central process in all living cells that involves a series of oxidation-reduction reactions where a variety of stored constituents within the cells are oxidized to CO_2 and energy is subsequently released (Kays, 1991; Mahajan & Goswami, 2001; Bhande, Ravindra, & Goswami, 2008). This method of self-consumption leads to a shorter shelf life of the fruits and vegetables. The rate of respiration is important because it gives an indication of the overall rate of metabolism of the plant or plant part. All metabolic changes occurring after harvest are important, especially those that have a direct bearing on product quality (Kays, 1991). The postharvest respiratory response of fruits and vegetables mainly depends on two factors, first is the storage temperature and the second is the storage air composition in terms of O_2, CO_2 and ethylene (Kays, 1991; Mahajan & Goswami, 2001; Bhande et al., 2008). The subjection of fresh product to low temperature, low O_2 and slightly high CO_2, in general, reduces the self-utilization process and increases the shelf life of the product beyond its normal span (Mahajan & Goswami, 2001; Bhande et al., 2008). Chill (cold) and frozen storage are the two widely used low-temperature preservation methods for fruits and vegetables. Like other processing techniques, the low-temperature processes may also cause some artefacts. For example, low-temperature (chilling and freezing) injuries can happen in fruits and vegetables. In this chapter, the freezing injuries as well as the mechanism of freeze damage in fruits and vegetables are being discussed. A comprehensive study on the methods that are being used to evaluate the freeze damage in fruits and vegetables is provided. Further than the principles and the applications of those methods, the advantages and the limitations are also being pointed out.

I.2.2 Freeze damage

I.2.2.1 Cellular structure of fruits and vegetables

Prior to the discussion of freeze damage mechanisms and the assessment methods, it is essential to describe the nature and the features of fruits and vegetables cellular structure as its condition/status determines the overall quality perceived by humans. The plant tissues are composed of various cells such as parenchyma, collenchyma, sclerenchyma and vascular bundles. The plant tissue system contains air gaps (1-25%) which can substantially affect the texture (Jackman & Stanley, 1995); the amount depends on the type, spatial arrangement and

relative shapes of constituent cells. The edible portion of most of the fruits and vegetables are composed of parenchyma cells (Figure 19) (Potter & Hotchkiss, 1998). The parenchyma cells are polyhedral or spherical in shape and measure 50-500 µm across (Jackman & Stanley, 1995). The cell internally contains, cell organelles to regulate cell metabolism; inclusion bodies incorporating important food components (starch, proteins and lipids); a vacuole (containing water, inorganic salts, organic acids, oil droplets, sugar, water soluble pigments, amino acids, vitamins, etc.) for regulating the osmotic pressure of cytoplasm (Jackman & Stanley, 1995; Potter & Hotchkiss, 1998; Li, Zhu, & Sun, 2018). The cytoplasm is the fluid surrounding the intracellular components and is confined within plasmalemma/cell membrane. The cell membrane is responsible for maintaining the cell turgor pressure and its viability (Li et al., 2018). Exterior to the plasma membrane is the primary cell wall. Fruits and vegetables lack secondary cell wall, but if present lies interior to the primary cell wall (Jackman & Stanley, 1995). The primary cell wall contains similar proportions of the pectic substances, hemicelluloses and cellulose (Buren, 1979); each of these substances provides certain functionality to the cell wall. Cellulose imparts rigidity and tearing resistance to the cell wall, while pectic substances and hemicelluloses provide plasticity and the ability to stretch. The extension of the primary cell walls of a matrix material that lacks cellulose fibrils is referred as middle lamella (Figure 20). Middle lamella acts as an adhesive that adheres the cells together. The plant cell also contains plasmodesmata, a small opening present in the cell walls that connects the cytoplasm of neighbouring plant cells to each other, thus establishing a living bridge between cells (Jackman & Stanley, 1995; Potter & Hotchkiss, 1998).

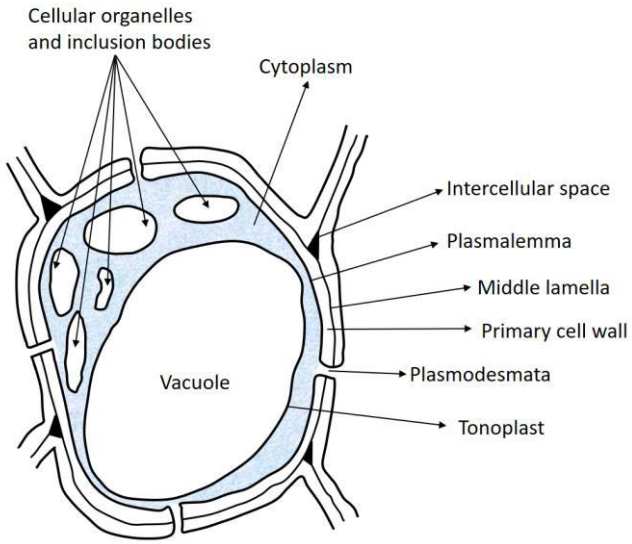

Figure 19: Diagram of a typical parenchyma cell present in plant tissues. Adapted from Jackman & Stanley (1995).

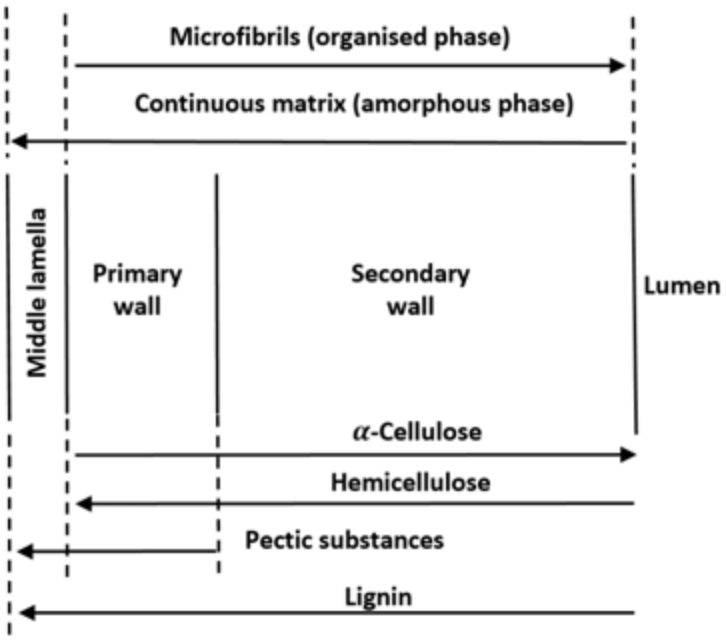

Figure 20: Variations in the concentrations of the major components of plant cell walls. Adapted from Buren (1979).

I.2.2.2 Freeze damage mechanisms

Freeze damage has been associated with ice formation, either directly (e.g., mechanical effects) or indirectly (e.g., changes in solute concentration in the unfrozen phase), (i) through migration of water from cell interior to cell exterior, producing cell shrinkage and membrane damage; (ii) through changes in gas solubility; and (iii) by phase transformation in non-aqueous membrane components (e.g., lipids) (Reid, 1997). The most common symptom of freeze damage is a water soaked appearance. Tissues damaged by freezing also lose their rigidity and become flaccid upon thawing (Ramsey, Wiant, & Link, 1938; Levitt, 1956; Wang, 2016). Fruits and vegetables suffer textural loss (loss of firmness) by two ways; the first one is caused by the loss of turgidity of cell due to puncturing of plasma membrane by the growing ice crystals. The second one is associated to the breakdown of cell wall structure, leading to the tissue breakage and a release of degradative enzymes. These enzymes can modify pectins and hemicelluloses during thawing and may contribute to the collapse of the cell walls, resulting in cell separation with the presence of larger intercellular spaces (Chassagne-Berces, Poirier, et al., 2009). In general, small cells with few or tiny intercellular spaces form a compact texture, while large cells often with large intercellular spaces form a coarse or spongy texture (Reeve, 1970). Moreover, the degradative

enzymes can also cause deleterious changes in colour, odour, flavour, and nutritive value (Skrede, 1996).

I.2.2.3 Factors governing freeze damage

The magnitude of freeze damage that fruits and vegetables would suffer during freezing preservation techniques depends on many factors, and it can be broadly divided into two categories. Those are related to either the product or the process or to both (Lasztity, Sebok, & Major, 1992; Skrede, 1996; Cano 1996; Silva, Goncalves, & Brandao, 2008; Wang, 2016).

Some of the influential factors of the product are listed as follows:

- raw materials type and variety
- maturity and quality of raw materials
- degree of ripening
- time spent between harvesting and processing
- resistance (inherent) to freeze damage.

The first four process parameters are very well discussed by Skrede (1996) and Cano (1996), only the last point will be discussed in this review. The susceptibility of fruits and vegetables to freezing injury depends on the inherent structural characteristics (Haard & Chism, 1996; Wang, 2016). Most vegetables, however, have fibrous structures that allow to maintain their structure when they are thawed after freezing (Silva et al., 2008).

Whereas, most fruits present softer structures, being physically much more susceptible to firmness loss (Silva et al., 2008). Based on the sensitivity toward freezing, the fruits and vegetables can be divided into three categories: highly susceptible (highly prone to the freeze damage), moderately susceptible (can recover from one or two short freezing periods), and the final one is the least susceptible (those that can be frozen several times for short periods without serious damage) (Table 1) (Wang, 2016).

Similarly, several process parameters in the overall processing steps govern the severity of freezing injury, such as: pre-treatments, freezing method, process time-temperature combination, frozen storage conditions, and thawing conditions. Minimal pretreatments such as peeling, trimming, dicing, chopping and slicing prior to freezing process eliminate the foreign materials, curtail microbial load, and minimize the product variation, at the meantime, they also ravage the protective barrier and exposes the inner constituents to oxygen (Fennema, 1988; Cano, 1996; Skrede, 1996; Silva et al., 2008). The resulting outcomes include enzymatic

browning, leaching of nutrients, moisture loss, which can promote undesirable changes in quality attributes such as nutrient composition, colour, and texture (Fennema, 1988; Cano, Marin, & Carmen Fuster, 1990; Silva et al., 2008). Pretreatments like blanching are commonly used for vegetables and for few fruits. Blanching is a common mild thermal pre-treatment, traditionally carried out by hot water or steam, prior to freezing aiming to inactivate deteriorative enzymes, decrease the microbial load and remove the air from the pores which subsequently can affect the nutritional characteristics of the fruits and vegetables upon storage (Xanthakis and Valdramidis, 2017). It has several advantages as well as number of disadvantages; the advantages include (1) stabilization of texture (changes caused by enzymes), colour, flavour and nutritional quality, and (2) diminishing foreign materials such as pesticides, and harmful pathogens. Whereas the disadvantages include (1) alteration of plant tissue system and subsequent texture change, (2) leaching of nutrients in the blanching medium, (3) weight changes, and (4) colour change (Fennema, 1988; Cano, 1996; Gregory III, 1996; Skrede, 1996; Silva et al., 2008; Xanthakis, Gogou, Taoukis, & Ahrné, 2018). During freezing time-temperature combination relates to the freezing rate. Freezing rate determines the population and the size of ice crystals in the product (Fennema, 1966; Delgado & Sun, 2001; Smith, 2011).

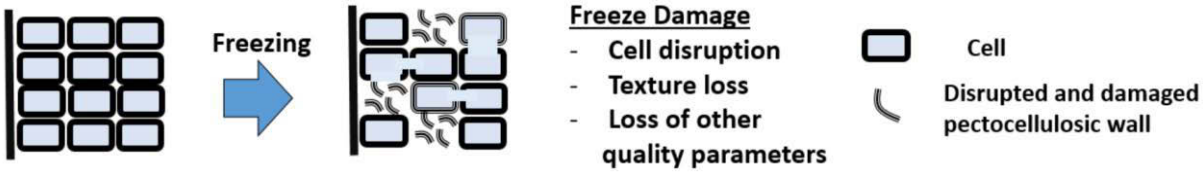

Figure 21: Schematic representation of the mechanical aspects of freeze damage in fruits and vegetables. Cell membrane and vacuole are usually disrupted during freezing resulting in tugor pressure loss and in loss of crispiness of fresh fruits and vegetables. The pectocellulosic wall remains the main skeleton that will be in charge of preserving the initial cellular structure. Damage of the pectocellulosic wall results in disruption of the cellular structure and higher level of loss in texture.

The size of the ice crystals is considered critical for the quality of frozen food products as it causes irreversible damages at cellular level; cell membrane is expected to break for any freezing process. Besides, distortion of cell structure, and pectocellulosic wall disruption is likely to occur resulting in major freeze degradation of the quality (texture, colour, nutritive value, etc.) of the product (Reid, 1997; Delgado & Sun, 2001; Smith, 2011). It is a well-known fact that slow freezing process produces a few larger ice crystals (mainly in intercellular domain) and increases the damage to the food products. Whereas, higher freezing rates produce numerous smaller ice crystals in both intercellular and intracellular domain, resulting in minimal quality loss (Fennema, 1966; Delgado & Sun, 2001; Orlowska, Havet, & Le-Bail,

2009; Singh & Heldman, 2009; Sadot, Curet, Rouaud, Le-bail, & Havet, 2017). However, when a product is too quickly frozen, the external layer of the food being frozen is exposed to compressive stress during water-to-ice-transition (until maximum freeze concentration temperature is reached). Then this ice has to support tensile stress due to contraction during further cooling. The layer being frozen moves into the direction of the centre of the product and has to support compressive stress. The difference between the compressive and tensile stresses results in cracks if the tensile stress passes the rupture stress of the frozen material (Shi, Datta, & Throop, 1998; Shi, Datta, & Mukherjee, 1998; Shi, Datta, & Mukherjee, 1999). Hence, lead to an inferior quality frozen product.

Table 1. Susceptibility of fresh fruits and vegetables to freezing injury. Inspired from Wang (2016).

Most susceptible	Moderately susceptible	Least susceptible
Apricots	Apples	Beets
Asparagus	Broccoli	Brussels sprouts
Avocados	Carrots	Cabbage, mature and savory
Bananas	Cauliflower	Dates
Beans, snap	Celery	Kale
Berries (except cranberries)	Cranberries	Kohlrabi
Cucumbers	Grapefruit	Parsnips
Eggplants	Grapes	Rutabagas
Lemons	Onion (dry)	Salsify
I.ettuce	Oranges	Turnips
Limes	Parsley	
Okra	Pears	
Peaches	Peas	
Peppers, sweet	Radishes	
Plums	Spinach	
Potatoes	Squash, winter	
Squash, summer		
Sweet potatoes		
Tomatoes		

Frozen storage factors, such as: storage temperatures, temperature fluctuations and storage duration, also referred to as TTT (time-temperature-tolerance) influence the quality of the frozen fruits and vegetables. Lower frozen storage temperature increases the practical storage life of the product. For example, the storage life of peas and cauliflower at − 24 ℃ increases up to 30 months and 18 months compared to 24 and 12 months at − 18 ℃ respectively (Cano, 1996). Fluctuation in the storage temperature leads to the recrystallization of ice, and this

phenomenon favors the further growing of the ice crystals which thereby will increase damages to the tissues (Reid, 1997). The best way to slow down the recrystallization process would be to store the sample at a temperature below its glass transition temperature (T'g). At this temperature, the pure water of food freezes and leaves behind a very viscous concentration of solutes that trap the remaining water. As an outcome, water has a limited movement and the deterioration that can result from water migration during storage can be minimized. However, achieving this in practice is challenging as the glass transition temperature of the product can be very low (as low as ≈ − 58 ℃ for apple and onion, and ≈ − 50 ℃ for grape and strawberry (Sa & Sereno, 1994; Bai, Sha, Perera, Smith, & Melton, 2001), making storage of majority of the fruits and vegetables at temperature below their T'g economically infeasible in the present scenario.

I.2.3 Freeze damage assessment methods

The qualitative and quantitative methods and technologies that are able to evaluate with accuracy the freeze damage are of great importance. The assessment of freeze damage in fruits and vegetables can be achieved by direct or indirect methods (Khan & Vincent, 1996; Mousavi, Miri, Cox, & Fryer, 2005, 2007; Chassagne-Berces, Poirier, et al., 2009; Parniakov, Lebovka, Bals, & Vorobiev, 2015). Direct methods constitute of cryo-confocal laser scanning microscopy (C-CLSM) (Evans et al., 1996; Vidot et al., 2018), cryo-scanning electron microscopy (C-SEM) (Bomben & King, 1982; Chassagne-berces, Fonseca, Citeau, & Marin, 2010), cold stage brightfield light microscopy (Donhowe, Hartel, & Bradley, 1991), X-rays microtomography in frozen state (Vicent, Verboven, Ndoye, Alvarez, & Nicolaï, 2017), and cold stage fluorescence microscopy (Kono, Tobari, Araki & Sagara, 2017). Whereas, indirect methods include: SEM (scanning electronic microscopy), TEM (transmission electron microscopy) and X-ray tomography of freeze substituted and/or freeze fixed and/or freeze-dried sample (Mousavi et al., 2007); confocal laser scanning (CLSM) imaging, macrovision imaging (Chassagne-Berces et al., 2009) and hyperspectral imaging (Gowen, Taghizadeh, & O'Donnell, 2009) of frozen-thawed samples; texture analysis (Sirijariyawat & Charoenrein, 2012); drip loss; impedance measurement (Zhang & Willison, 1992a,b; Angersbach, Heinz, & Knorr, 1999); solute diffusivity measurement (Parniakov et al., 2015); nuclear magnetic resonance (NMR) spectroscopy and magnetic resonance imaging (MRI) (Hills & Remigereau, 1997)**;** and analysis of chemical and biochemical changes (Murray, Shipton, Whitfield, Kennett, & Stanley, 1968; Murray, Shipton, Whitfield, & Last, 1976; Cano, Fuster, & Marín, 1993; Fúster, Préstamo, & Cano, 1994; Cano, 1996; Skrede, 1996; Oruna-Concha, Gonzalez-Castro, Lopez-Hernandez, &

Simal-Lozano, 1997; Lim, McFetridge, & Liesebach, 2006; de Ancos, Sánchez-Moreno, Pascual-Teresa, & Cano, 2012). This review provides a comprehensive study about both the direct and indirect methods that are being used to evaluate the freeze damage.

I.2.3.1 Microstructure investigations

Microstructure examination of frozen fruits and vegetables has been carried out for a number of reasons that include monitoring the morphology of ice crystals formed during freezing process, estimation of the damage that the cells suffered during freezing/storage/thawing process, observation of re-distribution of solutes, and determination of the heterogeneity degree of the foodstuff as well as to acquire important correlations between microstructure and mouth texture (Wilson, 1991; Kiani & Sun, 2011). Understanding of the structure-function relationship becomes crucial for controlling and improving the quality of frozen foods (Mallikarjunan & Hung, 1997).

The microstructure studies can be conducted by several methods, some of them are:, light microscopy (includes polarised microscopy (Khan & Vincent, 1996), cold-stage light microscopy (Donhowe et al., 1991) and confocal laser scanning microscopy (CLSM) (Chassagne-Berces, Poirier, et al., 2009), electron microscopy (2 types: transmission electron microscopy-TEM, and scanning electron microscopy-SEM) (Bomben & King, 1982; Rimkeeree & Charoenrein, 2014 and many others), X-rays tomography (Mousavi et al., 2005, 2007), MRI (Magnetic Resonance Imaging) (Duce, Carpenter, & Hall, 1992; Gamble, 1994) and macrovision imaging (Chassagne-Berces, Poirier, et al., 2009). The aforementioned methods provide both qualitative and quantitative information about the ice crystal size, shape and distribution.

I.2.3.1.1 Light microscopy

Light microscopy is a widely and commonly used method for microstructure evaluation. The observation and visualization of the structure of frozen foods with light microscopy can be executed at ambient temperatures after controlled dehydration or thawing of the sample or even at low temperatures when the sample is frozen (Kiani & Sun, 2011). The dehydrated sample for the first method can be obtained either by freeze substitution method or by freeze drying method (Martino & Zaritzky, 1986). The freeze substitution method is mainly used in case of fruits and vegetables and is performed in two steps: one is fixation step and another is substitution step. During fixation step, fixative such as carnoy's, glutaraldehyde, etc. engenders a new

crosslinking between and within the molecules of the tissue constituents, and thus, produces a fixed and stable structure. In the case of fruits and vegetables, fixation can be performed at temperature above 0 ℃ for frozen/thawed product using fixatives like glutaraldehyde in phosphate buffers (primary fixation) and osmium tetroxide (secondary fixation) or can also be performed at – 20 ℃ for frozen sample by using fixatives like carnoy's (Fuchigami, Miyazaki, Kato, & Teramoto, 1997; Otero, Martino, Zaritzky, Solas, & Sanz, 2000). Whereas in the substitution step, the ice/water present in the specimen is replaced by a polar solvent. Organic solvents capable of replacing ice/water, such as ethanol/methanol/acetone can be used for substitution process (Feder, 1958; Wilson, 1991; Giddings et al., 2001; Phothiset & Charoenrein, 2014). Freeze substitution technique has been employed to evaluate the damage imparted by ice crystals in different products including carrot frozen by high pressure freezing and different conventional freezing methods (Rahman, Henning, & Westcott, 1971; Fuchigami et al., 1997), peach and mango (Otero et al., 2000; Rimkeeree & Charoenrein, 2014), dates (Shomer, Borochov-neori, Luzki, & Merin, 1998), apple (Ramírez, Troncoso, Muñoz, & Aguilera, 2011), and papaya frozen/thawed for several times (Phothiset & Charoenrein, 2014). Light microscopy of the frozen food tissue after thawing has also been performed for studying the ice crystal characteristics and the damages of the tissue (Khan & Vincent, 1996; Sterling, 1968). The aforementioned method brings some errors due to changes occurring during thawing, nonetheless, it can provide useful information (Figure 22). Alternatively, microstructure of the fruits and vegetables can also be observed and evaluated in the frozen state using a cold stage light microscope (cryo-microscope). This technique minimizes the artefacts that can occur to the product structure during sample preparation step of normal light microscopy. Moreover, it also allows dynamic observation of cells during freezing and thawing (McLellan, Morris, Grout, & Hughes, 1991; Wilson, 1991), and thus can be used to estimate the freeze damage in real time. There are a few limitations associated to the aforementioned light microscopy techniques, these include:

- Sample should be very thin: not suitable for imagining of thick cryo-sections as out-of focus structures above and below the focal plane will cause flare and will considerably reduce the amplitude contrast (Wilson, 1991).
- Lengthy sample preparations (Evans, Adler, Mitchell, Blanshard, & Rodger, 1996)
- The process of obtaining 3-D structure of product using this method is quite tedious as it involves microscopic analyses of thin, serial sections followed by stereological analysis or

three-dimensional (3-D) reconstruction of physical slices (Gray, Kolesik, Høj, & Coombe, 1999).

- The use of confocal laser scanning microscopy (CLSM) can overcome these limitations as it can examine the opaque solid sample, and therefore there is no need for very thin slices to be cut which would destroy the microstructure (Evans et al., 1996). It allows optical sectioning of the specimen, and thus, facilitates non-destructive 3-D analysis of food structure (Wilson, 1991; Kalab, Allan-Wojtas, & Miller, 1995; Gray et al., 1999). It requires the sample to fluoresce, either by being autofluorescent or by having absorbed sufficient fluorophore (Evans et al., 1996).

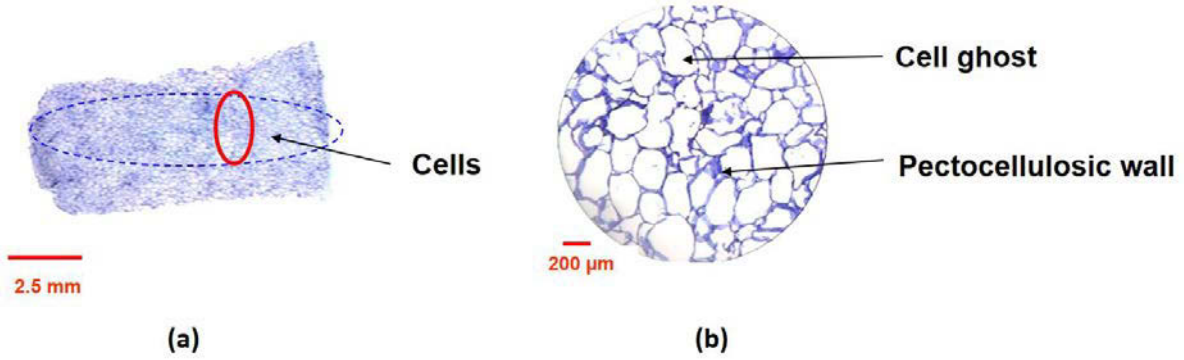

Figure 22: Melon sample that was cut in a cryomicrotom prior to thawing. The cells can be depicted with light blue colour under light microscopy (Le-Bail et al., 2017). Dirsuption of pectocellulosic wall can be observed on the image on the right.

I.2.3.1.1.1 Confocal laser scanning microscopy (CLSM)

CLSM comprises of laser light illumination, fluorescence microscopy and computer imaging (Gray et al., 1999). In CLSM, the sample is illuminated and imaged one point at a time through the pinhole (Guillemin, Devaux, & Guillon, 2004; Kalab et al., 1995). The pinhole is placed at a focal plane of the image to remove out-of-focus light and generate a clearer image. Moreover, it allows optical sectioning of specimen, thus facilitating generation of 3-D data set (Gray et al., 1999; Wilson, 1991). Applications of CLSM to the study of plant microstructure includes 3-D reconstruction of guard cells in Commelina leaves (White, Errington, Fricker, & Wood, 1996), quantitative measurement of cell wall profile (volume, area, perimeter and thickness) in maize (Travis, Murison, Perry, & Chesson, 1997), in vivo observation of sieve elements in fava bean leaves (Knoblauch and van Bel, 1998), and visualization of 3-D shape and size of parenchyma cells of developing grape fruits (Gray et al., 1999).

With respect to freeze damage assessment, CLSM was used by Charoenrein & Owcharoen (2016) to study the effect of freezing protocols (i.e. freezing at – 80, – 40 and – 20 °C) and

freeze-thaw cycles on the cellular structure of mangoes. Using this method, they were able to observe the freezing-thawing related degradation of cellular structure. Moreover, based on CLSM images, they were able to discriminate the different freezing protocols.

The main advantages of using CLSM techniques are: (i) sample preparation requires minimal cutting of organ and therefore reduces chance of cell distortion (Kalab et al., 1995; Evans et al., 1996; Chassagne-Berces, Poirier, et al., 2009) (ii) obtaining the 3-D structure of the product is far easier by using CLSM than the aforementioned light microscopy methods (Gray et al., 1999); it also permits dynamic observation and recording of freezing-thawing process if equipped with heat transfer stage (cooling/heating stage on which sample rests); and lastly, ice crystals size and shape can also be determined if the sample is well stained with fluorescein (Evans et al., 1996). This technique has a potential in future to be used as tool to access freeze damage in fruits and vegetables with a minimal destruction to the product's original structure.

Some limitations of this technology can be identified, the major one is that the sample must be able to fluoresce. Auto fluorescent samples and samples that have fluorescent labeling have advantages over samples which have simply soaked up a fluorophore since the material of interest can be directly observed (Evans et al., 1996). Another weakness is that the black pixels per optical slices increase linearly with depth. This phenomenon causes an increase in the wall-enclosed area which in-turn increases the unit volume of cell and may lead to overestimation of individual cell size. In order to minimize this error, the attenuation of the fluorescent signal should be corrected by increasing sequentially the thresholding intensity (Gray et al., 1999).

In order to obtain higher resolution image electron microscopy is generally preferred over light microscopy.

I.2.3.1.2 Electron microscopy

Electron microscopy has been widely used to study the microstructure of frozen fruits and vegetables. The image formation in the electron microscopy (EM) is similar to in light microscopy, but the illumination source is electrons focused with magnetic lenses rather than photons focused with glass lenses (Kalab et al., 1995). Since electrons get absorbed by air, the EM is carried out in vacuum condition. Moreover, the sample used should not liberate any volatile compounds when placed in microscope: this requirement is generally fulfilled by either drying or freezing the product, or covering it with platinum and carbon. Different types of EM techniques, such as transmission electron microscopy (TEM), conventional scanning electron microscopy (SEM), cryo-SEM, and environmental SEM (ESEM) have been employed to

evaluate the freeze damage in food products (Bomben & King, 1982; Kalab et al., 1995; Chassagne-Berces, Fonseca, et al., 2010; Kiani & Sun, 2011; Phothiset & Charoenrein, 2014).

TEM can be used to visualize the internal structure of the food products. It can be an effective method for routine examination of frozen products. The samples can be either in freeze-substituted condition (chemically fixed) or freeze-dried prior to the TEM analysis (Wilson, 1991). Thin (15-90 nm) slice of a dehydrated sample embebbed in epoxy resin or platinum carbon-replica of the sample is placed in the path of the electron beam, and the image is obtained on the fluorescent screen. The image of the sample is generated based on the varying degree of energy loss that the electron beam suffers when it passes through the sample specimen. The degree of energy loss from electron depends on the electron density of the structure stained in the resin section with heavy-metal salts (e.g. of uranium or lead) or on varying thickness of metal replica created due to difference in angles at which the metal is deposited on the fractured sample (Kalab et al., 1995).

TEM has been successfully used to evaluate the freeze damage in mango (Rimkeeree & Charoenrein, 2014), papaya (Phothiset & Charoenrein, 2014), dates (Shomer et al., 1998), carrot (Fuchigami, Hyakumoto, Miyazaki, Nomura, & Sasaki, 1994) and blueberry (Fava, Alzamora, & Castro, 1996). Shomer et al. (1998) observed ultrastructural injuries in both the exocarp and the mesocarp cells of thawed Madjhoul dates as viewed by transmission electron microscopy (TEM). The damaged cell walls appeared torn or crushed resulting in the formation of intracell-wall spaces. Rimkeeree & Charoenrein (2014) and Phothiset & Charoenrein (2014) in their TEM analysis found that the freezing and thawing caused a loss of cell wall materials in the middle lamella, and thus, reduced the adhesion among the cells. As an outcome, cell separation happened and led to the development of larger intercellular spaces. TEM results from Fava et al. (1996) showed that the freezing-thawing process causes folding of the cell wall of the epicarp.

Even though this technique produces better quality images, there are some drawbacks related to TEM such as the sampling process which is time consuming and may also produce some artefacts in the final image of specimen. Moreover, replications by this technique are difficult, while the evaluated area viewed is only a very small fraction of the entire sample (Bomben & King, 1982).

SEM is used to examine surfaces (Kalab et al., 1995). It provides an opportunity to study the structure of the food product at a wide range of magnifications, and can achieve a depth of field

roughly 500 times than that of the light microscopy (Aguilera & Stanley, 1999; Kiani & Sun, 2011). It produces better image quality due to lower diffraction effect; when doing light microscopy to produce magnified image of objects, diffraction (bending of light around the corners of an obstacle or aperture) may limit the resolution and hence the image quality in terms of fine details (Mehta, 2012). The lights used in light microscopy have a wavelength in the range of 380-740 nm, while electron beam used in SEM have much shorter wavelengths. The wavelength of the electron beam depends on the accelerating voltage being used and can be calculated using Eq. (3) (Anon 2018a). Using the following equation, the accelerating voltage of 10 and 20 kV would generate electron beam having wavelength of 0.01225 and 0.0086 nm respectively. The dependence of diffraction on the wavelength of the beam (Eq. (4)) makes electron beam more suitable than beams of wavelengths in the optical region. Eq. (4) reveals that if the wavelength is higher, the diffraction effects are greater which in turn lead to a lower image quality in terms of fine details. Moreover, the SEM fills and overlaps the magnification gaps between the light microscope and TEM (Aguilera & Stanley, 1999).

$$\lambda = \frac{12.25 \times 10^{-10}}{\sqrt{V}} \tag{3}$$

where λ is the wavelength of a particle and V is the operating accelerating voltage.

$$\sin\theta = \lambda/d \tag{4}$$

where d is aperture width, θ is diffraction angle and λ is wavelength.

In general, SEM consists of an electron gun able to produce the electron beams, electromagnetic optics to guide and focus the beam on the sample, and the detector to collect the backscattered or secondary electrons. The energy of the detected electron, their intensity (number density) and location of emission are combined to create an image (Mehta, 2012). The sample is either dry (conventional SEM) or frozen below -80 ℃ (cryo-SEM) or wet (ESEM). While performing conventional SEM and cryo-SEM, the sample's surface is in general coated with 5-20 nm-thick metal (gold) layer to provide electron conductivity and the operating conditions are maintained under vacuum to avoid absorption of electrons by air. Whereas, in ESEM, the sample does not require vacuum environment and any coating, but the sample chamber need to kept under a low gas pressure (Bache & Donald, 1998). The choice of the gas depends on the kind of food: hydrated food is kept under water vapour (Falcone et al., 2006). Nowadays, SEM can also be used to perform energy dispersive X-ray microanalysis (using X-ray detectors

attached to SEM) to detect the chemical elements likely to be of interest in the frozen food specimen (Wilson, 1991; Kalab et al., 1995; Mehta, 2012)

Xu et al., (2014) used conventional SEM to observe the microstructure of carrot frozen by three different freezing methods. The three freezing protocols used by them were (i) liquid nitrogen immersion (LNI) freezing, (ii) high pressure carbonic immersion (HPCI) freezing, and (iii) freezing in a refrigerator at − 80 °C. The samples were freeze-dried prior to SEM imaging. The SEM images showed that the size of ice crystals of freeze-dried carrot slices was greatly dependent on the freezing rate. For instance, freezing in HPCI system and freezing by immersion in liquid nitrogen (LN) yielded a homogeneous porous structure which contained numerous fine crystals inside the cells, meanwhile, samples structural integrity was protected under these conditions. However, portions of carrot slices in LNI freezing were visualized to have lost their structure integrity. Micrograph of carrot frozen at − 80 °C showed maximum damage of tissue structure; collapse of carrot tissue structure was found to be more important in sample frozen at −80 °C than in the other freezing conditions. Conventional SEM has also been used to study the microstructure of other frozen fruits and vegetables, such as strawberries (Delgado & Rubiolo, 2005), potato (Mousavi et al., 2007), peach (Otero et al., 2000), lotus root (Tu, Zhang, Xu, & Liu, 2015), mango (Otero et al., 2000), raspberry (Sousa, Canet, Alvarez, & Tortosa, 2006), broccoli (Xin et al., 2014), and blackberry (Sousa et al., 2006).

Ammar et al. (2010) and Jalté et al. (2009) used ESEM to observe the structural change that occurs during freezing-thawing of potato. By applying this method, the structural disorder, deformation and damage of the polyhedral shaped cells were observed in frozen-thawed samples.

The cryo-SEM method has been very much beneficial in accessing the ice crystal size distribution in fruits and vegetables (Bomben & King, 1982; Chassagne-Berces, Poirier, et al., 2009; Chassagne-Berces, Fonseca, et al., 2010; Sun & Li, 2003) (Figure 23). Compared to the other two SEM techniques, cryo-SEM method causes least alteration to the structure of the product as it provides rapid physical fixation (Kiani & Sun, 2011), thus allowing to obtain much precise information about the structural changes and the formed ice structure during freezing processes. The typical sample preparations methods (freeze fixation and thawing) used for the other two types of SEM can sometimes cause artefacts such as structural collapse, shrinkage, etc. in the samples leading to the loss of detailed ice structure. For instance, freeze fixation method such as freeze substitution sometimes cause the loss of the solidified solutes structure

due to the dissolution of cell solutes along with the ice in the solvent, ultimately leading to the modification of ice crystal morphology (Bomben & King, 1982). Similarly, freeze drying process can lead to the collapse of some solutes (especially soluble carbohydrate) present in plant materials, thus modifying the original ice morphology (Bellows & King, 1973; Bomben & King, 1982). The thawing process causes some structural changes, and hence may tarnish the real effect of freezing processes on the cell structure.

Although the electron microscopy is one of the best methods to evaluate the freezing process, limitations such as high cost and difficult sample preparation makes its usage limited, thus providing opportunity for the development of some alternative methods.

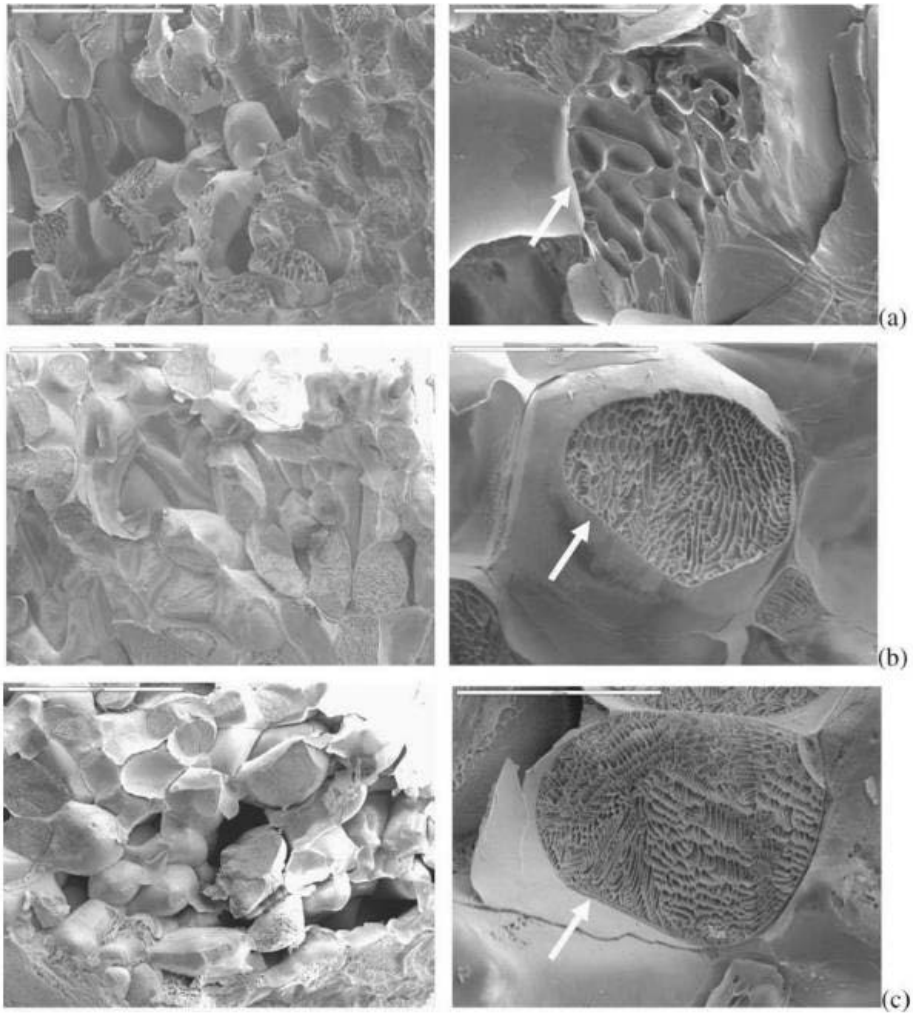

Figure 23: Cryo-Scanning Electron Microscopy images of apple tissue frozen in three different protocols. (a) Freezing at − 20 ℃; (b) Freezing at − 80 ℃; (c) Freezing by immersion in liquid nitrogen. Cell membranes are arrowed. Left-scale bar = 500 μm and right-scale bar = 100 μm (Chassagne-Berces, Poirier, et al., 2009).

I.2.3.1.3 X-rays tomography

The above-mentioned microscopy methods (both light (except CLSM) and electronic) are widely used to gather 2-D information of the product. In most of these cases, obtaining 3-D information of the product is very complicated but offers more representative imaging of the entire sample. 3-D visualization can be achieved by first obtaining the 2-D information of cross-sections acquired by serially slicing of the sample (very thin slices $\approx 1\ \mu$m) and then using image reconstruction techniques or directly from 2-D information by appropriate software. But, according to Mousavi et al. (2007), the 3-D information acquired with respect to the frozen product using these techniques is not reliable as the sample preparation technique can alter the inherent ice structure and the distance between the slices ($\geq 1\ \mu$m) would be too coarse to avoid loss of 3-D information (Gray et al., 1999; Mousavi et al., 2005).

X-ray micro-computed tomography (XMT) is a non-invasive technique which permits visualisation and evaluation of complete 3-D structure of the product with a minimal sample preparation (Farber, Tardos, & Michaels, 2003; Lim & Barigou, 2004; Mousavi et al., 2005, 2007; Moussawi, Xu, Nouri, & Lubineau, 2014; Ullah, Takhar, & Sablani, 2014; Tan, Chin, Yusof, & Abdullah, 2016; Vicent, Verboven, Ndoye, Alvarez, & Nicolaï, 2017). It is a combination of X-ray microscopy and tomographical algorithms. The principle lying behind it is based on contrast of the X-ray images which is generated by differences in X-ray attenuation arising principally from differences in density within the specimen. The resulting image is a superimposed information (projection) of a volume in a 2-D plane. In order to obtain 3-D information, a large number of radiographs are acquired while rotating the specimen between 0 and 180°. 3-D images are then reconstructed from these radiographs using a filtered back-projection algorithm (Feldkamp, Davis, & Kress, 1984).

In the recent times, this technique has been successfully used to compare the effect of the different freezing parameters on ice crystal size distribution and the microstructure of fruits and vegetables (e.g. apple, potato and carrot) (Mousavi et al., 2007; Voda et al., 2012; Ullah et al., 2014; Vicent et al., 2017; Zhao & Takhar, 2017). This method can observe and visualize the structure of frozen products both at ambient temperature after freeze drying (Mousavi et al., 2007; Ullah et al., 2014; Zhao & Takhar, 2017) but also at low temperature when the sample is still in a frozen state (Vicent et al., 2017). Mousavi et al. (2007) found a good correlation between the freezing rate and the average ice crystal size using XMT. Similarly, Ullah et al. (2014) and Zhao & Takhar (2017) in the case of potato sample were able to find a good

interconnection between the ice crystal growth and different frozen storage conditions (storage time, temperature and temperature fluctuation level) (Ullah et al., 2014; Zhao & Takhar, 2017) (Figure 24). At this point, it worth to be mentioned that these researchers investigated the ice crystal distributions in freeze-dried products. Freeze drying removes moisture from the material by sublimation and creates a network of solid fibers and pores. The pore present in the dried product corresponds to the ghost of ice microcrystal that sublimes during the freeze drying process. Nevertheless, the freeze drying process may possibly alter the structure of interest through shrinkage (Voda et al., 2012). The level of shrinkage can be related to the properties of the sample such as solid content, glass transition temperature, freezable water and others, but also with the freeze drying cycle operation conditions such as temperature and pressure. Most recently, Vicent et al. (2017) developed and validated a methodology to determine the size of ice crystals in the apple fruit held in a frozen state using XMT. They established an image analysis protocol to segment ice crystals in the frozen product by using the X-ray attenuation coefficients of the material components. For instance, segmentation of ice crystals in frozen apple sample was done using X-ray attenuation coefficients of reference model samples such as frozen pure water and concentrated apple juice. This technique clearly identified the decrease in the size of ice crystal with the increase of the freezing rate. Thus, this method allows visualization, quantification and understanding of the 3-D microstructure of frozen fruits and vegetables in direct and non-destructive means in a realist sample environment without modifying their structures and generating artefacts.

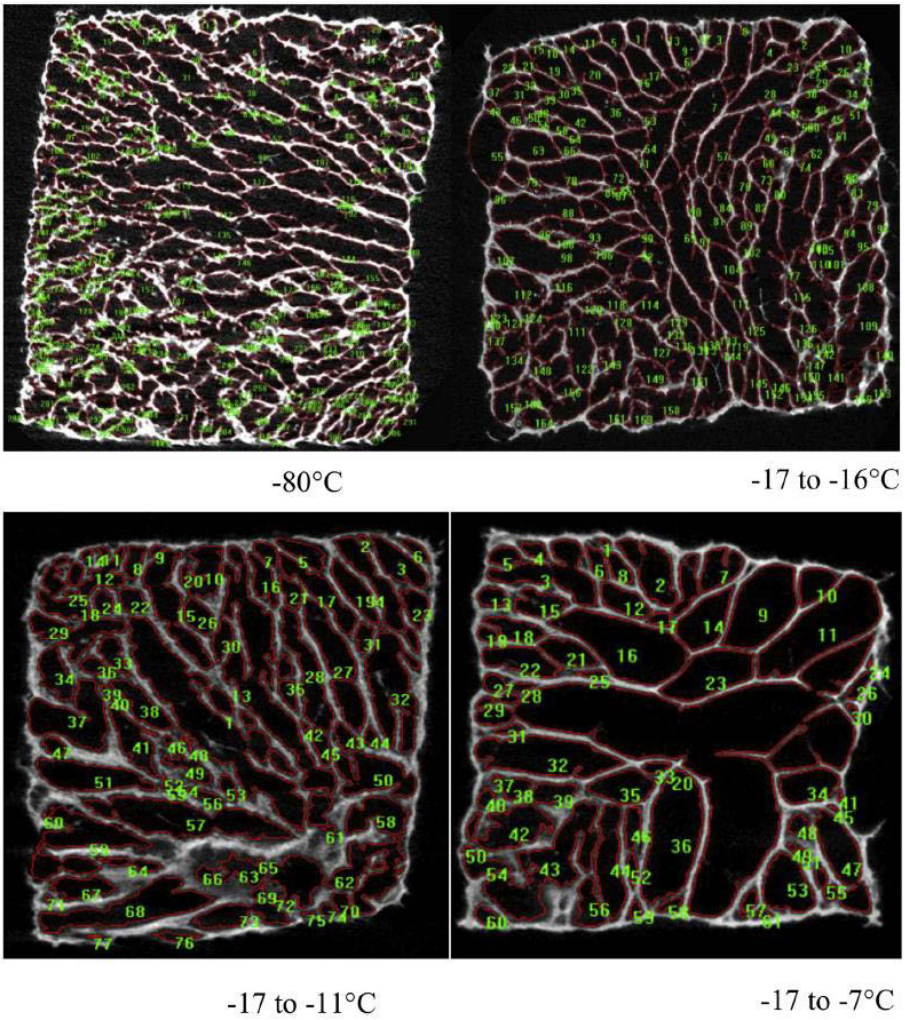

Figure 24: XMT scan micrographs of freeze-dried potatoes showing the pores sizes as a function of fluctuation in freezing temperature. Larger size ice crystals and higher level of destruction were observed for the storage condition having higher amplitude of temperature fluctuation (Ullah et al., 2014).

This method of image analysis contains a number of advantages compared to other techniques, they are:

- XMT process requires little or no sample preparation and thereby it preserves the information in the original form.
- The sample analysis can be performed at normal atmospheric conditions (temperature and pressure) and therefore making the technique simple in operation compared to electronic microscopy that requires certain environment for the sample analysis (e.g. SEM requires vacuum conditions during the imaging process, while cryo-SEM requires low temperature and vacuum condition to perform the imaging process).
- It provides information about the internal 3-D structure of the product. In contrary, most of the other imaging techniques being used observe the surface morphology of the object or a

transmission image through a thin section, which means that the internal 3-D structure can only be investigated invasively.

XMT for use within the food discipline is subject to a number of limitations, some of them are (Wang et al., 2018):

- The cost of high-resolution benchtop systems is easily in the six to seven figures.
- The data sets are typically on the order of gigabytes per sample, and studies can easily exceed the terabyte mark, thus large amount storage space is required.
- The data acquisition using XMT is time consuming (scan times are typically a few minutes to an hour per sample depending up on the resolution of scan).

I.2.3.1.4 Magnetic Resonance Imaging (MRI) / NMR imaging

MRI is another non-invasive technique that allows observation of internal structure of food product in two or three dimensions without destroying the product. MRI scanner is an NMR (nuclear magnetic resonance) instrument equipped with magnetic gradient coils that can spatially gather the data related to MRI parameters (such as proton density, relaxation times (T_1 and T_2), and self-diffusion coefficient) of molecules, and thus, create two-dimensional and/or three-dimensional images that display areas having different physico-chemical properties (e.g. water content) with different contrasts (Clark, Hockings, Joyce, & Mazucco, 1997; Thybo, Karlsson, Bertram, & Andersen, 2004; d'Avila et al., 2005; Defraeye et al., 2013; Kirtil & Oztop, 2016).

MRI technique has been employed for the detection of freeze damage in blueberries, courgette, kiwifruit, orange, mandarin and cucumber (Duce, Carpenter, & Hall, 1992; Gamble, 1994; Kerr, Clark, Mccarthy, & Ropp, 1997; Hernández-Sánchez, Barreiro, Ruiz-Altisent, Ruiz-Cabello, & Fernández-Valle, 2004; Kim, Milczarek, & Mccarthy, 2008; Kotwaliwale, Curtis, Othman, & Naganathan, 2012). Duce et al. (1992) implied MRI technique to investigate the internal structure of fresh and frozen-thawed courgette. By using MRI technique, they obtained an image of fresh courgette in which the skin, vascular tissue, cortex, seed-bed and seeds were clearly delineated, whereas, the image of frozen/thawed courgette showed very little contrast between the different tissues. Moreover, the overall intensity of the image of the thawed courgette was greater than that of the fresh courgette, similar results were obtained in the case of frozen/thawed blueberry by Gamble (1994). Rupture of cells by freezing leading to release of the cellular contents on thawing which affects the transverse relaxation of water in the tissue,

and this, in turn, changes the image contrast and intensity. It was also found that the intensity increase was higher at particular location upon freezing-thawing. In the case of blueberry, the greatest intensity increase occurred in placental tissue and locules, where seeds are located , while for pickling cucumber the subsurface rind area had the highest intensity increase (Gamble, 1994; Kotwaliwale et al., 2012).

In addition to these aforementioned methods, some other imaging techniques have also been used to evaluate the freeze damage in fruits and vegetables. Chassagne-Berces, Poirier, et al. (2009) by using macrovision imaging technique were able to estimate the severity of freeze-damage (at the cellular level) suffered by apple tissues when subjected to different freezing rates. Hyperspectral imaging has also shown to be an effective and good method in early detecting the freeze damage in white button mushrooms (Gowen et al., 2009).

I.2.3.2 Low-Field nuclear magnetic resonance relaxometry (NMR)

NMR relaxometry is a non-invasive, hence non-destructive technique, which allows the assessment of intact sample's freeze damage (e.g. fruits and vegetables). By using this technique, the changes occurring to the compartment and the mobility of water in the food product when subjected to various processing conditions can be monitored (e.g. freezing). In that way, the extent of damage that the cellular tissue suffers can be estimated (Hills & Remigereau, 1997; Hills & Nott, 1999). An example of T_2 (spin-spin or transverse) relaxation time peak obtained while performing NMR of fresh carrot is illustrated in Figure 25a. Hills & Remigereau (1997) used T_2 time of water proton to monitor the changes in sub-cellular water compartmentation in the parenchyma tissue of apple during freezing and subsequent thawing. They reported that the vacuolar compartment is the first area which gets frozen at 270 K, but because of their higher biopolymer content, the cytoplasm and cell wall compartments require temperatures below 263 K before they freeze. NMR studies on the thawed products showed that relaxation time of the frozen-thawed vacuole at room temperature was only 250 ms compared to the value of 650 ms of fresh apple vacuole (Figure 25b). This T_2 time shift of the vacuolar component (main peak in T_2 relaxation curve) is indicative of a change in molecular environment attributed to a loss in cell compartmentalization. The relaxation peaks for the cell wall and cytoplasm compartments were not so clearly resolved for the freeze-thawed sample at room temperature. Most recently, it has been reported that along with reducing the T_2 time of vacuole water, freezing-thawing also shortened the T_2 time of cell wall water, cytoplasm and extracellular water compared to the fresh sample in the case of blueberry fruit (Cao, Zhang,

Zhao, Zhu, & Li, 2018). The self-diffusion coefficient of water determined using NMR was found to increase upon freezing-thawing compared with the fresh sample depicting the loss of membrane integrity (Arunyanart, Siripatrawan, Makino, & Oshita, 2015; Kerr et al., 1997).

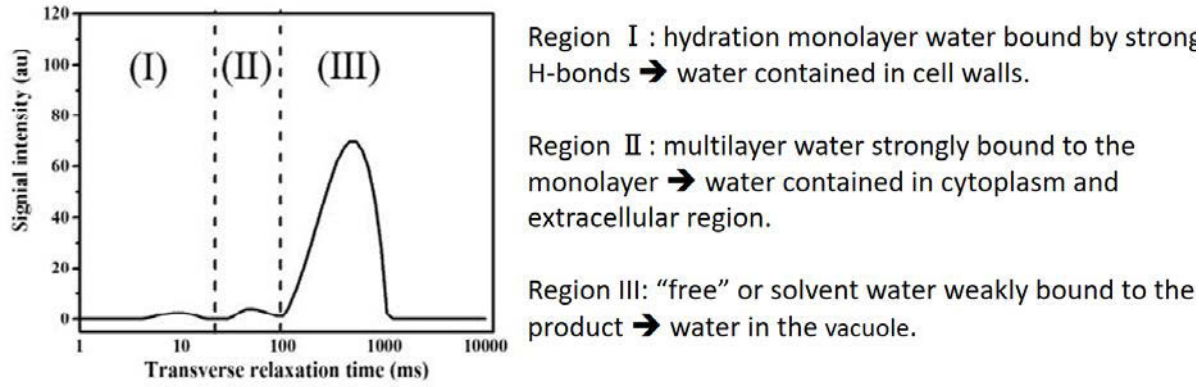

(a)

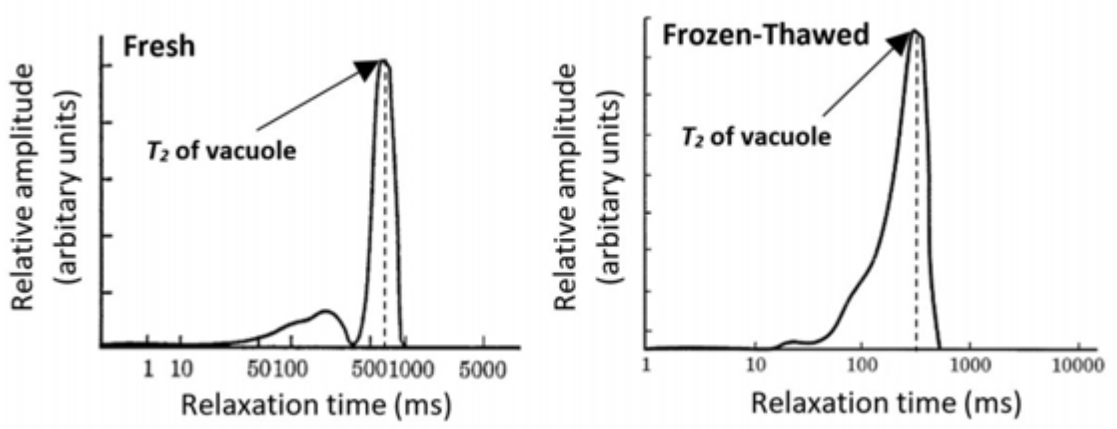

(b)

Figure 25: (a) T_2 times as function of water location in carrot sample (Based on Wang, Xu, Wei, & Zeng, 2018), (b) T_2 curves of fresh and frozen-thawed apples (Hills & Remigereau (1997)).

NMR can also be used to determine the amount of non-freezable water in a food matrix after a steady-state has been reached. In this context, the non-freezable water content can be determined from the residual NMR signal obtained from the frozen sample, compared with the fresh one (measured at a positive temperature) and then normalized to the total weight of the sample. The estimation of non-freezable water becomes important as partial crystallisation of water can result in quality changes, ice recrystallisation or further chemical reactions caused by increasing solute concentration in unfrozen matrices or by changing reaction conditions such as pH or ionic strength (Sadot et al., 2017).

There are also some limitations and disadvantages associated with NMR and MRI techniques:

- High cost (investment and operating costs) (Kiani & Sun, 2011).

- Low sensitivity (Hills & Remigereau, 1997; Kiani & Sun, 2011).
- MRI requires small sample size (typically a millimeter or less) to achieve very high spatial resolutions, thus imaging of subcellular changes during the processing of large pieces of cellular tissue are still beyond the current capability of the technique (Hills & Nott, 1999).

I.2.3.3 Textural analysis

Texture is a collective term that encompasses the structural and mechanical properties of a food and their sensory perception in the hand or in the mouth (Abbott, 2004). The most comprehensive and useful definition of texture was proposed by Bourne (1982) as: "Texture properties of the food are the group of physical characteristics that result from the structural elements of the food. They are sensed by the sensation of touch in the hand or in the mouth and they are related to the deformation, disintegration, and flow of food under force. Texture properties are measured by the function of force, distance, and time using a texture analyzer". Texture is not only one of the most important quality characteristics but also a critical parameter that determines acceptability by the consumer (Abbott, 2004; Van Buggenhout, Lille, et al., 2006; Waldron, 2004). There are several terms used to describe the sensory texture of various fruits and vegetables, some of them are hardness, firmness, softness, grittiness, crunchy, mealy, juicy and many others (Abbott, 2004). However, there are not accepted complementary methods for instrumental measurements of each sensory attributes (Abbott, 2004).

In the case of fruits and vegetables, the structural, physiological and biochemical characteristics of the cell determine its texture. For instance, the texture of fruits and vegetables is mainly influenced by (i) turgidity of cell (ii) cell wall and middle lamella polysaccharide composition, structure and strength (iii) cell arrangement and density and (iv) cell to cell bonding (Brown, 1977; Buren, 1979; Reid, Carr, Sajjaanantakul, & Labavitch, 1986; Van Buggenhout, Messagie, et al., 2006).

The freezing process affects the texture of fresh fruits and vegetables largely. Freeze-damaged fruits and vegetables often lose their rigidity, have a water-soaked appearance on thawing and become mushy (Ramsey et al., 1938; Ramsey & Smith, 1961; Brown, 1977; Wang, 2016). The textural change happens majorly due to (i) the loss of turgor pressure as an outcome of the breakdown and loss of cell membrane's semi-permeability (plasma membrane and vacuolar membrane) during freezing-thawing (Brown, 1977; Brown, 1979; Grout, Morris, & McLella, 1991; Abbott, 2004; Sousa et al., 2006; Chassagne-Berces, Poirier, et al., 2009), and (ii) the loss of the structural integrity of the cell components (cell wall and middle lamella) leading to

the collapse of the cell walls, ultimately resulting in cell separation (Brown, 1979; Chassagne-Berces, Poirier, et al., 2009; Phothiset & Charoenrein, 2014). The second phenomenon happens as a consequence of the first phenomenon: in short, when the tissue compartments are destroyed, the water and cellular contents (organic acids, phenols and hydrolytic enzymes) leak out of the cell and come in contact with cell walls. This interaction may lead to cell wall enzymatic dissolution during thawing. Further information on this topic is provided in section I.2.3.4.

In order to quantify the degree of textural damage that a product has suffered during freezing, various methods of texture analysis can be performed. It can either be objective (instrumental analysis) or sensory evaluation or preferably a combination of both, and may be accompanied by microscopic, biochemical, and NMR studies (Barrett, Garcia, & Wayne, 1998; Thybo et al., 2004; Waldron, 2004; Chassagne-Berces, Poirier, et al., 2009; Kiani & Sun, 2011). An instrumental analysis can either be destructive or non-destructive.

Sensory and instrumental analysis of texture is very well discussed by several researchers (Bourne, 1982; Barrett et al., 1998; Waldron, 2004; Abbott, 2004; Chen & Opara, 2013 and many others), so this topic will not be extensively discussed in this review. Sensory analysis involves the codification of sensory experiences (such as mouthfeel, hand feel, olfaction, visual and auditory perceptions), and it is commonly carried out by trained panels (Bourne, 1982;Barrett et al., 1998; Kilcast, 2001; Waldron, 2004; Chen & Opara, 2013). The instrumental measurements are preferred over sensory evaluations for both research and commercial applications as they reduce the variation that may arise due to the human perceptions; give more accurate results; can provide common language to researchers, industries and consumers (Abbott, 2004). The instrumental methods based on their measurement principles may be classified into empirical, imitative, and fundamental (Kilcast, 2001; Lu & Abbott, 2004; Waldron, 2004; Abbott, 2004; Chen & Opara, 2013). In short, the empirical tests often measure ill-defined variables that are indicated by practical experience which is related to some aspect of textural quality. The imitative methods have been considered to be a subset of empirical test that seeks to mimic methods used in the sensory analyses. Fundamental methods can offer better understanding of the mechanical behaviour of a food, its structural features, and their changes upon processing (Kilcast, 2001; Lu & Abbott, 2004; Waldron, 2004; Chen & Opara, 2013).

Fruits and vegetables exhibit viscoelastic behaviour under mechanical loading, which means that the force, distance, and time involved in loading determine the value of any measurement

(Lu & Abbott, 2004). Based on the pattern of loading, destructive instrumental methods may include puncture, compression, shearing, torsion (twisting), extrusion, crushing, tension, bending, and others (Lu & Abbott, 2004). There are four basic values that can be obtained from destructive instrumental analysis tests: force (load), deformation (distance, displacement, penetration), slope (ratio of force to deformation), and area under the force/deformation curve (energy) (Bourne, 1982; Hung, McWatters, & Prussia, 1998; Lu & Abbott, 2004). The engineering terms for these are stress, strain, modulus, and energy, respectively (Abbott, 2004).

Destructive instrumental measurements, compression test ((i) TPA (texture profile analysis), (ii) uniaxial compression test of food samples between two plates and (iii) confined compression tests, such as Kramer shear test and back extrusion test), puncture test, and tensile test have been used in the past to measure and evaluate the mechanical properties of fruit tissues prior and after freezing (Khan & Vincent, 1993; Fuchigami et al., 1994; Khan & Vincent, 1996; Koch, Seyderhelm, Wille, Kalichevsky, & Knorr, 1996; Kidmose & Martens, 1999; Sousa et al., 2006; Van Buggenhout, Messagie, et al., 2006; Chassagne-Berces, Poirier, et al., 2009; Chassagne-Berces, Fonseca, et al., 2010; Sirijariyawat & Charoenrein, 2014; Phothiset & Charoenrein, 2014; Wiktor, Schulz, Voigt, Witrowa-Rajchert, & Knorr, 2015; Purnell et al., 2017, and many others). Chassagne-Berces, Poirier, et al. (2009), by using penetration and uniaxial compression tests, were able to determine the textural loss of apple subjected to different freezing conditions. They found that the textural loss of apple fruit depended on the freezing rate. For example, freezing at −80 °C generated less degradation (54%) in firmness than freezing at − 20 °C (79%) or immersion in liquid nitrogen (91%) during the puncture tests. The compression test showed that freezing at − 80 °C and immersion in liquid nitrogen made less Young's modulus decrease (97%) than freezing at − 20 °C (99%). At this point, we have to mention that the puncture test evaluates local fracture behaviour (Chassagne-Berces, Poirier, et al., 2009). In the case of freezing by immersion in liquid nitrogen, the higher temperature difference between the sample and cryogenic fluid generated cracks in the sample mainly at the level of vascular bundles, where the cell size was smaller, and this might have resulted in larger deformation during the puncture test. For the compression test, the situation is different, it evaluates the deformability of the tissue taken as a whole (Chassagne-Berces, Poirier, et al., 2009). In another study, Sousa et al. (2006) used Kramer shear cell (KSC), back extrusion, compression and multiple penetration tests to determine the texture of fruits (raspberry and blackberry) before and after freezing. They were able to detect significant differences between the samples frozen under different freezing protocols by using all the above mentioned

mechanical texture measurement methods. Similar to Chassagne-Berces, Poirier, et al. (2009), they also observed that the ultrarapid freezing (e.g. liquid nitrogen immersion freezing and freezing by a means of a combination of immersion followed of vapours of liquid nitrogen at ≈ -88 °C) caused more textural loss than a rapid freezing (e.g. forced convection with liquid nitrogen vapour at -24 and -40 °C). Koch et al. (1996) performed TPA and Kramer shear test to estimate the textural loss sustained by potato samples under different freezing protocols. Their textural measurements revealed that conventional freezing leads to the softening of potato tissue system. Khan & Vincent (1996) performed a tensile test on frozen and thawed strips of apple and potato tissues. They reported that the tensile stiffness of both frozen potato and apple decreased as the freezing temperature was reduced from 0 to -20 °C. The tensile stiffness reduction rate was observed to be the fastest between 0 °C and -10 °C, which was found to be closely associated with the fastest rate of tissue damage that occurred between -3 °C and -10 °C. When the freezing temperatures were decreased below -10 °C the tissue stiffness began to level off indicating that most of the cells (> 80%) were damaged. The tensile stiffness value was also found to be dependent on the freezing rate; higher freezing rate (10 °C/min) led to lesser degradation of tensile stiffness value of apple than the slower freezing rate (1 °C/min).

Non-destructive testing using force deformation (laser-air puff), impact force (impact or bounce test), vibrational behaviour (low frequency vibration, sonic vibration and acoustic response), optical method (hyperspectral scattering imaging), light scattering, MRI (Magnetic resonance imaging) and NMR (nuclear magnetic resonance) have been successfully implemented to study the texture attributes of fresh fruits and vegetables (Chen & Sun, 1991; Hung et al., 1998; Mcglone & Jordan, 2000; Thybo, Bechmann, Martens, & Engelsen, 2000; Abbott, 2004; Peng & Lu, 2008; Chen & Opara, 2013). To the best of our knowledge, to date, none of these methods has been used to study the textural attributes of frozen/thawed fruits and vegetables. However, the textural alterations of meat and fish as a result of freezing and frozen storage had been studied using NMR relaxometry technique (Steen & Lambelet, 1997; Yano, Tanaka, Suzuki, & Kanzaki, 2002).

I.2.3.4 Chemical and structural composition of cell wall

The pectic substances are brought into solution more easily than other cell wall polymers and are more chemically reactive. This leads to the frequent observation that processes that result in textural changes, such as ripening, storage and cooking, are accompanied by significant changes in the characteristics of the pectic substances (Buren, 1979).

Reid in 1986 (Reid, 1986) reported that the changes in the cell wall, in particular, changes in the pectic fraction of the cell wall complex during freezing-thawing contributed to some extent in softening of Aiko strawberries. Among all pectin fractions, the water-soluble pectin fraction (WSP) showed the most dramatic change upon freezing and frozen storage compared to unfrozen sample. WSP decreased upon freezing and frozen storage, paralleling a decrease in the firmness value. Moreover, based on the compositional studies of the WSP, the researchers suggested that some of the changes were associated with the pectin rhamno-galacturonan backbone. In another study, Simandjuntak et al. (1996) reported that the total sugar composition of cell wall polysaccharides (CWP) of muskmelon decreases with the frozen storage prolongation indicating the modification and solubilisation of pectins and hemicellulose fraction of CWP. Moreover, during the frozen storage period of 10 months, the highest change in pectin content happened during the first five months of frozen storage and this was attributed to the maximum ice crystals growth during the initial period of frozen storage. However, no quantitative data on ice crystals growth during frozen storage period was reported by them.

Recently, Chassagne-Berces, Poirier, et al. (2009) studied the impact of three different protocols (− 20 °C, − 80 °C using nitrogen gas convection and − 196 °C by immersion in liquid nitrogen) on the sugar composition of cell walls. They observed a reduction in the proportion of cell wall neutral sugars and uronic acids of apple during freezing and thawing for all freezing protocols. Among the three freezing protocols being studied, slow freezing (at − 20 °C) created more damages than the other freezing conditions (− 80 °C and dipped in liquid nitrogen). The main sugars, the amounts of which were modified after freezing at − 20 °C, concern arabinose representative of the pectin and mannose, which is a cellulosic–hemicellulosic sugar. The reduction in the arabinose content as a consequence of freezing-thawing could be due to the loss of arabinan from the rhamnogalacturonan I domains of pectin, which is supposed to participate in the cell wall mechanical characteristics by forming an interaction with the cellulose (Zykwinska, Ralet, Garnier, & Thibault, 2005). The modification of pectins and hemicelluloses was considered responsible for the collapse of the cell walls, resulting in cell separation (larger intercellular spaces) and development of softer texture in samples frozen at − 20 °C.

The biochemical modifications of cell walls can also be studied using non-invasive techniques such as Fourier transform infrared (FT-IR) spectroscopy technique (Largo-Gosens et al., 2014). To date, this technique has been used for analyzing cell walls architectures and monitoring cell wall changes due to various factors, such as growth and development processes, genetic

modifications, exposition or habituation to cellulose biosynthesis inhibitors and responses to other abiotic or biotic stresses, as well as its biotechnological applications. Besides, it also provides abundant information about cell walls polymers, functional groups, and *in muro* entanglement (Largo-Gosens et al., 2014).

I.2.3.5 Impedance measurement

Measurement of electrical impedance can be a simple, rapid and inexpensive method of detecting freeze-thaw damage in fruits and vegetables (Zhang & Willison, 1991, 1992a,b). This technique is based on the fact that the undamaged tissues have resistance and capacitance.

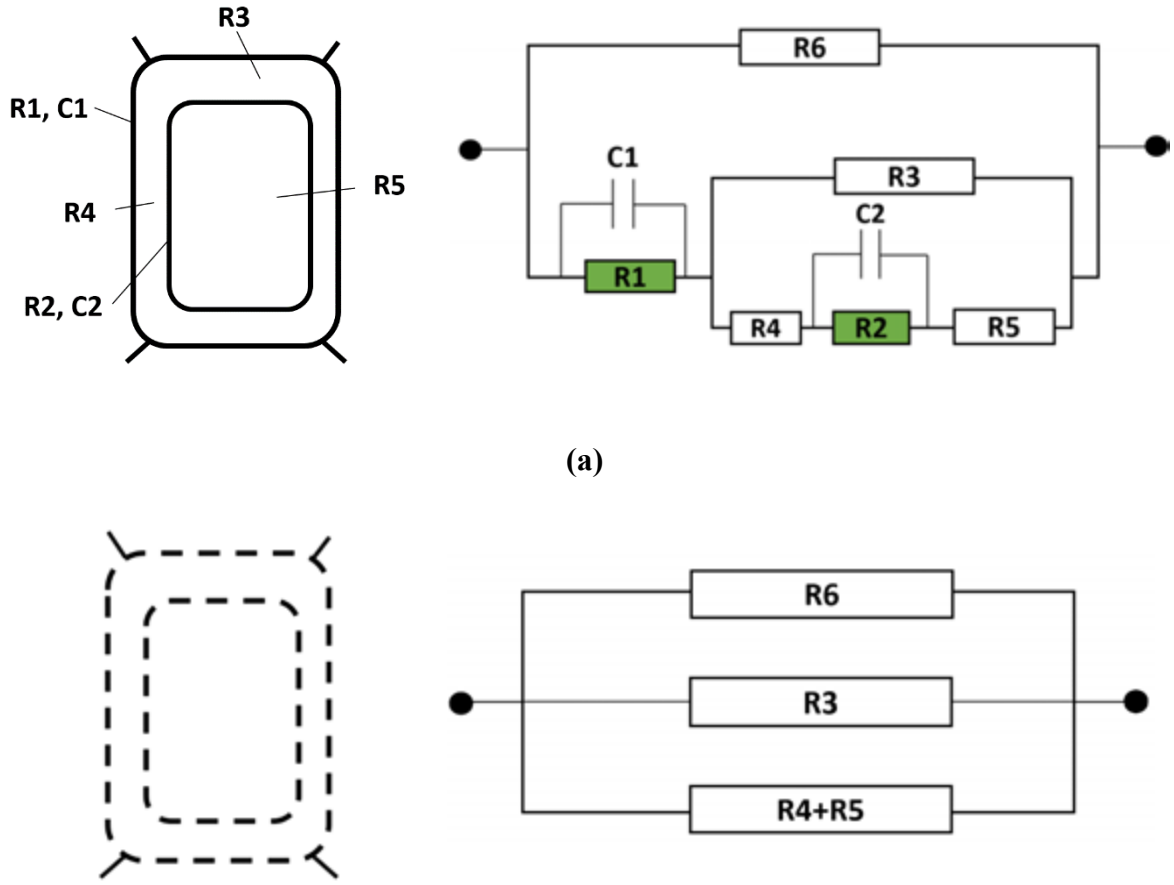

Figure 26: Schematic representation of a cell as an electrical circuit; (a) intact cell, (b) ruptured cell. R1, R2, plasma and vacuole membrane (tonoplast) resistance; C1, C2, plasma and vacuole membrane (tonoplast) capacitance; R3, cytoplasmic resistance surrounding the vacuole in the direction of current; R4, cytoplasmic resistance in vacuole direction; R5, resistance of the vacuole interior; R6, resistance of the extracellular compartment. This figure was adapted from Angersbach et al. (1999).

On the contrary, fully damaged plant tissue has no capacitance (Figure 26). Capacitance corresponds to intercellular domains, whereas intracellular domains are rather resistive

domains. Capacitance components will increase in electrical impedance with increasing frequency whereas resistive domain's impedance will not be function of the frequency. Usually, the impedance measured before freezing is compared to that measured after thawing to determine the extent of freeze damage tissues suffer during the processing. Upon knowing the conductivity of initial intact and treated (freeze-thawed) samples at low and high frequencies, one can calculate the cell disintegration index (p_0) in Eq. (5). This disintegration index characterizes the proportion of damaged (permeabilized) cells within the plant product (for intact cells, p_0 is 0; for total cell disintegration, p_0 is 1) (Knorr & Angersbach, 1998; Angersbach et al., 1999; Parniakov et al., 2015; Wiktor et al., 2015).

$$p_0 = 1 - b\,\frac{(K_h' - K_l')}{(K_h - K_l)}; \quad b = \frac{K_h}{K_h'} \tag{5}$$

where K_l and K_l' are the electrical conductivity of samples in low frequency range (1–5 kHz), for intact and treated (freeze-thawed) samples, respectively. While, $K_h$and K_h' are electrical conductivities of samples in high frequency range (3–50 MHz), for intact and treated samples.

Greenham in 1966 (Greenham, 1966) was the first to study the freezing injury caused to four varieties of alfalfa *(Medicago saliva* L.) by the means of impedance measurement. He found that the impedance value decreased due to the freezing-thawing process. Later in 1991, Zhang and Willison developed a new system for tissue impedance measurement and implemented it to detect injuries in frozen potato, carrot, and cabbage tissues in the years 1992 and 1993 (Zhang & Willison, 1991; Zhang & Willison, 1992a,b; Zhang & Willison 1993). They extracted the tissue impedance value from directly measured impedance (DMI) by performing multiple measurements at different inter-electrode spacing. Their data can be considered more relevant than Greenham's as the impedance value proposed by him included both tissue impedance and electrode impedance. They reported that the impedance value of the frozen-thawed sample was lesser than the intact cell as a result of membrane injuries happening during the freezing-thawing process. Hayden et al. (1972) found this technique potentially useful in determining the frost resistance among four Solanum clones without causing any appreciable damage to the plant under test.

To the best of our knowledge, this technique has not been used to compare the impact of different freezing rates which are known to control the freeze damage in plant tissues, thus, it is worthy, the effectiveness of this method in assessing the freeze damage to be further explored.

I.2.3.6 Solute diffusivity test

Mass transfer during osmotic treatment occurs through semi-permeable cell membranes present in biological materials, which imparts dominant resistance to the mass transfer process. Depending on the processing conditions, the state of cell membrane can change from being partially to totally permeable and this can lead to significant changes in the tissue architecture. The increase in cell membrane permeability increases the mass transfer rate of solutes and water during osmotic treatment process (Rastogi, Eshtiaghi, & Knorr, 1999; Alizadeh, Chapleau, de-Lamballerie, & Le-Bail, 2009). The diffusivity of solutes also depends on other factors, such as: the temperature and concentration of the osmotic solution, the size and geometry of the material, the solution-to-material mass ratio, and the level of agitation of the solution (Rastogi, Raghavarao, Niranjan, & Knorr, 2002). If all these factors are kept constant then the diffusity of solutes into the product can be related to cell damage that the product suffers during the processing steps. Since freezing has a detrimental effect on a cellular system (ruptures the cell membranes), the diffusion methods can be used to quantify freeze damage in fruits and vegetables at a global level. Figure 27 portrays the relationship between the freeze damage and solute mass diffusivity. Mass diffusivity values can be calculated by fitting the dry matter vs. time data to diffusion models (based on sample configuration), an example is presented in Figure 27. Until now, only Alizadeh et al. (2009) used this method to compare different freezing parameters. They found that the frozen/thawed sample (Atlantic salmon) had a higher mass diffusivity than the untreated sample. Moreover, different mass diffusivity rates were observed for samples treated with different freezing conditions. For example, high pressure shift frozen sample had a higher mass diffusivity than samples frozen at – 20 °C in static freezer. High pressure-induced permealisation was considered as a candidate factor for the higher mass diffusivity in the high pressure shift frozen sample.

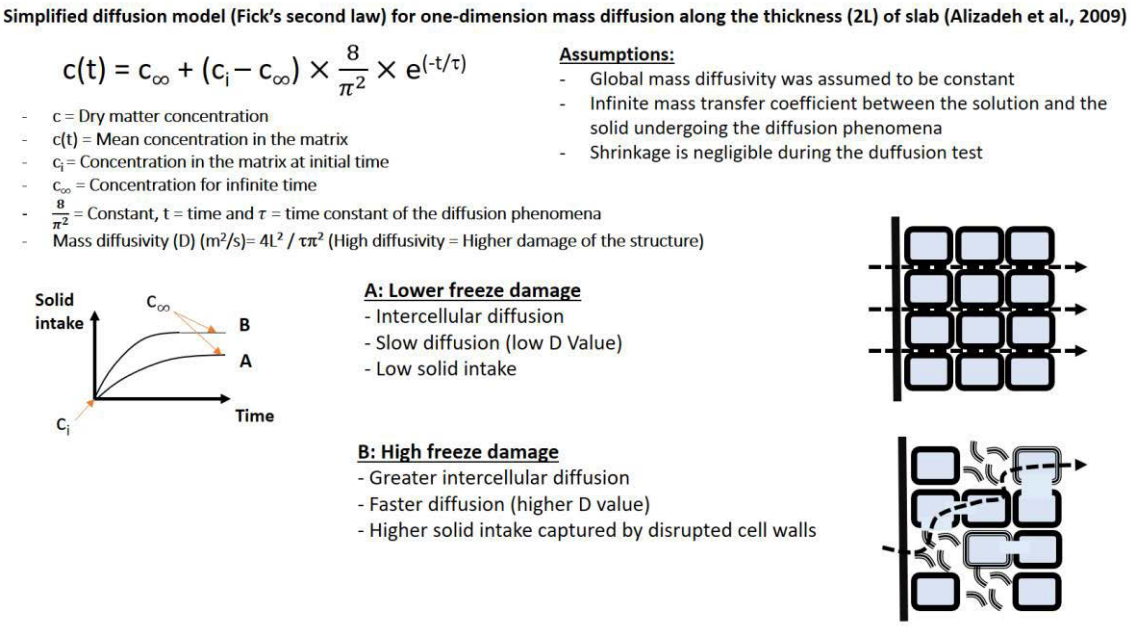

Figure 27: Diffusion occurs mainly in the intercellular spaces (Floury, Le Bail, & Pham, 2008). When pectocellulosic walls are disrupted, different paths appear resulting in mass diffusivity increase. Furthermore, the damage of the disrupted pectocellulosic walls could explain the higher solid intake for damaged tissues. Dry matter concentration (c) is expresssed as g of dry matter/g of sample. Time constant ($\boldsymbol{\tau}$) unit is [s].

I.2.3.7 Other methods

Drip loss measurement is one of the easiest and commonly used method to estimate the freeze damage in fruits and vegetables. In simpler terms, drip loss is a measurement of cellular content losses from cellular matrices. Drip loss is dependent on both the freezing rate (which determines the size and location of ice crystals) and the thawing rate (Van Buggenhout, Messagie, et al., 2006). In general, slower freezing rates promote the formation of larger ice crystals in the cellular matrix, and thus cause a higher destruction of the cellular structure, ultimately leading to a higher drip loss. On the contrary, rapid freezing methods produce numerous fine ice crystals in the cellular structure and impart less damage to the tissue structure, this will lead to lesser leakage of cellular content out of the cell. However, a very fast freezing rate (obtained using cryogenic liquids) may also lead to crack development in the sample and hence can increase the drip loss. Charoenrein & Owcharoen (2016) studied the relationship between the drip loss and the freezing rate during freezing of mangoes. The pattern of drip loss after being subjected to three different freezing protocols (high (2.91 °C/min), medium (1.69 °C/min) and low (0.05 °C/min) freezing rates) was as such: slow freezing > medium freezing > fast freezing. Similar

to Charoenrein & Owcharoen (2016), Fuchigami, Hyakumoto, & Miyazaki (1995) reported that the amount of drip increased as the freezing rate decreased in frozen carrots.

Freeze damage can be assessed by quantifying the chemical and biochemical changes. These include studies related to other changes such as colour, flavour, texture (discussed in section I.2.3.4), pH, vitamins status during freezing and frozen storage of fruits and vegetables (Murray et al., 1968; Murray et al., 1976; Cano et al., 1993; Fúster et al., 1994; Cano, 1996; Skrede, 1996; Oruna-Concha et al., 1997; Lim et al., 2006; de Ancos et al., 2012).

The study of colour change becomes important as colour is the first quality attribute that is perceived by the consumer and is the basis for judging the product acceptability (Cano, 1996; Skrede, 1996). Most of the colour in fruit and vegetables are provided by chlorophylls (green leafy vegetables), carotenoids (orange, yellow and red fruits and vegetables) and anthocyanins (the majority of berries and red to purplish vegetables) (Cano, 1996; Skrede, 1996; Lim et al., 2006; de Ancos et al., 2012). Frozen fruits and vegetables are subjected to colour modification upon freezing, frozen storage and thawing (Table 2). The most important colour alterations are related to chemical, biochemical, and physicochemical mechanisms: (i) breakdown of cellular chloroplasts and chromoplasts, (ii) natural pigments (chlorophylls, carotenoids, and anthocyanins) degradation, and (iii) development of enzymatic browning (Cano et al., 1993; Cano & de Acnos, 1994; Larsen & Poll, 1995; Cano, Ancos, & Monreal, 1996; Cano, 1996; Skrede, 1996; Oruna-Concha et al., 1997; Lisiewska & Kmiecik, 2000; Chaovanalikit & Wrolstad, 2004; Lim et al., 2006; Hager, Howard, Prior, & Brownmiller, 2008; Poiana, Moigradean, & Alexa, 2010; de Ancos et al., 2012; Leong & Oey, 2012).

Freezing, frozen storage and thawing processes also cause off-flavour development in fruits and vegetables. These processes affect the flavour profile in different ways depending on the type of fruit and variety. The flavour change have been associated to factors such as change in aroma profile, lipid oxidation, accumulation of ethanol and other volatile compounds, and decrease in the organic acids (Buck & Joslyn, 1953; Murray et al., 1968; Murray et al., 1976; Larsen & Poll, 1995; Cano, 1996; Skrede, 1996; Bartolomé, Rupérez, & Fúster, 1996; González-Castro, Oruña-Concha, López-Hernández, & Simal-Lozano, 1997). The vitamin C content in fruits and vegetables decreases slightly when subjected to freezing treatment, but its degradation increases remarkably during the frozen storage period (Marin, Cano, & Fuster, 1992; Cano et al., 1993; Lisiewska & Kmiecik, 2000; Poiana et al., 2010; Goncalves, Abreu, Brandão, & Silva, 2011; Xanthakis et al., 2018). The vitamin status was inferred as a shelf life

limiting factor for frozen fruits and vegetables (Cano, 1996; Skrede, 1996; Martins & Silva, 2004; Lim et al., 2006; de Ancos et al., 2012). β-carotene (precursor of vitamin A) and the phenolic compounds can also be degraded during freezing and frozen storage period (Cano & Marin, 1992; Marin et al., 1992; Cano et al., 1996; Lisiewska & Kmiecik, 2000; Poiana et al., 2010; Veberic et al., 2014). The extent of chemical and biochemical changes in final product (frozen/thawed) depends on various factors including product (type, cultivars, and maturity), pre-treatment (e.g. blanching), freezing and frozen storage conditions (light, oxygen, heavy metals, temperature, water activity, pH, oxidizing and reducing agents) (Cano et al., 1993; Fúster et al., 1994; Cano, 1996; Skrede, 1996; de Ancos, Ibanez, Reglero, & Cano, 2000; Lin & Brewer, 2005; Lim et al., 2006; de Ancos et al., 2012). Table 2 summarises further information about the chemical and biochemical changes related to freezing, frozen storage and thawing.

Table 2. Chemical and biochemical changes related to freezing, frozen storage and thawing.

Freeze damage type	Observations from literature	Meachanism
Colour change (a) Colour pigments (chlorophylls, carotenoids, and anthocyanins) degradation (b) Enzymatic browning	- Total chlorophylls content decreased as a result of freezing and frozen storage in kiwi fruit and green beans (Oruna-Concha et al., 1997; Cano et al., 1993). - Freezing treatment reduced the carotenoid content in mango, papaya, green beans and tomato (Cano & de Acnos, 1994; Cano et al., 1996; Oruna-Concha et al., 1997; Lisiewska & Kmiecik, 2000). - Freezing (at − 196 ℃) and frozen storage (at − 20 ℃, until analysis was made) increased the anthocyanins content in cherries, peaches and plums (Leong & Oey, 2012). - Reduction in total monomeric anticyanins content in black raspberries was observed upon freezing (at − 70 ℃) and storage at − 20 ℃ for 1 day. Further, monomeric anthocyanins were retained well during frozen storage of 6 months (Hager et al., 2008) - Anthocyanins in sweet cherry and strawberries fruit degraded remarkably during frozen storage (Larsen & Poll, 1995; Chaovanalikit & Wrolstad, 2004).	- Conversion of chlorophylls a and b to the corresponding pheophytins. - Bleaching of chlorophylls during fat peroxidation. - *cis-trans* isomerisation and epoxidation reactions and other oxidative changes are responsible for carotenoids pigments loss. - Freezing enhances the release of membrane bound anthocyanins, resulting in higher content after processing compared to fresh commodities. - Enzymatic degradation of anthocyanins. Polyphenoloxidase (PPO) and peroxidase (POD) enzymatic activities have been related to anthocyanin degradation. - Oxidative degradation catalysed by light. - Freezing and frozen storage disrupts the cell membrane and increase the loss of

	- Freezing, frozen storage, and thawing of fruits and vegetables such as mangoes, peaches, bananas, apples, potato, mushrooms etc., quickly developed colour changes that resulted in non-reversible browning or darkening of the tissues (Cano, 1996; Skrede, 1996; Lim et al., 2006; de Ancos et al., 2012).	anthocyanins (a water-soluble pigment) due to leaching. - Browning in fruits and vegetables was caused by enzymatic oxidation of phenolic compounds by PPO in the presence of oxygen.
Flavour modification	- Off-flavour development in frozen fruits and vegetables (Buck & Joslyn, 1953; Murray et al., 1968; Murray et al., 1976; Cano, 1996; Skrede, 1996; Bartolomé et al., 1996; González-Castro et al., 1997).	- Rancidity development in the lipid matter catalyzed by lipoxidase. - Development of off-flavour due to generation of ethanol and other volatile compounds. - Flavour modifications due to the decrease in the organic acids.
Vitamin degradation	- Frozen fruits and vegetables suffer considerable loss of Vitamin C during frozen storage, and such loss is mainly dependent on the storage temperature (Marin et al., 1992; Cano et al., 1993; Lisiewska & Kmiecik, 2000; Poiana et al., 2010; Goncalves et al., 2011). - The major part of vitamin C degradation in mangoes was related with freezing and frozen storage rather than the blanching pretreatment (Xanthakis et al., 2018).	- Oxidation: the oxidation of L-ascorbic acid may be enzymatic or non-enzymatic and proceeds in the presence of oxygen. - The loss happens due to activity of enzymes (POD, LOX (lipoxygenase), catalase (CAT)) during storage period in the presence of oxygen.

	- β-carotene (precursor of vitamin A) content in tomato, papaya, kiwi fruits, and mango during frozen storage period (Cano & Marin, 1992; Marin et al., 1992; Cano et al., 1996; Lisiewska & Kmiecik, 2000). - The β-carotene content of apricot, cherry, peaches, plums, carrots was not affected by the freezing (at -196 ℃) and storage (storage period prior to analysis) at -20 ℃. Meanwhile, freezing and storage under similar condition, the carotenoid content in nectarines decreased, while its amount increased in peppers (Leong & Oey, 2012).	- No explanation for the increase in the carotenoid content in peppers as a result of freezing process was specified.
Phenolic compounds loss	- During freezing (in home-scale freezer) and storage at – 18 ℃ over a long period (10 months), total phenolic compounds in cherries and strawberries decreased (Poiana et al., 2010). - Total phenolic content in Bing cherries (frozen in liquid nitrogen) underwent pronounced degradation during frozen storage at – 23 ℃ but were relatively stable at – 70 ℃ (Chaovanalikit & Wrolstad, 2004). - Blackberry frozen slowly and stored at -20 ℃ for 7 months enhanced the extraction of phenolic compound content, meanwhile, the liquid nitrogen frozen sample under similar	- Destruction is believed to be because of native enzymes, particularly PPO - Slow freezing process imparted higher damage to the cellular structure and this, in turn, enhanced extraction of phenolic compounds.

	condition showed no significant change when compared to the fresh sample (Veberic et al., 2014).	

➔**Intermediate conclusions:**

Various methods capable of assessing the freeze damage in fruits and vegetables were comprehensively described and compared in this chapter. In order to evaluate the freeze damage in fruits and vegetables, methods related to microstructure, texture, colour analysis, and drip loss estimation are the commonly preferred methods by the researchers. Other methods such as NMR, solute diffusivity, impedance measurements although that they have found limited applications till now, they seem to have a great potential to be used for assessing freeze damage in fruits and vegetables. The chemical and biochemical changes related to freezing, frozen storage and thawing have been studied by numerous researchers, however, maximum studies are focused on the changes happening during frozen storage. Fast evaluation methods that would enable the accurate characterization of the frozen product's quality during the industrial production are still missing although that they could be very helpful on the improvement of the quality attributes of the final frozen products.

II. MATERIALS AND METHODS

This chapter presents the materials, equipment and methods used to investigate the effect of conventional and innovative microwaves assisted freezing (MAF) processes on the quality attributes of the apples and potatoes.

II.1 Product properties

II.1.1 Food matrices description

Apples and potatoes were the two food matrices on which the effects of different freezing processes were investigated. The apples (Royal Gala) purchased from the local supermarket (Nantes, France) and the potatoes (TROPATOR variety) supplied by McCain Foods (Harnes, France) were used for the freezing tests.

Information about batches and storage time of apple and potato used for the freezing tests are mentioned below:

i) **Conventional freezing of apple:** For this study, the samples (having similar size) were purchased on the same day from the same shelf of the supermarket. However, it has to be mentioned that the entire sample came in a pack of 2 kg each. The total sample was divided into 3 batches randomly; each batch was meant for each freezing conditions being studied. The samples were stored at 2 °C and processed within 7 days of the purchase from the supermarket.

ii) **Conventional freezing of potato:** Two batches of potato were used for this test. The first batch of potato was used for NMR tests. For each freezing condition, samples meant for NMR test were taken from the same potato. Potatoes from another batch were used for time-temperature history study and freeze damage assessment tests. Both the batches of potato were stored at 8 °C and tests were performed within one and half month of storage period.

iii) **MAF of apple:** For MAF of apples, the samples from the same batch stored not more than one month at 2 °C were used for freezing curve test and quality evaluation test. Cryo-SEM tests were performed on apple from two different batches; samples for control and pulsed microwave assisted freezing conditions came from the same batch, while different batch was used for constant MAF condition. The samples intended for cryo-SEM analysis was stored less than a week at 2 °C after purchase.

iv) **MAF of potato:** Samples from the same batch were used for MAF of potato. All the tests related to MAF of potato were performed on potato sample stored for one month at 8 °C.

II.1.2 Moisture content measurements

The moisture content measurements were performed by drying the apple and potato flesh (about 5.5 ± 0.2 g) at 104 ± 2 ℃ for about 24 h. The ratio of the weight lost during drying to the original weight of the product gives the moisture content of the product on wet basis. The value is expressed in percentage basis and is calculated using Eq. (6). A minimum of 10 samples randomly picked from the lot were used for these measurements.

$$\text{Moisture content (\%)} = \frac{W_1 - W_2}{W_1} \times 100 \qquad (6)$$

W_1 = initial weight of the sample before drying (g), W_2 = final weight of the sample after drying (g).

II.1.3 Total soluble solids (TSS) content determination

For measuring the TSS content (°Brix) of the apples, around 20 g of sample was cut from the parenchyma section and were ground in a mortar and pestle until a thick slurry was obtained. Then the slurry was strained and the juice acquired was used for TSS measurement. The TSS measurement was performed using a refractometer (LR-01, Maselli Instrument Systems, Northampton, UK). A minimum of 10 samples was selected randomly for this test.

II.1.4 Estimation of freezable water

The freezable water available in the apple was determined by using μ-DSC 7 EVO DSC (Setaram, Caluire, France). Apple and potato (unblanched) flesh weighing around 85-150 mg was cut and immediately transferred into the sample cell; the apple flesh included only the middle parenchyma section. The sample cell along with a reference cell (empty cell without sample) was then placed into the DSC scanning chamber and was scanned (at 1 ℃/min) in two steps. In the first step, the sample was cooled from 20 ℃ to − 35 ℃ and was held at − 35 ℃ for 30 min, then it was brought back to 20 ℃ (second step). The melting curve (endothermic curve) obtained during the second step corresponds to the amount of energy required to melt the ice in the sample. The amount of freezable water was calculated by the Eq. (7). The results were obtained as an average of fifteen measurements from the fifteen apples randomly selected from the different batches of apples (includes nine samples for conventional freezing of apples (three replications each for batches meant three conventional freezing conditions of apple) and 6 replications form the batches of apple meant for MAF process. For potato (unblanched), the experiment was performed in duplicate.

$$\text{Amount of freezable water (\%)} = \frac{\text{Integral of area under the melting curve}}{\text{Heat of fusion of 1g of pure ice } \left(\frac{333.5\ \text{J}}{\text{g}}\right)} \times 100 \quad (7)$$

II.2 Sample preparations for different freezing tests

II.2.1 In the case of apple

For the freezing test (both conventional and MAF processes), cylindrical pieces of apple (0.47 ± 0.03 g) with a diameter (Ø) of 8 mm and height (H) of 10 mm were cut using a sharp cylindrical punch in tangential orientation from the middle parenchyma of the fruit (Figure 28). A minimum of 4 cylinders was cut from each fruit. The samples were then placed in zip-lock bag and stored at 4 ± 1 ℃ to avoid any moisture loss from the product and to achieve a uniform temperature prior to the freezing tests. However, it is important to mention that during conventional freezing of apple the temperature of the sample reached around 11 ℃ prior to freezing treatment because of time spent on spreading the sample on the trays at an ambient temperature.

Note: The precooling time was monitored based on a temperature measurement made by placing a thermocouple at the geometric centre of one of the sample. It was found that 1 h was sufficient enough to bring the temperature of the product to around 5 ℃.

II.2.2 In the case of potato

II.2.2.1 Conventional freezing of potato

The sample size used to study the effect of conventional freezing processes on the quality parameters depended on the freeze damage assessment methods. For instance, to study the effect of freezing rates on freezing characteristics, texture, colour and drip loss, cuboids of potato ($1.3 \times 1.3 \times 1$ cm^3 – length × height × width; weight 1.95 ± 0.5 g) were used. The potatoes were cut in cuboid shape using a dicer (Ibili Manage, Inc. Spain). The potato samples used for NMR relaxometry and cryo-SEM analysis were cylindrical in shape (Ø = 8 mm and H = 10 mm). For confocal laser scanning microscopy (CLSM) analysis, cylindrical potato samples (Ø = 8 mm and H = 5 mm) were chosen. The cylinders of potato were cut following the same method as used for apples. The samples were then immediately transferred into the freezer and were cooled from the ambient temperature to the desired temperature.

Note: Potatoes used for this test were neither blanched nor precooled prior to freezing.

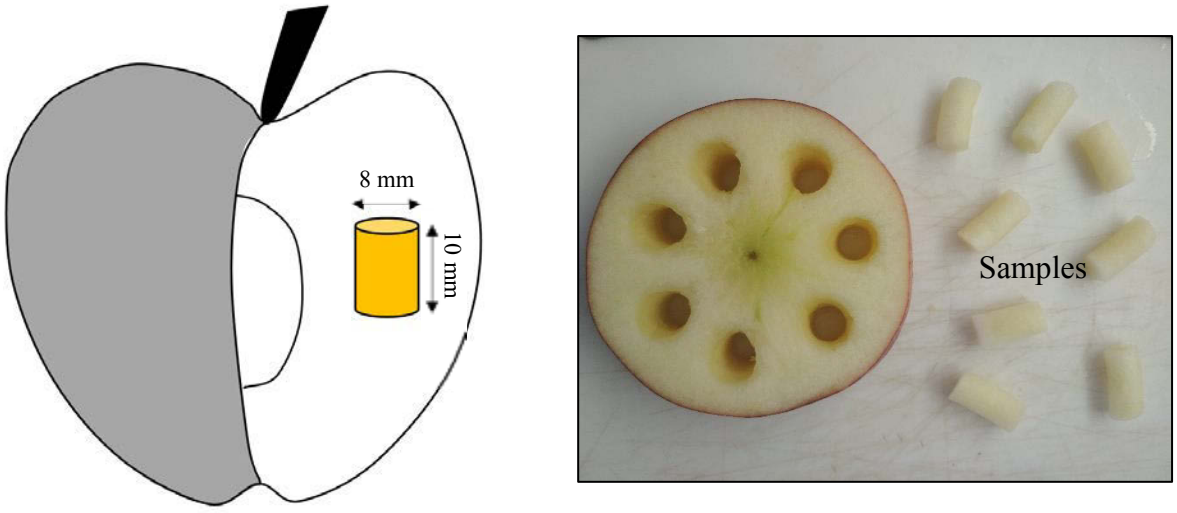

(a) (b)

Figure 28: Cylindrical shape of apple cut from the middle parenchyma of apple. (a) Pictorial representation of region from which sample was cut, (b) cylindrical sample cut from the apple.

II.2.2.2 MAF of potato

The cuboids of potato having the dimensions and weight same as mentioned in the section II.2.2.1 were selected for MAF of potato. The samples were blanched prior to the freezing tests. The blanching of potato was performed by immersing around 500 g of sample in the hot water (at 85 ± 1 ℃) until 1 min 50 s. The blanching time was fixed based to the suggestion from the "McCain Foods", according to them, keeping the temperature at the geometric centre of the product to 75 ℃ for at least 1 min would give an adequate blanching. After blanching, the samples were cooled to the room temperature by dipping in cold water at ambient temperature for 9 min. The samples were then spread on absorbent paper to remove the surface moisture of the product. Lastly, the samples were placed in a zip-lock bag and kept at 4 ± 1 ℃ to achieve a uniform temperature prior to the freezing tests.

Table 3. Geometry of samples used for different freezing and freeze damage assessment tests.

<table>
<tr><th rowspan="2">Tests</th><th colspan="2">Apple freezing</th><th colspan="2">Potato freezing</th></tr>
<tr><th>Conventional</th><th>MAF</th><th>Conventional</th><th>MAF</th></tr>
<tr><td>Freezing process parameters (time-temperature history)</td><td rowspan="5" colspan="2">Cylinders (Ø and H = 8 mm and 10 mm)</td><td colspan="2">Cubes (1.3 × 1.3 × 1 cm^3 – L×H×W)</td></tr>
<tr><td>Cryo-SEM</td><td rowspan="2">Cylinders (Ø = 8 mm and H = 10 mm)</td><td rowspan="2">Not applicable</td></tr>
<tr><td>NMR</td></tr>
<tr><td>Texture</td><td rowspan="2" colspan="2">Cubes (1.3 × 1.3 × 1 cm^3)</td></tr>
<tr><td>Drip loss</td></tr>
<tr><td>Colour</td><td rowspan="2" colspan="2">Not applicable</td><td rowspan="2">Cylinders (Ø = 8 mm and H = 5 mm)</td><td rowspan="2">Not applicable</td></tr>
<tr><td>CLSM</td></tr>
<tr><td>X-rays tomography</td><td>Not applicable</td><td>Cylinders (Ø and H = 8 mm and 10 mm)</td><td>Not applicable</td><td>Cubes (1.3 × 1.3 × 1 cm^3)</td></tr>
</table>

Ø = diameter (m), H = height (m), L = length (m), H = height (m), W = width (m).

Note: The freezing tests of apples were performed in the beginning, followed by freezing tests on potatoes. In the case of apples, we wanted samples from the middle parenchyma of the apple excluding portions from seed cortex and the extreme periphery of the sample. The sample preparation was quite tedious. Learning from the experience, we thought to use some fast means to prepare the sample for potato freezing tests. Upon researching, we found that dicer was available for the potato that can produce cubes of potato with a good uniformity and in a short course of time. Hence, sample configuration used for apple and potato for the freezing tests were different.

Moreover, one of our aims was to analyze the sample in its original state without causing any alterations, thus we had to vary sample size for potato according to the freeze damage assessment methods (mainly for conventional freezing of unblanched potatoes). For instance, NMR tube has a diameter of 1 cm and hence required sample having a diameter < 1 cm. Also, another requirement of NMR test is to have the NMR tube filled minimum up to 1 cm in height. The cylindrical sample with a diameter of 8 mm and height of 1cm perfectly matched both the requirements. For cryo-SEM, sample size similar as NMR facilitated cutting of sample in the frozen state and allowed pooling of sample from nearly the same location for each condition. For CLSM, small sample size helped in proper and fast staining of the sample.

Besides, similar to cryo-SEM, small sample size eased extraction of sample from the same location.

II.3 Freezing apparatus and freezing protocols

II.3.1 Freezers and freezing conditions used for conventional freezing of apple and potato

The apples were frozen under three freezing conditions at − 18 ℃ in a static chest freezer (FCB400EA, Firstline, Denmark), at − 40 ℃ and 2 m/s air velocity in an air blast freezer (Servathin, Poesy, France), and at − 72 ℃ and air velocity of 1 m/s in an air blast freezer (VC7018, Vötsch, Avionik Straubing Entwicklungs GmbH, Germany). Similarly, conventional freezing of unblanched potatoes was performed at − 18 ℃ in a cold room, at − 30 ℃ and 0.5 m/s air velocity in an industrial batch freezer (MATAL, France), and at − 74 ℃ in an ultra-low temperature freezer (TSE240V, Thermo Scientific, Marietta, Georgia, USA). The three conditions will be referred to as slow freezing (SF), intermediate freezing (IF) and fast freezing (FF) in further sections of the thesis. The samples were frozen to the respective end temperature (i.e. − 18, − 40, − 72 ℃ for apples and − 18, − 30, − 74 ℃ for potatoes). Once frozen, the samples were packed in the zip-lock bags and stored at − 40 ℃ (≈ for 2-3 days) until quality evaluation tests were performed.

The time-temperature history during the freezing process was recorded using a K-type thermocouple inserted at the geometric centre of the product. For comparison purpose, temperature profile from the initial temperature (i.e. 11 ℃ for apples and 18-20 ℃ for potatoes) to − 18 ℃ was considered. The characteristic freezing time and overall freezing time were determined using time-temperature data. The characteristic freezing time is the time taken by the product to reach −7 ℃ from −1 ℃ (described precisely in section II.3.2). The overall freezing time is the time required to lower the temperature of the geometrical centre of the product from the initial value (around 10-11 ℃ for apple and 18-20 ℃ for potatoes) to a given final temperature (− 18 ℃ considered in this study).

Note: The freezing conditions used for this study were selected based on a study from Charoenrein & Owcharoen (2016). In their study, the effect of three freezing conditions (freezing at – 20 ℃, – 40 ℃ and – 80 ℃) on the texture, microstructure and pectic substances of mango was investigated.

II.3.2 Microwave assisted freezer prototype and different MAF freezing strategies

A custom-built microwave freezer which consisted of a domestic MW cavity installed in a blast freezer (RS 10/RL, ACFRI, France) was used for microwave assisted freezing (MAF) of apples (Figure 29). This experimental unit had no provision to adjust the airflow rate.

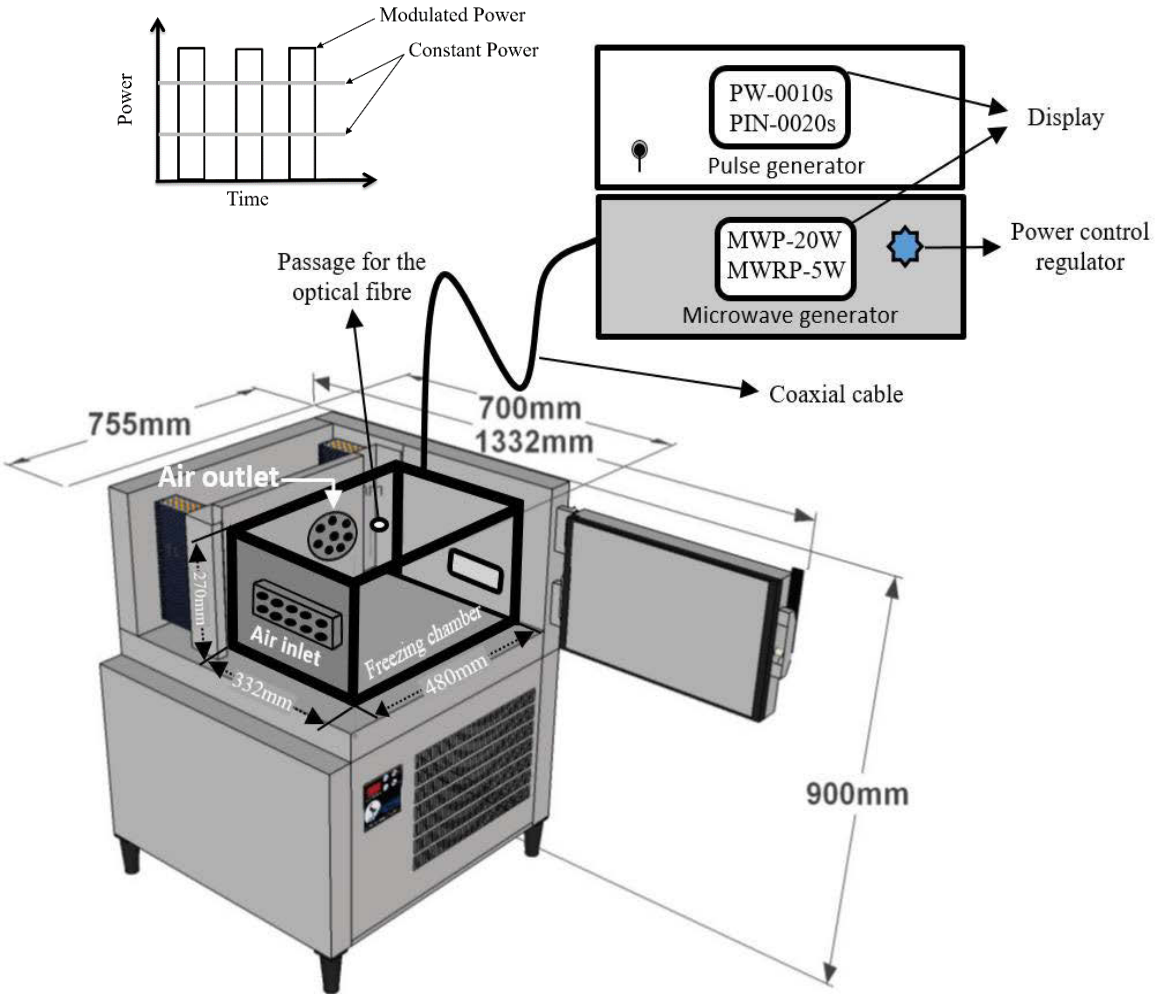

Figure 29: Schematic diagram of the MAF experimental system. A domestic MW cavity was connected to a solid state MW emitter with adjustable power from 1 to 200 W (SAIREM-France). Different strategies were applied to the food undergoing freezing within the MW cavity (top right corner). PW = pulse width; PIN = pulse interval; MWP = microwave incident power; and MWRP = microwave reflected power.

The experimental set-up used for MAF of potato was a little different from that of MAF of apple. Three main modifications were made in the experimental set-up used for MAF of apple, one is that the domestic MW cavity was installed in a different freezer (Industrial batch freezer (MATAL, France)), second is that the air inlet and outlet point were reversed, and the

last one is that a blower was attached to the air entry point of MAF unit in order to provide the flexibility to manipulate the airflow rate (Figure 30).

(a)

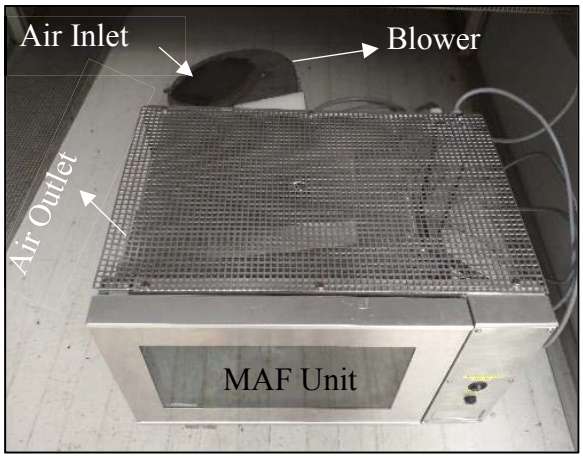

(b)

Figure 30: Experimental unit used for MAF of potato. (a) Entire experimental setup, and (b) MAF unit with blower attached to the air entry point for improving the airflow rate during the freezing operation.

The microwaves (MWs) of 2450 MHz required for the freezing tests were generated using a solid-state generator (Sairem, Lyon, France); the generator was designed to dissipate power from 0-200 W. A pulse generator (fabricated in our lab) connected to microwave producing source helped to achieve microwaves with different ON/OFF duty ratios. The freezing chamber was precooled with cold air current of – 30 °C moving at a speed of 1.1 m/s (for apple) and 2.30-2.50 m/s (for potato) prior to each freezing tests. MAF of apples and potatoes was performed by placing the samples (30 g) in the freezing chamber and simultaneously applying microwaves of various power levels. Table 4 portrays the different microwaves modalities used for this study.

Table 4. Microwaves modalities used for this study.

Conventional (control)	**MW conditions**		
	Constant (CMAF)	**Pulsed**	
		P1MAF	**P2MAF**
No MW irradiation	- 5 W or 167 W/kg applied continuously	- 15 W or 500 W/kg with 10 s pulse width and 20 s pulse interval - Average power (167 W/kg)	- 20 W or 667 W/kg with 10 s pulse width and 20 s pulse interval - Average power (222 W/kg)

The time-temperature profile during the freezing tests was studied by inserting a fibre optic at a geometric centre of the product. The optical fibre was calibrated against a reference platinum probe (Comptoir Lyon Allemand – Lyon-France). During measurements temperature changes of the sample were recorded every 5 s with the data logger with an accuracy of ± 0.1 °C. The freezing test was terminated once the geometric centre of the product reached − 18 °C.

In this study, characteristic freezing time and overall freezing time was determined for each freezing condition. The characteristic freezing time is the measure of local freezing rate and is defined as the time during which the temperature at a particular point changes from the initial freezing point to a temperature at which 80% of the water (at that point) is converted to ice. The temperature range considered for the characteristic freezing time was from − 1 to − 7 °C, similar temperature range was used by Delgado et al. (2009) and Li & Sun (2002) for the determination of characteristic freezing time during ultrasound assisted freezing of apples and potatoes. The overall freezing time is the time required to lower the temperature of the geometrical centre of the product from the initial value (5 °C in the present study) to a given temperature (− 18 °C in this study). Samples for quality analysis were frozen using the same

procedure but without optical fibre inserted into it. Each experiment was performed at a minimum of three times.

II.4 Thawing protocol

The frozen samples (both apple and potato) were thawed at room temperature (20 ± 1 °C) for 2 h in a zip-lock bag before performing colour, drip loss measurements, texture and solute diffusion tests. In other words "static air thawing" procedure was used for these studies. For NMR analysis the thawing protocol was slightly different, the samples were thawed at 4 °C for 4 h in the NMR tube.

II.5 Colour analysis

The colour of the potatoes was measured using a portable and handheld chroma meter CR-400 (Konica Minolta, Inc. Japan). Using this equipment, the L^*, a^*, b^* value for samples from each condition was obtained with high accuracy. The maximum value for L^* is 100 (represents a perfectly white surface or a perfectly reflecting diffuser) and its minimum value is 0 (represents perfectly black surface). The positive and negative a^* corresponds to red and green colour. Similarly, positive and negative b^* represents yellow and blue colour, respectively (Figure 31).

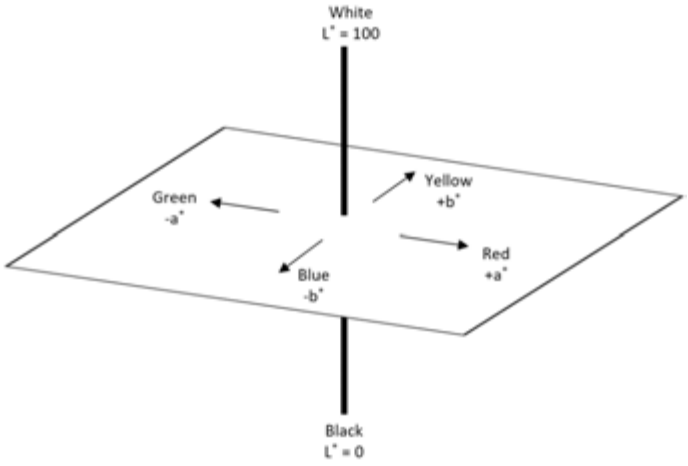

Figure 31: Diagram representing colour space. This image is inspired from Anon (2018b).

A single value for the colour difference was achieved by calculating the overall colour difference (ΔE) value; it takes into account the differences between L^*, a^*, b^* of the specimen (e.g. frozen-thawed sample) and reference (fresh sample), and is obtained using Eq. (8) (Anon, 2018b). The frozen samples were thawed before the colour measurements. At least eight measurements were recorded for each freezing protocols.

$$\Delta E = \sqrt{\Delta L^{*2} + \Delta a^{*2} + \Delta b^{*2}} \quad (8)$$

II.6 Drip loss measurement

The drip loss was determined on the basis of weight difference between frozen sample (W_1), and thawed sample (W_2). The drip loss (%) was calculated using Eq. (9). At least 9 samples were analyzed for each freezing conditions.

$$\text{Drip Loss (\%)} = \frac{W_1 - W_2}{W_1} \times 100 \quad (9)$$

II.7 Texture analysis

II.7.1 Firmness/hardness and Young's modulus measurement

The frozen apple and potato samples were thawed and compressed in a texture analyzer (AMETEK, Lloyd Instruments, France) (Figure 32a) to beyond failure point which was marked by a significant drop in the force reading (Figure 32b). A similar procedure was used by Khan & Vincent (1993, 1996) for determining the failure stress, Young's modulus, and failure strain of apple and potato. Based on our preliminary trials and results from Khan & Vincent (1993) and Alvarez, et al. (2002), compression of the sample to 50% strain was found more than sufficient to cause the failure of the sample (Figure 32b). The maximum force exerted during the compression test was recorded as the firmness/hardness (N) of the samples (Figure 32b). Other test parameters for firmness/hardness measurement of apples and potatoes are discussed in Table 5. Moreover, the stress vs. strain curves during compression tests were examined and Young's modulus (E) (the slope of the loading curve at the point of its highest gradient) was also acquired (Chassagne-Berces, Poirier, et al., 2009). The Young's modulus measurements were only performed for potatoes. The test parameter for Young's modulus determination of potato were same as used for firmness determination of potato. All measurements were performed at 21 $\pm$ 2 ºC. A minimum of 12 samples was analyzed for each freezing conditions.

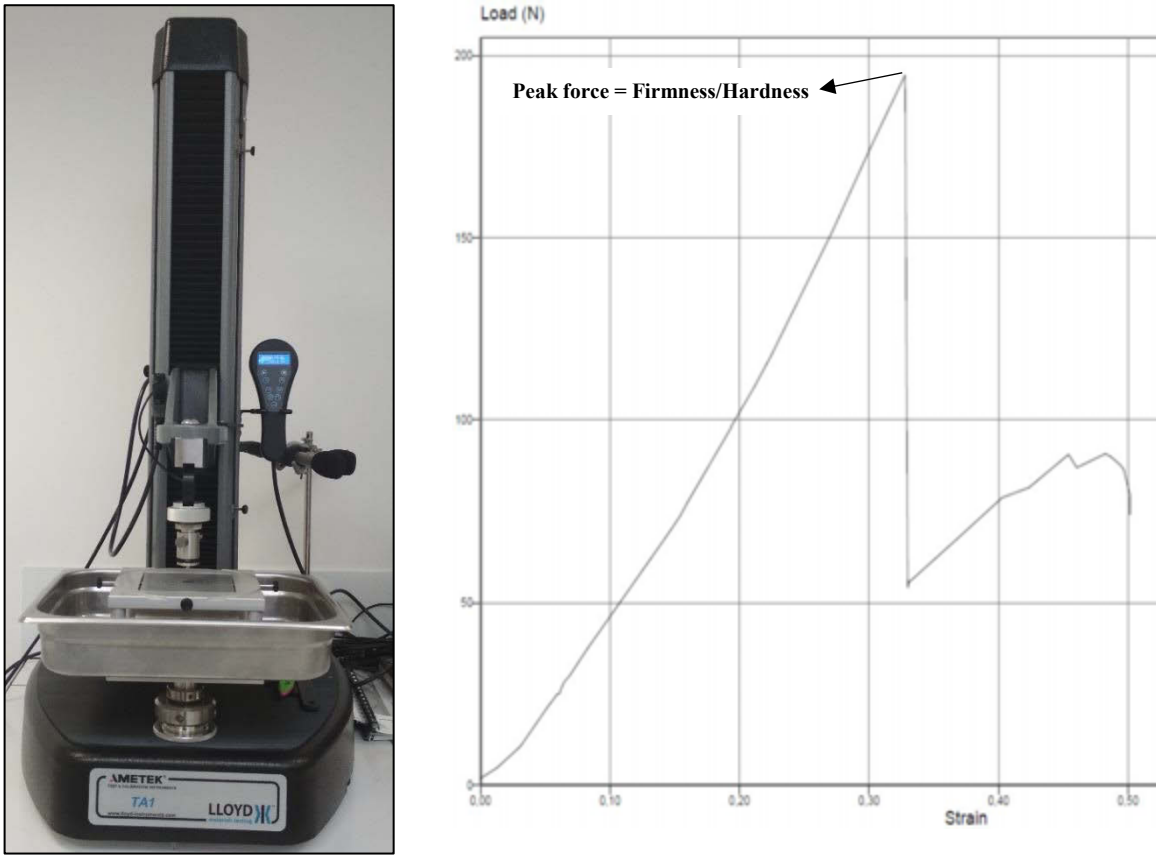

(a) (b)

Figure 32: (a) Texture analyzer used for performing compression test, (b) load-strain curve providing detail about the firmness of the potato.

Table 5. Parameters used during firmness determination of apple and potato.

Parameters	Firmness and/ Young's modulus	
	Apple	Potato
Load cell	50 N	1000 N
Operating test speed	100 mm/min	50 mm/min
Diameter of circular compression plate	21 mm	50 mm

II.7.2 Laser-Puff firmness tester

A laser-puff firmness tester designed in our lab was used for measuring the texture of fresh and frozen-thawed potatoes non-destructively (Figure 33). The firmness tester comprises the following components: a means to generate impulsive jet of air; a nozzle to direct the air onto the surface of the specimen under investigation; a deformation measurement unit containing a laser source to generate coherent source of light directed on the surface of object impacted by the air jet, a detector to catch the light reflected from the specimen surface, and an analyzer to

estimate the amount of deformation sustained by the product surface; a control panel to change the pressure value; a software (developed in our lab) to run the test. Based on the preliminary trials, for measuring the firmness of frozen-thawed potato, the air pressure of 5×10^5 Pa (5 bar) and air jet exposure time of 100 ms was found most appropriate. Prussia, Astleford, Hewlett, & Hung (1994) used impact pressure of 3.10×10^5 Pa (45 psia) to determine the firmness of potato. Similar to the authors, Hung, McWatters, & Prussia (1998) used the same exposure time to determine the firmness of peaches.

The sample under test was placed on the sample platform below the air delivery nozzle and the position of the sample was adjusted (using a positioner) in order to ensure (i) the air jet and the laser hit the same point on the sample and (ii) the distance between end of the nozzle and the sample surface was same for all trials. Then using the software air jet was directed on the sample and the deformation was measured. The software yielded deformation results in volts (Figure 34). The maximum deformation can be referred to as the difference between the highest initial value and lowest value recorded by the deformation unit during the test. The conversion of volts to mm (millimeter) based unit was made by multiplying with a conversion factor (in the present case, volt value was multiplied by 2 to obtain final value in mm). The final deformation value was an average of sixteen measurements.

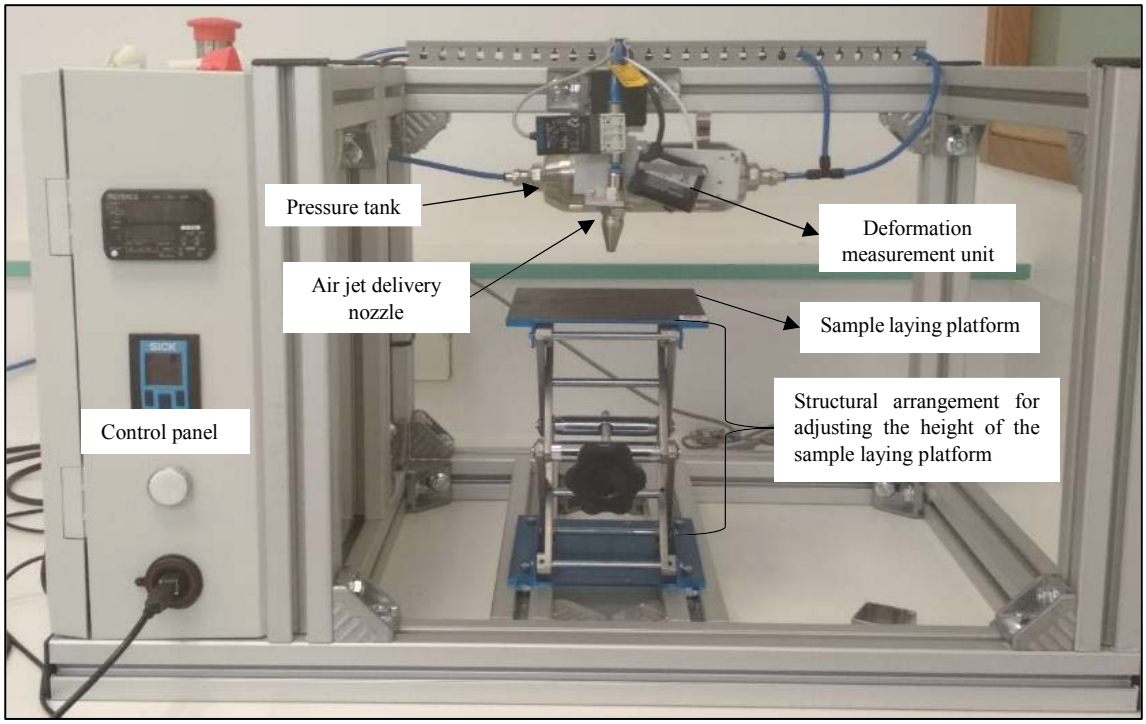

Figure 33: Laser-puff firmness tester machine.

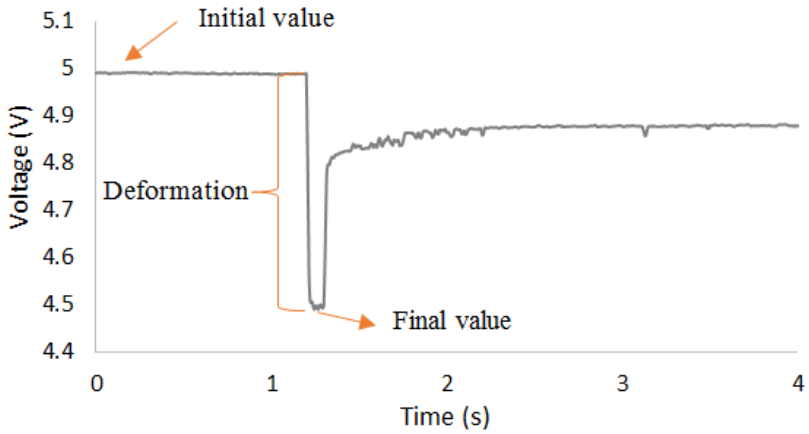

Figure 34: Deformation curve obtained while performing the laser puff test. Conversion of volts to mm: 1 V = 2 mm.

II.8 Solute diffusion test

An attempt was made to evaluate the freeze damage suffered by the apple during different conventional freezing processes using the solute diffusivity method. The experimental setup used for sugar diffusivity test is shown in Figure 35. Six frozen apple cylinders of known weight were thawed first and placed in tea snap ball infuser. They were then put in a vessel containing sugar solution (20% of sucrose in distilled water (wt/wt)). The TSS content of the sugar measured at the beginning of the test was ≈ 16.30 °Brix. An agitator (Stuart, Magnetis Stirret, SM8, England) was used to ensure homogeneous concentration during 3 h of experiment at a temperature of 20 ± 0.1 °C. The samples were removed from the sugar solution after every 30 min during the test period (till 3 h) and were placed in a hot air oven (maintained at 105 ± 2 ºC) for 24 hours to determine the dry matter content of the samples. From the dry matter values, the amount of sugar gain (i.e. the difference between the initial dry matter of the respective batch and the dry matter after diffusion test) as a function of time was obtained. The TSS content of the osmotic solution measured at the beginning and at the end of the test and was not significantly affected during the test (measured ≈ 16.30 °Brix before and after the test). The experiments were repeated for three times for each freezing conditions.

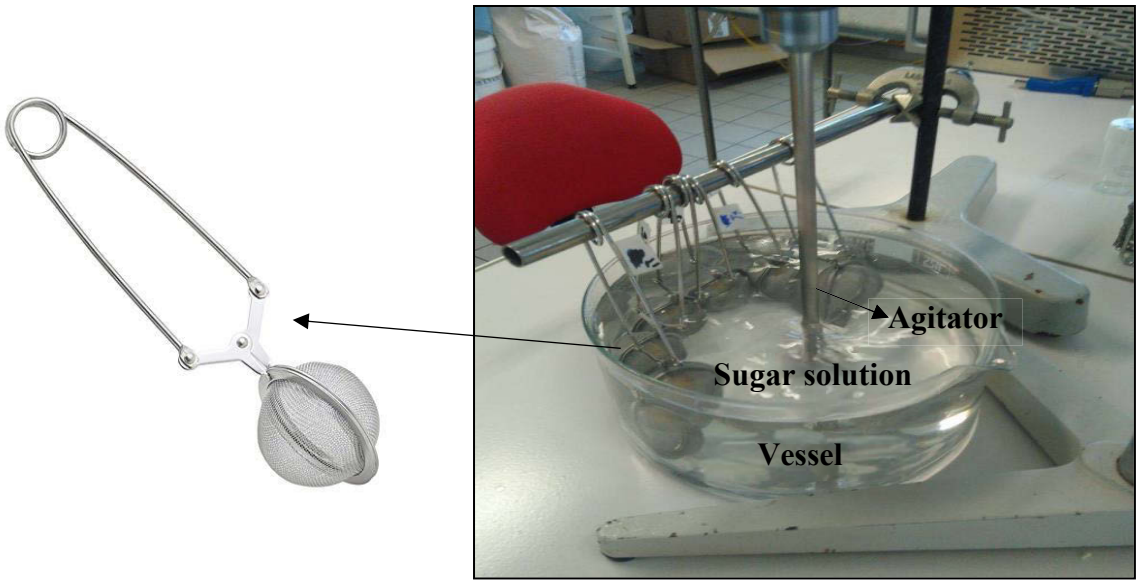

(a) (b)

Figure 35: Experimental set up for sugar diffusivity measurement. (a) Tea snap ball infuser used for holding the samples during sugar diffusivity test, (b) diffusivity test step up.

II.9 Microstructure examination

II.9.1 Cryo-SEM analysis

For cryo-SEM analysis, a very thin specimen (e.g. slab) was cut from the middle of the frozen apple and potato samples using a sharp scalpel and was fixed into the groove notched in a copper sample holder using an OCT (optimal cutting temperature) compound (Tissue-Tek, Sakura, Finetek, USA). The cutting operation was performed in cold condition (on a glass petri plate placed in a box filled with dry CO_2) so as to avoid thawing of the sample. The sample was left for 2 min in a box filled with dry CO_2 to harden the OCT compound. After that, the sample was loaded onto a precooled copper specimen stub and was quickly transferred in the cryo-preparation chamber of cryo-SEM (LS10, ZEISS EVO, Germany) (Figure 36) maintained under vacuum at − 80 ℃, where it was cryo-fractured using a precooled sharp knife mounted inside the chamber. The fractured sample was etched in the preparation chamber for about 10 min to expose the subsurface information. The sample was finally coated with a thin conducting layer of gold (5 nm) in the cryo-preparation chamber and then was transferred to the cold stage in the cryo-SEM (maintained at − 80 ℃) where microstructural observation was performed. The fractured surface of apples and potatoes were examined with an accelerating voltage of 11 kV. The pictorial representation of the sample preparation steps is presented in Figure 37.

Figure 36: Cryo-SEM equipment used for imaging the products in frozen state.

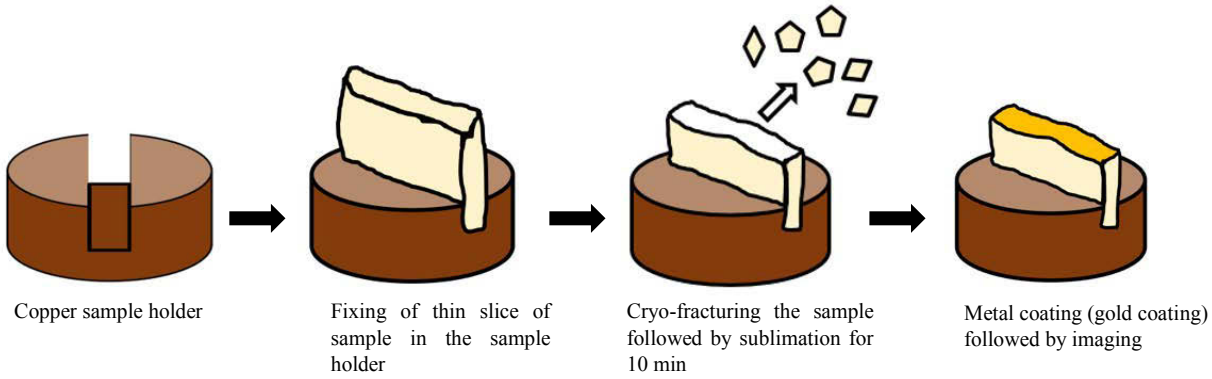

Figure 37: Illustration of sample preparation step prior to imaging in cryo-SEM.

II.9.2 X-rays tomography

The sequence of steps required for acquiring the 2-D and 3-D information about the product using an X-ray tomography are discussed below:

II.9.2.1 Sample preparation

For X-ray tomography analysis, the entire frozen samples were first dehydrated using a freeze dryer (at − 85 ℃ and 5.33-8 Pa (40-60 mtorr)). Freeze drying process removed the moisture inside the material by sublimation and left a network of solid fibers and pores. The pores present in the product correspond to the ghost of ice microcrystals that sublimed during freeze drying.

II.9.2.2 Image acquisition

The freeze-dried samples were then scanned by an X-ray micro-computed tomography scanner (SkyScan 1174v2, Bruker microCT, Kontich, Belgium) operating at a voltage of 50 kV and current of 800 µA. A CCD (charge-coupled device) camera with resolution of 1,304 × 1,024 pixels was used to record the projection images. The acquisition was performed at a voxel size of 9 µm (for apple) and 13.5 µm (for potato). The exposure time was 1,600 ms, and the samples were rotated from 0° to 180° with a step angle of 0.2°. Three images per angular position were taken and averaged. A total of 923 images in TIFF format (16 bits) were acquired at the end of the process. Flat field correction was carried out to remove the artefacts (white or dark dots or blotches in the image) that arise due to the variations in the pixel-to-pixel sensitivity of the detector and/or by distortions in the optical path.

II.9.2.3 Image processing

Image processing comprises of two steps one is the reconstruction and another image analysis to acquire the distribution characteristics of pores.

II.9.2.3.1 Reconstruction

From the series of images (16-bit TIFF) obtained during the image acquisition process, 2-D images were reconstructed using NRecon reconstruction software (Bruker microCT, Kontich, Belgium). Firstly, the zone to be reconstructed was set up; in the present case, the images comprising the entire sample were considered for the reconstruction process. Then, the alignment of the images with each other was checked and corrected automatically. In the next step, the intensity range of the image was adjusted by its histogram, the lower limit of histogram was fixed at 0 (considered reasonable choice for many applications) and the upper limit was fixed as 0.068 (which was ≈ 20% higher than the maximum in the histogram for each case). The output image format was fixed as TIFF (16-bits), and upon reconstruction process, a series of images having a resolution of 1,304 × 1,304 pixels was obtained.

II.9.2.3.2 Image analysis

The image analysis was performed using CTAN 1.16.4.1 image analysis software (Bruker microCT, Kontich, Belgium). In the first step, the image on which 3-D analysis would be performed was selected. A stack of 750-800 slices images was selected for the further processing. For all conditions around 75-85 slices from the top and bottom were systematically removed, because of their low quality. In the second step, the region of interest (ROI) on which

analysis would be carried out was defined. The ROI used for this study covered the sample entirely while excluding the information from the extreme periphery of the sample; the ROI accounted roughly more than 80% of the raw image (Figure 38). Moreover, the ROI for each image slice was checked and was adjusted according to the configuration of the slice so as to avoid the information from the extreme periphery of the sample. The ROI was then thresholded (using automatic Otsu thresholding method) to separate the pixels into 2 categories: the brightest (corresponding to the cellular matrix), and the darkest (corresponding to the pores). The resulting image, thus, had only black and white pixels. Next, despekling was performed; by this method the floating pixels (generally due to noise) which are not attached to the main solid matrix are removed from the image. The pore (or matrix) distribution is then measured directly (which is model independent) in 3-D using distance transform method described by Remy and Thiel (2002). The process starts with a "skeletonisation" process in order to determine the medial axes of all pores (or matrix). The local thickness measurement is then done for all voxels lying along this axis to obtain the pore size (or matrix size). The local thickness for a point in pores (or matrix) corresponds to the diameter of the largest sphere fulfilling two conditions:

(i) the sphere should encompass the point (the point should not be necessarily the centre of the sphere)
(ii) the sphere should be circumscribed by the pore boundary (or matrix boundary).

Upon knowing the pore size distribution, other distribution characteristics such as mean pore size (using log-normal fitting Eq. (10)) and the D-Values (D10, D50 and D90, the intercepts for 10%, 50% and 90% of the cumulative pore size distributions (Figure 39)) were also calculated (Chevallier et al., 2014; Hafsa et al., 2014).

$$\mathrm{f}(x) = \frac{1}{\sigma \times \sqrt{2\pi}} \times \exp\left[-\frac{1}{2}\left(\frac{x-\mu}{\sigma}\right)^2\right] \qquad (10)$$

where x is the pore size, f its volume fraction, μ its mean value and σ its standard deviation (Chevallier et al., 2014). For each freezing conditions, not less than three repetitions were done.

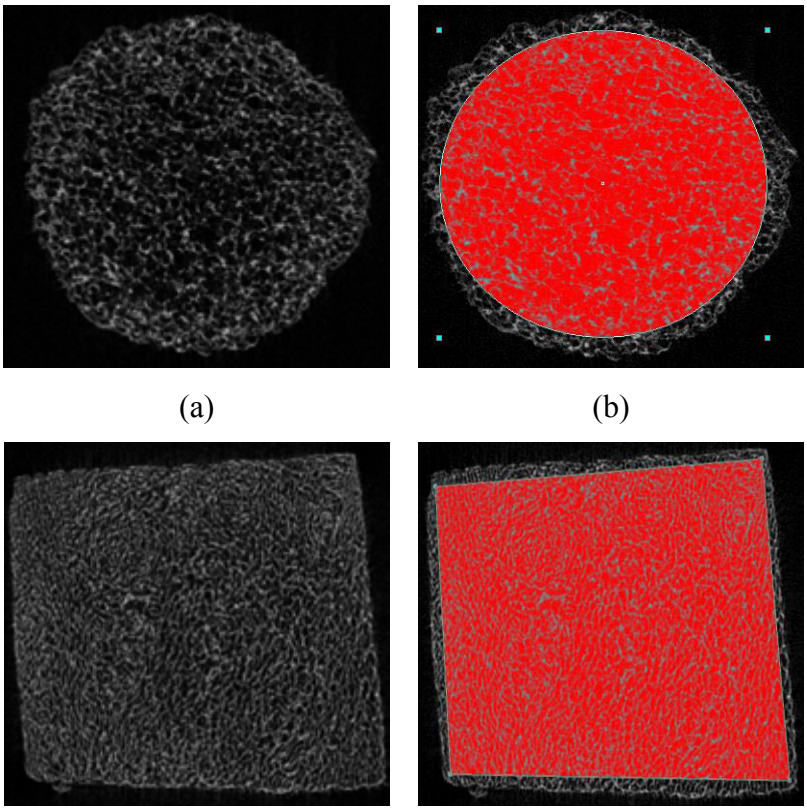

Figure 38: Process for selection of region of interest. (a) and (c) untreated image of apple and potato obtained from X-rays tomography; (b) and (d) region of interest covering more than 80% of the untreated image of apple and potato (red area masking the raw image corresponds to the region of interest).

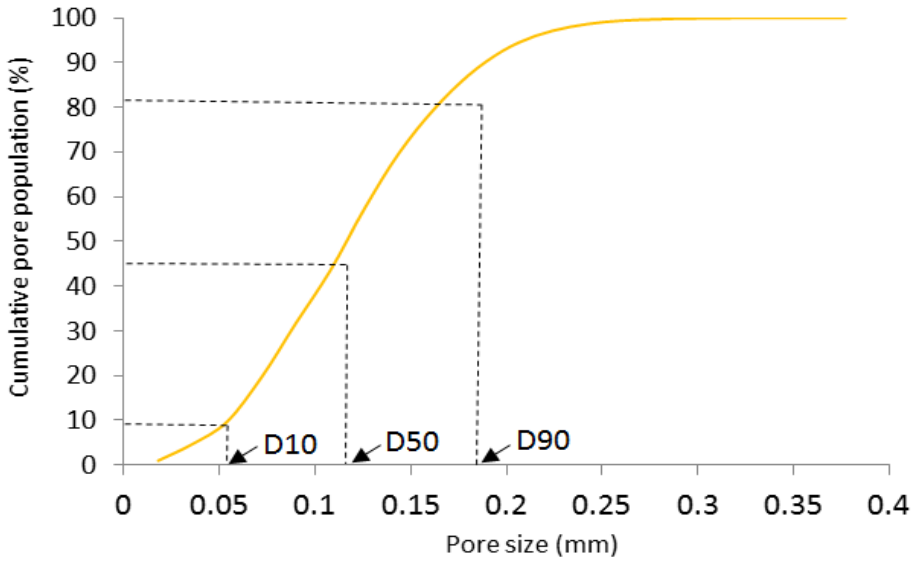

Figure 39: D-Values (D10, D50 and D90 values) of pores present in the sample.

II.9.3 Confocal laser scanning microscopy (CLSM)

The confocal laser scanning microscopy was only used for potatoes samples. Figure 40 provides a brief description of the protocol followed to prepare potatoes for the CLSM observations. The CLSM was performed using an Eclipse Ti inverted microscope (Nikon Ti A1, Japan). For each freezing condition, three replications were performed.

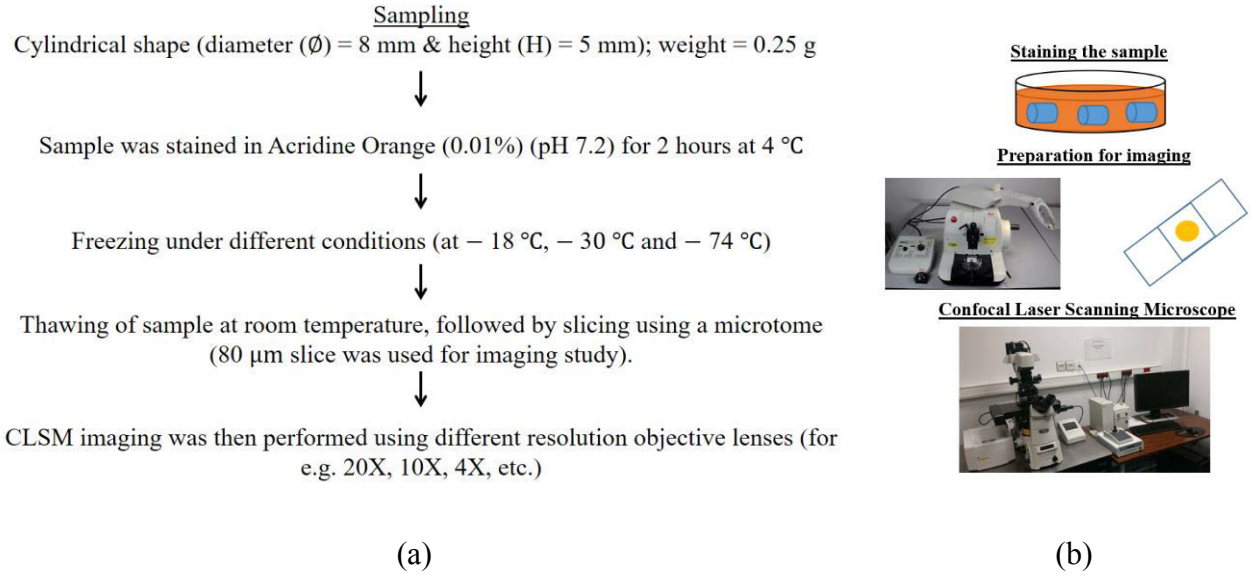

Figure 40: Protocol followed for CLSM imaging of unblanched potato.

Note: The acridine orange is well known to be a metachromic dye, especially for staining DNA and RNA. Such dye is able to give fluorescence with emissions wavelength depending on its interaction with chemical functions, charge or geometry of a compound. The acridine orange was chosen here as a dye to stain simultaneously the different cell layers of the fruits and vegetables as it has been widely applied for fluorescent staining of plant tissue with a high fluorescence emission.

II.10 NMR relaxometry

For each freezing protocols, NMR tests were performed for the sample in a frozen state (at − 20 °C) and frozen-thawed state (at 4 °C). Firstly, the frozen samples were placed in NMR tube (Ø = 10 mm) precooled to − 20 °C. Then the tube was quickly placed in the spectrometer (maintained at − 20 °C) and left for 10 min to ensure that the samples were at − 20 °C at the beginning of NMR test at a negative temperature. Upon completion of NMR tests in frozen condition, the same samples were thawed (at 4 °C for 4 h) and then NMR tests on frozen-thawed

samples (at 4 °C) were carried out. In order to compare the damage caused by different freezing procedures, the NMR measurements of fresh sample were performed at 4 °C and were compared with results obtained for frozen-thawed samples obtained under various freezing protocols. The Minispec mq20 spectrometer (Bruker) at 0.47 T (20 MHz proton resonance frequency) equipped with a thermostated ($\pm$ 0.1 °C) ^{1}H probe was used for NMR analysis. Three replications were performed for each freezing conditions for potato. While a minimum of two replications were done for apple frozen by MAF process.

In the present study, T_2 (transverse) relaxation time of protons and their respective population in the product was evaluated. The T_2 distributions were determined using a Carr−Purcell−Meiboom−Gill (CPMG) sequence. For the NMR test at frozen and frozen-thawed state, the 180° pulse separation was 0.04 and 0.1 ms, 2000 and 10000 even echoes were collected and the 1024 and 256 scans were acquired with a recycle delay of 1 and 5 s resulting in a total acquisition time of about 20 and 40 min.

An inverse Laplace transformation (ILT) was applied to convert the relaxation signal into a continuous distribution of T_2 relaxation components. For this purpose, a numerical optimization method was used by including non-negativity constraints and L1 regularization and by applying a convex optimization solver primal–dual interior method for convex objectives (PDCO).

II.11 Statistical analysis

One way ANOVA (analysis of variance) was used to determine any significant difference (in terms of freezing and quality characteristics) among the freezing conditions. Duncan's multiple range test was performed to determine differences between the means ($p < 0.05$).

III. RESULTS AND DISCUSSION

This chapter has two parts. In the first part, the impact of different freezing rates on the quality parameters of apples and potatoes (unblanched) are presented and discussed. The second part deals with the results and observation related to microwave assisted freezing (MAF) of apples and potatoes (blanched). Moreover, in this chapter, new methods developed for assessment of freeze damage are also introduced and their applicability is discussed.

Prior to reporting the results related to freezing treatments effects on freezing and quality parameters of apple and potato, we would like to present the information related to the product properties. The moisture content, freezable water amount and TSS content of apples used for this study were around $88.4 \pm 1\%$ (wet basis), $76.62 \pm 0.88\%$ and 11.89 ± 0.86 °Brix. Similarly, the average moisture content and freezable water content of potato (unblanched) were $75.70 \pm 1.40\%$ and $67.5 \pm 2.1\%$.

III.1 PART I

III.1.1 Conventional freezing of apples

III.1.1.1 Freezing curves and freezing parameters

In order to study the effect of freezing kinetic on apple's quality, different freezing protocols were applied: at − 18 ºC (slow freezing or SF), at − 40 ºC and 2 m/s air velocity (intermediate freezing or IF) and at − 72 ºC and 1 m/s air velocity (fast freezing or FF). Figure 41 shows the freezing curves of the apple cylinders under these different protocols. The SF process yielded freezing curves having three stages i.e. the supercooling, nucleation, and phase change. Meanwhile, intermediate freezing (IF) and fast freezing (FF) conditions had no evident characteristics of the above three stages, and this might be due to a rapid decrease in temperature at higher freezing rates. Similar curves (lacking distinct three stages of freezing curves) at higher freezing rates (at − 80 ºC and liquid nitrogen immersion freezing) were obtained by Cao et al. (2018) while freezing blueberries. According to them, the absence of evident three stages of the freezing curve at a higher freezing rate might be due to the instability, or lack of persistence, of the super-cooled state. The initial freezing temperature (T_{IFP}) of the apple cylinders when frozen under SF conditions were -1.83 ± 0.19 ºC, while it was not detected for IF and FF conditions. The characteristic freezing time found to be the least for FF (0.48 ± 0.19 min) followed IF (1.67 ± 0.50 min) and SF (18.61 ± 2.31 min) respectively. The shorter the time

during this stage, the lesser would be the damage to the cell structure of the apple. The overall freezing time and freezing rate followed the similar trend as characteristic freezing time and their values are presented in Table 6.

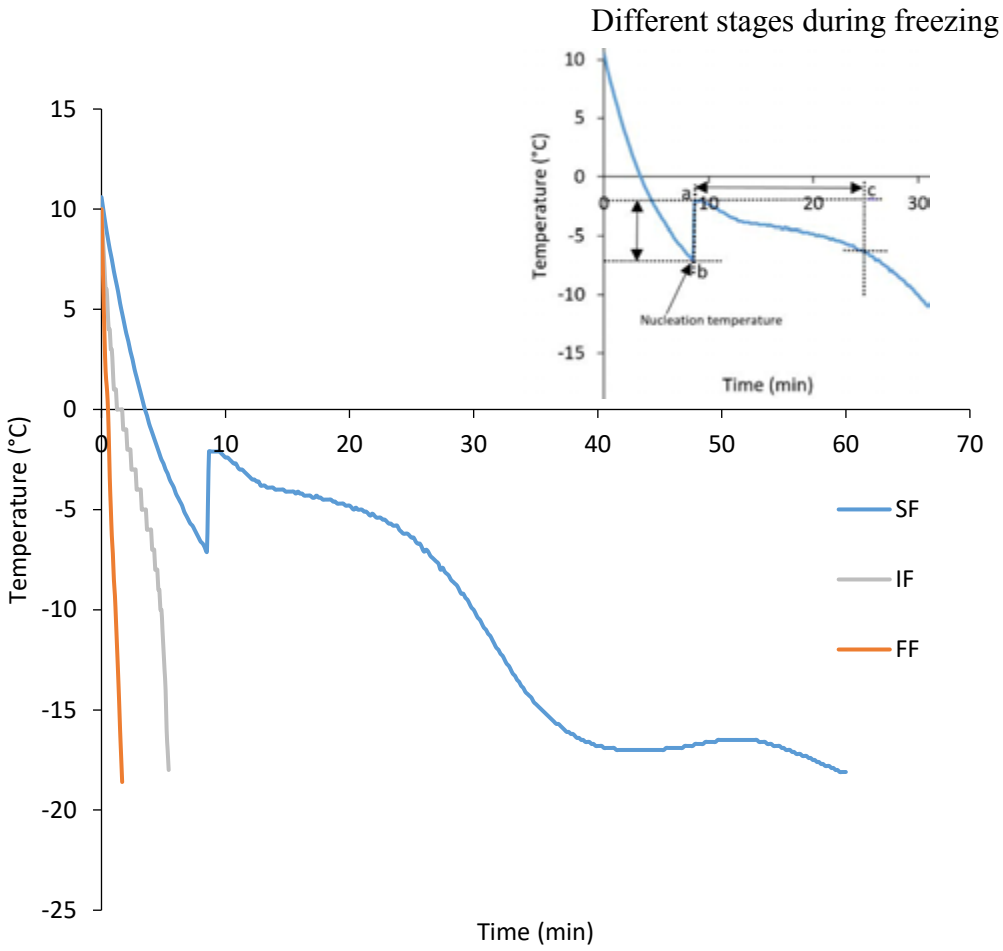

Figure 41: Time-Temperature profile of apple cylinders under various freezing conditions. The absolute value of the difference between the temperature at point "b" and point "a" is the degree of supercooling. From "a" to "b" is called the rupture of supercooling. The temperature at point "b" is the nucleation temperature. The period from ''a'' to ''c'' is the phase transition time.

Table 6. Freezing parameters of apple under different freezing rates.

Freezing condition	Characteristic freezing time (min)	Overall freezing time (min)	Overall freezing rate (ºC/min)
SF	18.61 ± 2.31	59.33 ± 0.49	0.49 ± 0.01
IF	1.67 ± 0.50	4.71 ± 0.71	6.08 ± 0.92
FF	0.52 ± 0.19	2 ± 0.33	15.16 ± 2.44

III.1.1.2 Quality parameters

III.1.1.2.1 Texture analysis

The firmness/hardness values of apple cylinders as measured by compression test cylinders are shown in Figure 42. The firmness of fresh apple cylinders was 10.62 ± 0.62 N and was significantly ($p < 0.05$) higher than the firmness values frozen-thawed samples acquired after SF, IF, and FF conditions (3.12 ± 0.53, 4.18 ± 0.28 and 4.39 ± 0.39 N for SF, IF and FF conditions, respectively). The softening of apple tissues on freezing-thawing is majorly due to the combined effect of turgor pressure decrease and cell wall modification (Chassagne-Berces, Poirier, et al., 2009). No significant difference in texture value was seen for IF and FF conditions, while these conditions had significantly firmer texture than the SF conditions. The SF condition (with lower freezing rate) yielded fewer ice crystals of large size, while IF and FF produced numerous small size ice crystals in the food. According to Mazur (1984) and Chassagne-Berces, Fonseca, et al. (2010), lower dehydration associated with small ice crystals induces less breakage of cell walls, and hence, better texture preservation is achieved at higher freezing rates than compared to the slow freezing rate. The fast freezing rates also decrease the collapse of cell walls and generate less intercellular spaces, and hence result in better texture preservation (Chassagne-Berces, Poirier, et al., 2009). No significant difference between the IF and FF process could be explained by the fact the ice crystals formed during the FF process were smaller and could have grown faster during the thawing process than compared to IF process. The migratory recrystallisation of ice, which happens when molecular mobility increases, makes possible the crystallization of residual water that is kinetically inhibited during cooling (Chassagne-Berces, Fonseca, et al., 2010). Thus, positive effect FF could have been counter-balanced by phenomenon such as recrystallization and volume changes which occurs in foods during thawing.

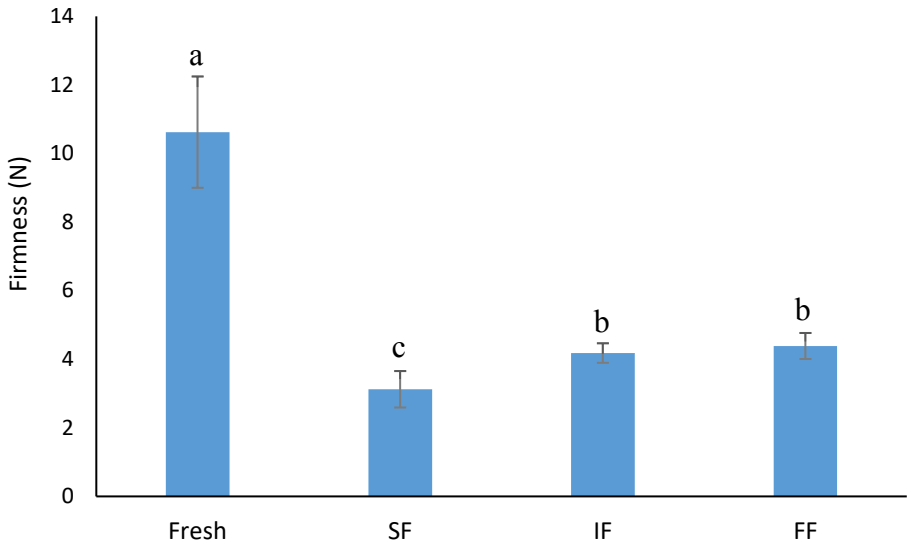

Figure 42: Effect of different protocols on firmness/hardness value of apple cylinders.

III.1.1.2.2 Impact of different freezing rates on drip loss

The drip loss from the product is linked to ice crystal size. Faster freezing rates causes fine crystals in the product that is uniformly distributed throughout the product and minimizes the decompartmentalization of water. As a result, the destruction to cell membranes is less and fewer mass is lost during thawing. Another reason for fewer drip loss due to smaller ice crystals is the larger specific surface area, which assist the water re-absorption during thawing (Sadot et al., 2017). Figure 43 represents the drip loss (%) measurements made after thawing the samples frozen under different conditions. The result showed that drip loss value had an inverse dependence on freezing rates, and a significant difference ($p < 0.05$) could be detected between FF sample and SF samples. No significant difference existed between IF and FF samples or IF and SF samples. Our results are in accordance with Charoenrein & Owcharoen (2016) and Fuchigami et al. (1995), who found that the drip loss (from frozen mangoes and carrot) followed a reducing tendency when the freezing rate was increased.

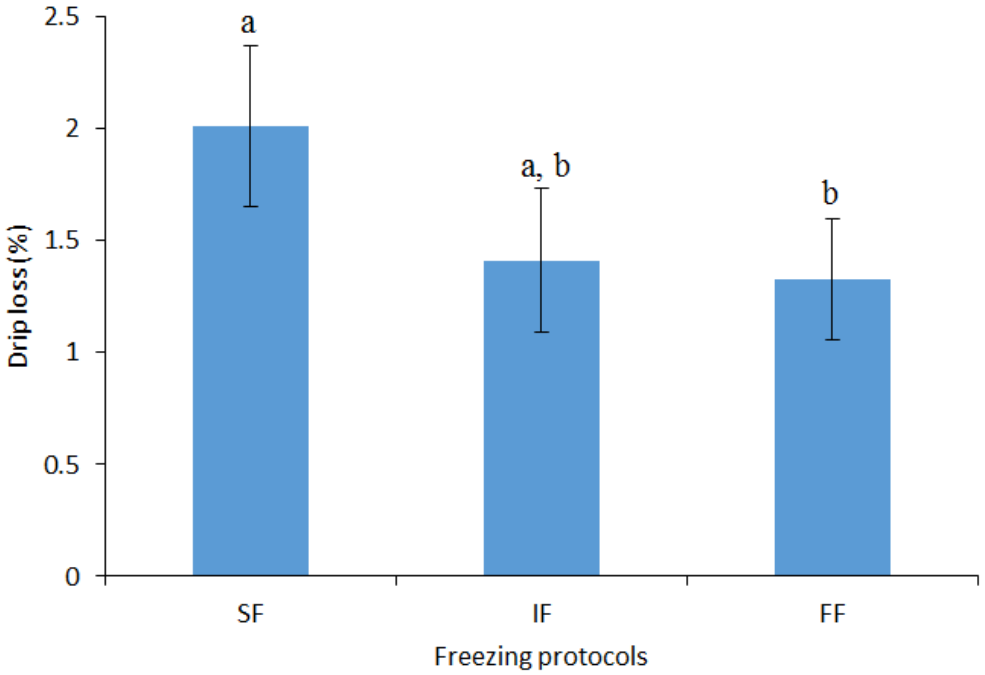

Figure 43: Exudate loss from apple after freezing at different freezing rates.

III.1.1.2.3 Solute gain

From the preliminary studies, it was evident that an unstable phenomenon of gaining and losing solute occurred during the treatment period. At present, the mechanism for such trend of solute gain (during diffusion test) inside the apple cylinders is a bit complicated to explain. However, some interesting results related to solute diffusivity in the case of fresh and frozen-thawed sample are presented below.

Figure 44 presents the solid gain by the fresh and frozen-thawed sample during osmotic treatment of three hours. It can be seen that the fresh sample gained comparatively less solute than all frozen and thawed samples. This provides an evidence that ice formation and melting during the freezing-thawing process might have distorted the cell structures and increased the permeability of cell membranes, ultimately resulting in a higher solute gain (Alizadeh et al., 2009). In fact, diffusion in intact cellular tissues (e.g. fruits and vegetables) occurs mainly in the intercellular spaces. When the pectocellulosic walls are disrupted, different path appears resulting in an increase in mass diffusivity. Furthermore, the damage of the disrupted pectocellulosic walls could explain the higher solid intake for damaged tissues. The solute uptake for all freezing condition was found to be inconsistent during the test period; the phenomenon of gaining and losing solute occurred during the treatment period for all conditions. Thus, fitting these data into diffusion model and obtaining mass transfer coefficient

value that would allow easy comparison (between freezing protocols) was not possible. The inconsistency in the solute gain was observed mainly between 0.5 to 2 h for all freezing trials. The solute gain for each condition reached steady state after 2 h. In order to compare the freezing methods, the average value of solute gain after steady state was considered (average of data at 2, 2.5 and 3 h). It was observed that FF conditions resulted in significantly ($p < 0.05$) lower solute gain ($4.71 \pm 0.60\%$) during treatment period than SF ($6.26 \pm 0.51\%$) condition depicting better preservation of cellular structure and cell membranes integrity under FF condition. As evident in Figure 45, SF process favoured the formation larger ice crystal in the apples, and this would have caused higher dehydration of the cells, thus resulting in greater breakage of cell wall and higher solid intake (during osmotic treatment). The solute uptake by IF ($5.63 \pm 0.74\%$) sample was neither significantly different with FF sample nor with SF sample. The trend followed by solute gain was found to be coherent with drip loss pattern (Figure 43) observed for different freezing conditions. Based on these results, it can be concluded that mass diffusivity methods can only detect a large difference in the quality or can discriminate the freezing protocols when the magnitude of the difference between freezing rates (offered by freezing conditions) is very high.

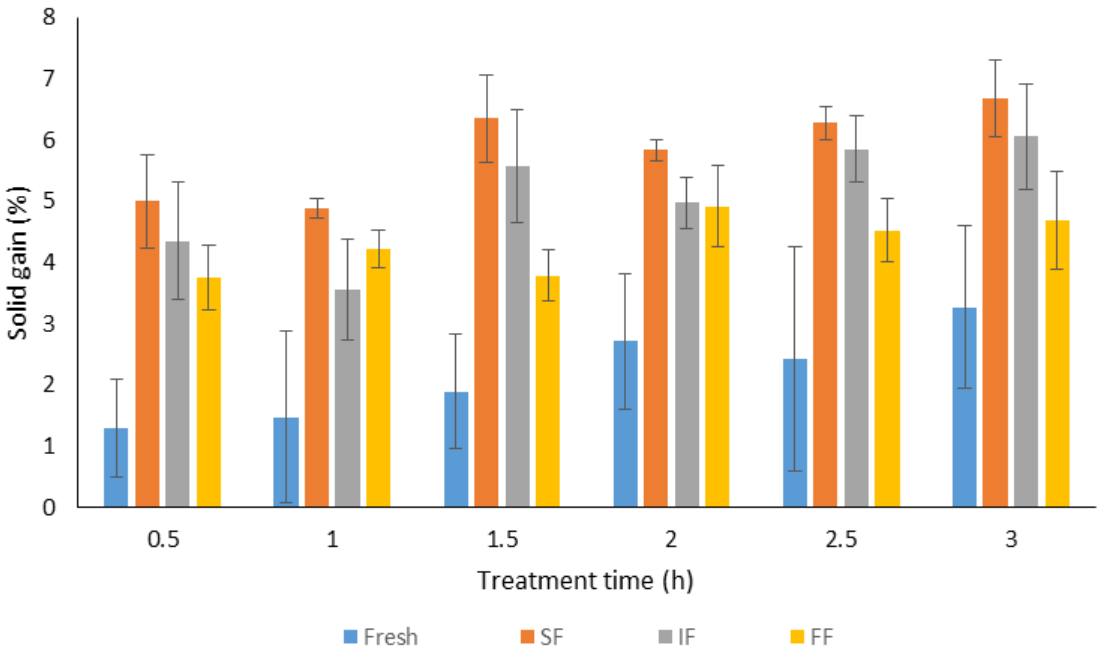

Figure 44: Solid gain for fresh and frozen-thawed sample.

III.1.1.2.4 Microstructure analysis using cryo-SEM

The impact of different freezing rates on ice crystals size was studied using cryo-SEM method. Figure 45 shows images of apples frozen with different freezing protocols. The bright regions

in the micrographs are the solidified solutes of the cell sap, the cytoplasmic membrane, and the cell walls. The darker regions in the micrographs are ice; some dark regions (indicated by letter A in the pictures) are the air space between two cells. As expected, SF sample had larger ice crystals. IF sample had relatively smaller ice crystals than SF sample but was a little larger than FF sample. FF sample had numerous small size ice crystals. The calculations for ice crystals size were no made as it was difficult to locate the boundary of the ice crystals. Moreover, the ice crystals had a 3D structure and if the calculation were made we could get only 2D information, this would have led to wrong estimation of the size of the ice crystals. Similar to Bomben & King (1982), Chassagne-Berces, Poirier, et al. (2009) and Chassagne-Berces, Fonseca, et al. (2010), we also observed that slow freezing process altered the shape of the cell wall than compared to the fast freezing processes (cell wall pointed with arrow in the Figure 45).

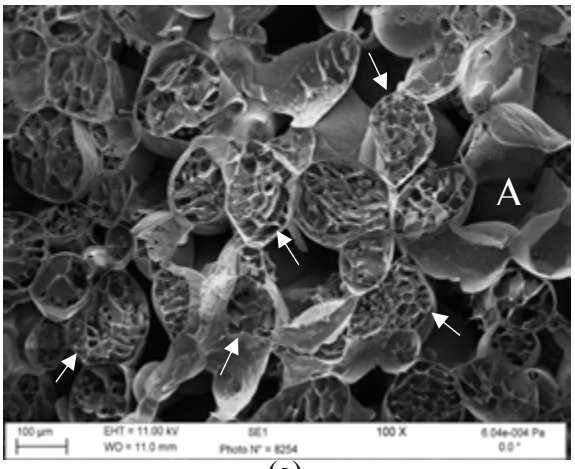

(a)

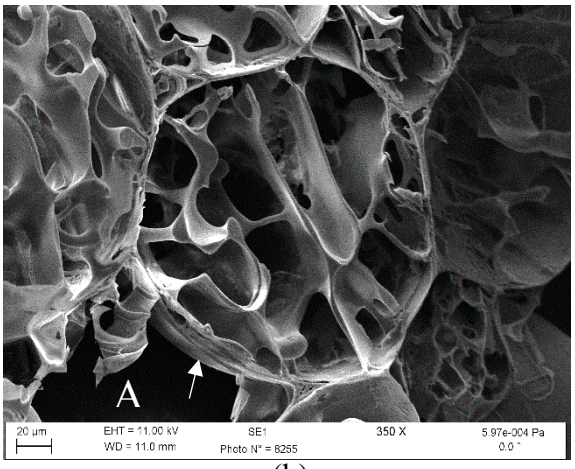

(b)

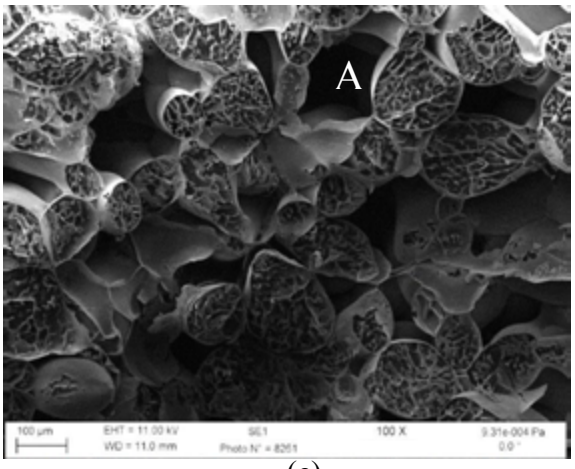

(c)

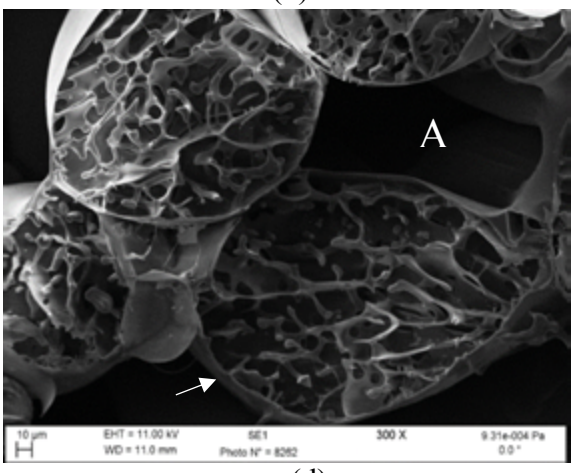

(d)

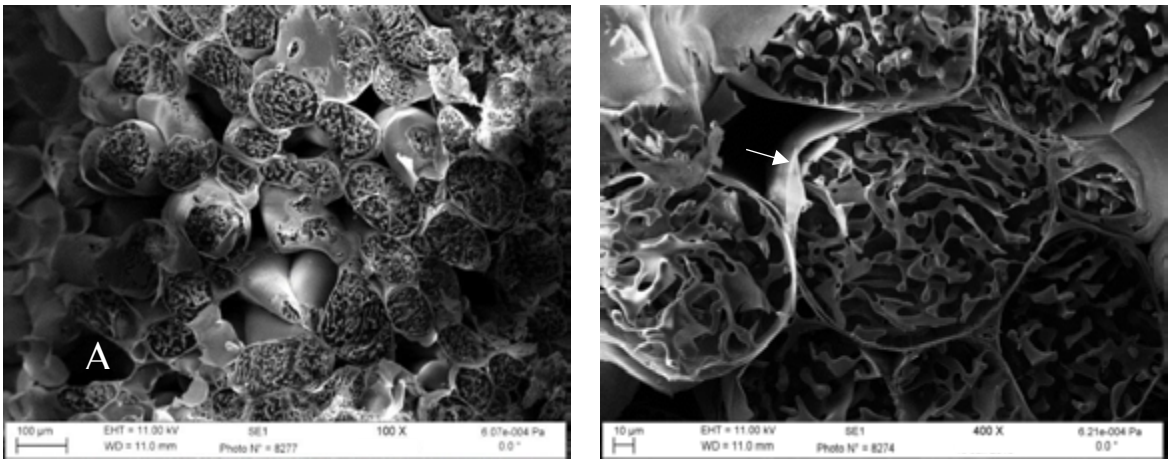

(e) (f)

Figure 45: Microstructure of apple under different freezing conditions: (a), (b) SF (at – 18 ℃); (c), (d) IF (– 40 ℃); and (e), (f) FF (at – 72 ℃). Cell membranes are arrowed. "A" is the intercellular air space present in the sample.

III.1.2 Potato freezing under different freezing rates

III.1.2.1 Effect of different freezing rates on freezing profile

The freezing curve profile of potatoes frozen by different freezing methods is presented in Figure 46. The supercooling curve was seen only for SF condition. The degree of supercooling of 0.15 ± 0.07 ºC was observed for the SF condition. No supercooling curve was noticed for other freezing conditions. The initial freezing point for SF and IF condition was recorded as -0.3 ± 0.14 and -0.73 ± 0.06 ºC (Table 7). It seems that depression in freezing point happened upon increasing the freezing rate. For FF condition, it was hard to detect the initial freezing point due to a rapid decline in the temperature during the freezing process. Among other freezing parameters being studied, the characteristic freezing time was found to be the shortest for FF condition (8.52 ± 1.53 min), followed by IF and SF condition (17.18 ± 0.79 min and 29.12 ± 3.94 min respectively) (Table 7). The time spent in this zone is very crucial as it determines the quality of the final product. From the perspective of better quality preservation, a shorter width of this zone is desired. Similar to characteristic freezing time, the overall freezing time and the overall freezing rate also exhibited the similar trend.

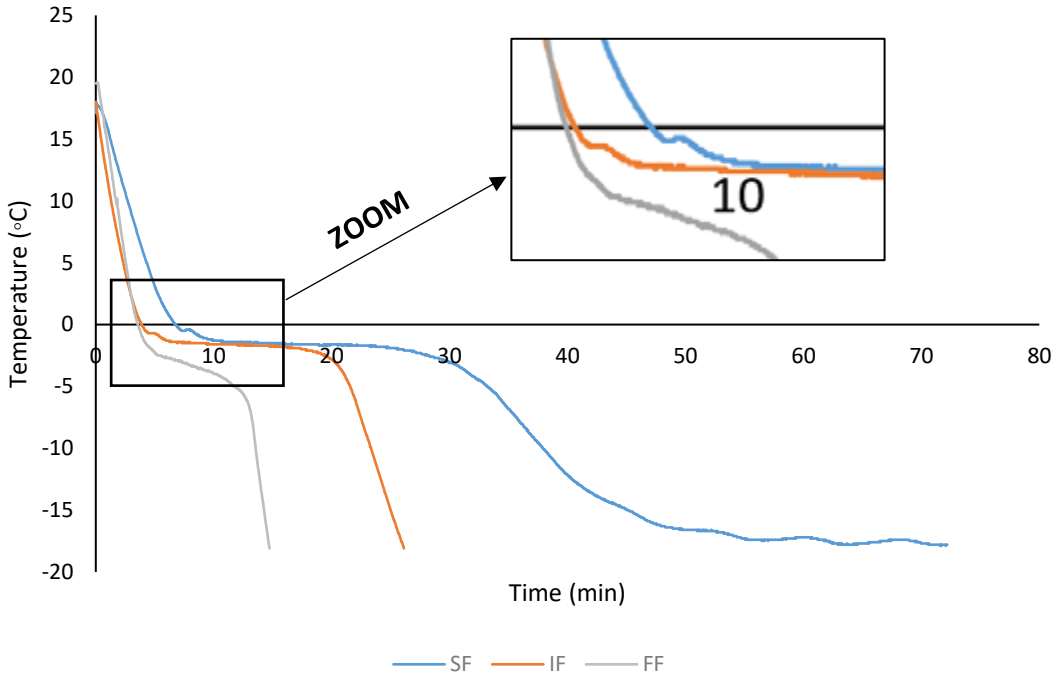

Figure 46: Freezing curves of potatoes under different freezing methods.

Table 7. Effects of different freezing protocols on the freezing properties of potatoes.

Freezing condition	Initial freezing point (°C)	Characteristic freezing time (min)	Overall freezing time (min)	Overall freezing rate (°C/min)
− 18 °C (SF)	− 0.3 ± 0.14	29.12 ± 3.94	72.30 ± 0.14	0.48 ± 0.00
− 30 °C (IF)	− 0.73 ± 0.06	17.18 ± 0.79	26.31 ± 0.62	1.36 ± 0.05
− 74 °C (FF)	-	8.52 ± 1.53	14.77 ± 1.48	2.54 ± 0.26

III.1.2.2 Texture analysis

III.1.2.2.1 Conventional method

The confined compression test was the conventional method used to determine the texture of potatoes. The hardness and Young's modulus values of fresh and thawed sample (from different freezing conditions) are shown in Table 8. The values of fresh sample were significantly different ($p < 0.05$) from those of frozen-thawed samples. FF process caused less decay in hardness value (≈ 50%) than IF process (≈ 62%) or SF process (≈ 74%). However, significant difference in hardness value was observed only between SF and FF samples. Young's modulus values exhibit a similar tendency as hardness values Table 8.

Table 8. Textural parameters measured for potatoes under different freezing conditions.

Parameters	Hardness (N)	Young's modulus (MPa)
Fresh	190 ± 19[a]	5.46 ± 0.44[a]
SF (at − 18 °C)	47 ± 11[c]	1.37 ± 0.33[c]
IF (at − 30 °C)	68 ± 16[b, c]	2.09 ± 0.41[b, c]
FF (at − 74 °C)	90 ± 8[b]	2.60 ± 0.45[b]

III.1.2.2.2 Laser-Puff firmness tester

Laser-Puff firmness tester allows rapid and non-destructive texture analysis of the food products (Hung et al., 1998; McGlone & Jordan, 2000; Prussia et al., 1994). An attempt was made to use this method, to the best of our knowledge for the first time, to measure the texture of frozen-thawed fruits and vegetables. In this section, the results from laser-puff firmness analysis of potato will be presented and discussed. The deformation curves and deformation values obtained during laser-puff firmness test of fresh and frozen-thawed potatoes (under different freezing rates) are shown in Figure 47a and b. The fresh sample had significantly ($p < 0.05$) lower deformation value than all frozen-thawed sample (Figure 47b). As expected, SF sample suffered the highest deformation during the test. The deformation sustained by IF sample was less than SF sample, but more than the FF sample. However, the deformation values of IF

samples were not significantly different ($p > 0.05$) with values of SF and FF samples. The FF sample showed lower deformation than the other conditions. Its values were found to be significantly lower than SF sample values, but not significantly different with IF sample values. The obtained results (in terms of deformation) are coherent with those obtained by classical method (discussed above). Using this method, it was possible not only to distinguish fresh and frozen-thawed samples but also to distinguish the different freezing conditions.

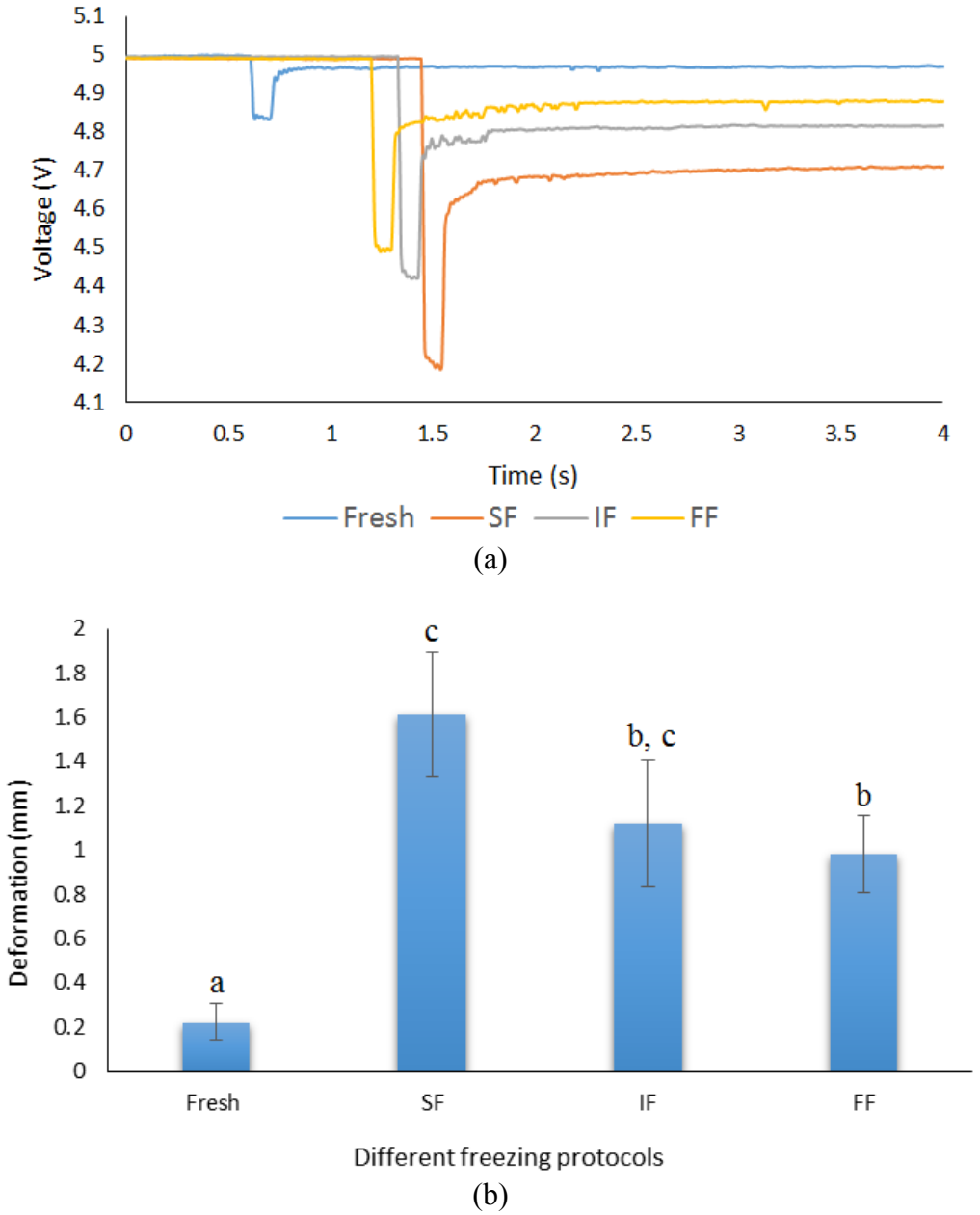

Figure 47: (a) Deformation curve obtained for fresh and frozen-thawed samples (conversion of volts to mm: 1 V = 2 mm) and (b) deformation values (in mm) for fresh and frozen-thawed potatoes (under different freezing rates) acquired using laser-puff firmness tester. SF (slow freezing at − 18 °C), IF (intermediate freezing at − 30 °C) and FF (fast freezing at − 74 °C).

III.1.2.3 NMR relaxometry

Figure 48 shows the results from NMR relaxometry of potato in a frozen state (at − 20 °C). The relaxation peaks, T_2^* (including magnetic field inhomogeneities) and T_2 of frozen samples provide information about the structure of the samples and about the unfrozen water at − 20 °C, that is to say water in very strong interaction (Figure 48). $T_{2\alpha}^*$ is the relaxation peak of protons associated with the macromolecules. $T_{2\beta}^*$, $T_{2\gamma}$, and $T_{2\delta}$ are the relaxation peaks associated with the protons of unfrozen water. Results showed that the $T_{2\alpha}^*$ values (relaxation time and proton population) for all freezing conditions were similar (Figure 48a). If we follow the hypothesis that the faster the freezing, the less is the destruction, the values of relaxation peak components of non-freezable water ($T_{2\beta}^*$, $T_{2\gamma}$, and $T_{2\delta}$) associated with the samples frozen quickly provides an evidence of better preservation of structures. Only samples that were frozen slowly (at − 18 °C) showed different values for these relaxation peak components (Figure 48a and b). It was observed that $T_{2\gamma}$ component values (relaxation time and proton population) for IF and FF conditions were not significantly different ($p > 0.05$) from each other, meanwhile, these values were significantly different ($p < 0.05$) with that obtained for SF condition. The lowest value of $T_{2\gamma}$ time observed for slow freezing (0.72 ms instead of around 0.80 ms for the other freezing conditions) can be explained by a greater destruction followed by a diffusion of "solutes" inducing a relative increase in viscosity. The $T_{2\delta}$ component relaxation times for all freezing conditions were not different from each other. But, the $T_{2\delta}$ component proton population was significantly lower ($p < 0.05$) for SF than compared to other conditions. This indicates loss of fluid from the respective water compartment due to greater damage offered by SF process. No significant difference ($p > 0.05$) (with respect to $T_{2\delta}$ component proton population) was observed among IF and FF samples.

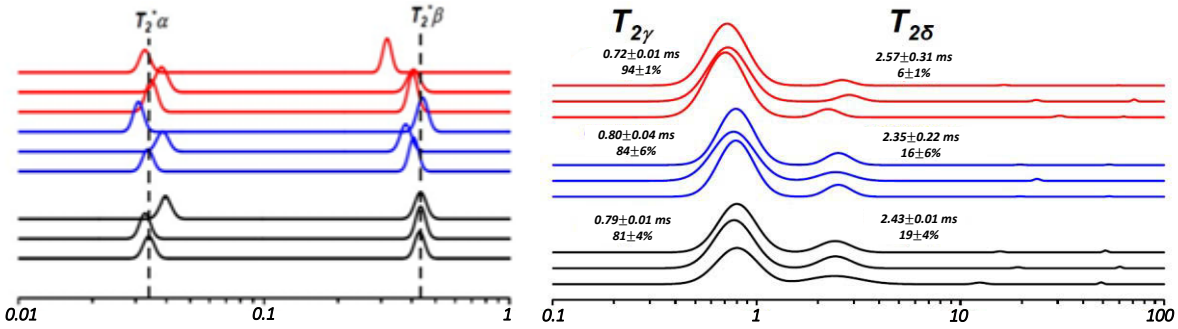

(a) (b)

Figure 48: Distributions of relaxation peak components ((a) T_2^* and (b) T_2) at − 20 ℃ of potato samples frozen by various freezing protocols: slow freezing at − 18 ℃ (red lines), intermediate freezing at − 30 ℃ (blue lines), and fast freezing at − 74 ℃ (black lines). (The x-axis correspond to the relaxation times expressed in ms (miliseconds)).

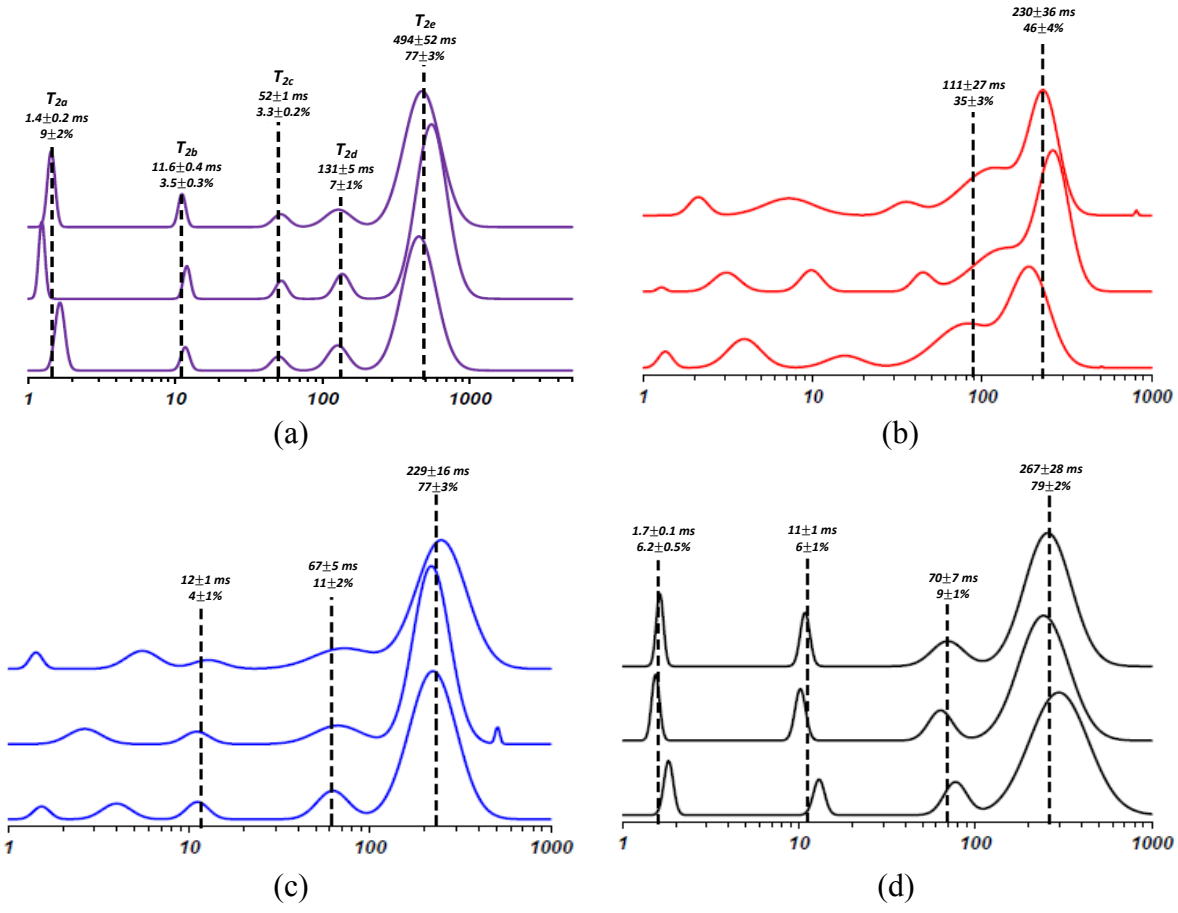

(a) (b)

(c) (d)

Figure 49: T_2 relaxation peak data of frozen-thawed potatoes at 4 ℃: (a) fresh sample, (b) after freezing at − 18 ℃ (c) after freezing at − 30 ℃ and (d) after freezing at − 74 ℃.

Figure 49 represents the T_2 peaks of fresh and frozen-thawed samples at 4 ℃. With regard to fresh samples, the distribution of T_2 relaxation peak has five components (T_{2a}, ..., T_{2e}), whose values averages are in good agreement with the literature data (Rutledge, Rene, Hills, & Foucat,

1994). Based on these data, an allocation of different components of T_2 are proposed: T_{2a} and T_{2b} are the relaxation peaks associated with water present in the cell walls and the vacuolar membrane. T_{2c} is the relaxation peak of water in starch grains. T_{2d} and T_{2e} are the relaxation peaks of water in the non-starch vacuoles, the nucleus and the cytoplasm (Rutledge et al., 1994). The measurement of the T_2 components values (relaxation time and proton population) of the samples after thawing makes it possible to observe the influence of different freezing protocols on the mobility of the water compared with the fresh samples. It can be seen that the freezing-thawing process affects the resolution of the T_2 distribution peaks (Figure 49). For instance, the T_{2c} and T_{2d} components which were distinctively visible in the fresh sample could no longer be differentiated in the frozen-thawed sample. Apart from this, T_{2d} and T_{2e} time of fresh potato decreased upon freezing-thawing.

Among freezing conditions, only FF (at -74 °C) preserved T_2 components distributions with good resolution over the entire time range studied. Four T_2 components were characterized for FF (against five for fresh samples), meanwhile, for IF and SF conditions, three and two T_2 components could only be characterized. For all freezing conditions, the mobility of water associated with non-starch vacuoles, nuclei and cytoplasm (T_{2d} and T_{2e}) decreased. This reflects a reorganization of the fluids following a partial rupture of the cellular structures (Lahaye, Falourd, Limami, & Foucat, 2015) irrespective of the freezing speed. Compared to fresh sample, the decrease in T_{2e} time was least for FF process ($\approx$ 46%), and was followed by SF ($\approx$ 53%) and IF ($\approx$ 54%) process. However, no significant difference among freezing processes (in terms of T_{2e} time) was observed. T_{2e} component proton population data reveal that FF and IF samples had similar values ($p > 0.05$) as the fresh sample, while it significantly decreased ($p < 0.05$) in the case of SF samples. This decrease was followed by an increase in proton population of the consecutive peak in the T_2 distribution curve for SF samples (Figure 49b), depicting the transfer of water between two compartments which might have probably happened due to the breakdown of vacuolar membrane. However, no such trend was observed for other freezing conditions (Figure 49c and d). The T_2 component values (relaxation time and proton proportion) adjacent to the T_{2e} for SF samples was significantly different ($p < 0.05$) from that of FF and IF conditions. The T_{2a} and T_{2b} components of FF samples had similar relaxation times as the fresh samples, illustrating the overall preservation of membranes and walls (despite a reorganization at the level of populations). IF also fairly maintained the T_{2b} component values and were found similar to the fresh sample. Due to poor resolution, it was

difficult to extract T_{2a} component value for IF samples. T_{2a} and T_{2b} component values for SF sample also could not be resolved due to the poor resolution of the peak.

III.1.2.4 Drip loss

Figure 50 shows the dependence of drip loss on freezing rate. The results reveal that drip loss decreased slightly when freezing rate was increased, however, significant difference was observed only between samples that were frozen under FF and SF conditions. IF samples were not significantly different ($p > 0.05$) with samples from other two freezing rates. The drip loss results exhibited similar trends to those of T_{2e} component proton population from NMR that showed that the application of − 18 °C freezing protocol least maintained the intracellular water content.

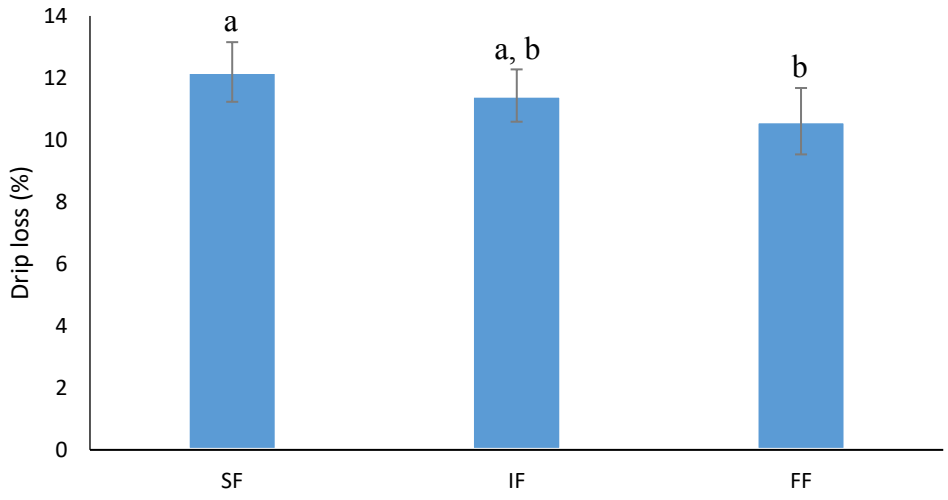

Figure 50: Effect of different freezing conditions on the drip loss of potato.

III.1.2.5 Colour

Freezing-thawing process significantly ($p < 0.05$) affected the colour parameters (L^*, a^*, and b^* values) of the unblanched potatoes (Figure 51). The L^* value (or lightness) and b^* value (or yellowness) decreased, while the a^* value (redness) increased for potatoes after freezing-thawing (Figure 51a, b and c). These results are in agreement with the previously reported study on freezing-thawing of unblanched potatoes (Koch et al., 1996). The colour change during the freezing-thawing process of unblanched potato has been attributed to the browning reaction that generally happens due to enzyme activity during thawing process (Cano, 1996; Koch et al., 1996). The freezing rates had little effect on the colour parameters of potatoes. Interestingly, it

was found that FF process increased the redness value of potatoes significantly ($p < 0.05$) than compared to SF process. Chassagne-Berces, Fonseca, et al. (2010) reported that freezing at − 80 °C increased the redness value of Golden Delicious apple compared to freezing performed at − 20 °C. The redness value of IF samples was not significantly different with that from FF and SF samples. No significant difference for other colour parameters (L^* value, b^* value and ΔE) were observed among the freezing protocols.

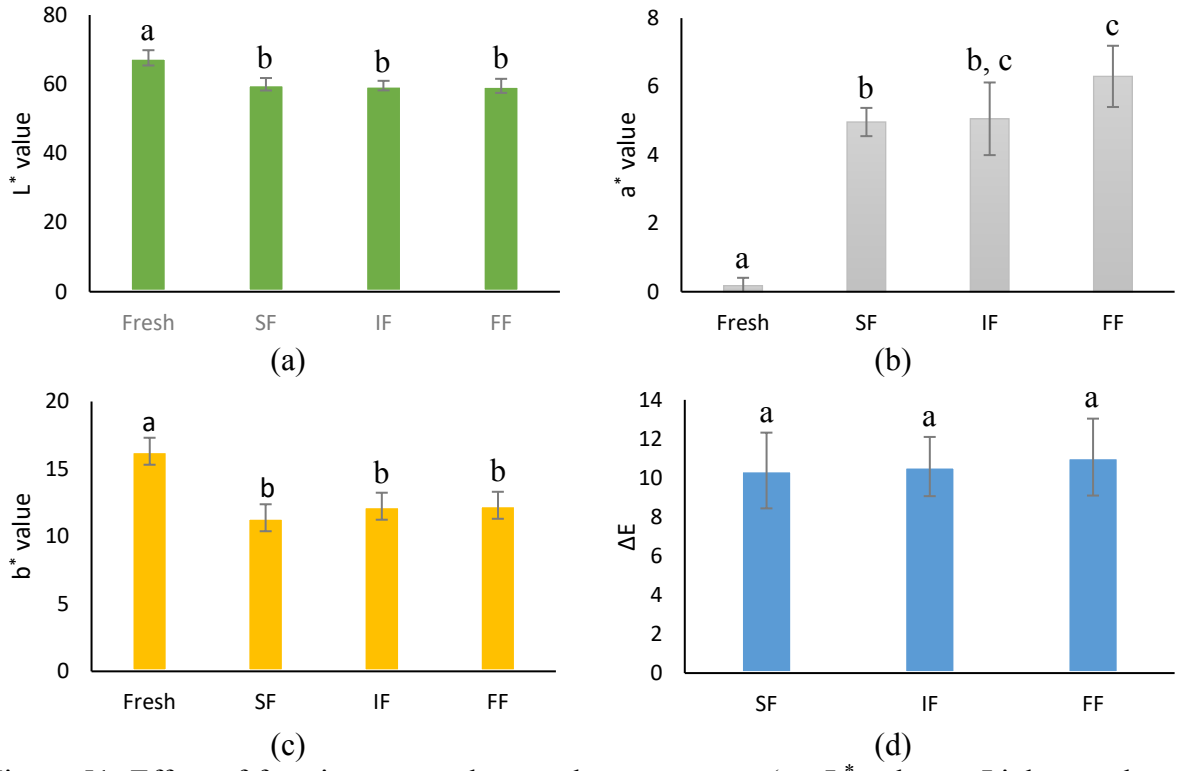

Figure 51: Effect of freezing protocols on color parameters (a - L^* value or Lightness, b - a^* value or Redness, c - b^* value or Yellowness and d - ΔE) of potato. Means of 9 repetitions are represented with confidence interval.

III.1.2.6 Microstructure analysis

III.1.2.6.1 Cryo-SEM analysis

Figure 52 illustrates the SEM images of fresh and frozen potatoes. The images of fresh and frozen potato were obtained using an environmental SEM (E-SEM) and cryo-SEM, respectively. It can be seen in the figure that the fresh potato has polyhedral cells with starch imbedded in them. The microstructure morphology upon freezing depended highly on the freezing rate being applied. The SF process not only created bigger ice crystals in the cells but also caused the highest damage to the cellular structure. The cells were highly distorted (deformed cells with broken and irregular cell wall structure) under SF conditions. The IF

process maintained the cellular structure and produced smaller ice crystals than the SF conditions. The FF process yielded smallest ice crystals compared to other freezing processes. Moreover, it also well maintained the cellular structure.

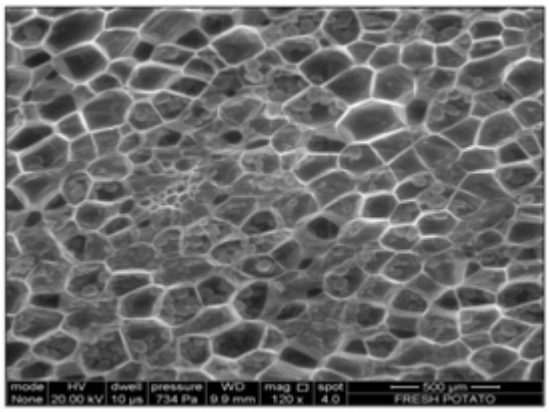
(a)

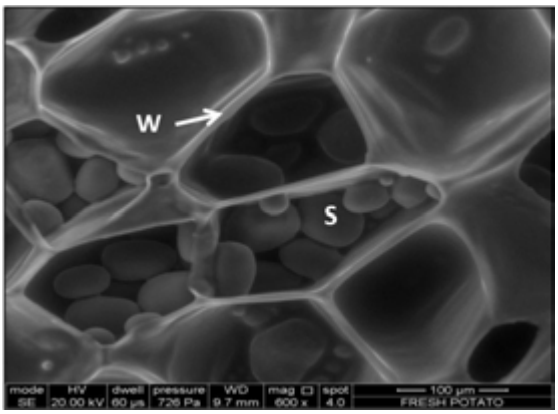

(b)

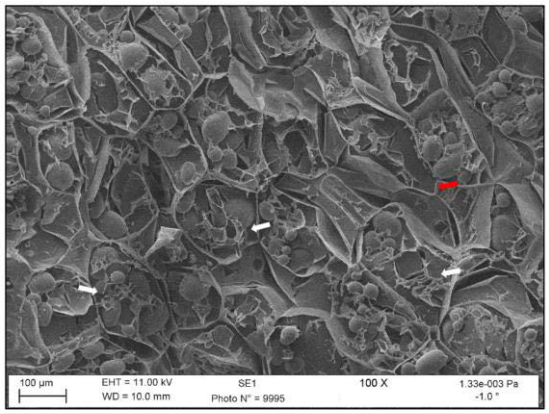

(c)

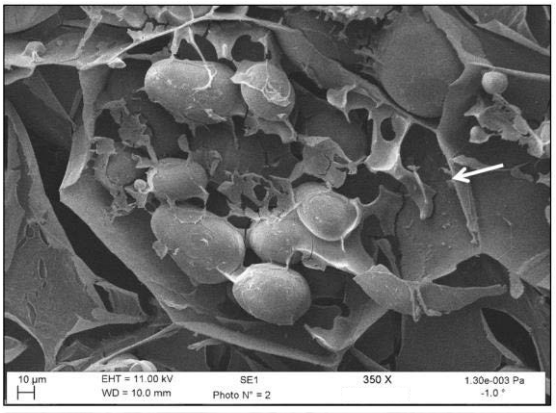

(d)

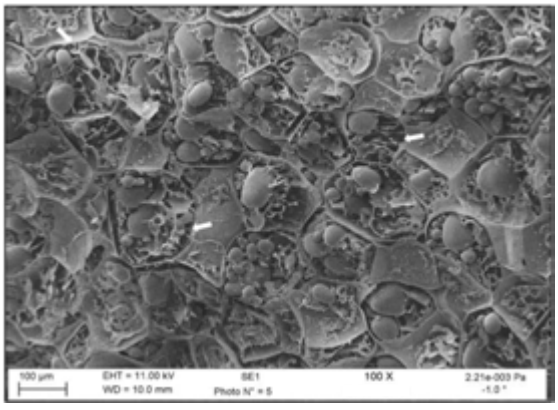

(e)

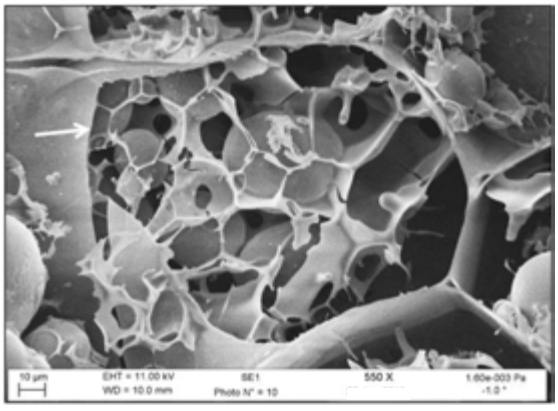

(f)

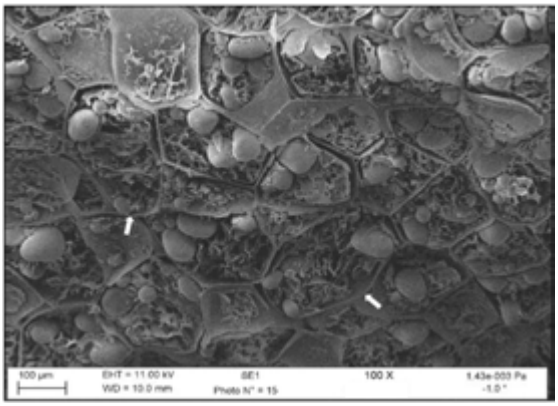
(g)
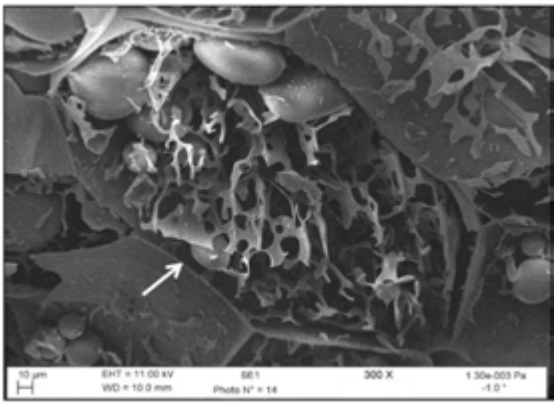
(h)

Figure 52: Microstructure of potato before and after freezing under various freezing protocols. (a, b) environmental SEM images of the fresh cell showing the cellular structure and starch granules imbedded into it. Cryo-SEM after freezing at − 18 ℃-SF (c, d), at − 30 ℃-IF (e, f) and at − 74 ℃-FF (g, h), respectively. White colored arrows in images are pointing the cells containing ice crystals. Red arrow showing the area where the breakdown of cell structure happened. Other abbreviations in the picture are A: air space; S: starch granule; W: cell wall and membrane structure.

III.1.2.6.2 CLSM analysis

CLSM images of fresh and frozen-thawed potatoes are presented in Figure 53. This method provides information about the status of the cell such as the shape of cells and integrity of the pectocellulosic walls. Compared to the fresh sample, the cells were highly disorganised and distorted in SF samples. The altered shape of the cell and damaged cell wall structure in the slowly frozen sample are clearly evident in the CLSM images (Figure 53). The buckled and folded cell wall structure in SF samples indicates a major dehydration related damage that generally happens at a lower freezing rates. IF process affected the shape of the cell, meanwhile it seemed to preserve the integrity of the cellular structure. FF condition helped to preserve the original shape and integrity cellular structure. Charoenrein & Owcharoen (2016) used CLSM to study the effect of freezing rates and freeze-thaw cycles on the cellular structure of mangoes. Using this method, they were able to observe the freezing-thawing related degradation of cellular structure. Moreover, based on CLSM images, they were able to discriminate the different freezing protocols (i.e. freezing at − 80, − 40 and − 20 ℃).

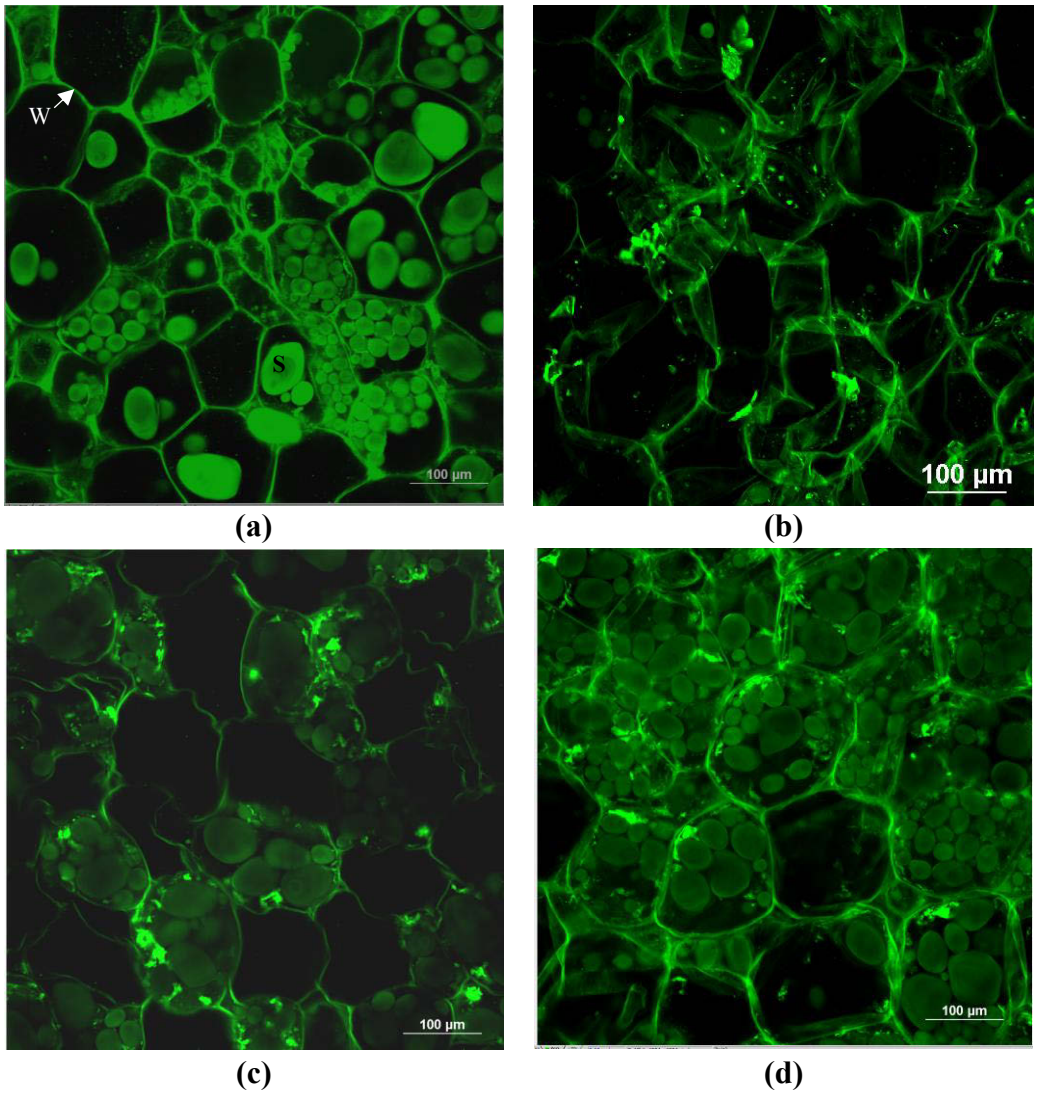

Figure 53: Microstructure evaluation using CLSM: (a) fresh potato; frozen-thawed after freezing at − 18 ℃-SF (b), at − 30 ℃-IF (c) and at − 74 ℃-FF (d). Other abbreviations in the picture are S: starch granule; W: cell wall and membrane structure.

➔**Intermediate conclusions:**

The impact of three freezing protocols on the quality parameters of apple and unblanched potato was investigated using different classical and new analytical methods in this section. As expected fast freezing process produced smaller ice crystals distributed uniformly throughout the food matrix (evident in cryo-SEM micrograph), and thus caused least dislocation of water. As an outcome, damage to the cellular structure was less, and hence greater quality preservations (in terms of texture, water holding capacity) could be achieved. On the contrary, the slow freezing process caused greater freeze damage (higher drip loss and texture loss) due to the production of larger ice crystals that facilitated dislocation of water leading to greater shrinkage and damage of the cellular structure.

The benchmarking study on freeze damage assessment methods reveals microstructure evaluation as the best choice to compare different freezing protocols as it can detect small quality changes. Meanwhile, the global methods such as texture analysis, NMR, drip loss and mass diffusivity tests provide important information about the freeze damage, however, they can only reflect large quality changes.

To the best of our knowledge, for the first time, laser-puff firmness analyzer was used for determining the texture potato. Similarly, mass diffusivity test was also performed for the first time to evaluate the damage occurring in apples due to the freezing-thawing process. Both methods were able to discriminate fresh and frozen-thawed samples. Besides, they were also able to differentiate fast and slow frozen samples.

III.2 PART II

III.2.1 MAF of apples

For the freezing of apples further than the conventional freezing (in the absence of microwave), pulsed power MAF conditions such as P1MAF (10 s /500 W/kg – 20 s /0 W/kg) and P2MAF (10 s /667 W/kg – 20 s /0 W/kg), constant power MAF condition (CMAF = 167 W/kg) were used. In this section, the results (in terms of freezing and quality parameters) obtained upon freezing apples under the aforementioned freezing conditions will be presented and discussed.

III.2.1.1 Effect of MAF on freezing process of apple cylinders

The shapes of the freezing curves obtained during conventional freezing and MAF of apples were identical to each other (Figure 54). Further, the representative time-temperature profile (Figure 54) demonstrated that the application of microwaves (MWs) during the freezing process had no significant impact on overall freezing time. The characteristic freezing times for all tested conditions were not significantly different from each other (Table 9). The current findings are in accordance with Hafezparast-Moadab et al. (2018) who found that the application of RF (radio frequency) during the freezing of fish matrices did not affect the shape of the freezing curve and the total freezing time. Xanthakis et al. (2014b) observed lower freezing rate and thus longer freezing time during MAF freezing of pork meat at different power levels. At this point, we need to remark that the freezing time during MAF of food depends not only on the power of microwaves but also on the S/V (surface to volume ratio) of the food product (Figure 55 and Table 9). For instance, when the S/V of the product was decreased from 7 cm^{-1} to 5 cm^{-1}, the characteristic freezing time for sample frozen under control freezing condition, CMAF, P1MAF and P2MAF increased from 6.58 ± 0.50, 7.14 ± 0.55, 6.75 ± 1.54 and 6.25 ± 0.52 min to 8.25 ± 0.41, 10.56 ± 0.86, 10.83 ± 0.35 and 10.47 ± 0.86 min, respectively. The larger S/V ratio might have aided in quicker dissipation of heat generated during microwave exposure and this, in turn, may have prevented an increase in the characteristic freezing time. These results indicate that the S/V of product can affect the characteristic freezing time during MAF of food.

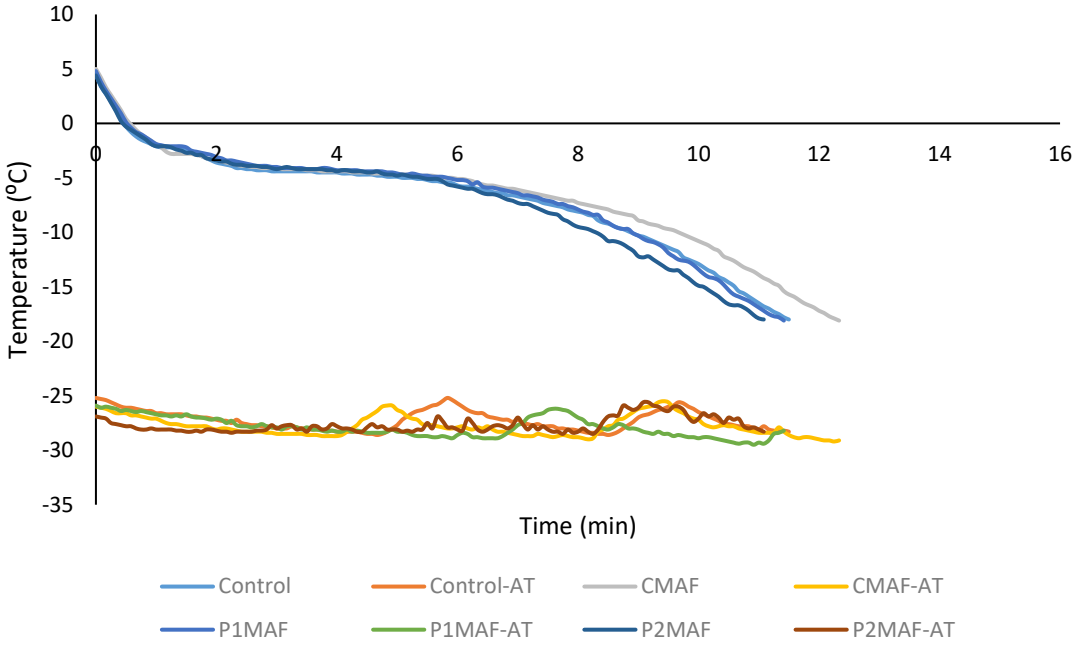

Figure 54: Freezing curve obtained during MAF of apple for sample having S/V of 7 cm^{-1}. "AT" attached in the legend for each freezing conditions relates to the ambient temperature maintained during the freezing processes.

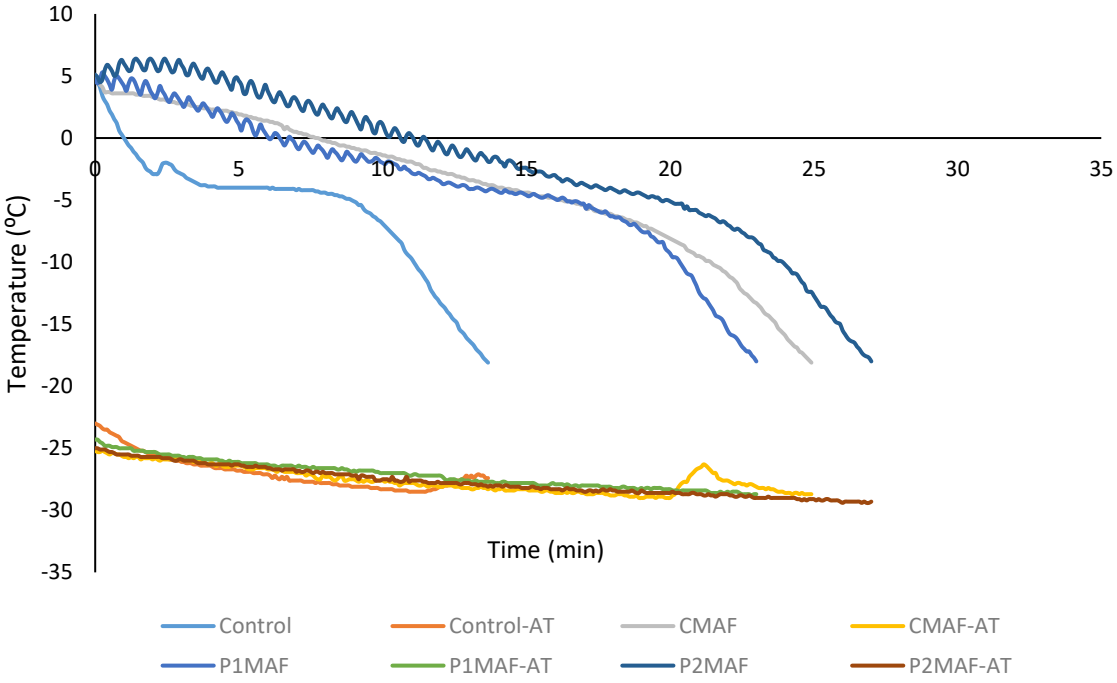

Figure 55: Freezing curve obtained during MAF of apple for sample having S/V of 5 cm^{-1}. "AT" attached in the legend for each freezing conditions relates to the ambient temperature maintained during the freezing processes.

Table 9. Freezing parameters obtained during MAF of apple with different configurations.

Apple having S/V ratio of 7 cm^{-1}				
Parameters	**Control**	**CMAF**	**P1MAF**	**P2MAF**
Characteristic freezing time (min)	6.58 ± 0.50	7.14 ± 0.55	6.75 ± 1.54	6.25 ± 0.52
Overall freezing time (min)	12.28 ± 0.79	12.36 ± 1.21	11.92 ± 1.88	11.89 ± 1.40
Overall freezing rate (°C/min)	1.88 ± 0.08	1.85 ± 0.17	1.99 ± 0.30	1.96 ± 0.20
Apple having S/V ratio of 5 cm^{-1}				
Parameters	**Control**	**CMAF**	**P1MAF**	**P2MAF**
Characteristic freezing time (min)	8.25 ± 0.41	10.56 ± 0.86	10.83 ± 0.35	10.47 ± 0.86
Overall freezing time (min)	13.78 ± 0.59	25.39 ± 2.33	22.92 ± 2.71	26.36 ± 3.09
Overall freezing rate (°C/min)	1.67 ± 0.07	0.91 ± 0.08	1.01 ± 0.12	0.88 ± 0.11

III.2.1.2 Effect on quality parameters

III.2.1.2.1 Effect on microstructure

The pore size distributions for each freezing conditions obtained using X-ray tomography are presented in Figure 56. It can be seen that MAF conditions produced better microstructure (less large pores and more homogeneous structure) than the control condition.

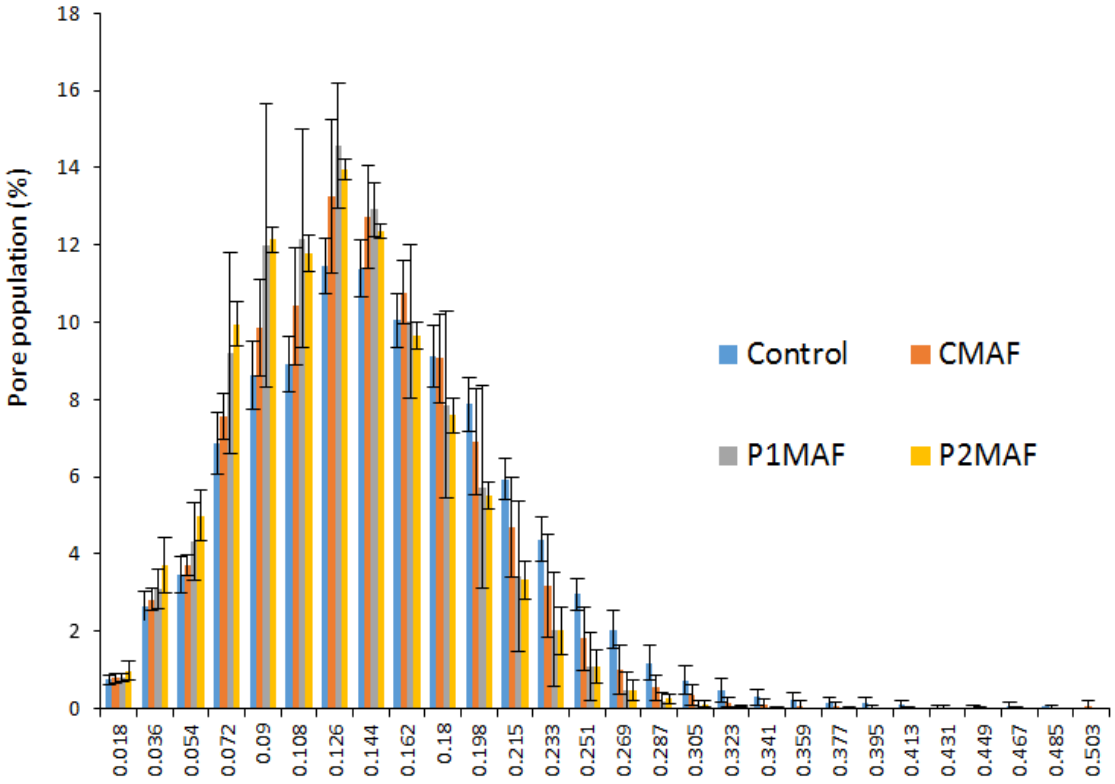

(a)

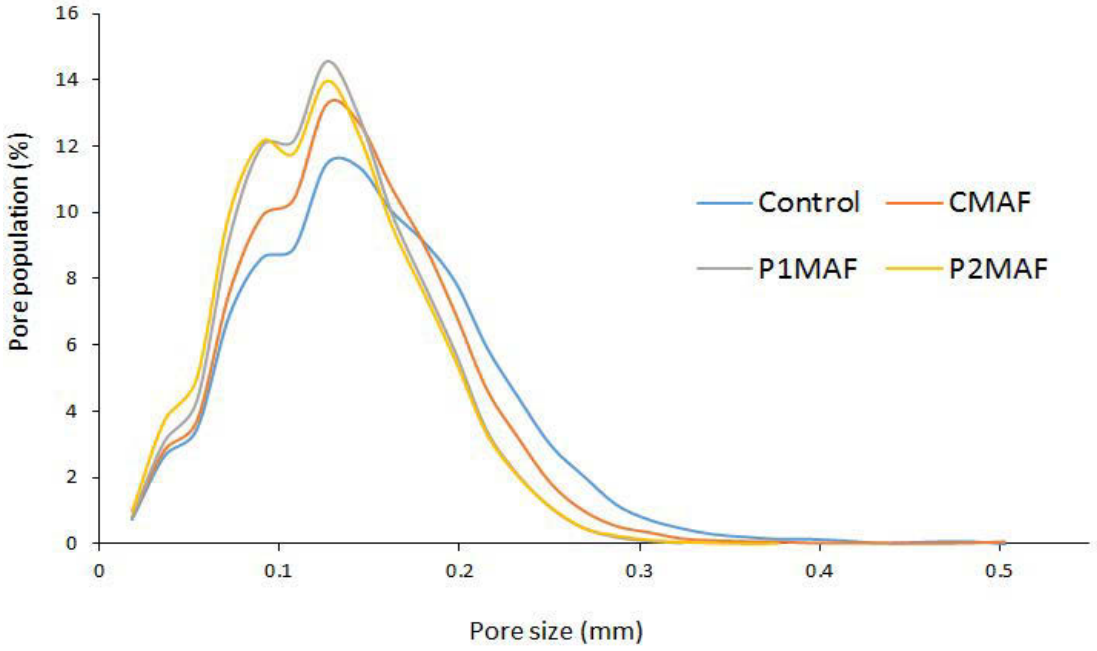

(b)

Figure 56: Frequency curve for apple sample treated under various conditions: (a) with and (b) without standard error bars. Control = no microwaves exposure, CMAF = constant microwave condition, and PMAF (includes both P1MAF and P2MAF) = Pulsed microwave conditions.

Further, these distributions were fitted to a normal distribution function and mean pore size present in the product were determined (Figure 57). The mean pore size for each freezing conditions was also obtained from the image analysis software.

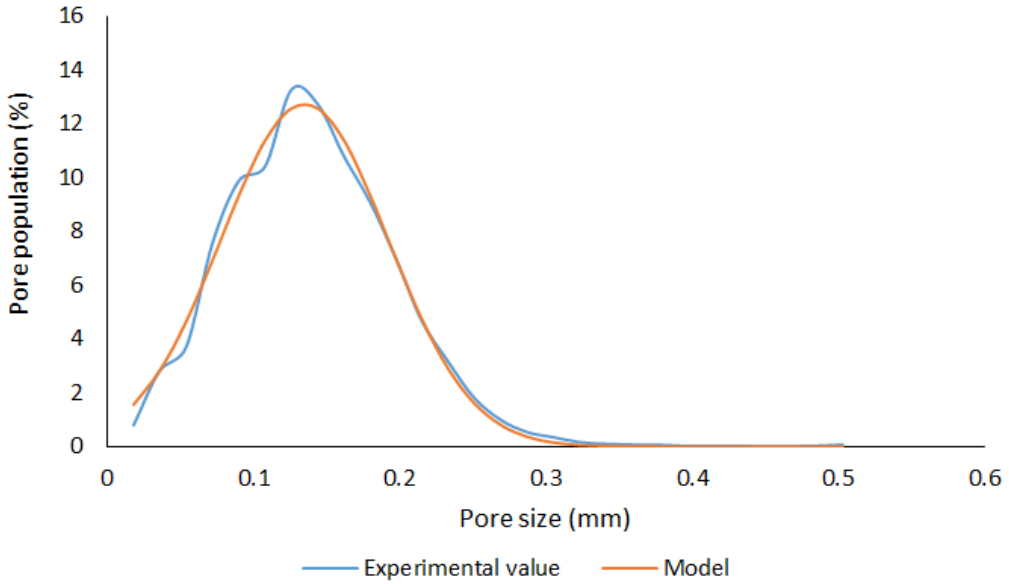

Figure 57: Experimental and modeled data (using normal distribution function) for pore size distribution in the apple.

The mean pore sizes obtained from the model fitting and the software are presented in Figure 58. The model fitting yielded slightly higher value than that given by the software, however, the mean pore size acquired for each freezing condition exhibited similar trend. The samples frozen in the absence of microwave exposure had the largest mean pore size (model = 151.76 ± 7.45 µm and software = 145.27 ± 4.23 µm), meanwhile, P2MAF condition resulted in smallest pore in the apples (i.e. model = 127.63 ± 4.63 µm, software = 123.32 ± 3.63 µm). The order of the mean pore size obtained under tested conditions was control freezing condition > CMAF condition > P1MAF condition > P2MAF condition. The statistical analysis of mean pore size depicted that P2MAF conditions significantly reduced the pore size in apple compared to the control condition. Meanwhile, mean pore size under CMAF condition were not significantly different with that of control and PMAF conditions. The MW form (constant mode or pulsed mode) and power level were found to govern the pore size distribution in the apple sample. For instance, the mean pore size decreased significantly ($p < 0.05$) with the introduction of MW pulsed conditions and with the increase in MW power.

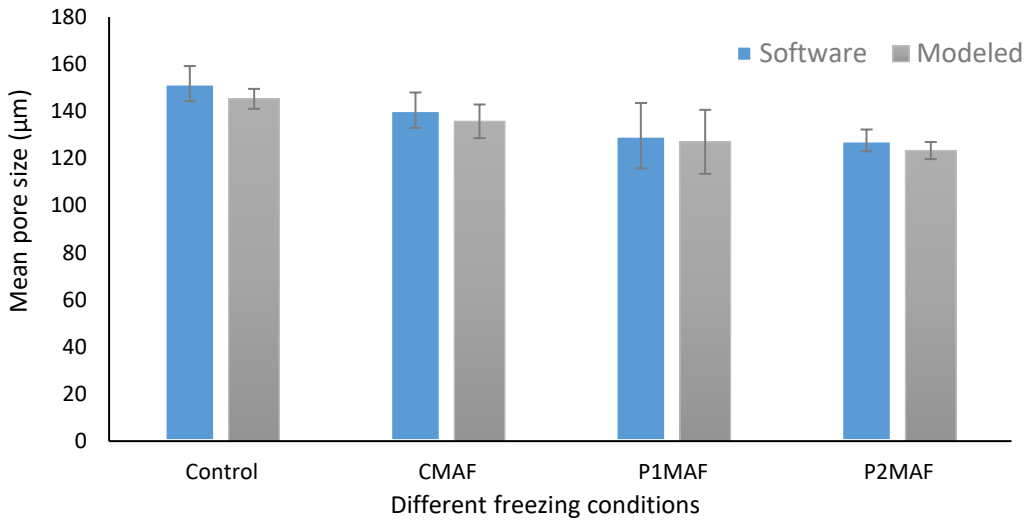

Figure 58: Mean pore size obtained with the software and the normal distribution fitting for apples frozen by different freezing protocols.

Moreover, better understanding of pore size distribution, the cumulative pore size distribution (Figure 59) and the D-Values (D10, D50 and D90 values, the intercepts for 10%, 50% and 90% of the cumulative pore size distributions) were also calculated (Table 10). The cumulative pore size distribution clearly shows that the control condition produced relatively larger pore throughout the distribution range than compared to the MAF conditions (Figure 59). For instance, the control condition had the largest D10, D50 and D90 values i.e. 62.53 ± 3.27,

137.59 ± 5.86 and 227.21 ± 13.85 µm, while these values were relatively lower in apple frozen under MAF conditions (Table 10).

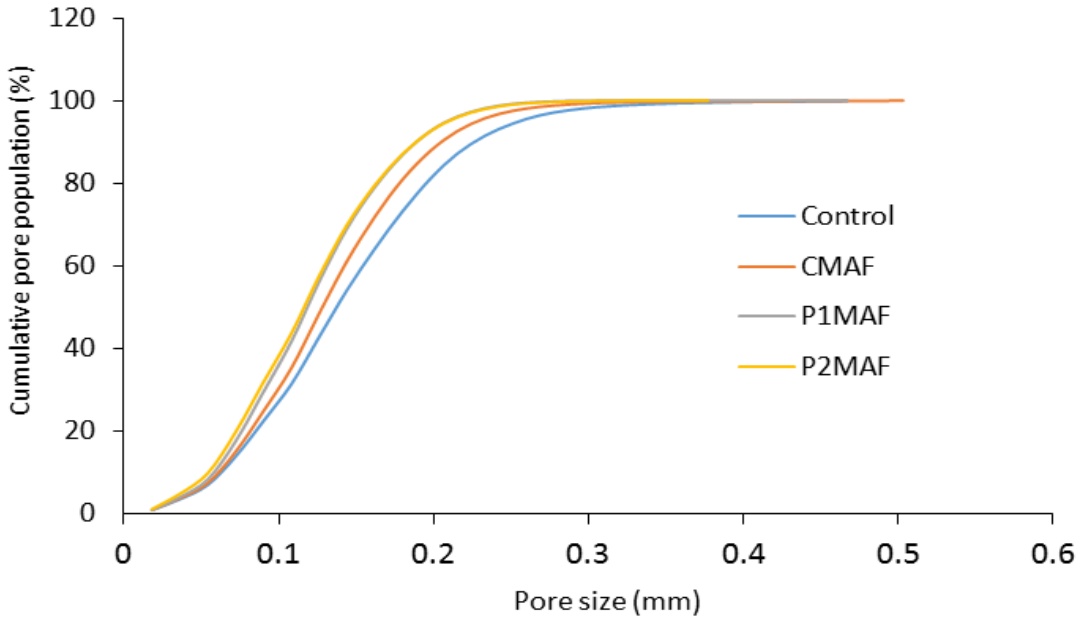

Figure 59: Cumulative pore size distribution for apple samples treated under various conditions: Control vs. CMAF and PMAFs.

The D-Values (D10, D50 and D90 values) for P2MAF condition were significantly smaller than the control freezing conditions. The D50 and D90 value for P1MAF was significantly smaller than the control condition, meanwhile, D10 value for P1MAF and control freezing conditions were not significantly different from each other. Among MAF conditions, no significant difference in D-Values were observed. From these results, it can be understood that upon increasing the power level of microwave, the amount of large size ice crystals decreased and at the same time amount of smaller ice crystals increased.

Table 10. D-Values (D10, D50 and D90) of pore size distribution obtained for apples frozen by different freezing protocols.

Freezing Conditions	Control	CMAF	P1MAF	P2MAF
D10 (µm)	62.53 ± 3.27^{a}	60.44 ± 1.70$^{a, b}$	58.32 ± 4.40$^{a, b}$	53.93 ± 4.16$^{b, c}$
D50 (µm)	137.59 ± 5.86^{a}	128.77 ± 6.78$^{a, b}$	119.41 ± 14.31^{b}	116.32 ± 3.57^{b}
D90 (µm)	227.21 ± 13.85^{a}	205.21 ± 16.52$^{a, b}$	186.51 ± 21.08^{b}	189.16 ± 7.17^{b}

III.2.1.2.2 Texture

The firmness values of apples under different freezing conditions are presented in Figure 60. The firmness of fresh apple was 13.01 ± 1.36 N, and it significantly reduced ($p < 0.05$) once frozen-thawed. Among the freeze-thawed sample, the firmness value was slightly better

conserved under P2MAF (5.59 ± 0.91 N) and P1MAF (5.11 ± 0.89 N) conditions than compared to the control (4.57 ± 0.92 N) and CMAF (4.63 ± 0.82 N) conditions (Figure 60). The firmness value was slightly better preserved when microwave used was in pulsed form and had a higher power level.

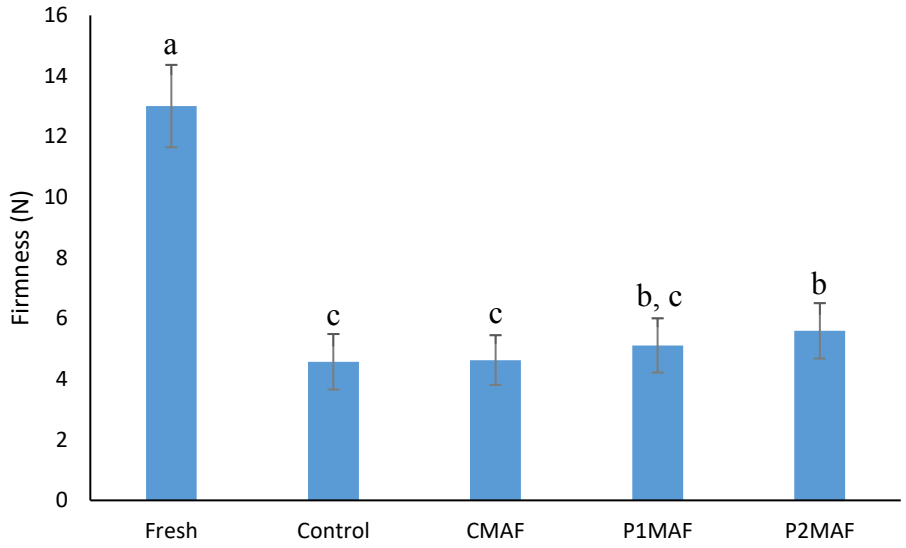

Figure 60: Texture (firmness) of fresh and frozen-thawed apple samples.

III.2.1.2.3 NMR (nuclear magnetic resonance) relaxometry of apple

Results from NMR tests on frozen (at $-$ 20 °C) and frozen-thawed samples (at 4 °C) will be discussed in this section. Figure 61 illustrates the T_2 relaxation peaks of non-freezable water (at – 20 °C) in control and MAF samples. At $-$ 20 °C, the observed signal is that of the protons of non-freezing water (in very strong interaction with macromolecules), which gives information on the macromolecular structure after the freezing process. For all conditions, a minimum of three distinct peaks were obtained. A fourth peak was always observed for the control sample, while it did not appear always for sample frozen under MAF conditions. However, the relaxation time and proton population for the fourth peak could not be resolved due to the weak resolution of the peak. Based on three relaxation peaks data obtained for each condition, it can be inferred that the non-freezable water status (T_2 time of peaks and their respective population) in apple was not affected by the introduction of microwaves during freezing. This method could be useful to compare the consequences of the freezing processes on the macromolecular structure.

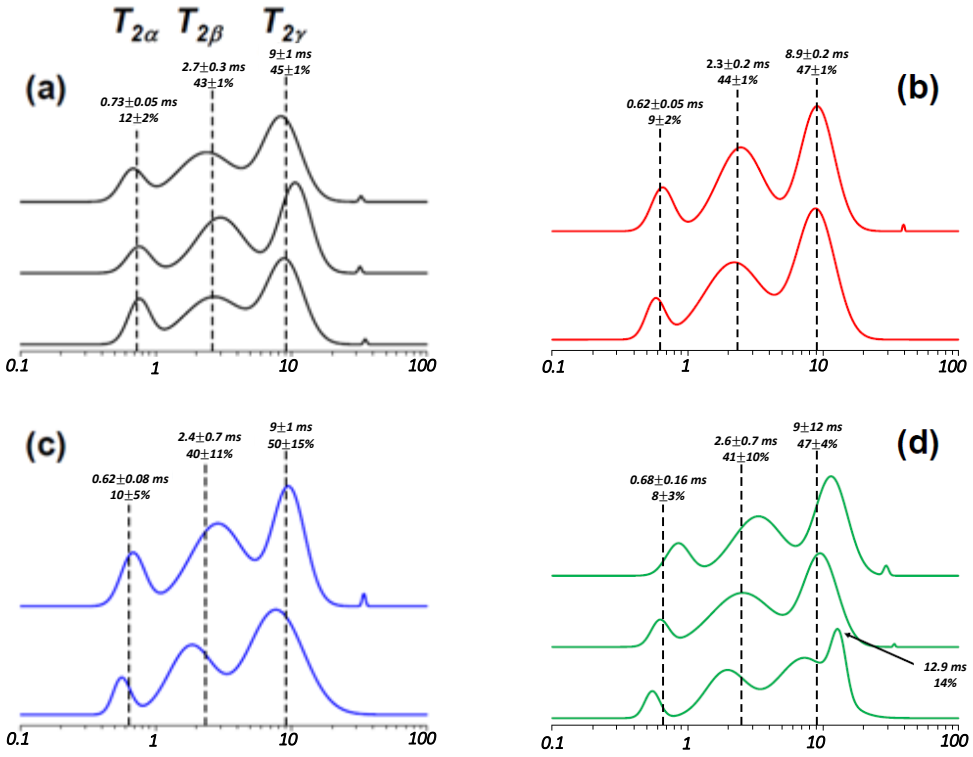

Figure 61: Distributions of T_2 peaks at − 20 ℃ from apple samples (a) control condition, (b) CMAF condition, (c) P1MAF condition, and (d) P2MAF condition (The x-axis correspond to the relaxation times expressed in ms (milliseconds)).

The freezing-thawing process induced alteration to the mobility and distribution of water in apples was studied (at 4 °C) using NMR relaxometry. The measurement of the T_2 relaxation peaks values of the samples after thawing makes it possible to observe the influence of different freezing protocols on the mobility of the water compared with the fresh samples. With respect to fresh samples, the distribution of T_2 relaxation peaks has five components (T_{2a}, ..., T_{2e}). Their average value (both relaxation time and proton population) which are in good agreement with the data from the literature (Marigheto, Venturi, & Hills, 2008) is proposed in Figure 62. The vacuole water had the longest T_2 time and it accounted for 77-79% of the total water content in the apple, indicating that the most water exists in the vacuole. Water in the cytoplasm and extracellular space accounted for 16.8-18.6% of the total water content, while the water in the cell walls accounted for approximately 3-3.8%.

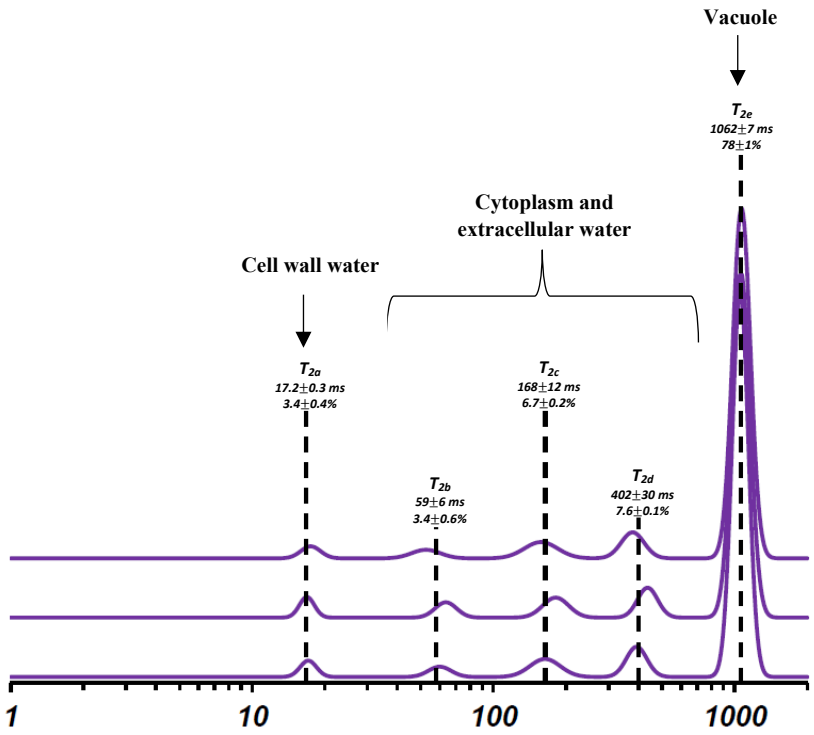

Figure 62: Relaxation peaks of the water proton in the different cell compartments of fresh apple samples at 4 °C (The x-axis correspond to the relaxation times expressed in ms (milliseconds)). Similar relaxation peaks for fresh 'Red Delicious' apple was obtained by Marigheto et al. (2008).

Figure 63 illustrates the distribution of T_2 relaxation peaks in frozen-thawed sample from various freezing conditions. Four relaxation peaks are characterized in the frozen-thawed sample (against 5 for fresh samples) (Figure 63). The T_{2b} and T_{2c} components could no longer be differentiated due to a loss of resolution. For all freezing conditions, mobility of vacuole and cytoplasm/extracellular space water decreased compared to the fresh sample. Moreover, the freezing process decreased the vacuole water in the apple, conversely it increased the proportion of cytoplasm and extracellular water. This reflects a reorganization of the fluids following a partial rupture of the cellular structures upon freezing-thawing.

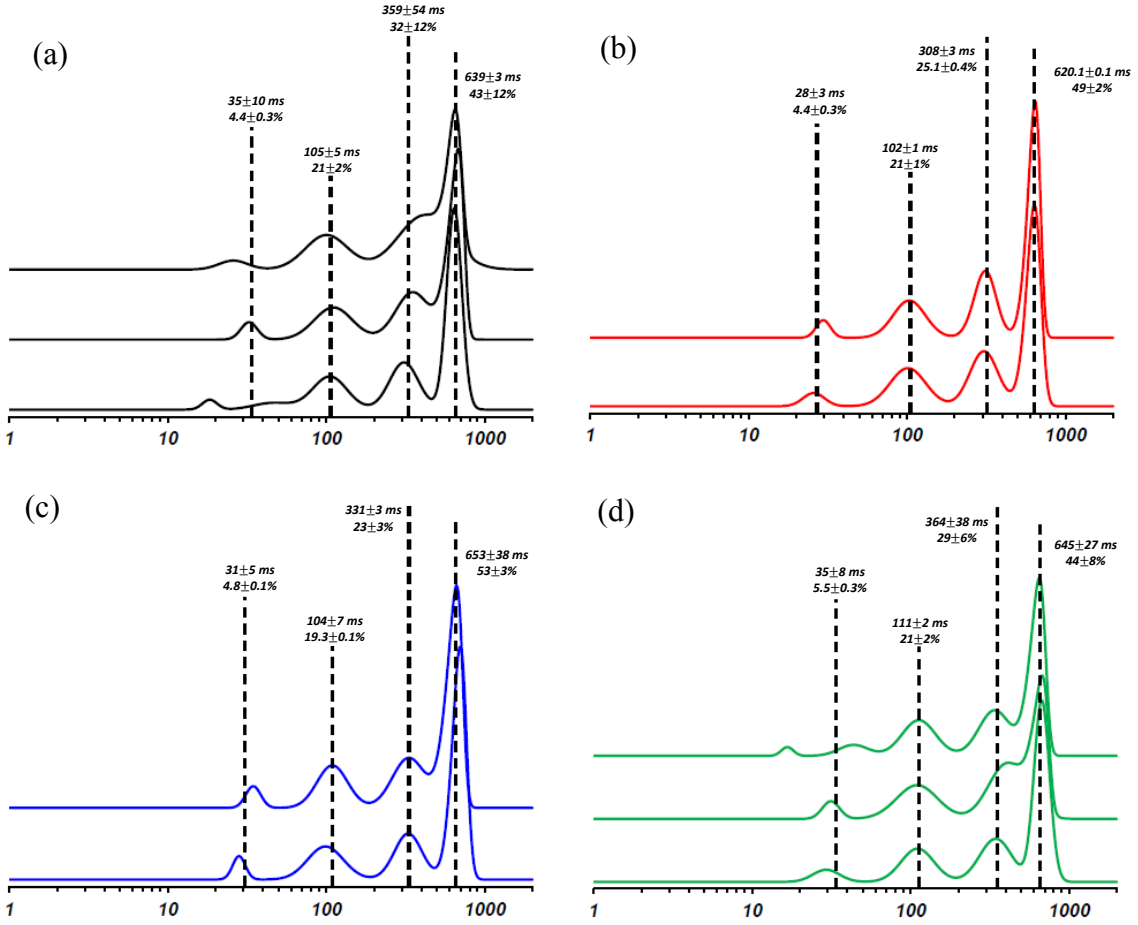

Figure 63: Distributions of T_2 relaxation peaks at 4 ℃ of apple samples after (a) control freezing, (b) CMAF, (c) P1MAF, and (d) P2MAF (The x-axis correspond to the relaxation times expressed in ms (milliseconds)).

Compared to the fresh sample, T_2 time of vacuole decreased the most for CMAF sample (up to 41.61%) whilst it was least for P1MAF condition (up to 38.51%) (Figure 62 and Figure 63). The PMAF conditions were found to have higher T_2 time values of vacuole than the control and CMAF conditions depicting better preservation of tonoplast. CMAF condition seemed to have negative impact on tonoplast as T_2 time value of vacuole component was lowest for this condition. However, the difference among the four groups (in terms of T_2 time value of vacuole) was not significant. Upon comparing the population of water in different compartments, it can be observed that control condition affected the vacuole water population the most, followed by P2MAF, CMAF and P1MAF (Figure 62 and Figure 63). The decrease in the population of vacuole water was followed by a subsequent increase in the population of cytoplasm and extracellular water, and it was the most for control condition. This indicates that the destruction of tonoplast was higher for control and, this in turn led to migration of water from vacuole to

cytoplasm and extracellular space. However, no significant difference (in terms of peak area proportions) was observed among the freezing conditions. At this point, it is difficult to draw a conclusion from NMR test, and as per our understanding, many replications of NMR are required to confirm the observed tendencies and reach a concrete conclusion.

III.2.1.2.4 Drip loss

Figure 64 shows the effect of MAF on drip loss. Compared to the control condition, the drip loss value decreased by ≈ 3, 23 and 42% under CMAF, P1MAF and P2MAF conditions. However, a significant reduction ($p < 0.05$) in drip loss could be obtained only under P2MAF condition. The change in drip loss could be related to ice crystal size. The MAF process produced small and homogeneously distributed ice crystals in the apple sample. As an outcome, the cellular structure was less damaged and hence resulted in lesser exudate loss upon thawing.

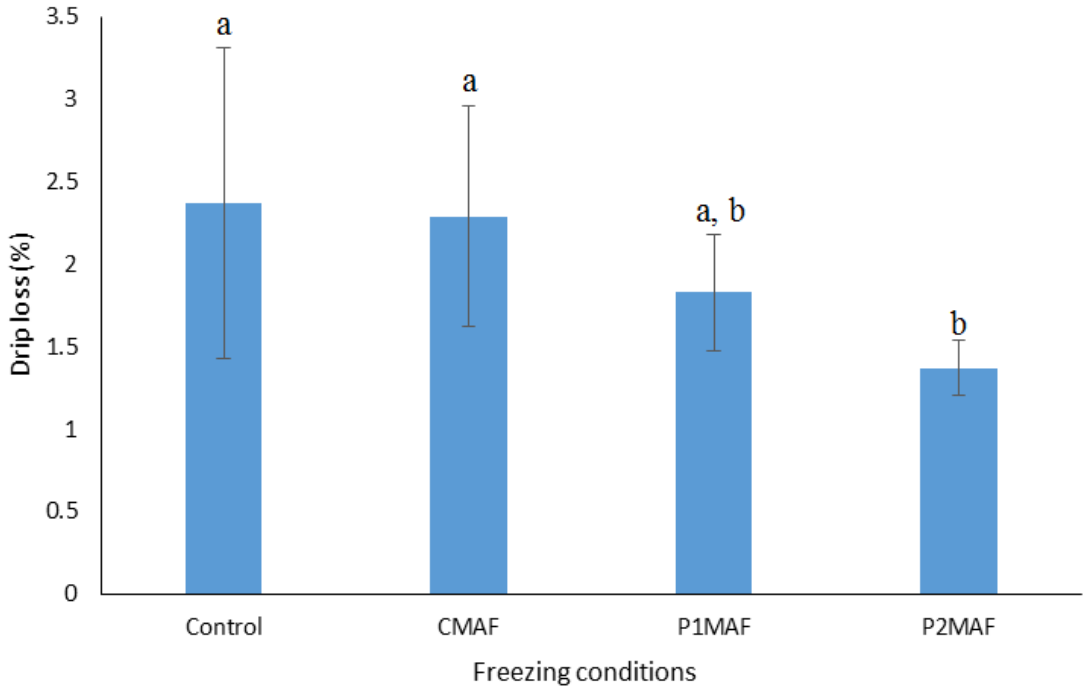

Figure 64: Effect of control and MAF conditions on the drip loss of apples. The different letters indicate significant differences ($p < 0.05$).

III.2.1.2.5 Cryo-SEM imaging

The cryo-SEM was also performed for apple frozen under control and MAF conditions (Figure 65). The bright regions in the micrographs (Figure 65b-e) are the solidified solutes of the cell sap, the cytoplasmic membrane, and the cell walls. The darker regions in the micrographs are ice; some dark regions (indicated by letter A in the Figure 65b-e) are the air space between the two cells). Upon analyzing the microstructure morphology, it was found that all of the freezing

conditions maintained cell structure when compared to the structure of the fresh sample (Figure 65a). However, the freezing conditions had an effect on the inner morphology of the cell i.e. the size of ice crystals was influenced. The control freezing condition had the most detrimental effect on the inner morphology of the cell. It had relatively bigger ice crystals than the microwaves assisted frozen samples. Also, compared to the MAF conditions, control freezing condition led to a non-homogenous inner structure. Furthermore, the control sample had a few larger ice crystals, while no such large crystals were observed under microwaves conditions. Among MAF conditions, CMAF conditions led to bigger ice crystals than compared to PMAF conditions. P2MAF condition produced smallest ice crystals among all conditions. The results from cryo-SEM confirm the outcomes of X-ray tomography analysis.

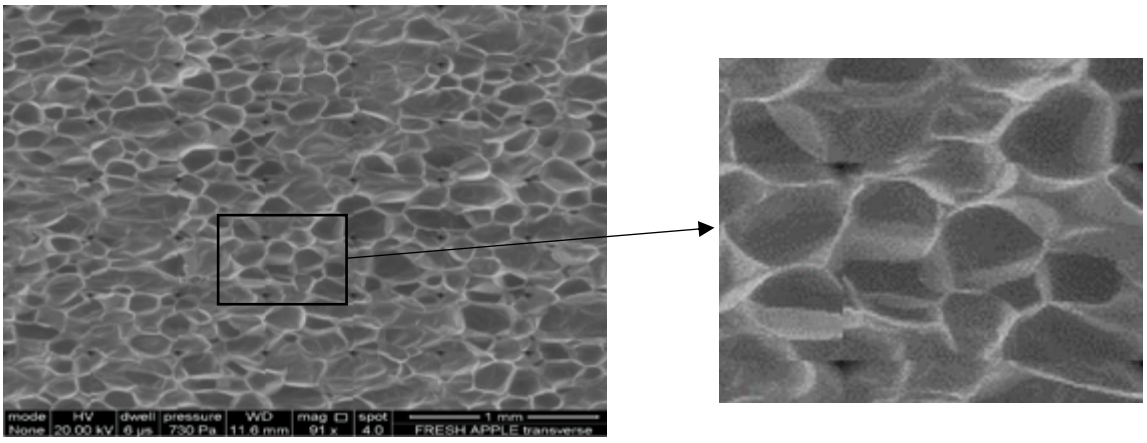

(a)

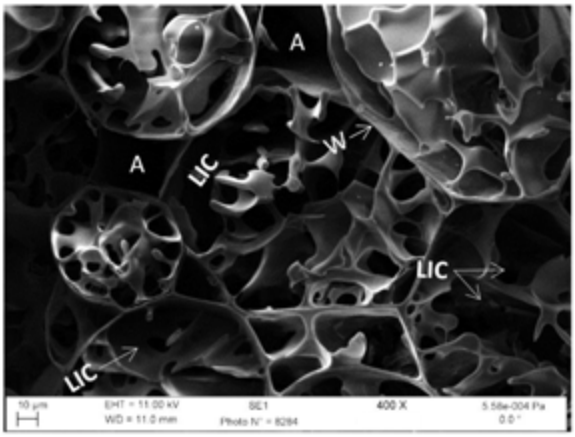

(b)

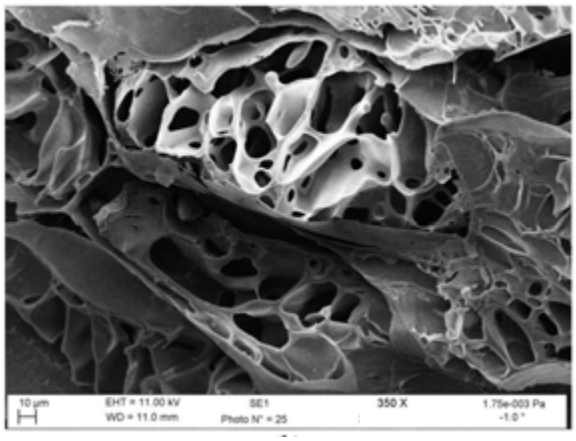

(c)

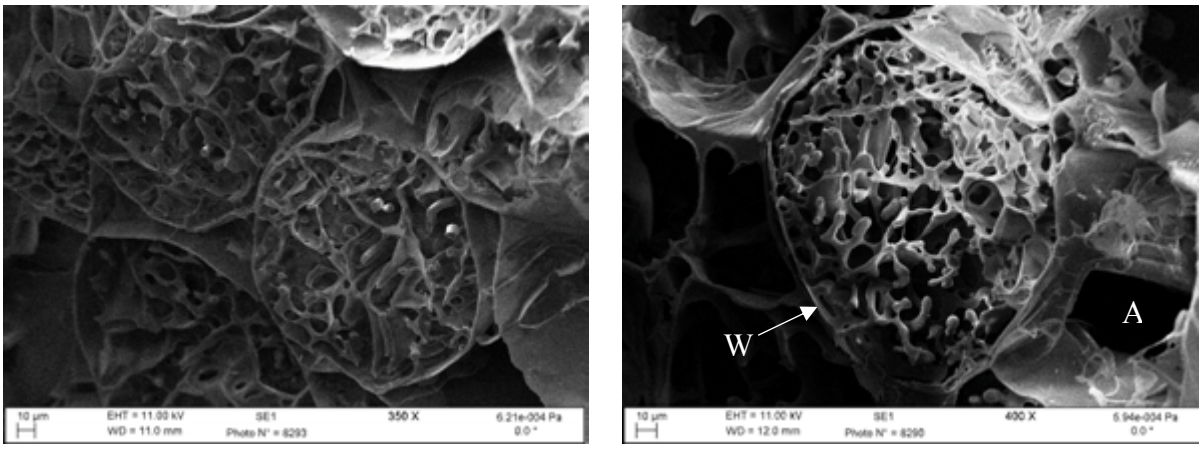

(d) **(e)**

Figure 65: (a) Environmental SEM image of fresh apple; cryo-SEM images of apple under (b) control freezing condition, (c) CMAF condition, (d) P1MAF condition and (e) P2MAF condition. Abbreviations used in the above picture: A = air space, W = cell wall and membrane structure, LIC = large ice crystals size.

➔Intermediate conclusions:

The apples were frozen by three MAF conditions (one constant power MAF (CMAF) and two pulsed power MAF (CMAF) conditions) and the conventional method. The freezing curve's shape and parameters (e.g. characteristic freezing time, overall freezing time and rate) values were similar for MAF conditions and no MAF condition. PMAF conditions improved the microstructure significantly compared to the control sample. The P2MAF samples were significantly firmer than control samples. The drip loss was also significantly lower for P2MAF samples than the control sample. No significant difference in drip loss and firmness values were observed among CMAF, P1MAF and control conditions. Among the studied conditions, P2MAF condition gave the best result in terms of microstructure and other quality attributes such as drip loss and texture.

III.2.2 MAF of potatoes

Based on the results from apple freezing under control and MAF conditions, it can be inferred that PMAF conditions would produce better quality product than control and CMAF conditions. Considering this fact, freezing trials of potatoes were performed only under PMAF conditions and were compared with the control conditions.

III.2.2.1 Freezing curves

The freezing history i.e. the time-temperature curves during control and MAF processes are depicted in Figure 66. It can be seen that the freezing curve exhibited similar shape irrespective of the freezing conditions being used. No supercooling was observed for any of the freezing conditions. The characteristic freezing time and overall freezing time increased slightly while overall freezing rate decreased somewhat upon the introduction of microwaves and with increasing power level of microwaves (Table 11), but, these differences were found to be insignificant.

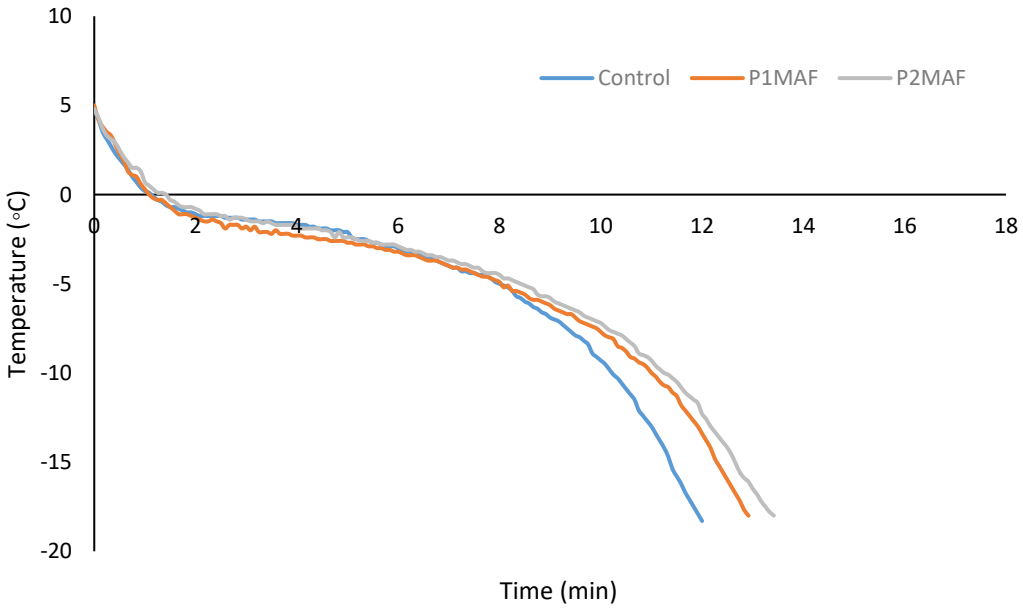

Figure 66: Potato freezing curves during control and MAF process.

Table 11. Freezing curve parameters under control and MAF conditions of potato.

Freezing condition	Characteristic freezing time (min)	Overall freezing time (min)	Overall freezing rate (°C/min)
Control	7.24 ± 0.40	11.71 ± 1.27	1.98 ± 0.20
P1MAF	7.58 ± 1.04	12.47 ± 1.47	1.83 ± 0.18
P2MAF	7.69 ± 0.21	12.81 ± 0.55	1.79 ± 0.08

Case study:

Why freezing time and freezing curves for MAF of potato (S/V = 5.08 cm^{-1}) (Table 11.) was less than MAF of apple (S/V = 5 cm^{-1}) (Section III.2.1.1 and Figure 55)?

The difference observed for apple and potato could be due to two main reasons: (i) the freezing conditions used for the two products and (ii) the pre-treatment given to the product prior to freezing. The freezing condition for MAF of apple (S/V = 5 cm^{-1}) and potato (S/V = 5.08 cm^{-1}) were different. As mentioned in the materials and methods, the freezing condition for MAF of apple (S/V = 5 cm^{-1}) were − 30 ℃ and 1.1 m/s air velocity, while for potato (S/V = 5.08 cm^{-1}) freezing it was − 30 ℃ and 2.3 to 2.5 m/s air velocity. The difference in freezing condition could be the reason for different freezing times for these two cases. The enhanced airflow rate might have improved the convective heat transfer coefficient around the sample thus facilitating the heat transfer. Moreover, the samples were blanched prior to freezing in the case of potato. The blanching process might have caused a partial breakdown of the cellular structure leading to enhanced heat transfer during freezing. It is a well-proven fact that intact cellular structure impedes the heat transfer, while any sort of alteration (like poration or breakdown of cellular structure) would allow better heat transfer. Our claim has a backing, it can be seen in the Figure 67a that unblanched potato (S/V = 4.9 cm^{-1}) had a characteristic freezing time of 11.50 min at − 30 ℃ and 1.1 m/s air velocity). Meanwhile, blanched potato (S/V = 5.08 cm^{-1}) had the characteristic freezing time of 7.3 min (Table 11.) for the freezing conditions of − 30 ℃ and 2.3 to 2.5 m/s air velocity. This higher freezing rate in the case of blanched was majorly due to the freezing condition and the blanching process. A similar comparison can be made for the overall freezing time.

The apple sample (S/V = 5 cm^{-1}) showed substantial temperature oscillation during pulsed MAF conditions (Figure 55), while temperature oscillation was quite minute during PMAF of potatoes (S/V = 5.08 cm^{-1}) (Figure 66). The loss of resolution of temperature oscillation during PMAF of potato compared to PMAF of apple is majorly due to the improved freezing condition (− 30 ℃ and 2.3 to 2.5 m/s air velocity for potato Vs. − 30 ℃ and 1.1 m/s for apple) and on the pre-processing step (blanching) used during PMAF of potato. Both factors (i.e. improved freezing condition and blanching of sample) led to higher freezing rate during MAF of potatoes, and hence, counterbalanced the heat generation during the PMAF condition.

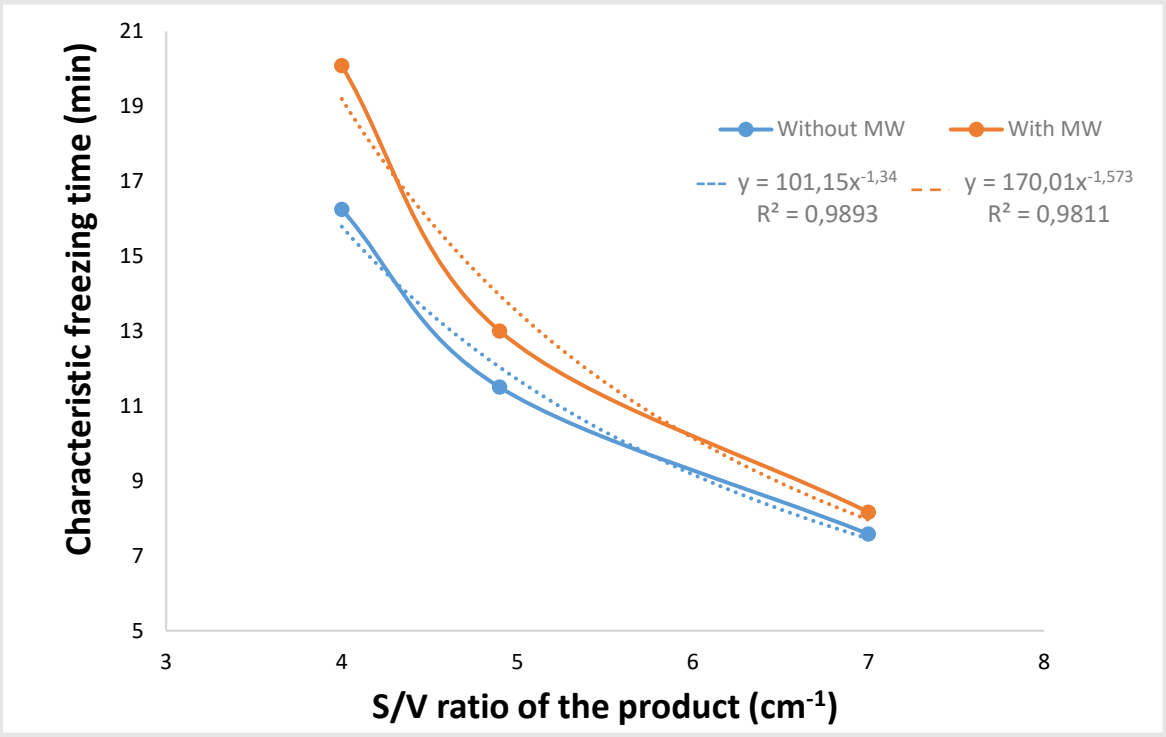

(a)

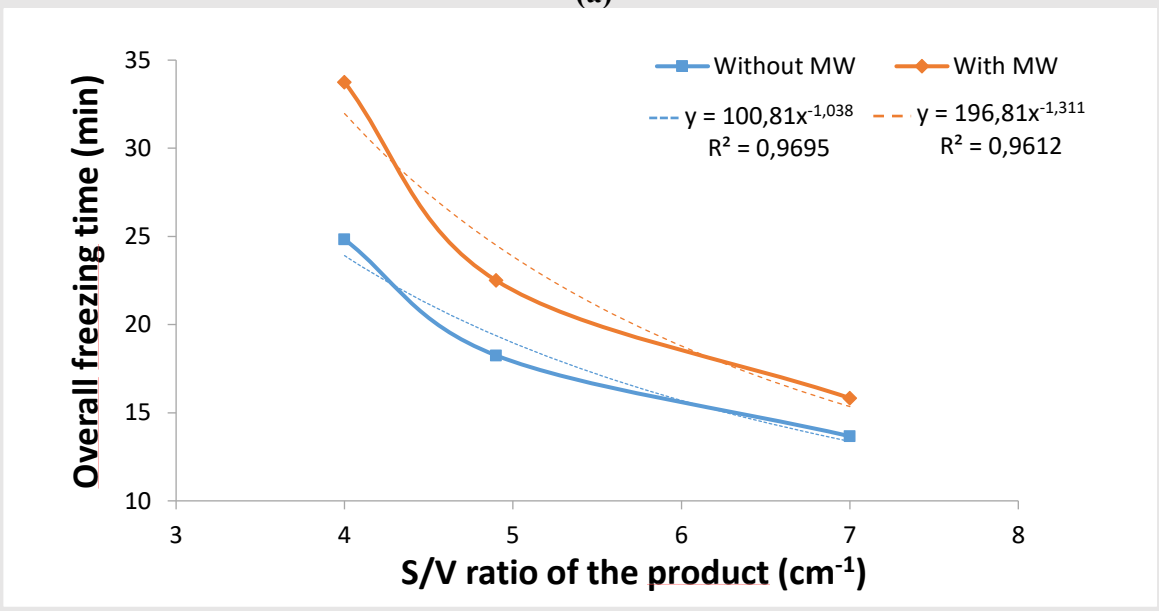

(b)

Figure 67: Dependence of (a) c (b) and overall freezing time of unblanched potato on S/V ratio of the product in the absence (blue curve) and presence of microwave (orange curve) (at an average power level 222 W/kg). Freezing condition (−30 ℃ and 1.1 m/s air velocity). The freezing time Vs. S/V ratio of the potato data best fitted to power law model. The samples were frozen from 5 ℃ to − 22 ℃ during these freezing tests.

The conclusion that could be drawn out from this comparison is that the freezing time during MAF process depends on the freezing rate, the S/V of the product, and the pre-processing steps such as blanching.

III.2.2.2 Quality attributes

III.2.2.2.1 Effect on ice crystals size

The ice crystals size distributions created during control and MAF conditions were quantified using X-rays microcomputed tomography. Figure 68 illustrates the pore size distribution under control and MAF conditions. It is evident from the figure that P2MAF condition produced smaller pores than the P1MAF and control conditions. Control condition not only produced relatively larger ice crystals but also had broad distribution range than compared to the MAF conditions. In other words, the pore distribution range under MAF conditions were narrower and hence much uniform than control condition.

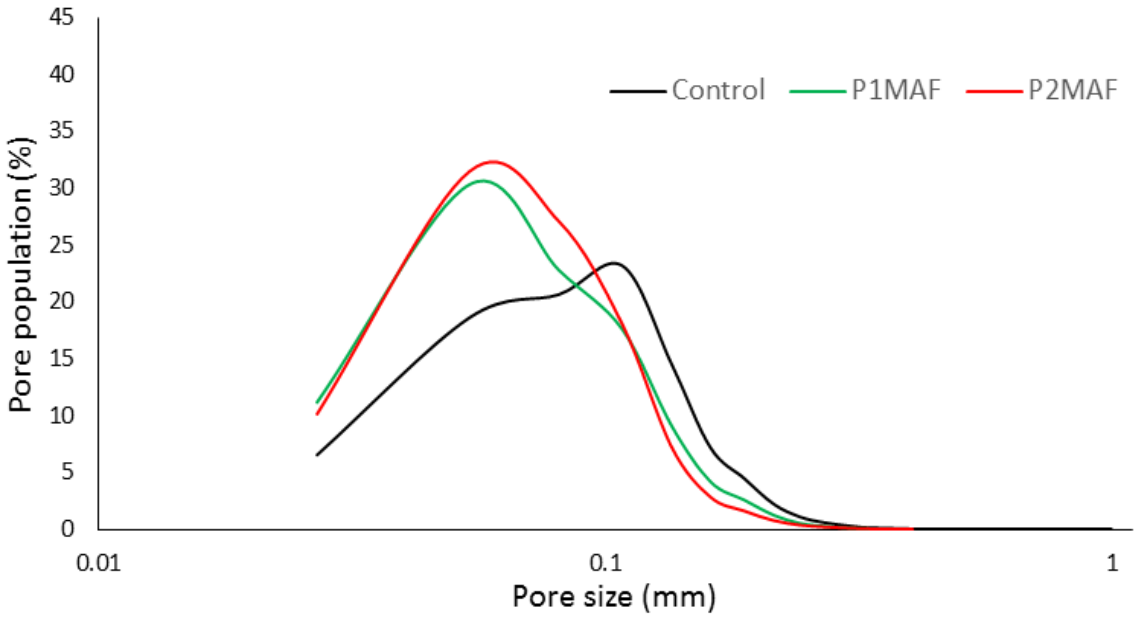

Figure 68: Frequency curve for pore size distribution in potato after freezing under control and MAF conditions. The x-axis has a logarithmic scale.

The mean pore size obtained for each freezing conditions is shown in Table 12. Compared to control condition, P1MAF and P2MAF condition reduced the mean pore size by 22.20% and 18.91% respectively. The difference in mean pore size was significant ($p < 0.05$) between control and P2MAF condition. While the pore size formed under P1MAF condition was not significantly different with that formed under P2MAF and control condition. Further,

cumulative pore size distribution and D-Values (D10, D50 (median) and D90) were also calculated for in-depth understanding of pore size distribution in the product (Figure 69 and Table 12). The D10 value could only be calculated for the control condition, while it was impossible to obtain D10 values for PMAF conditions. This is because of the resolution (i.e. voxel size of 13.5 µm) that was chosen for the test. Using this voxel size the smallest pore size that could be detected is 27 µm. In the case of MAF conditions, it was observed that pore below 27 µm accounted for more than 10% on an average. Since the calculation of D10 value requires two points one representing the value below 10% and other representing value above 10%, lack of value below 10% in the case of MAF conditions made it impossible to calculate the D10 value. The D50 (median) values of pores under P1MAF and P2MAF conditions were 22.36% (but $p > 0.05$) and ≈ 30% ($p < 0.05$) smaller than that obtained after freezing under control condition. The D90 value of pores exhibited similar trend as mean and median pore size for the studied conditions (Table 12). From these above findings, it can be understood that freezing under MAF condition produces smaller ice crystals having a narrow range of distribution, and hence would result in a product having more homogenous structure than the control condition (Figure 70).

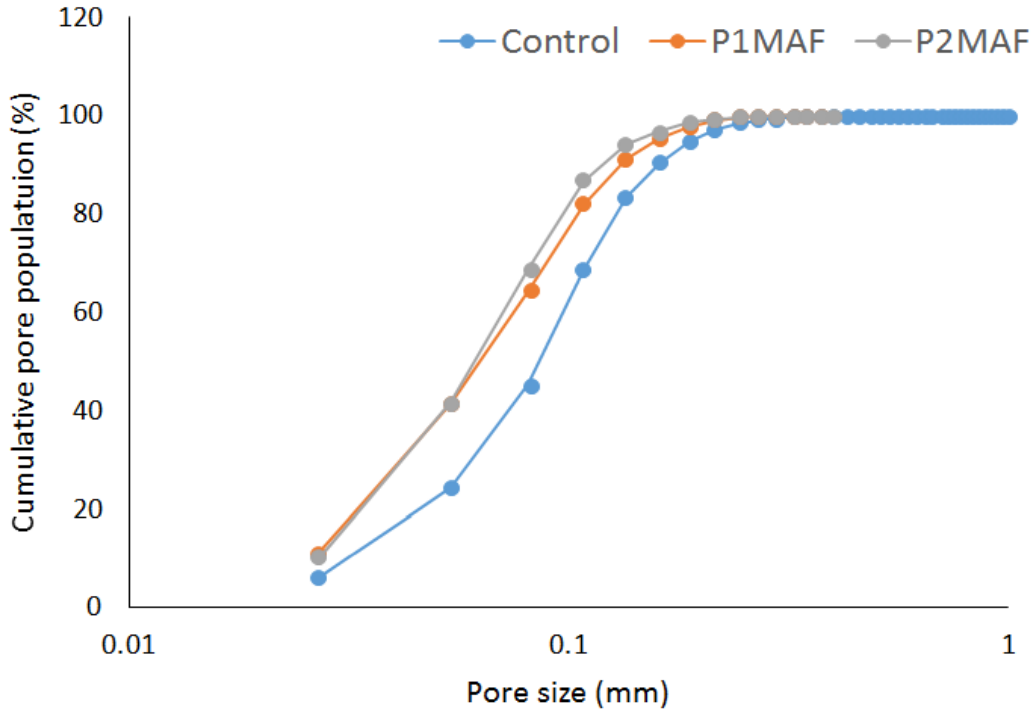

Figure 69: Cumulative pore size distribution in potato after freezing under control and MAF conditions. The x-axis has a logarithmic scale.

Table 12. Mean, D10, D50 (median) and D90 pore size obtained for various freezing conditions for potato.

Freezing Conditions	Control	P1MAF	P2MAF
Mean pore size (µm)	105.52 ± 4.66^{a}	$85.86 \pm 17.68^{a, b}$	82.10 ± 6.31^{b}
D10 (µm)	33.42 ± 4.94	-	-
D50 (µm)	85.59 ± 5.16^{a}	$66.45 \pm 19.29^{a, b}$	59.95 ± 7.58^{b}
D90 (µm)	162.93 ± 20.54^{a}	$127.92 \pm 27.59^{a, b}$	115.86 ± 9.98^{b}

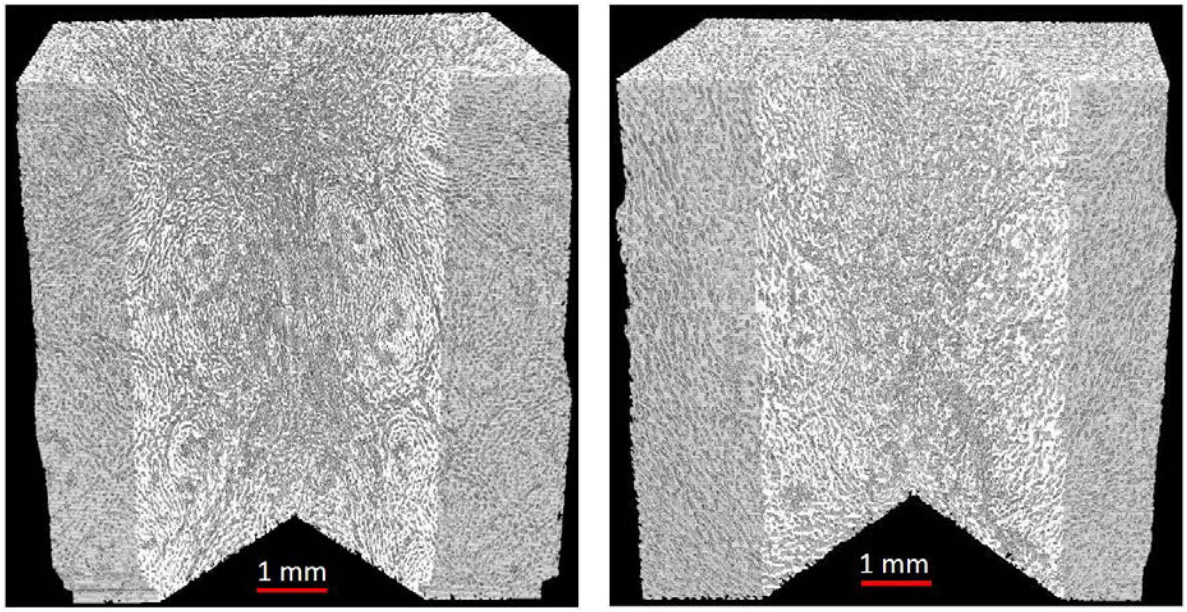

(a) (b)

Figure 70: Microstructure of potatoes after (a) control freezing (b) P2MAF freezing process. The white regions in the figure correspond to the cellular matrix, while grey regions correspond to the ghost of ice microcrystal that sublimed during freeze drying.

III.2.2.2.2 Texture

Figure 71a and b represents the hardness and Young's modulus of the potatoes at different processing steps. The hardness and Young's modulus value of the fresh potato were the highest averaging 189.94 ± 18.80 N and 5.46 ± 0.44 MPa. Blanching process reduced both the hardness and Young's modulus values (approx. by 17%). The blanching process causes thermal destruction of cell membranes and hence tissue loses its turgor pressure and rigidity. As an outcome, softening of tissues happens (Reid et al., 1986; Reis, 2017; Verlinden et al., 2000). The blanched frozen-thawed potatoes were found to be softer than both the fresh and blanched samples. The hardness of fresh potatoes, upon blanching and subsequent freezing degraded the least under P2MAF (by ≈ 88%) than under P1MAF condition (by ≈ 89%) or under control freezing condition (by ≈ 90%). Similarly, Young's modulus value of fresh potatoes suffered

the least degradation under P2MAF condition (≈ 86%) than under P1MAF condition (≈ 89%) or under control freezing condition (≈ 91%).

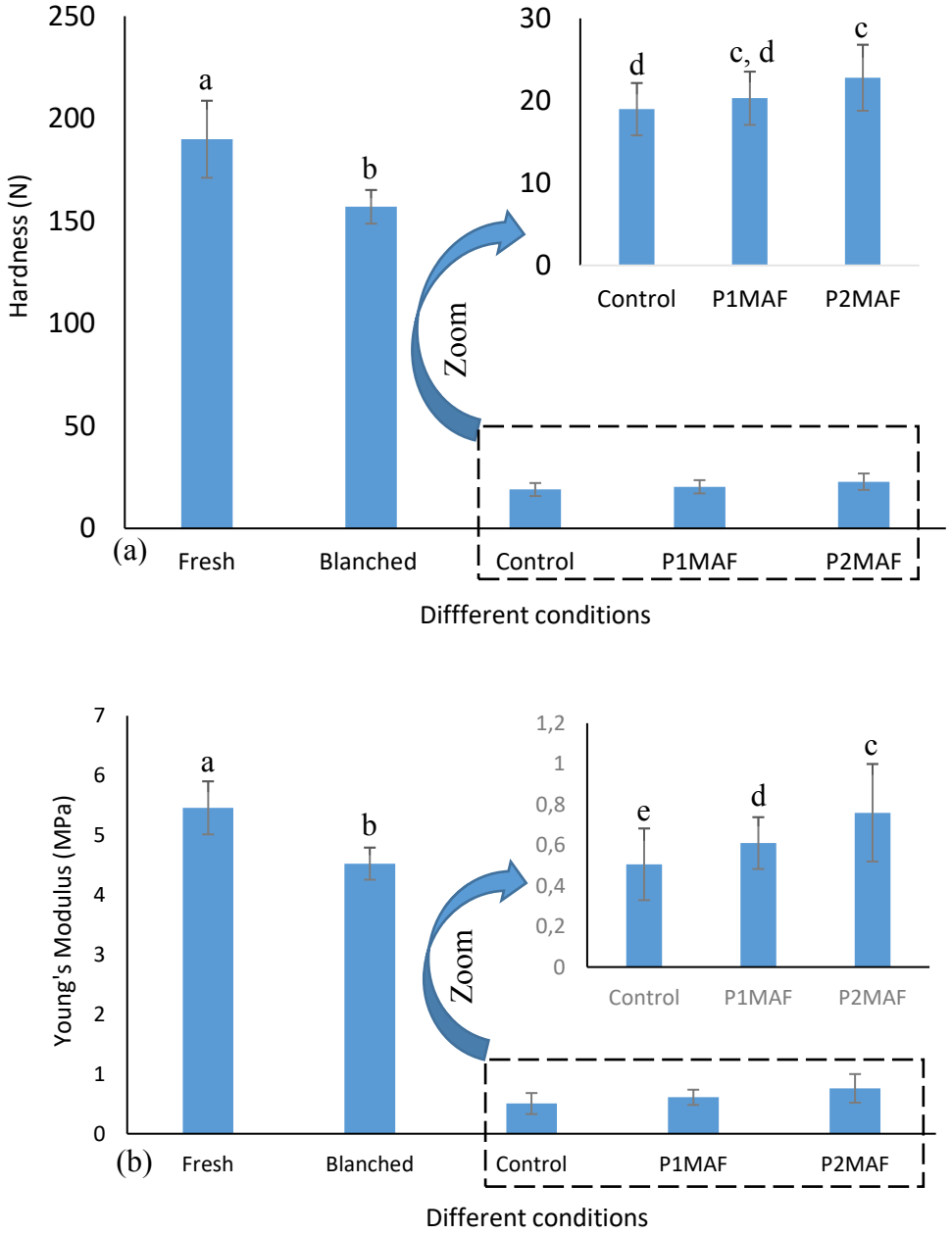

Figure 71: Texture parameters ((a) Hardness and (b) Young's modulus) of fresh, blanched and frozen-thawed potatoes.

III.2.2.2.3 Drip loss

The exudate loss data for control and MAF samples are portrayed in the Figure 72. Freezing under control freezing condition resulted in higher drip loss (2.67 ± 1.12 %) than either of the

MAF conditions (P1MAF = 2.03 ± 0.88% (but $p > 0.05$) and P2MAF = 1.62 ± 0.70% ($p < 0.05$)).

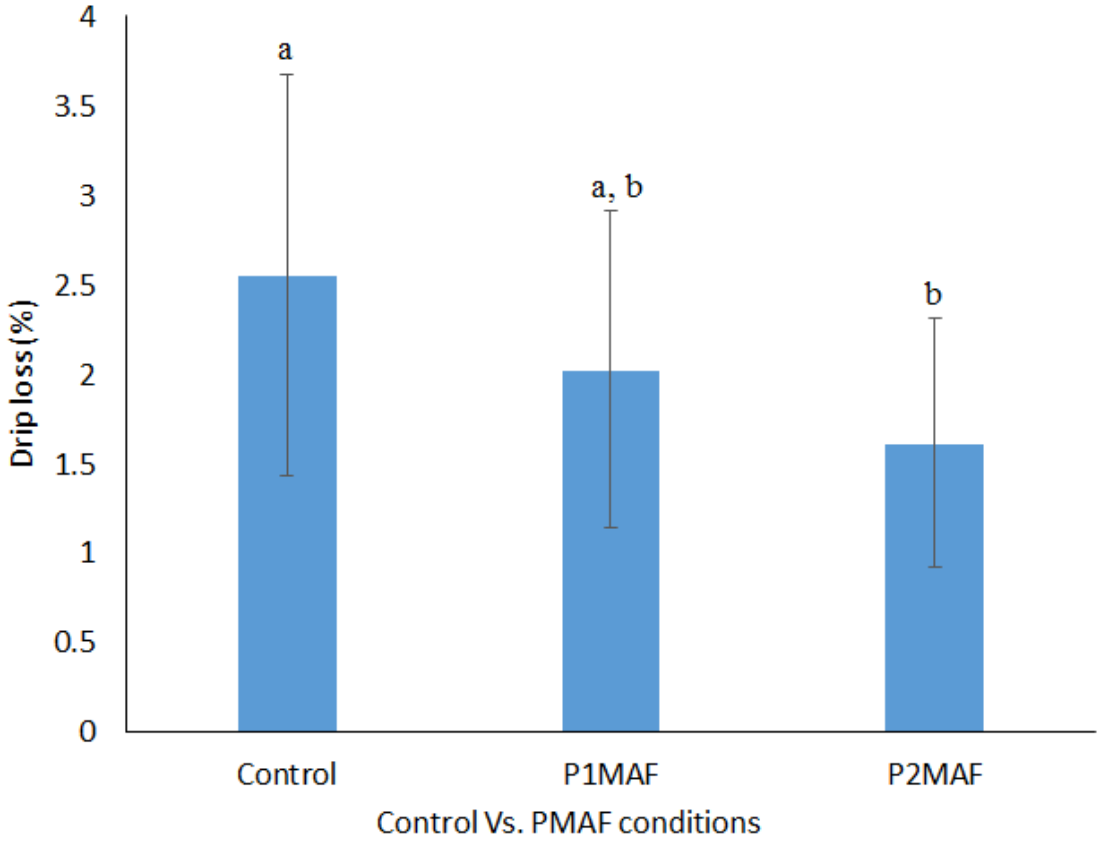

Figure 72: Drip loss (%) from potato samples after freezing under control and MAF conditions.

III.2.2.2.4 Colour

The colour of fresh, blanched, and blanched-frozen-thawed potato is represented in the Figure 73. The blanching process did not affect L^* (lightness) value, meanwhile, it decreased the b^* (yellowness) value and imparted negative a^* (green) value to fresh samples. The freezing-thawing process of blanched sample did not affect the colour characteristics. Moreover, none of the freezing protocols caused any significant effect to the colour characteristics of blanched potato. As mentioned earlier, the colour change in potatoes upon freezing-thawing is mainly associated to the browning that generally happens due to enzyme activity during thawing process. In the present case, the blanching process seems to have inactivated the enzymes and prevented the colour change.

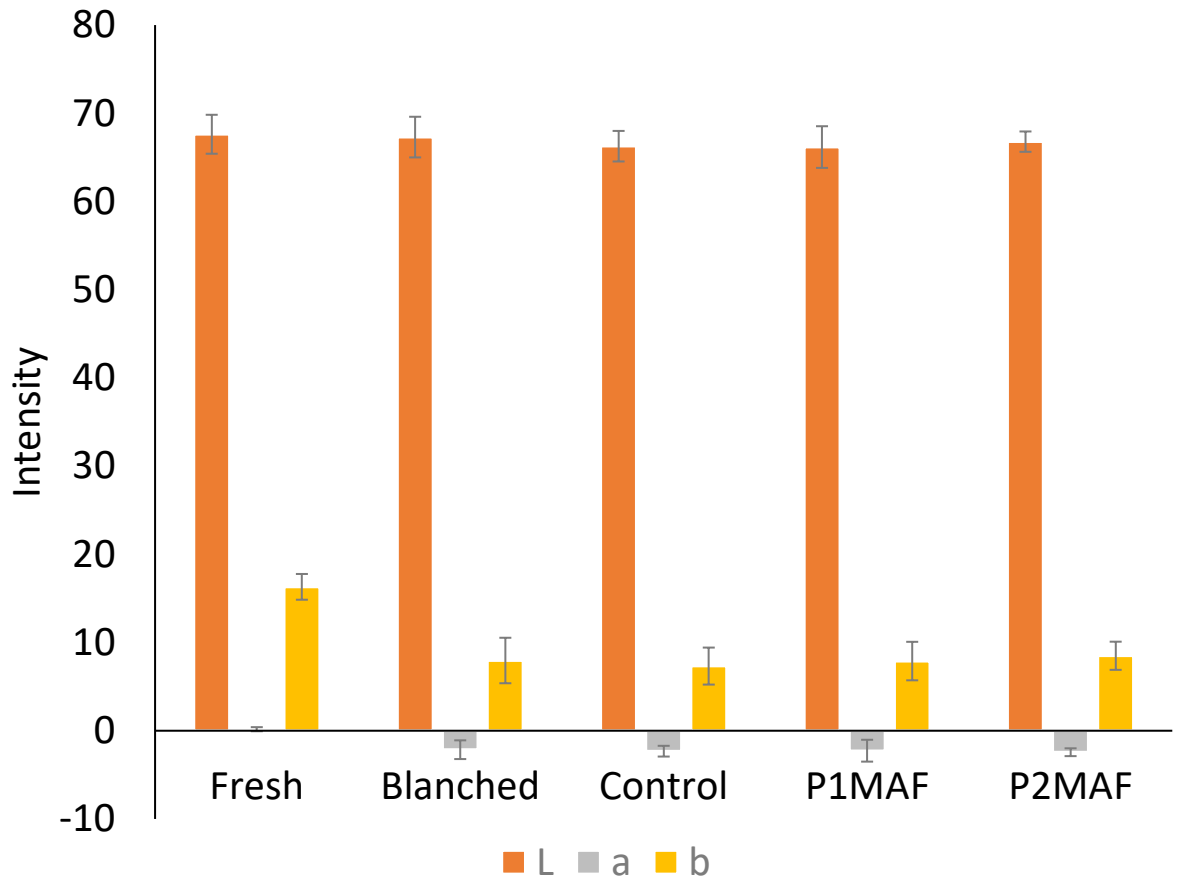

Figure 73: Colour attributes of potato at different processing steps.

➔Intermediate conclusions:

In this section, the effect of pulsed MAF (PMAF) conditions and control freezing condition (no MAF) on the freezing and quality characteristics of blanched potatoes were studied. The results reveal that the introduction of microwaves did not affect the freezing curve; they were found identical to control freezing condition. Compared to control freezing condition, PMAF conditions resulted in samples having more small pores and thinner pore size distribution range. Besides, PMAF samples exhibited less exudate and texture loss than the control samples. Colour parameters of blanched potato were unaffected by the freezing process. Among the test conditions, P2MAF condition caused highest reduction in ice crystals size and offered least freeze damage.

SUMMARY AND CONCLUSIONS

This PhD project aimed at the following 3 key objectives:

(i) To understand the impact of freezing on the cohesion and damage in fruits and vegetables.
(ii) To develop techniques to access the freeze damage of horticulture product (mainly fruits and vegetables) at various level (cellular to organ level).
(iii) To optimize microwave assisted freezing process from the product quality point of view.

The context of the PhD was related to fruits and vegetables, which are a rich source of nutrients (especially micronutrients), dietary fibre and phytochemicals. They offer low fat, and low calories and are termed cholesterol free product. The consumption of fruits and vegetables provides health benefits. For instance, routine consumption of fruits and vegetable reduces the risk of obesity and many diseases including cardiovascular diseases, cancer, diabetes, certain non-communicable diseases, etc. World health organisation (WHO) recommends consuming more than 400 grams of fruits and vegetables per day (in 5 portions per day) in order to improve the overall health and to reduce the chances of aforementioned diseases.

Fruits and vegetables are seasonal, and hence they are required to be persevered (using different preservation techniques) for their year-round availability. Various short-term (refrigeration, controlled atmospheric storage, modified atmospheric packaging, etc.) and long-term (freezing, canning and drying) preservation techniques have been used to extend the shelf life of fruits and vegetables. Among the long-term preservation techniques, freezing technology causes less deterioration to nutrients and other important health beneficial compounds present in fruits and vegetables. However, it also causes some irreversible damages such as texture loss, colour change, etc. Blanching of the product prior to freezing can resolve the colour change problem.

With respect to freezing and frozen storage of frozen products, three things are of uttermost importance (i) better understanding of the nature and mechanism of freezing injuries (ii) the selection of appropriate freeze damage assessment technique (qualitative and quantitative) that can estimate the freeze damage efficiently, accurately, cost-effectively and can be easily operated, and (iii) development of new freezing technologies that imparts minimum damage to the product.

In this PhD work, the nature and/or extent of freeze damage suffered by apples and potatoes at different freezing rates were studied using several conventional and new analytical methods.

The impact of frozen storage was not regarded for the sake of time. Moreover, the impact of innovative microwave assisted freezing (MAF) process on freezing parameters and quality indicators were also explored. The conclusions from the outcomes of the project are listed below.

Effectiveness of freeze damage assessment methods in terms of efficiency, accuracy, cost-of operation, and ease of operation

- Table 13 summarizes the results, and also the pros and cons related to methods used for assessing the freeze damage in fruits and vegetables. A summary of the type of information given by each analytical technique is presented in Table 14. It is hoped that these observations would provide more useful information about the analytical techniques that can be used to estimate freeze damage efficiently.
- The focused freeze damage assessment technology like CLSM, and global freeze damage assessment techniques like texture analysis (also includes laser-puff texture analysis), mass diffusivity test, low field NMR relaxometry, and colour analysis tests used in this study were found to be relevant methods to distinguish the fresh samples from frozen-thawed sample.
- The results suggest that cryo-SEM, CLSM and X-rays microcomputed tomography are suitable for validating small quality changes among the different freezing protocols. Meanwhile, the global methods such as texture (also includes laser-puff texture analysis), NMR, drip loss and mass diffusivity tests, can only reflect larger quality changes.
- To compare freezing protocols, the colour analysis was found to be an unsuitable parameter.
- Efficiency and accuracy wise, cryo-SEM, CLSM and X-rays microcomputed tomography can be termed as best methods to analyze the freezing injuries.
- NMR, cryo-SEM, X-rays microcomputed tomography, CLSM techniques are expensive techniques, whereas mass diffusivity tests, texture analysis, drip loss measurements, colour analysis are cost-effective methods.
- The analyses time for NMR, X-rays microcomputed tomography and mass diffusivity are long, while other methods take substantially less time.

From a global point of view, a debate could be opened on which is the most relevant technique to assess freeze damage. Two key parameters can be tackled, (i) the size of the field that is embraced by the technique and (ii) the representative size of the technique. For example, NMR will tackle a sample of ca 1 cm and will provide information at the level of a water molecule

(2.75 Å). Cryo-SEM will look at field of ca 100 µm with information at 0.1 µm, even though in this case the freeze damage is observed at the scale of an ice crystal (ca 10 µm). The ratio between the size of field and the representative size of technique could be considered as a kind of "freeze damage assessment index" (FDA Index) to assess the relevance of each technique. The higher will be this FDA index, the most useful will be (a priori) the technique. From such point of view NMR looks like the best candidate, even though the interpretation and quantification of the freeze damage based on T_1 and T_2 values are quite subjective. The major concerns relates to the size of the field. Observation of the freeze damage on a single cell can be very informative and detailed, but ca a hundred of cells should be analysed to obtain an averaged information, which is out of reach for time reasons. Another aspects relies on the possibility to repeat the analysis and on the time needed for a single measurement. It is almost impossible to conclude on which is the best technique anyway. CLSM, cryo-SEM bring informative images that can help to visualize the defaults and that can support observations done with other techniques at a broader field like NMR, texture, drip losses. The proper assessment of freeze damage remains a challenge and requires a mass of experimental work before drawing any conclusion. The impact of storage time and temperature add one more "dimension" to the problem, making it very important for the experimental work to finish quickly.

Impact of different freezing protocols on the freezing characteristics and quality attributes of apples and potatoes

The impact of different freezing rates on the freezing parameters and quality attributes of apple was studied under this project. The slow freezing process (− 18 ℃) yielded freezing curves having three stages i.e. the supercooling, nucleation, and phase change. Meanwhile, intermediate freezing (− 40 ℃ and 2 m/s air velocity) and fast freezing conditions (− 72 ℃ at 1 m/s air velocity) had no evident characteristics of all the above three stages. As expected, finer ice crystals were formed when freezing speed was increased. The difference in ice crystals among three freezing protocols were clearly visible in the cryo-SEM micrographs. The drip loss, texture and solid gain data reveals that a significant improvement happens only when the difference in freezing rate offered by the process is very large (i.e. freezing rate offered at − 18 ℃ Vs. − 72 ℃ in the present case).

Similar to apple, the potatoes were also frozen by freezing protocols and their quality was evaluated. The slowly frozen (− 18 ℃) potatoes exhibited supercooling during freezing while

no supercooling was noticed for other freezing conditions (i.e. − 30 ℃-intermediate freezing process and − 74 ℃-fast freezing process). The initial freezing point could be detected for slow freezing and intermediate freezing conditions, while it was hard to detect the initial freezing point for the fast freezing condition. The initial freezing point temperature data for slow freezing and intermediate freezing conditions revealed that a depression in freezing point happened when freezing rate was increased. The slow freezing process resulted in bigger ice crystals and caused the highest damage to the cellular structure. The cells were highly distorted (deformed cells with buckled and folded cell wall structure) when the slow freezing condition was used. Intermediate freezing process produced relatively small ice crystals than slow freezing process and maintained the cell wall structure integrity, however, it could not preserve the cell shape. The fast freezing process not only promoted the formation of very fine ice crystals but also preserved the morphology of the cells. The NMR analytical parameters, texture and drip loss values showed that significant effect of the freezing process on these parameters could be obtained when freezing rate difference used during the freezing process was higher (i.e. freezing rate offered at − 18 ℃ Vs. − 74 ℃ in the present case). None of the freezing protocols preserved the colour parameters of the fresh potato.

As a global conclusion of this section, fast freezing process (at − 72 ℃ and − 74 ℃ for apple and potato) could be considered as the best choice among the studied freezing conditions for freezing small size products since it promotes the formation of the small size ice crystals in the products and also imparts lower freeze damage.

Table 13. Benchmarking study on freeze damage assessment methods.

Freeze damage assessment methods for fruits and vegetables	Focused Methods		Global methods						
	Cryo-SEM	CLSM	Texture Analysis		NMR	Drip loss	Colour	Mass diffusivity	X-ray tomography
			Conventional	Laser-Puff					
Sample preparation	Difficult	Difficult	Easy	Easy	Easy	Easy	Easy	Easy	Easy
Ability to detect differences between fresh and frozen-thawed sample	×	++++	++++	++++	++++	++++	++++	++++	×
Ability to distinguish different freezing protocols	++++	++++	++	++	+	++	-	+++	++++
Analysis time (sample preparations + data acquisition and treatment)	++	++	+	+	+++	+	+	++++	++++
Interpretation of measured analytical parameters	Easy	Easy	Easy	Easy	Difficult	Easy	Easy	Easy* & Difficult**	Easy
Nature of sample	F	F-T	F-T	F-T	F & F-T	F-T	F-T	F-T	FD
Cost of operation	High	High	Low cost	Low cost	High	Low cost	Low cost	Low cost	High
Status of method	OU	NUO	VC	NM	NUO	VC	VC	NM	NUO

+ = Lowest value; ++++ = Highest value; × = Not applicable; - = No effect; * = Immediately after freezing-thawing; ** = Mass diffusion during the test period of 3h (readings were taken at a time interval of 0.5h during the test).

Abbreviations of the words: F = Frozen; F-T = Frozen-Thawed; FD = Freeze-dried; OU = Often used; NUO = Not used often; VC = Very common; NM = New method.

Table 14. Summary of the type of information given by each analytical technique.

Analytical method	Information gathered
Cryo-SEM	Ice crystals morphology and cellular structure status.
CLSM	Cellular structure detail such as (a) integrity of pectocellulosic wall and (b) shape of the cells.
X-ray tomography	3-D information about the product (pore size distribution), quantitative measurement.
NMR	Information about the water contained in the different cellular compartments.
Mass diffusivity test	Well-being of the cellular structure. The solute diffusivity is higher when the damage to the cellular structure is greater.
Texture (conventional and laser-puff firmness tester) and drip loss	Provides global information about the damage caused to the product. Higher the damage to the cellular structure higher would be the texture and drip loss.

Impact of microwave assisted freezing (MAF) on the freezing parameters and quality factors of apple and potato

MAF of apples and potatoes was performed by applying constant microwave power (CMAF = 167 W/kg) and pulsed microwave power (P1MAF and P2MAF = 500 and 667 W/kg with 10 s pulse width and 20 s pulse interval) during the freezing process. A custom-built microwave freezer which consisted of a domestic microwave cavity installed in a blast freezer was used for MAF. To the best our knowledge, this is the first time that the MAF process is used for freezing plant products (i.e. apples and potatoes). In this study, the impact of MAF conditions on freezing parameters and quality attributes (for e.g. microstructure, texture, drip loss, etc.) of apples and potatoes were studied using several analytical techniques.

In the case of apple, microwave use during freezing did not affect the freezing parameters. For instance, the shapes of the freezing curve obtained during conventional freezing and MAF of apples were identical to each other. No supercooling was observed for any of the freezing conditions. The characteristic freezing time and the overall freezing time and freezing rate values were found to be similar for all conditions. Concerning quality parameters, the application of microwaves during freezing process produced superior microstructure (homogenous pore size distribution with a larger population of small pores) than the control sample. Moreover, MAF of apple resulted in a lower drip loss, meanwhile, it also led to a lower reduction in firmness/hardness compared to reference sample. The microwave form (constant mode or pulsed mode) and power level were found as critical parameters that controlled the quality attributes of apple sample. For instance, average pore size, texture loss, and drip loss significantly ($p < 0.05$) decreased with the introduction of pulsed microwave conditions and with the increase in microwave power level. P2MAF condition gave the best result in terms of microstructure and other quality attributes such as drip loss and texture.

Similar to apple, the freezing curve shape and freezing parameter (characteristic freezing time, and the overall freezing time and freezing rate) were unaffected by the introduction of the microwave during freezing of potato. The MAF samples exhibited microstructure with more small size pores that were distributed uniformly throughout the sample, while no MAF condition resulted in a product having relatively larger pores and a wider pore size distribution range. The texture loss and drip loss were lower for MAF sample than the control sample. No significant effect of any of the freezing conditions on the colour parameters was observed. The quality preservation was greater when microwave intensity was increased. Among all freezing conditions, P2MAF condition yielded the best result in terms of microstructure and other quality attributes such as drip loss and texture.

As a result, the key objectives of this PhD project, for the most, have been achieved. Studying fruits and vegetable undergoing freezing is among the most challenging topic, compared to meat for example for which it is relatively easier to assess freeze damage. The precise impact of MW on freezing is still under debate. Two hypothesis were proposed by Xanthakis et al. (2014b) about the possible effect of MW during freezing, either disruption of ice crystals with continuous MW power emission (CMAF), either nucleation induced by MW duty ratio (Pulsed MW Assisted Freezing = PMAF). From our results, it seems that PMAF hypothesis is the right hypothesis. However, further investigations are needed as optimal combinations of power level and duty ratio may exist for a given food with a given geometry. The second point is the power level that is needed. Our experimental system was a small domestic cavity with multimode conditions; in such configuration, it is almost impossible to ensure that all the emitted energy will be trapped by the sample, some of it may be indeed reflected toward the emitter. Therefore, at this stage of the research, the value of specific energy reported in this study for MAF (PMAF and CMAF) should be considered as an indicative value.

Despite these minor issues, the very final conclusion of this study is that MW assisted freezing has a clear effect in reducing the size of ice crystals in the case of freezing of fruits and vegetables. The reduction of size is not huge but is significant. Further, follow up studies could address the following aspects for example:

- It could be worth to keep on the investigation to optimize the duty ratio for PMAF process.
- Applying MW assisted freezing at larger scale in a continuous system.
- Assessing the quality during frozen storage to check up to which point the initial advantage of MW assisted freezing is preserved during storage in comparison to a control.
- Investigating different MW or RF wavelength; in particular, RF is much less powerful than MW and provided very interesting results in several studies (Anese et al., 2012; Hafezparast-Moadab et al., 2018). Still, the way these authors have proceeded and the specific energy that was used is not fully clear and further studies are obviously needed.

REFERENCES

Abbott, J. A. (2004). Textural quality assessment for fresh fruits and vegetables. In F. Shahidi, A. M. Spanier, C. T. Ho, & T. Braggins (Eds.), *Quality of Fresh and Processed Foods* (pp. 265–279). New York: Springer Science+Business Media, LLC.

Aguilera, J. M., & Stanley, D. W. (1999). *Microstructural principles of food processing and engineering* (2nd ed., pp. 1-70). Maryland: Aspen Publishers, Inc..

Alizadeh, E., Chapleau, N., de-Lamballerie, M., & Le-Bail, A. (2009). Impact of freezing process on salt diffusivity of seafood: Application to salmon (salmo salar) using conventional and pressure shift freezing. *Food and Bioprocess Technology*, *2*(3), 257–262.

Alvarez, M. D., Canet, W., & López, M. E. (2002). Influence of deformation rate and degree of compression on textural parameters of potato and apple tissues in texture profile analysis. *European Food Research and Technology*, *215*(1), 13–20.

Ammar, J. B., Lanoisellé, J. L., Lebovka, N. I., Van Hecke, E., & Vorobiev, E. (2010). Effect of a pulsed electric field and osmotic treatment on freezing of potato tissue. *Food Biophysics*, *5*(3), 247–254.

Anese, M., Manzocco, L., Panozzo, A., Beraldo, P., Foschia, M., & Nicoli, M. C. (2012). Effect of radiofrequency assisted freezing on meat microstructure and quality. *Food Research International*, *46*(1), 50–54.

Angersbach, A., Heinz, V., & Knorr, D. (1999). Electrophysiological model of intact and processed plant tissues: Cell disintegration criteria. *Biotechnology Progress*, *15*(4), 753–762.

Anon (2018a). https://advanced-microscopy.utah.edu/education/electron-micro/. Retrieved on 10 June 2018.

Anon (2018b). http://cobra.rdsor.ro/cursuri/cielab.pdf. Retrieved on 3rd July 2018.

Arunyanart, T., Siripatrawan, U., Makino, Y., & Oshita, S. (2015). Rapid method based on proton spin – spin relaxation time for evaluation of freezing damage in frozen fruit and vegetable. *Journal of Food Processing and Preservation*, *39*, 2802–2810.

Bache, I. C., & Donald, A. M. (1998). The structure of the gluten network in dough: a study using environmental scanning electron microscopy. *Journal of Cereal Science*, *28*(2), 127–133.

Bai, Y., Sha, M., Perera, C. O., Smith, B., & Melton, L. D. (2001). State diagram of apple slices : glass transition and freezing curves. *Food Research International*, *34*, 89–95.

Barba, F. J., Ahrné, L., Xanthakis, E., Landerslev, M. G., Orlien, V. (2017). Innovative

technologies (Chapter 2.). *In* F. J. Barba; M. Koubaa; V. Orlien; A. Sant´Ana, *Innovative Technologies for Food Preservation: Inactivation of spoilage and pathogenic microorganisms.* Elsevier Academic Press. London: 25-51.

Barrett, D. M., Garcia, E., & Wayne, J. E. (1998). Textural modification of processing tomatoes. *Critical Reviews in Food Science and Nutrition*, *38*(3), 173–258.

Bartolomé, A. P., Rupérez, P., & Fúster, C. (1996). Non-volatile organic acids, pH and titratable acidity changes in pineapple fruit slices during frozen storage. *Journal of the Science of Food and Agriculture*, *70*(4), 475–480.

Bellows, R. J., & King, C. J. (1973). Product collapse during freeze drying of liquid foods. *AIChE Symposium Series*, *69*(132), 33–41.

Bhande, S. D., Ravindra, M. R., & Goswami, T. K. (2008). Respiration rate of banana fruit under aerobic conditions at different storage temperatures. *Journal of Food Engineering*, *87*, 116–123.

Bomben, J. L., & King, C. J. (1982). Heat and mass transport in the freezing of apple tissue. *Journal of Food Technology.*, *17*, 615–632.

Bourne, M. C. (Ed.). (1982). *Food Texture and Viscosity : Concept and Measurement*. London: Academic Press, INC.

Brown, M. S. (1979). Frozen fruits and vegetables: their chemistry, physics, and cryobiology. *Advances in Food Research*, *25*, 181–235.

Brown, M. S. (1977). Texture of frozen fruits and vegetables. *Journal of Texture Studies*, *7*, 391–404.

Buck, P. A., & Joslyn, M. A. (1953). Broccoli processing, accumulation of alcohol in underscalded frozen broccoli. *Journal of Agricultural and Food Chemistry*, *1*(4), 309–312.

Buren, J. P. V. (1979). The chemistry of texture in fruits and vegetables. *Journal of Texture Studies*, *10*, 1–23.

Cano, M. P., de Acnos, B, & Monreal, G. L. M. (1996). Effects of freezing and canning of papaya slices on their carotenoid composition. *Zeitschrift für Lebensmittel-Untersuchung und -Forschung*, *202*, 279–284.

Cano, M. P. (1996). Vegetables. In L. E. Jeremiah (Ed.), *Freezing effects on food quality* (pp. 247-298). New York: Marcel- Dekker.Inc.

Cano, M. P., & de Acnos, B. (1994). Carotenoid and carotenoid ester composition in mango fruit as influenced by processing method. *Journal of Agricultural and Food Chemistry*, *42*, 2737–2742.

Cano, M. P., Fuster, C., & Marin, M. A. (1993). Freezing preservation of four Spanish kiwi

fruit cultivars (Actinidia chinensis, Planch): chemical aspects. *Zeitschrift für Lebensmittel-Untersuchung und Forschung*, *196*(2), 142–146.

Cano, M. P., & Marin, M. A. (1992). Pigment composition and color of frozen and canned kiwi fruit slices. *Journal of Agricultural and Food Chemistry*, *40*, 2141–2146.

Cano, P., Marin, M. A., & Carmen Fuster. (1990). Freezing of banana slices. Influence of maturity level and thermal treatment prior to freezing. *Journal of Food Science*, *55*(4), 1070–1072.

Cao, X., Zhang, F., Zhao, D., Zhu, D., & Li, J. (2018). Effects of freezing conditions on quality changes in blueberries. *Journal of the Science of Food and Agriculture.* In press accepted manuscript.

Chaovanalikit, A., & Wrolstad, R. E. (2004). Anthocyanin and polyphenolic composition of fresh and processed cherries. *Journal of Food Science*, *69*(1), FCT73-FCT83.

Charoenrein, S., & Owcharoen, K. (2016). Effect of freezing rates and freeze-thaw cycles on the texture, microstructure and pectic substances of mango. *International Food Research Journal*, *23*(2), 613–620.

Chassagne-Berces, S., Fonseca, F., Citeau, M., & Marin, M. (2010). Freezing protocol effect on quality properties of fruit tissue according to the fruit , the variety and the stage of maturity. *LWT - Food Science and Technology*, *43*, 1441–1449.

Chassagne-Berces, S., Poirier, C., Devaux, M. F., Fonseca, F., Lahaye, M., Pigorini, G., Girault, C., Marin, M., & Guillon, F. (2009). Changes in texture, cellular structure and cell wall composition in apple tissue as a result of freezing. *Food Research International*, *42*(7), 788–797.

Chen, L., & Opara, U. L. (2013). Texture measurement approaches in fresh and processed foods — A review. *Food Research International*, *51*, 823–835.

Chen, P., & Sun, Z. (1991). A review of non-destructive methods for quality evaluation and sorting of agricultural products. *Journal of Agricultural Engineering Research*, *49*, 85–98.

Cheng, L., Sun, D. W., Zhu, Z., & Zhang, Z. (2017). Emerging Techniques for Assisting and Accelerating Food Freezing Processes─A Review of Recent Research Progresses. *Critical Reviews in Food Science and Nutrition*, *57*(4), 769–781.

Chevallier, S., Réguerre, A., Le-Bail, A., & Della Valle, G.. (2014). Determining the cellular structure of two cereal food foams by X-ray micro-tomography. *Food Biophysics*, *9*, 219–228.

Choi, Y. S., Ku, S. K., Jeong, J. Y., Jeon, K. H., & Kim, Y. B. (2015). Changes in ultrastructure and sensory characteristics on electro-magnetic and air blast freezing of beef during frozen

storage. *Korean Journal for Food Science of Animal Resources*, *35*(1), 27–34.

Clark, C. J., Hockings, P. D., Joyce, D. C., & Mazucco, R. A. (1997). Application of magnetic resonance imaging to pre- and post-harvest studies of fruits and vegetables. *Postharvest Biology and Technology*, *11*, 1–21.

Cnudde, V., & Boone, M. N. (2013). Earth-Science Reviews High-resolution X-ray computed tomography in geosciences : A review of the current technology and applications. *Earth Science Reviews*, *123*, 1–17.

Dalvi-Isfahan, M., Hamdami, N., Xanthakis, E., & Le-Bail, A. (2016). Review on Control of Ice Nucleation by Ultrasound Waves, Electric and Magnetic Fields. *Journal of Food Engineering*, *195*, 222–234.

Dalvi-Isfahan, M., Hamdami, N., & Le-Bail, A. (2016). Effect of freezing under electrostatic field on the quality of lamb meat. *Innovative Food Science and Emerging Technologies*, *37*, 68–73.

Dalvi-isfahan, M., Hamdami, N., & Le-bail, A. (2017). Effect of freezing under electrostatic field on selected properties of an agar gel. *Innovative Food Science & Emerging Technologies*, *42*, 151–156.

Dalvi-Isfahan, M., Hamdami, N., & Le-Bail, A. (2018). Effect of combined high voltage electrostatic with air blast freezing on quality attributes of lamb meat. *Journal of Food Process Engineering*, 1–6.

d'Avila, M. A., Powell, R. L., Phillips, R. J., Shapley, N. C., Walton, J. H., & Dungan, S. R. (2005). Magnetic resonance imaging (MRI): A technique to study flow an microstructure of concentrated emulsions. *Brazilian Journal of Chemical Engineering*, *22*(1), 49–60.

de Ancos, B., Ibanez, E., Reglero, G., & Cano, M. P. (2000). Frozen storage effects on anthocyanins and volatile compounds of raspberry fruit. *Journal of Agricultural and Food Chemistry*, *48*, 873–879.

de Ancos, B., Sánchez-Moreno, C., Pascual-Teresa, D., & Cano, M. P. (2012). Freezing preservation of fruits. In N. K. Sinha, J. S. Sidhu, J. Barta, J. S. B. Wu, & M. P. Cano (Eds.), *Handbook of Fruits and Fruit Processing* (2nd ed., pp. 103–119). Iowa: Wiley-Blackwell.

Defraeye, T., Lehmann, V., Gross, D., Holat, C., Herremans, E., Verboven, P., Verlinden, B. E., & Nicolai, B. M. (2013). Application of MRI for tissue characterisation of "Braeburn" apple. *Postharvest Biology and Technology*, *75*, 96–105.

Delgado, A. E., Zheng, L., & Sun, D. W. (2009). Influence of ultrasound on freezing rate of immersion-frozen apples. *Food and Bioprocess Technology*, *2*(3), 263–270.

Delgado, A. E., & Rubiolo, A. C. (2005). Microstructural changes in strawberry after freezing and thawing processes. *LWT-Food Science and Technology, 38*, 135–142.

Delgado, A. E., & Sun, D. W. (2001). Heat and mass transfer models for predicting freezing processes – a review. *Journal of Food Engineering*, *47*(3), 157–174.

Deshmukh, K., Sankaran, S., Ahamed, B., Sadasivuni, K. K., Pasha, K. S. K., Ponnamma, D., Rama Sreekanth, P.S., & Chidambaram, K. (2017). Dielectric Spectroscopy. In S. Thomas, R. Thomas, A. Zachariah, & R. Mishra (Eds.), *Spectroscopic Methods for Nanomaterials Characterization* (1st ed., pp. 237–299). Amsterdam: Elsevier Inc.

Donhowe, D. P., Hartel, R. W., & Bradley, R. L. (1991). Determination of ice crystal size distributions in frozen desserts. *Journal of Dairy Science*, *74*, 3334–3344.

Duce, S. L., Carpenter, T. A., & Hall, L. D. (1992). Nuclear magnetic resonance imaging of fresh and frozen courgettes. *Joumal of Food Engineering*, *16*, 165–172.

Dufour, L. (1861). Ueber das Gefrieren des Wassers und über die Bildung des Hagels. *Annalen der Physik*, *190*(12), 530–554. Evans, J., Adler, J., Mitchell, J., Blanshard, J., & Rodger, G. (1996). Use of confocal laser scanning microscope in conjunction with a conduction heat transfer stage in order to observe dynamically the freeze–thaw cycle in an autofluorescent substance and to measure ice crystal sizein situ. *Cryobiology*, *33*(1), 27–33.

Falcone, P. M., Baiano, A., Conte, A., Mancini, L., Tromba, G., Zanini, F., & Del Nobile, M. A. (2006). Imaging techniques for the study of food microstructure: a review. *Advances in Food and Nutrition Research*, *51*(6), 205–263.

Farber, L., Tardos, G., & Michaels, J. N. (2003). Use of X-ray tomography to study the porosity and morphology of granules. *Powder Technology*, *132*(1), 57–63.

Fava, J., Alzamora, S. M., & Castro, M. A. (1996). Structure and nanostructure of the outer tangential epidermal cell wall in *Vaccinium corymbosum* L. (Blueberry) fruits by blanching, freezing–thawing and ultrasound. *Food Science and Technology International*, *12*(2), 241–251.

Feder, N. (1958). Methods and principles of fixation by freeze-substitution. *The Journal of Cell Biology*, *4*(5), 593–602.

Feldkamp, L. A., Davis, L. C., & Kress, J. W. (1984). Practical cone-beam algorithm. *Journal of the Optical Society of America A*, *1*(6), 612–619.

Fennema, O. (1966). An overall view of low temperature food preservation. *Cryobiology*, *3*(3), 197–213.

Fikiin, K. A. (1998). Ice content prediction methods during food freezing: a survey of the

Eastern European literature. *Journal of Food Engineering*, *38*(3), 331-339.

Fikiin, K. A., & Fikiin, A. G. (1999). Predictive equations for thermophysical properties and enthalpy during cooling and freezing of food materials. *Journal of food engineering*, *40*(1-2), 1-6.

Fennema, O. (1988). Effects of freeze preservation on nutrients. In E. Karmas & R. S. Harris (Eds.), *Nutritional evaluation of food processing* (3rd ed., pp. 269–317). New York: Van Nostrand Reinhold Company Inc.

Fletcher, N. H. (1970). *The chemical physics of ice*. (A. Herzenberg, M. M. Woolfson, & J. M. Ziman, Eds.). Cambridge: Cambridge University Press.

Floury, J., Le Bail, A., & Pham, Q. T. (2008). A three-dimensional numerical simulation of the osmotic dehydration of mango and effect of freezing on the mass transfer rates. *Journal of Food Engineering*, *85*, 1–11.

Fuchigami, M., Miyazaki, K., Kato, N., & Teramoto, A. (1997). Histological changes in high-pressure-frozen carrots. *Journal of Food Science*, *62*(4), 809–812.

Fuchigami, M., Hyakumoto, N., & Miyazaki, K. (1995). Programmed freezing affects texture, pectic composition and electron microscopic structures of carrots. *Journal of Food Science*, *60*(1), 137–141.

Fuchigami, M., Hyakumoto, N., Miyazaki, K., Nomura, T., & Sasaki, J. (1994). Texture and histological structure of carrots frozen at a programmed rate and thawed in an electrostatic field. *Journal of Food Science*, *59*(6), 1162–1167.

Fúster, C., Préstamo, G., & Cano, M. P. (1994). Drip loss, peroxidase and sensory changes in kiwi fruit slices during frozen storage. *Journal of the Science of Food and Agriculture*, *64*, 23–29.

Gamble, G. R. (1994). Non-invasive determination of freezing effects in blueberry fruit tissue by magnetic resonance imaging. *Journal of Food Science*, *59*(3), 571–573.

Gao, D., & Critser, J. K. (2000). Mechanisms of Cryoinjury in Living Cells. *ILAR Journal*, *41*(4), 187–196.

Giddings, T. H., O'Toole, E. T., Morphew, M., Mastronarde, D. N., McIntosh, J. R., & Winey, M. (2001). Using rapid freeze and freeze-substitution for the preparation of yeast cells for electron microscopy and three-dimensional analysis. *Methods in Cell Biology*, *67*, 27–42.

Goncalves, E. M., Abreu, M., Brandão, T. R. S., & Silva, C. L. M. (2011). Degradation kinetics of colour, vitamin C and drip loss in frozen broccoli (*Brassica oleracea* L. ssp. *Italica*) during storage at isothermal and non-isothermal conditions. *International Journal of Refrigeration*, *34*(8), 2136–2144.

González-Castro, M. J., Oruña-Concha, M. J., López-Hernández, J., & Simal-Lozano, J. (1997). Effects of freezing on the organic acid content of frozen green beans and Padrón peppers. *Zeitschrift für Lebensmittel-Untersuchung und -Forschung*, *204*, 365–368.

Gowen, A. A., Taghizadeh, M., & O'Donnell, C. P. (2009). Identification of mushrooms subjected to freeze damage using hyperspectral imaging. *Journal of Food Engineering*, *93*(1), 7–12.

Gray, J. D., Kolesik, P., Høj, P. B., & Coombe, B. G. (1999). Confocal measurement of the three-dimensional size and shape of plant parenchyma cells in a developing fruit tissue. *The Plant Journal*, *19*(2), 229–236.

Greenham, C. G. (1966). The stages at which frost injury occurs in alfalfa. *Canadian Journal of Botany*, *44*, 1471–1483.

Gregory III, J. F. (1996). Vitamins. In O. R. Fennema (Ed.), *Food Chemistry* (3rd ed., pp. 531–616). New York: Marcel Dekker, Inc.

Grout, B. W. W., Morris, G. J., & McLellan, M. R. (1991). Freezing of fruit and vegetables. In W. B. Bald (Ed.), *Food Freezing: Today and Tomorrow* (pp. 113–122). London: Springer-Verlag.

Guillemin, F., Devaux, M. F., & Guillon, F. (2004). Evaluation of plant histology by automatic clustering based on individual cell morphological features. *Image Anal Stereol*, *23*, 13–22.

Hafezparast-Moadab, N., Hamdami, N., Dalvi-Isfahan, M., & Farahnaky, A. (2018). Effects of radiofrequency-assisted freezing on microstructure and quality of rainbow trout (Oncorhynchus mykiss) fillet. *Innovative Food Science and Emerging Technologies*, 47, 81-87.

Hafsa, I., Cuq, B., Jin Kim, S., Le-Bail, A., Ruiz, T., & Chevallier, S. (2014). Description of internal microstructure of agglomerated cereal powders using X-ray microtomography to study of process – structure relationships. *Powder Technology*, *256*, 512–521.

Haard, N. F., & Chism, G. W. (1996). Characteristics of Edible Plant Tissues. In O. R. Fennema (Ed.), *Food Chemistry* (3rd ed., pp. 944–1011). New York: Marcel Dekker, Inc.

Hanyu, Y., Ichikawa, M., & Matsumoto, G. (1992). An improved cryofixation method: cryoquenching of small tissue blocks during microwave irradiation. *Journal of Microscopy*, *165*(2), 255–271.

Hager, T. J., Howard, L. R., Prior, R. L., & Brownmiller, C. (2008). Processing and storage effects on monomeric anthocyanins, percent polymeric color, and antioxidant capacity of processed blackberry products. *Journal of Food Science*, *73*, H134–H140.

Havet, M., Orlowska, M., & Le-Bail, A. (2009). Effects of an electrostatic field on ice

nucleation. In *International Conference on Bio and Food Electrotechnologies*. Compiègne, France (pp. 22-23).

Hayden, R. E., Dionne, L., & Fensom, D. S. (1972). Electrical impedance studies of stem tissue of Solanum clones during cooling. *Canadian Journal of Botany*, *50*, 1547–1554.

Hernández-Sánchez, N., Barreiro, P., Ruiz-Altisent, M., Ruiz-Cabello, J., & Fernández-Valle, M. E. (2004). Detection of freeze injury in oranges by magnetic resonance imaging of moving samples. *Applied Magnetic Resonance*, *26*(3), 436.

Hills, B. P., & Nott, K. P. (1999). NMR studies of water compartmentation in carrot parenchyma tissue during drying and freezing. *Applied Magnetic Resonance*, *17*, 521–535.

Hills, B. P., & Remigereau, B. (1997). NMR studies of changes in subcellular water compartmentation in parenchyma apple tissue during drying and freezing. *International Journal of Food Science and Technology*, *32*, 51–61.

Hu, S. Q., Liu, G., Li, L., Li, Z. X., & Hou, Y. (2013). An improvement in the immersion freezing process for frozen dough via ultrasound irradiation. *Journal of Food Engineering*, *114*(1), 22–28.

Hung, Y. C., McWatters, K. H., & Prussia, S. E. (1998). Peach sorting performance of a non destructive laser air-puff firmness detector. *Applied Engineering in Agriculture*, *14*(5), 513–516.

IIR (1986). Recommendations for the Processing and Handling of Frozen Foods (3rd ed. pp. 30). International Institute of Refrigeration.

Jackman, R. L., & Stanley, D. W. (1995). Perspectives in the textural evaluation of plant foods. *Trends in Food Science & Technology*, *6*, 187–194.

Jackson, T. H., Ungan, A., Critser, J. K., & Gao, D. (1997). Novel microwave technology for cryopreservation of biomaterials by suppression of apparent ice formation. *Cryobiology*, *34*(4), 363–372.

Jalté, M., Lanoisellé, J. L., Lebovka, N. I., & Vorobiev, E. (2009). Freezing of potato tissue pre-treated by pulsed electric fields. *LWT - Food Science and Technology*, *42*(2), 576–580.

Jha, P. K., Xanthakis, E., Jury, V., Havet, M., & Le-Bail, A. (2018b). Advances of electro-freezing in food processing. *Current Opinion in Food Science*, *23*, 85–89.

Jha, P. K., Jury, V., Chevallier, S., Xanthakis, E., & Le-Bail, A. (2018a). Freezewave H2020 project-microwave assisted freezing of potato. In *5th IIR Conference on Sustainability and the Cold Chain, ICCC 2018, 6 April 2018 through 8 April 2018* (pp. 190-195)..

Jha, P. K., Sadot, M., Vino, S. A., Jury, V., Curet-ploquin, S., Rouaud, O., Havet, M., & Le-Bail, A. (2017a). A review on effect of DC voltage on crystallization process in food

systems. *Innovative Food Science and Emerging Technologies*, *42*, 204–219.

Jha, P. K., Xanthakis, E., Jury, V., & Le-Bail, A. (2017b). An Overview on Magnetic Field and Electric Field Interactions with Ice Crystallisation; Application in the Case of Frozen Food. *Crystals*, *7*(10), 299.

Jia, G., He, X., Nirasawa, S., Tatsumi, E., Liu, H., & Liu, H. (2017). Effects of high-voltage electrostatic field on the freezing behavior and quality of pork tenderloin. *Journal of Food Engineering*, *204*, 18–26.

Kalab, M., Allan-Wojtas, P., & Miller, S. S. (1995). Microscopy and other imagining techniques in food structure analysis. *Trends in Food Science & Technolog*, *6*, 177–186.

Kashchiev, D. (1972). On the influence of the electric field. *Philosophical Magazine*, *25*(2), 459–470.

Kays, S. (1991). Metabolic Processes in Harvested Products. In *Post Harvest Physiology of Perishable Plant Products* (pp. 75-142). NY: Van Nostrand Reinhold Publication.

Kerr, W. L., Clark, C. J., Mccarthy, M. J., & Ropp, J. S. De. (1997). Freezing effects in fruit tissue of kiwifruit observed by magnetic resonance imaging. *Scientia Horticulturae*, *69*, 169–179.

Khan, A. A., & Vincent, J. F. V. (1993). Compressive stiffness and fracture properties of apple and potato parenchyma. *Journal of Texture Studies*, *24*, 423–435.

Khan, A., & Vincent, J. (1996). Mechanical damage induced by controlled freezing in apple and potato. *Journal of Texture Studies*, *27*(1996), 143–157.

Kiani, H., & Sun, D. W. (2011). Water crystallization and its importance to freezing of foods: A review. *Trends in Food Science and Technology*, *22*(8), 407–426.

Kidmose, U., & Martens, H. J. (1999). Changes in texture, microstructure and nutritional quality of carrot slices during blanching and freezing. *Journal of the Science of Food and Agriculture*, *79*, 1747–1753.

Kilcast, D. (2001). Modern methods of texture measurement. In E. Kress-Rogers & C. J. B. Brimelow (Eds.), *Instrumentation and sensors for the food industry* (2nd ed., pp. 518–549). Cambridge: Woodhead Publishing Limited.

Kim, S. C., Shin, J. M., Lee, S.-W., Kim, C. H., Kwon, Y. C., & Son, K. Y. (2013a). US008616008B2. Unlted States Patent and Trademark Office.

Kim, Y. B., Jeong, J. Y., Ku, S. K., Kim, E. M., Park, K. J., & Jang, A. (2013b). Effects of various thawing methods on the quality characteristics of frozen beef. *Korean Journal for Food Science of Animal Resources*, *33*(6), 723-729.

Kim, Y. B., Woo, S. M., Jeong, J. Y., Ku, S. K., Jeong, J. W., Kum, J. S., & Kim, E. M. (2013c).

Temperature changes during freezing and effect of physicochemical properties after thawing on meat by air blast and magnetic resonance quick freezing. *Korean Journal for Food Science of Animal Resources*, *33*(6), 763-771.

Kim, S. M. I. N., Milczarek, R., & Mccarthy, M. (2008). Fast detection of seeds and freeze damage of mandarines using magnetic resonance imaging. *Modern Physics Letters B*, *22*(11), 941–946.

Kirtil, E., & Oztop, M. H. (2016). ^{1}H Nuclear magnetic resonance relaxometry and magnetic resonance imaging and applications in food science and processing. *Food Engineering Reviews*, *8*(1), 1–22.

Kono, S., Tobari, Y., Araki, T., & Sagara, Y. (2017). Investigating the ice crystal morphology in frozen cooked rice based on size, fractal dimension and ANN modeling. *International Journal of Refrigeration*, *84*, 210-219.

Knoblauch, M., & van Bel, A. J. E. (1998). Sieve tubes in action. *The Plant Cell*, *10*, 35–50.

Knorr, D., & Angersbach, A. (1998). Impact of high-intensity electric field pulses on plant membrane permeabilization. *Trends in Food Science and Technology*, *9*(5), 185–191.

Koch, H., Seyderhelm, I., Wille, P., Kalichevsky, M. T., & Knorr, D. (1996). Pressure-shift freezing and its influence on texture, colour, microstructure and rehydration behaviour of potato cubes. *Molecular Nutrition & Food Research*, *40*(3), 125–131.

Kotwaliwale, N., Curtis, E., Othman, S., & Naganathan, G. K. (2012). Magnetic resonance imaging and relaxometry to visualize internal freeze damage to pickling cucumber. *Postharvest Biology and Technology*, *68*, 22–31.

Lahaye, M., Falourd, X., Limami, A. M., & Foucat, L. (2015). Water mobility and microstructure evolution in the germinating Medicago truncatula seed studied by NMR relaxometry. A revisited interpretation of multicomponent relaxation. *Journal of Agricultural and Food Chemistry*, *63*(6), 1698-1710.

Largo-Gosens, A., Hernández-Altamirano, M., García-Calvo, L., Alonso-Simón, A., Álvarez, J., & Acebes, J. L. (2014). Fourier transform mid infrared spectroscopy applications for monitoring the structural plasticity of plant cell walls. *Frontiers in plant science*, *5*, 303.

Larsen, M., & Poll, L. (1995). Changes in the composition of aromatic-compounds and other quality parameters of strawberries during freezing and thawing. *Zeitschrift für Lebensmittel-Untersuchung und -Forschung*, *201*(3), 275–277.

Lasztity, R., Sebok, A., & Major, J. (1992). Textural properties of fruits and vegetables and their changes during freezing and storage at low temperatures. *Periodica Polytechnica*

Chemical Engineering, *36*(4), 225–238.

Leong, S. Y., & Oey, I. (2012). Effects of processing on anthocyanins, carotenoids and vitamin C in summer fruits and vegetables. *Food Chemistry*, *133*(4), 1577–1587.

Levitt, J. (1956). *The hardiness of plants*. New York: Academic Press Inc., Publishers.

Le-Bail, A., Jha, P., Sadot, M., Chevallier, S., Curet, S., Jury, V., Rouaud, O., Toublanc, C., Havet, M. Conventional and Innovative food freezing; a review on processes and technics to assess freeze damage. 31st EFFoST International Conference, 13th – 16th November, 2017, Sitges, Spain.

Le-Bail, A., Jha, P. K., Xanthakis, E., Havet, M., & Jury, V. (2016). Phase change under static electrical field; in the case of lipids. In *4th IIR International Conference on Sustainability and the Cold Chain,*. Auckland, New Zealand,: IIR. DOI: 10.18462/iir.iccc.2016.0019.

Le-Bail, A., Chapleau, N., Anton-De Lamballerie, M., & Vignolle, M. (2008). Evaluation of the mean ice ratio as a function of temperature in a heterogeneous food: Application to the determination of the target temperature at the end of freezing. *International Journal of Refrigeration*, *31*(5), 816-821.

Le-Bail, A., Chevalier, D., Mussa, D. M., & Ghoul, M. (2002). High pressure freezing and thawing of foods: a review. *International Journal of Refrigeration*, *25*(5), 504-513.

Li, D., Zhu, Z., & Sun, D. W. (2018). Effects of freezing on cell structure of fresh cellular food materials : A review. *Trends in Food Science & Technolog*, *75*, 46–55.

Li, B., & Sun, D. W. (2002). Effect of power ultrasound on freezing rate during immersion freezing of potatoes. *Journal of Food Engineering*, *55*(3), 277–282.

Lim, K. S., & Barigou, M. (2004). X-ray micro-computed tomography of cellular food products. *Food Research International*, *37*(10), 1001–1012.

Lim, M. H., McFetridge, J. E., & Liesebach, J. (2006). Frozen food: components and chemical reactions. In Y. H. Hui (Ed.), *Handbook of Food Science, Technology and Engineering* (pp. 114-1-10). Boca Raton: CRC Press.

Lin, S., & Brewer, M. S. (2005). Effects of blanching method on the quality characteristics of frozen peas. *Journal of Food Quality*, *28*, 350–360.

Lisiewska, Z., & Kmiecik, W. (2000). Effect of storage period and temperature on the chemical composition and organoleptic quality of frozen tomato cubes. *Food Chemistry*, *70*, 167–173.

Lu, R., & Abbott, J. A. (2004). Force/deformation techniques for measuring texture. In D. Kilcast (Ed.), *Texture in food Volume 2: Solid foods* (pp. 109–145). Cambridge: Woodhead Publishing Ltd.

Ma, Y., Zhong, L., Gao, J., Liu, L., Hu, H., & Yu, Q. (2013). Manipulating ice crystallization of 0.9 wt.% NaCl aqueous solution by alternating current electric field. *Applied Physics Letters*, *102*(18), 183701.

Mahajan, P. V, & Goswami, T. K. (2001). Enzyme kinetics based modelling of respiration rate for apple. *Journal of Agricultural Engineering Research*, *79*(4), 399–406.

Mallikarjunan, P., & Hung, Y. C. (1997). Physical and Ultrastructural Measurements. In M. C. Erickson & Y. C. Hung (Eds.), *Quality in Food Frozen* (pp. 313–339). Dordrecht: Springer Science+Business Media.

Marand, H. L., Stein, R. S., & Stack, G. M. (1988). Isothermal crystallization of poly(vinylidene fluoride) in the presence of high static electric fields. I. Primary nucleation phenomenon. *Journal of Polymer Science Part B: Polymer Physics*, *26*(7), 1361–1383.

Marigheto, N., Venturi, L., & Hills, B. (2008). Two-dimensional NMR relaxation studies of apple quality. *Postharvest Biology and Technology*, *48*(3), 331-340.

Marin, M. A., Cano, P., & Fuster, C. (1992). Freezing preservation of four spanish mango cultivars (*Mangifera indica L.*): chemical and biochemical aspects. *Zeitschrift für Lebensmittel-Untersuchung und -Forschung*, *194*, 566–569.

Martino, M. N., & Zaritzky, N. E. (1986). Fixing conditions in the freeze substitution technique for light microscopy observation of frozen beef tissue. *Food Structure*, *5*(1), 19–24.

Martins, R. C., & Silva, C. L. M. (2004). Frozen green beans (*Phaseolus vulgaris* L.) quality profile evaluation during home storage. *Journal of Food Engineering*, *64*(4), 481–488.

Mazur, P. (1977). The role of intracellular freezing in the death of cells cooled at supraoptimal rates. *Cryobiology*, *14*(3), 251–272.

Mazur, P. (1984). Freezing of living cells: Mechanisms and implications. *American Journal of Physiology–Cell Physiology*, 247(3), C125–142.

Mcglone, V. A., & Jordan, R. B. (2000). Kiwifruit and apricot firmness measurement by the non-contact laser air-puff method. *Postharvest Biology and Technology*, *19*, 47–54.

McLellan, M. R., Morris, G. J., Grout, B. W. W., & Hughes, K. (1991). Light microscopy of foodstuffs during freezing and thawing. In W. B. Bald (Ed.), *Food Freezing: Today and Tomorrow* (1st ed., pp. 171–185). London: Springer-Verlag.

Mehta, R. (2012). Interactions, imaging and spectra in SEM. In V. Kazmiruk (Ed.), *Scanning Electron Microscopy* (1st ed., pp. 17–30). Rijeka: InTech.

Mok, J. H., Choi, W., Park, S. H., Lee, S. H., & Jun, S. (2015). Emerging pulsed electric field (PEF) and static magnetic field (SMF) combination technology for food freezing. *International Journal of Refrigeration*, *50*, 137–145.

Mousavi, R., Miri, T., Cox, P. W., & Fryer, P. J. (2005). A novel technique for ice crystal visualization in frozen solids using X-ray micro-computed tomography. *Journal of Food Science*, *70*(7), e437–e442.

Mousavi, R., Miri, T., Cox, P. W., & Fryer, P. J. (2007). Imaging food freezing using X-ray microtomography. *International Journal of Food Science and Technology*, *42*(6), 714–727.

Moussawi, A., Xu, J., Nouri, H., & Lubineau, G. (2014). Volume digital image correlation to assess displacement field in compression loaded bread crumb under X-ray microtomography. *Innovative Food Science & Emerging Technologies*, *25*, 78–87.

Murray, K. E., Shipton, J., Whitfield, F. B., Kennett, B. H., & Stanley, G. (1968). Volatile flavor components from green peas (*Pisum sativum*). *Journal of Food Science*, *33*, 290–294.

Murray, K. E., Shipton, J., Whitfield, F. B., & Last, J. H. (1976). The volatiles of off-flavored unblanched green peas (*Pisum sativum*). *Journal of the Science of Food and Agriculture*, *27*, 1093–1107.

Orlowska, M., Le-Bail, A., & Havet, M. (2014). Electrofreezing. In H. S. Ramaswamy, M. Marcotte, S. Sastry, & K. Abdelrahim (Eds.), *Ohmic Heating in Food Processing* (pp. 423–437). Boca Raton: CRC Press, Taylor & Francis Group.

Orlowska, M., Havet, M., & Le-Bail, A. (2009). Controlled ice nucleation under high voltage DC electrostatic field conditions. *Food Research International*, *42*(7), 879–884.

Oruna-Concha, M. J., Gonzalez-Castro, M. J., Lopez-Hernandez, J., & Simal-Lozano, J. (1997). Effects of freezing on the pigment content in green beans and padron peppers. *Zeitschrift für Lebensmittel-Untersuchung und -Forschung A*, *205*(2), 148–152.

Otero, L., Pérez-Mateos, M., Rodríguez, A. C., & Sanz, P. D. (2017). Electromagnetic freezing: Effects of weak oscillating magnetic fields on crab sticks. *Journal of Food Engineering*, *200*, 87–94.

Otero, L., Martino, M., Zaritzky, N., Solas, M., & Sanz, P. D. (2000). Preservation of microstructure in peach and mango during high-pressure-shift freezing. *Journal of Food Science*, *65*(3), 466–470.

Owada, N. (2007). *US 7,237,400 B2*. Unlted States Patent and Trademark Office.

Owada, N., & Saito, S. (2010). *US 7,810,340 B2*. Unlted States Patent and Trademark Office.

Owada, N., & Kurita, S. (2001). *US 6,250,087 B1*. *Patent*. Unlted States Patent and Trademark Office.

Parniakov, O., Lebovka, N. I., Bals, O., & Vorobiev, E. (2015). Effect of electric field and osmotic pre-treatments on quality of apples after freezing–thawing. *Innovative Food*

Science & Emerging Technologies, *29*, 23–30.

Pawley, J. B. (Ed.). (2006). *Handbook of biological confocal microscopy* (3rd.). New York: Springer Science+Business Media, LLC.

Poiana, M. A., Moigradean, D., & Alexa, E. (2010). Influence of home-scale freezing and storage on antioxidant properties and color quality of different garden fruits. *Bulgarian Journal of Agricultural Science*, *16*(2), 163–171.

Potter, N. N., & Hotchkiss, J. H. (1998). *Food Science* (5th ed., pp. 409-436). (D. R. Heldman, Ed.). New York: Springer Science+Business Media.

Peng, Y., & Lu, R. (2008). Analysis of spatially resolved hyperspectral scattering images for assessing apple fruit firmness and soluble solids content. *Postharvest Biology and Technology*, *48*, 52–62.

Phothiset, S., & Charoenrein, S. (2014). Effects of freezing and thawing on texture, microstructure and cell wall composition changes in papaya tissues. *Journal of the Science of Food and Agriculture*, *94*(2), 189–196.

Pruppacher, H. R., Steinberger, E. H., & Wang, T. L. (1968). On the Electrical Effects that Accompany the Spontaneous Growth of Ice in Supercooled Aqueous Solutions. *Journal of Geophysical Research*, *73*(2), 571–584.

Prussia, S. E., Astleford, J. J., Hewlett, B., & Hung, Y. C. (1994). Non-Destructive Firmness Measuring Device. *U.S. Patent No. 5,372,030*. Washington, D.C.: U.S. Patent and Trademark Office.

Purnell, G., James, C., & James, S. J. (2017). The effects of applying oscillating magnetic fields during the freezing of apple and potato. *Food and Bioprocess Technology*, *10*(12), 2113–2122.

Rahman, A. R., Henning, W. L., & Westcott, D. E. (1971). Histological and physical changes in carrots as affected by blanching, cooking, freezing, freeze drying and compression. *Journal of Food Science*, *36*(3), 500–502.

Ramírez, C., Troncoso, E., Muñoz, J., & Aguilera, J. M. (2011). Microstructure analysis on pre-treated apple slices and its effect on water release during air drying. *Journal of Food Engineering*, *106*, 253–261.

Ramsey, G. B., Wiant, J. S., & Link, G. K. K. (1938). *Market diseases of fruits and vegetables: Crucifers and cucurbits (No. 292)*. Washington D.C: US Department of Agriculture.

Ramsey, G. B., & Smith, M. A. (1961). *Market Diseases of Cabbage, Cauliflower, Turnips, Cucumbers, Melons, and Related Crops*. *Agriculture Handbook No. 184*, Washington D.C.: US Department of Agriculture.

Rastogi, N. K., Eshtiaghi, M. N., & Knorr, D. (1999). Accelerated mass transfer during osmotic dehydration of high intensity electrical field pulse pretreated carrots. *Journal of Food Science*, *64*(6), 1020–1023.

Rastogi, N. K., Raghavarao, K. S. M. S., Niranjan, K., & Knorr, D. (2002). Recent developments in osmotic dehydration : methods to enhance mass transfer. *Trends in Food Science & Technology*, *13*, 48–59.

Reeve, R. M. (1970). Relationships of histological structure to texture of fresh and processed fruits and vegetables. *Journal of Texture Studies*, *1*(3), 247–284.

Reid, D. S. (1997). Overview of physical/chemical aspects of freezing. In M. C. Erickson & Y. C. Hung (Eds.), *Quality in frozen food* (pp. 10–28). Dordrecht: Springer Science+Business Media.

Reid, D. S., Carr, J. M., Sajjaanantakul, T., & Labavitch, J. M. (1986). Effects of freezing and frozen storage on the characteristics of pectin extracted from cell walls. In *Chemistry and Function of Pectins* (Symposium, Vol. 310, pp. 200–216). Washington, DC: American Chemical Society.

Remy, E., & Thiel, E. (2002). Medial axis for chamfer distances: Computing look-up tables and neighbourhoods in 2D or 3D. *Pattern Recognition Letters*, *23*, 649–661.

Rimkeeree, K., & Charoenrein, S. (2014). Effect of cultivar and ripening stage on quality and microstructure of frozen mangoes (*Mangifera indica* Linn.). *International Journal of Food Properties*, *17*(5), 1093–1108.

Rutledge, D. N., Rene, F., Hills, B. P., & Foucat, L. (1994). Magnetic resonance imaging studies of the freeze-drying kinetics of potato. *Journal of Food Process Engineering*, *17*(3), 325-352.

Sa, M. M., & Sereno, A. M. (1994). Glass transitions and state diagrams typical natural fruits and vegetables. *Thermochimica Acta*, *246*, 285–297.

Saban, K. V., Thomas, J., Varughese, P. A., & Verghese, G. (2002). Thermodynamics of Crystal Nucleation in an External Electric Field. *Crystal Research and Technology*, *37*(11), 1188–1199.

Sadot, M., Curet, S., Rouaud, O., Le-bail, A., & Havet, M. (2017). Numerical modelling of an innovative microwave assisted freezing process. *International Journal of Refrigeration*, *80*, 66–76.

Salt, R. W. (1961). Effect of Electrostatic Field on Freezing of Supercooled Water and Insects. *Science*, *133*(3451), 458–459.

Salvo, L., Cloetens, P., Maire, E., Zabler, S., Blandin, J. J., Buffière, J. Y., Ludwig, W., Boller,

E., Bellet, D., & Josserond, C. (2003). X-ray micro-tomography an attractive characterisation technique in materials science. *Nuclear Instruments and Methods in Physics Research, Section B: Beam Interactions with Materials and Atoms*, *200*, 273–286.

Sharma, S., Thakur, A. K., & Maiti, R. (2016). Post-harvest technology for reducing stress on bioresource: recent advances and future needs. In R. Maiti, A. Kumari, A. K. Thakur, & N. C. Sarkar (Eds.), *Bioresource and Stress Management* (pp. 229–256). Singapore: Springer Science+Business Media.

Shevkunov, S. V., & Vegiri, A. (2002). Electric field induced transitions in water clusters. *Journal of Molecular Structure: THEOCHEM*, *593*(1–3), 19–32.

Shi, X., Datta, A. K., & Throop, J. A. (1998). Mechanical property changes during freezing of biomaterial. *Transactions of the ASAE*, *41(5)*, 1407-1414.

Shi, X., A. K. Datta, & Mukherjee, Y. (1998). Thermal stresses from large volumetric expansion during freezing of biomaterials. *Transactions of the ASME*, *120*, 720-726.

Shi, X., A. K. Datta, & Mukherjee, Y. (1999). Thermal fracture in a biomaterial during rapid freezing. *Journal of Thermal Stresses*, *22*, 275-292.

Shomer, I., Borochov-neori, H., Luzki, B., & Merin, U. (1998). Morphological, structural and membrane changes in frozen tissues of Madjhoul date (*Phoenix dactylifera* L.) fruits. *Postharvest Biology and Technology*, *14*, 207–215.

Silva, C. L. M., Goncalves, E. M., & Brandao, T. R. S. (2008). Freezing of Fruits and Vegetables. In J. A. Evans (Ed.), *Frozen Food Science and Technology* (pp. 165–183). Oxford: Blackwell Publishing Ltd.

Simandjuntak, V., Barrett, D. M., & Wrolstad, R. E. (1996). Cultivar and frozen storage effects on muskmelon (*Cucurnis melo*) colour, texture and cell wall polysaccharide composition. *Journal of the Science of Food and Agriculture*, *71*, 291–296.

Singh, R. P., & Heldman, D. R. (2009). Food engineering. In S. L. Taylor (Ed.), *Introduction to Food Engineering* (4th ed., pp. 501–541). San Diego: Academic Press publications.

Sirijariyawat, A., & Charoenrein, S. (2012). Freezing characteristics and texture variation after freezing and thawing of four fruit types. *Songklanakarin Journal Science Technology*, *34*(5), 517–523.

Sirijariyawat, A., & Charoenrein, S. (2014). Texture and pectin content of four frozen fruits treated with calcium. *Journal of Food Processing and Preservation*, *38*, 1346–1355.

Skrede, G. (1996). Fruits. In L. E. Jeremiah (Ed.), *Freezing effects on food quality* (pp. 183–245). New York: Marcel- Dekker.Inc.

Smith, P. G. (2011). Low-temperature preservation nomenclature. In *Introduction to Food*

Process Engineering (2nd ed., pp. 275–298). New York: Springer Science+Business Media.

Sousa, M. B., Canet, W., Alvarez, M. D., & Tortosa, M. E. (2006). Effect of processing on the texture and sensory attributes of raspberry (cv. Heritage) and blackberry (cv. Thornfree). *European Food Research and Technology*, *223*, 517–532.

Stan, C. A., Tang, S. K. Y., Bishop, K. J. M., & Whitesides, G. M. (2011). Externally applied electric fields up to 1.6×105 V/m do not affect the homogeneous nucleation of ice in supercooled water. *Journal of Physical Chemistry B*, *115*(5), 1089–1097.

Steen, C., & Lambelet, P. (1997). Texture changes in frozen cod mince measured by low-field nuclear magnetic resonance spectroscopy. *Journal of the Science of Food and Agriculture*, *75*, 268–272.

Sterling, C. (1968). Effect of low temperature on structure and firmness of apple tissue. *Journal of Food Science*, *33*(6), 577–580.

Sun, W., & Li, X. H. (2010). Study on ice construction of normal saline under alternated electric field by dielectric method. In *Proceedings - 2010 3rd International Congress on Image and Signal Processing, CISP 2010* (Vol. 6, pp. 2933–2936). Yantai, China: IEEE.

Sun, W., Chen, Z., & Huang, S. (2006). Effect of an external electric field on liquid water using molecular dynamics simulation with a flexible potential. *Journal of Shanghai University (English Edition)*, *10*(3), 268–273.

Sun, W., Xu, X., Sun, W., Ying, L., & Xu, C. (2006). Effect of Alternated Electric Field on the Ice Formation During Freezing Process of 0.9% K_2MnO_4 Water. In *8th International Conference on Properties and applications of Dielectric Materials* (pp. 774–777). Bali: IEEE.

Sun, W., Xu, X., Zhang, H., Sun, W., & Xu, C. (2006). The Mechanism Analysis of NaCI Solution Ice Formation Suppressed by Electric Field. In *8th International Conference on Properties and applications of Dielectric Materials* (pp. 770–773). Bali: IEEE.

Sun, D. W., & Li, B. (2003). Microstructural change of potato tissues frozen by ultrasound-assisted immersion freezing. *Journal of Food Engineering*, *57*(4), 337–345.

Suzuki, T., Takeuchi, Y., Masuda, K., Watanabe, M., Shirakashi, R., Fukuda, Y., Tsuruta, T., Yamamoto, K., Koga, N., Hiruma, N., Ichioka, J., & Takai, K. (2011). Experimental investigation of effectiveness of magnetic field on food freezing process. *Transactions of the Japan Society of Refrigerating and Air Conditioning Engineers*, *26*, 371–386.

Tan, M. C., Chin, N. L., Yusof, Y. A., & Abdullah, J. (2016). Novel 2D and 3D imaging of

internal aerated structure of ultrasonically treated foams and cakes using X-ray tomography and X-ray microtomography. *Journal of Food Engineering*, *183*, 9–15.

Thybo, A. K., Bechmann, I. E., Martens, M., & Engelsen, S. B. (2000). Prediction of sensory texture of cooked potatoes using uniaxial compression, near infrared spectroscopy and low field ^{1}H NMR spectroscopy. *LWT-Food Science and Technology*, *33*, 103–111.

Thybo, A. K., Karlsson, A. H., Bertram, H. C., & Andersen, H. J. (2004). Nuclear magnetic resonance (NMR) and magnetic resonance imaging (MRI) in texture measurement. In D. Kilcast (Ed.), *Texture in food Volume 2: Solid foods* (pp. 184–204). Cambridge: Woodhead Publishing Ltd.

Travis, A. J., Murison, S. D., Perry, P., & Chesson, A. (1997). Measurement of cell wall volume using confocal microscopy and its application. *Annals of Botany*, *80*, 1–11.

Tu, J., Zhang, M., Xu, B., & Liu, H. (2015). Effects of different freezing methods on the quality and microstructure of lotus (*Nelumbo nucifera*) root. *International Journal of Refrigeration*, *52*(0), 59–65.

Ullah, J., Takhar, P. S., & Sablani, S. S. (2014). Effect of temperature fl uctuations on ice-crystal growth in frozen potatoes during storage. *LWT-Food Science and Technology*, *59*(2), 1186–1190.

Van Buggenhout, S., Lille, M., Messagie, I., Von Loey, A., Autio, K., & Hendrickx, M. (2006). Impact of pretreatment and freezing conditions on the microstructure of frozen carrots: Quantification and relation to texture loss. *European Food Research and Technology*, *222*, 543–553.

Van Buggenhout, S., Messagie, I., Maes, V., Duvetter, T., Loey, A. Van, & Hendrickx, M. (2006). Minimizing texture loss of frozen strawberries: effect of infusion with pectinmethylesterase and calcium combined with different freezing conditions and effect of subsequent storage / thawing conditions. *European Food Research and Technology*, *223*, 395–404.

Veberic, R., Stampar, F., Schmitzer, V., Cunja, V., Zupan, A., Koron, D., & Mikulic-Petkovsek, M. (2014). Changes in the contents of anthocyanins and other compounds in blackberry fruits due to freezing and long-term frozen storage. *Journal of Agricultural and Food Chemistry*, *62*(29), 6926–6935.

Vegiri, A. (2004). Reorientational relaxation and rotational-translational coupling in water clusters in a d.c. external electric field. *Journal of Molecular Liquids*, *110*(1), 155–168.

Vegiri, A., & Schevkunov, S. V. (2001). A molecular dynamics study of structural transitions

in small water clusters in the presence of an external electric field. *The Journal of Chemical Physics*, *115*(9), 4175–4185.

Vicent, V., Verboven, P., Ndoye, F., Alvarez, G., & Nicolaï, B. (2017). A new method developed to characterize the 3D microstructure of frozen apple using X-ray micro-CT. *Journal of Food Engineering*, *212*, 154–164.

Vidot, K., Gaillard, C., Rivard, C., Siret, R., & Lahaye, M. (2018). Cryo-laser scanning confocal microscopy of diffusible plant compounds. *Plant Methods*, *14*(1), 89.

Voda, A., Homan, N., Witek, M., Duijster, A., van Dalen, G., van der Sman, R., Nijsse, J., van Vliet, L., Van As, H., & van Duynhoven, J. (2012). The impact of freeze-drying on microstructure and rehydration properties of carrot. *Food Research International*, *49*(2), 687–693.

Waldron, K. W. (2004). Plant structure and fruit and vegetable texture. In D. Kilcast (Ed.), *Texture in food Volume 2: Solid foods* (pp. 239–258). Cambridge: Woodhead Publishing Ltd.

Wang, C. Y. (2016). Chilling and Freezing Injury. In K. C. Gross, C. Y. Wang, & M. Saltveit (Eds.), *The Commercial Storage of Fruits, Vegetables, and Florist and Nursery Stocks. Agriculture Handbook Number 66* (pp. 62–67). Washington, D. C.: United States Department of Agriculture.

Wang, Z., Herremans, E., Janssen, S., Cantre, D., Verboven, P., & Nicolai, B. (2018). Visualizing 3D food microstructure using tomographic methods : advantages and disadvantages. *Annual Review of Food Science and Technology*, *9*, 1–21.

Wang, L., Xu, B., Wei, B., & Zeng, R. (2018). Low frequency ultrasound pretreatment of carrot slices : Effect on the moisture migration and quality attributes by intermediate-wave infrared radiation drying. *Ultrasonics-Sonochemistry*, *40*, 619–628.

Wei, S., Xiaobin, X., Hong, Z., & Chuanxiang, X. (2008). Effects of dipole polarization of water molecules on ice formation under an electrostatic field. *Cryobiology*, *56*(1), 93–99.

White, N. S., Errington, R. J., Fricker, M. D., & Wood, J. L. (1996). Aberration control in quantitative imaging of botanical specimens by multidimensional fluorescence microscopy. *Journal of Microscopy*, *181*(2), 99–116.

Wiktor, A., Schulz, M., Voigt, E., Witrowa-Rajchert, D., & Knorr, D. (2015). The effect of pulsed electric field treatment on immersion freezing, thawing and selected properties of apple tissue. *Journal of Food Engineering*, *146*, 8–16.

Wilson, A. J. (1991). Microscopical methods for examining frozen foods. In W. B. Bald (Ed.), *Food Freezing: Today and Tomorrow* (1st ed., pp. 97–112). London: Springer-Verlag.

Woo, M. W., & Mujumdar, A. S. (2010). Effects of Electric and Magnetic Field on Freezing and Possible Relevance in Freeze Drying. *Drying Technology*, *28*(4), 433–443.

Xanthakis, E., Huen, J., Eliasson, L., Jha, P. K., Le-Bail, A., & Shrestha, M. (2018). Evaluation of microwave assisted freezing (MAF) impact on meat and fish matrices. In *5th IIR Conference on Sustainability and the Cold Chain, ICCC 2018, 6 April 2018 through 8 April 2018* (pp. 176-181).

Xanthakis, E., Valdramidis, V. P. (2017). Impact of heating operations on the microbial ecology of foods. In A. Sant'Ana (Eds.), *Modeling the Microbial Ecology of Foods: Quantitative Microbiology in Food Processing* (pp.117-142). New Jersey: John Wiley & Sons, Ltd.

Xanthakis, E., Gogou, E., Taoukis, P., & Ahrné, L. (2018). Effect of microwave assisted blanching on the ascorbic acid oxidase inactivation and vitamin C degradation in frozen mangoes, *Innovative Food Science & Emerging Technologies*, *48*, 248-257.

Xanthakis, E., Le-bail, A., & Havet, M. (2014a). Freezing Combined with Electrical and Magnetic Disturbances. In D. W. Sun (Ed.), *Emerging Technologies for Food Processing* (2nd ed., pp. 563–579). San Diego: Elsevier Academic Press.

Xanthakis, E., Le-Bail, A., & Ramaswamy, H. (2014b). Development of an innovative microwave assisted food freezing process. *Innovative Food Science & Emerging Technologies*, *26*, 176–181.

Xanthakis, E., Havet, M., Chevallier, S., Abadie, J., & Le-Bail, A. (2013). Effect of static electric field on ice crystal size reduction during freezing of pork meat. *Innovative Food Science & Emerging Technologies*, *20*, 115–120.

Xin, Y., Zhang, M., Adhikari, B., Ying, X., & Min, Z. (2014). The effects of ultrasound-assisted freezing on the freezing time and quality of broccoli (*Brassica oleracea* L. var. *botrytis* L.) during immersion freezing. *International Journal of Refrigeration*, *41*, 82–91.

Xu, Z., Guo, Y., Ding, S., An, K., & Wang, Z. (2014). Freezing by immersion in liquid CO_2 at variable pressure: Response surface analysis of the application to carrot slices freezing. *Innovative Food Science and Emerging Technologies*, *22*, 167–174.

Yano, S., Tanaka, M., Suzuki, N., & Kanzaki, Y. (2002). Texture change of beef and salmon meats caused by refrigeration and use of pulse NMR as an index of taste. *Food Science and Technology Research*, *8*(2), 137–143.

Yuryev, Y., & Wood-Adams, P. M. (2012). Crystallization of Poly(L-/D-Lactide) in the Presence of Electric Fields. *Macromolecular Chemistry and Physics*, *213*, 635−642.

Zhang, M. I. N., & Willison, J. H. M. (1991). A microcomputer-based precision impedance atralyzer for measuring electncal impedance in plant tissues. *Canadian Journal of Plant*

Science, *7*, 1285–1288.

Zhang, M. I. N., & Willison, J. H. M. (1992a). Electrical impedance analysis in plant tissues: In vivo detection of freezing injury. *Canadian Journal of Botany*, *70*, 2254–2258.

Zhang, M. I. N., & Willison, J. H. M. (1992b). Electrical impedance analysis in plant tissues: The effect of freeze-thaw injury on the electrical properties of potato tuber and carrot root tissues. *Canadian Journal of Plant Science*, *72*(2), 545–553.

Zhang, M. I. N., & Willison, J. H. M. (1993). Electrical impedance analysis in plant tissues: impedance measurement in leaves. *Journal of Experimental Botany, 44*(265), 1369–1375.

Zhao, Y., & Takhar, P. S. (2017). Micro X-ray computed tomography and image analysis of frozen potatoes subjected to freeze-thaw cycles. *LWT-Food Science and Technology*, *79*, 278–286.

Zykwinska, A. W., Ralet, M. C. J., Garnier, C. D., & Thibault, J. F. J. (2005). Evidence for in vitro binding of pectin side chains to cellulose. *Plant Physiology*, *139*, 397–407.

PUBLICATIONS AND COMMUNICATIONS

Peer Reviewed Publications (Published (*); Under Review (**); In Preparation (***))

***P. K. Jha**, E. Xanthakis, V. Jury, M. Havet, A. Le-Bail: *Advances of electro-freezing in food processing*. Current Opinion in Food Science, 2018; 23: 85-89. DOI:10.1016/j.cofs.2018.06.007.

***P. K. Jha**, E. Xanthakis, V. Jury, A. Le-Bail: *An overview on magnetic field and electric field interactions with ice crystallisation; application in the case of frozen food*. Crystals 2017; 7(10): 299. DOI:10.3390/cryst7100299.

***P. K. Jha**, M. Sadot, S. A. Vino, V. Jury, S. Curet-Ploquin, O. Rouaud, M. Havet, A. Le-Bail: *A review on effect of DC voltage on crystallization process in food systems*. Innovative Food Science & Emerging Technologies 2017; 42: 204-219. DOI: 10.1016/j.ifset.2017.06.002.

***P. K. Jha**, E. Xanthakis, S. Chevallier, V. Jury, A. Le-Bail: *Assessment of freeze damage in fruits and vegetables*.. In Press, Accepted Manuscript, *Food Research International* (2018). 10.1016/j.cofs.2018.06.007.

A. Le-Bail, **P. K. Jha: *Application - Freezing of foodstuffs (Book chapter)*. In Gases in Agro-Food Processes, Academic Press, Elsevier, 2018.

*** **P. K. Jha**, et al.: Evaluation of Microwave Assisted Freezing (MAF) impact on apples and potatoes.

*** **P. K. Jha** et al.: Benchmarking of techniques used to access the freeze damage in potatoes.

*** P. N. Gururaj, **P. K. Jha**, V. Jury, A. Pare, A. Le-Bail: Impact of different freezing, thawing and storage conditions on structural damage and quality loss of Royal Gala apple.

Conference Proceedings/Workshops

- **P. K. Jha**, V. Jury, S. Chevallier, A. Le-Bail: *Recent advances of microwave assisted freezing (MAF) in food processing under FREEZEWAVE H2020 project.* 32nd EFFoST International Conference, 6th-8th November, 2018, Nantes, France (Oral presentation).
- **P. K. Jha,** V. Jury, S. Chevallier, M. Havet, A. Le-Bail: *Freezing under static and oscillating electromagnetic fields; overview and recent advances*. IUFoST, 23rd-27th October, 2018, Mumbai, India (Invited speaker, Oral).
- **P. K. Jha**, V. Jury, S. Chevallier, M. Havet , A. Le-Bail*: Freezing under static and oscillating electromagnetic fields; overview and recent advances*. IuFOST 23rd-27th October, 2018, Mumbai, India (Oral + Invited Speaker).
- **P. K. Jha**, V. Jury, S. Chevallier, A. Le-Bail: *Effect of innovative low energy microwave assisted freezing (MAF) on the microstructure, texture, drip loss and colour of apple and potato (FREEZEWAVE Project).* IFT-EFFoST 2018 International Nonthermal Processing Workshop and Short course. 25th-27th September, 2018, Sorrento-Salerno, Italy (Oral presentation).
- P. N. Gururaj, A. Pare, **P. K. Jha**, V. Jury, A. Le-Bail: *Freeze-Thaw damage evaluation in frozen Royal Gala apples*. iCRAFPT'18. 17th-19th August, 2018, Thanjavur, India (Poster).
- A. Le-Bail, **P. K. Jha**, M. Sadot, O. Rouaud, V. Jury, M. Havet, S. Chevallier, S. Curet, E. Xanthakis, S. Isaksson, L. Eliasson, J. Huen, M. Shrestha, J. P. Bernard: *Microwave assisted crystallization; recent advanced applied to freezing of foods (FREEZEWAVE Project).* The 52nd Annual Microwave Power Symposium (IMPI 52), 26th – 28th June, 2018, Long Beach, California, USA.
- **P. K. Jha**, V. Jury, S. Chevallier, E. Xanthakis, A. Le-Bail: *Freezewave H2020 project-microwave assisted freezing of Potato.* 5th IIR Conference on Sustainability and the Cold Chain (ICCC2018), 6th – 8th April, 2018, Beijing, China (Conference paper + Oral).
- E. Xanthakis, J. Huen, L. Eliasson, **P. K. Jha**, A. Le-Bail, M. Shrestha: *Evaluation of microwave assisted freezing (MAF) impact on meat and fish matrices.* 5th IIR Conference on Sustainability and the Cold Chain (ICCC2018), 6th – 8th April, 2018, Beijing, China (Conference paper + Oral).
- A. Le-Bail, **P. K. Jha**, E. Xanthakis, M. Sadot, V. Jury, S. Curet, O. Rouaud, M. Havet: *Review on the impact of electrical and magnetic disturbances during freezing.* 5th IIR Conference on Sustainability and the Cold Chain (ICCC2018), 6th – 8th April, 2018, Beijing, China (Conference paper + Oral).
- **P. K. Jha**, V. Jury, A. Le-Bail: *Phase change under static and oscillating electromagnetic fields*. Symposium on Thermodynamics and Phase Transitions in Food Processing, 29th – 30th, January, 2018, Wageningen, Netherlands (Invited Speaker).
- V. Jury, **P. K. Jha**, S. Chevallier, A. Le-Bail: *Innovative low energy microwave assisted freezing (MW-AF) permits to minimize freeze damage of fruits and vegetables; some results from FREEZEWAVE H2020 project*. 31st EFFoST International Conference, 13th – 16th November, 2017, Sitges, Spain (Oral).
- A. Le-Bail, **P. Jha**, M. Sadot, S. Chevallier, S. Curet, V. Jury, O. Rouaud, C. Toublanc, M. Havet. *Conventional and Innovative food freezing; a review on processes and technics to assess freeze damage*. 31st EFFoST International Conference, 13th – 16th November, 2017, Sitges, Spain (Poster).
- S. Chevallier, **P. K. Jha**, A. Le-Bail, O. Rouaud, V. Jury: *X-ray micro-tomography and enhancement methods to study food structure.* World Congress of Chemical Engineering, 1st – 5th October, 2017, Barcelona, Spain (Oral).
- A. Le-Bail, **P. Jha**, E. Xanthakis, M. Havet, V. Jury. *Crystallisation of lipids under static electric field*. 30th EFFoST International Conference, 28th – 30th November, 2016, Vienna, Austria (Oral).
- A. Le-Bail, **P. Jha**, E. Xanthakis, M. Havet, V. Jury: *Phase change under static electrical field; in the case of lipids*. *Refrigeration Science and Technology; IIF-IIR: Paris, France,* 2016: 138-143, (Conference paper + Oral), DOI:10.18462/iir.iccc.2016.0019.

RÉSUMÉ EN FRANÇAIS

La congélation est une méthode efficace de conservation des aliments. Il s'agit d'un procédé qui transforme l'eau libre disponible dans les produits alimentaires en glace, entraînant une réduction de l'activité de l'eau dans la matrice alimentaire. L'immobilisation de l'eau libre inhibe la croissance microbienne et ralentit les réactions de dégradation enzymatique et chimique entraînant une détérioration plus lente des produits alimentaires. Cependant, la congélation peut également provoquer des dommages irréversibles au niveau cellulaire, ce qui entraine une dégradation de la qualité globale des produits alimentaires congelés.

L'ampleur des dommages causés par la congélation aux produits alimentaires et visibles lors de la décongélation est liée en grande partie à la taille et à la localisation des cristaux de glace, laquelle est fonction de la vitesse de congélation utilisée. Les détériorations sont également liées à l'effet de cryoconcentration de la phase aqueuse du milieu cellulaire dont la concentration en solutés augmente avec la formation progressive de glace ; il en résulte une dénaturation des protéines et des autres biopolymères organisés (à savoir les systèmes à base de cellulose pour les fruits et légumes), qui dégradent à leur tour les propriétés mécaniques et, ainsi, la texture globale du tissu.

Les procédés de congélation sont souvent qualifiés de rapides ou de lents sur une base plus ou moins subjective. Un « taux de congélation » (freezing rate) est parfois proposé, soit sur une base subjective (rapude-lent), soit sur une base de cinétique de diminution de la température sur un intervalle de température donné (en °C/min habituellement), soit enfin à partir du temps nécessaire pour congeler un produit ayant des dimensions fixées (soit sous forme d'un temps caractéristique pour passer d'une température à une autre, ou le plus souvent en cm/h habituellement). À un taux de congélation lent, les eaux intracellulaires se déplacent vers les domaines extracellulaires (à partir de l'intérieur de la cellule), entraînant ainsi une augmentation de la taille des cristaux de glace et une déshydratation plus importante des cellules. La formation de gros cristaux de glace et les cellules fortement déshydratées provoqueraient une destruction plus importante de la structure cellulaire (membrane cellulaire hautement perforée, structure cellulaire effondrée et séparation cellulaire). Par conséquent, la fuite du liquide intra-cellulaire sera plus élevée et le produit aura un aspect imbibé d'eau et une texture molle. Une vitesse de congélation lente entraînera également une exposition prolongée du tissu à la solution concentrée résultant de l'effet de cryoconcentration et aboutira à un endommagement accru. Au contraire, la congélation rapide (vitesse de congélation élevée) favorise la genèse de cristaux de

glace fins répartis uniformément dans le produit, réduisant ainsi les mouvements d'eau avec une déformation moindre du produit. Le résultat est un endommagement cellulaire réduit et une meilleure préservation de l'état initial du produit. Cependant, les taux de congélation rapides ont deux inconvénients principaux : i) le procédé de congélation rapide consomme plus d'énergie, ce qui augmente les coûts d'exploitation, ii) l'utilisation de taux de congélation extrêmement élevés peut entraîner le développement de fissures dans les échantillons, en particulier dans le cas de la congélation cryogénique, ce qui peut entraîner une qualité finale médiocre du produit. Ce dernier phénomène est lié au fait qu'après avoir subi une expansion lors de la congélation (transition eau-glace), le tissu congelé va se contracter ; il en résulte une contrainte tangentielle différentielle de compression au niveau de la zone en cours de congélation et de traction au niveau des zones périphériques qui au final conduit à des fissurations radiales orientées perpendiculairement au flux de chaleur (objets de révolution).

Un dernier paramètre important qui peut être responsable des pertes de qualité des aliments congelés est le stockage ; les paramètres temps-température ainsi que les fluctuations de température sont les principaux responsables de la perte de qualité.

Même si la technologie de congélation est optimale en termes de blocage de la croissance de la plupart des microorganismes et des réactions de dégradation enzymatique qui se produisent dans les aliments frais, il est très difficile pour l'industrie des aliments surgelés de minimiser les dommages causés par la congélation en obtenant des petits cristaux de glace tout en minimisant les dépenses énergétiques. Plusieurs procédés de congélation innovants ont été récemment développés en tenant compte des économies d'énergie et / ou de la conservation de la qualité des produits lors de la décongélation. Parmi ces technologies, l'utilisation de la congélation assistée par ondes électromagnétiques s'est révélée une technologie prometteuse en raison de sa capacité à affiner les cristaux de glace et à réduire les dommages causés par la congélation. Il a été montré que la congélation assistée par radiofréquence (RF) n'affecte pas le temps de congélation, tandis que la congélation assistée par micro-ondes augmente légèrement le temps de congélation (Hafezparast-Moadab et al., 2018; Xanthakis et al., 2014b). En effet, les micro-ondes (MW) présentent une certaine dissipation d'énergie (plus que la RF) et une optimisation doit être réalisée pour réduire l'énergie du MW tout en améliorant efficacement la microstructure des tissus congelés. L'influence du rayonnement électromagnétique sur l'eau résulte de l'impact électrique plutôt que magnétique. Ce constat est lié au fait que le champ électrique est plus efficace pour modifier la conformation du réseau de l'eau (sous forme de clusters, pentamères pour la plupart = 5 molécules d'eau en réseau) en raison du moment

électrique dipolaire intrinsèque de la molécule d'eau, alors que des champs magnétiques beaucoup plus forts sont nécessaires pour exercer la même force. On suppose que le couple exercé par une composante de champ électrique alternatif du rayonnement électromagnétique peut déstabiliser l'état d'équilibre des agrégats d'eau (lors de la formation des cristaux de glace) et peut donc interférer avec la nucléation mais aussi la cinétique de croissance des cristaux conduisant à la formation de cristaux de glace de petite taille.

Les fruits et légumes congelés sont les produits de prochaine génération sur le marché mondial des aliments surgelés. Ils sont également beaucoup plus affectés par le procédé de congélation que d'autres aliments comme la viande. Ainsi, pour produire des fruits et légumes congelés de haute qualité, il est important :

(i) D'acquérir une meilleure compréhension de la nature et du mécanisme des dommages causés par la congélation.
(ii) De développer des méthodes (à la fois qualitatives et quantitatives) permettant d'estimer les dommages dus à la congélation de manière précise et à moindre coût.
(iii) De développer de nouvelles méthodes de congélation capables de réduire les dommages causés par la congélation.

Suite à une étude précédente de Xanthakis et al. (2014b), qui a montré que le MAF (Microwave Assisted Freezing - congélation assistée par micro-ondes) était capable de réduire la taille des cristaux de glace (application sur de la longe de porc), un projet européen collaboratif H2020 appelé FREEZEWAVE a été lancé en 2015 avec pour objectif d'étudier en profondeur les effets du procédé MAF sur différentes matrices alimentaires. Ce projet compte 4 partenaires ; ONIRIS (France) qui est coordinateur du projet, RISE (Suède), TTZ (Allemagne) et SAIREM (France). Le procédé MAF d'un système modèle (gel à base de tylose) et de produits végétaux spécifiques (pomme et pomme de terre), ainsi que la modélisation du procédé de MAF, sont réalisés à ONIRIS. Le procédé MAF de la matrice de viande et de poisson est effectué respectivement à RISE (Suède) et à TTZ (Allemagne). La société SAIREM (France) a conçu l'émetteur micro-ondes (générateur à semi-conducteurs) pour ce projet. À notre connaissance, cette technologie a été utilisée pour la première fois au sein de FREEZEWAVE pour la congélation de fruits et de matrices végétales. Outre le procédé MAF, les effets de plusieurs méthodes conventionnelles sur la qualité des fruits et légumes frais ont également été explorés à ONIRIS dans le cadre de cette thèse.

Ce travail de thèse a été initié avec 3 objectifs principaux :

(i) Comprendre l'impact de la congélation sur la cohésion et la détérioration des fruits et légumes.
(ii) Développer des techniques pour évaluer les dommages dus à la congélation des produits horticoles (principalement des fruits et des légumes) à différents niveaux d'échelle (niveau cellulaire au niveau macroscopique).
(iii) Optimiser le procédé de congélation assistée par micro-ondes du point de vue de la qualité du produit et de la consommation d'énergie.

Pour atteindre ces objectifs, un plan de travail stratégique a été établi avec les étapes clés suivantes :
(i) Mettre au point un prototype d'équipement de MAF capable de congeler une quantité suffisante d'échantillons pour pouvoir évaluer les dommages causés par la congélation avec une bonne significativité statistique.
(ii) Développer un ensemble de techniques permettant d'évaluer les dommages causés par la congélation à différentes échelles et comparer ces techniques.
(iii) Appliquer et optimiser le procédé MAF aux pommes et pommes de terre, les deux modèles de fruits et légumes choisis pour cette étude.

Ce manuscrit présente un aperçu du travail effectué au cours de mon projet de thèse. Dans le premier chapitre, un état de l'art est d'abord proposé; La cristallisation assistée par champ électromagnétique sera d'abord introduite, et sera suivie d'une description des études antérieures liées à l'évaluation des dommages causés par la congélation dans les fruits et légumes.

Le deuxième chapitre présente les matériels et les méthodes qui ont été utilisés, couvrant à la fois les aspects du procédé et les techniques d'évaluation des dommages causés par la congélation.

Le troisième chapitre rassemble les principaux résultats obtenus lors du projet sur les pommes et les pommes de terre.

La dernière partie de la thèse propose un résumé du travail réalisé et aborde certaines perspectives sur les futures recherches possibles sur ce procédé hautement innovant.

Les principales conclusions des résultats du projet sont présentées ci-dessous.

Efficacité des méthodes d'évaluation des dommages dus au gel en termes d'efficacité, de précision, de coût de fonctionnement et de facilité d'utilisation

- Le tableau 1 résume les résultats, ainsi que les avantages et inconvénients liés aux méthodes d'analyse utilisées pour évaluer les dommages causés par la congélation dans les fruits et légumes. Ces observations pourront fournir des informations intéressantes et une vision globale sur les techniques analytiques pouvant être utilisées pour estimer efficacement les dommages dus à la congélation.
- La technologie d'évaluation des dommages causés par la congélation comme la microscopie confocale à balayage laser (CLSM) et les techniques d'évaluation globale des dommages telles que l'analyse des textures, l'analyse de la diffusion massique, la relaxométrie RMN et les tests colorimétriques utilisés dans cette étude se sont révélées comme étant des méthodes pertinentes pour distinguer les échantillons frais des échantillons congelés / décongelés.
- Les résultats suggèrent que la cryo-Microscopie électronique à balayage (cryo-SEM), la CLSM et la tomographie à rayons X sont des méthodes appropriées pour valider et quantifier les petits changements de qualité entre les différents protocoles de congélation (meilleure discrimination), tandis que les méthodes globales telles que les mesures de texture (incluant également l'analyse de la texture au laser-puff test), la RMN, les tests de diffusivité de masse par exsudation semblent moins discriminants et ne sont en mesure de détecter que des changements de qualité plus importants.
- Pour comparer les protocoles de congélation, l'analyse de la couleur s'est révélée être une technique non discriminante et donc inapproprié.
- En termes d'efficacité et de précision, la tomographie-RX, la CLSM et la cryo-SEM semblent être les méthodes les plus performantes pour analyser les dommages dus à la congélation. Sous condition d'un procédé de préparation préalable de lyophilisation mené très progressivement afin de réduire les déformations au maximum, la tomographie RX appliquée à un échantillon de taille relativement importante (1 cm^3) est une technique qui permet d'apporter des éléments chiffrés (dimensions des pores laissés par les cristaux de glace) pertinents et obtenus sur un nombre important « d'objets » (empreintes des cristaux).
- Les techniques RMN, cryo-SEM, tomographie-RX et CLSM sont des techniques relativement coûteuses en termes d'investissement et parfois chronophages (Cryo-SEM en particulier), tandis que les tests de diffusivité massique, l'analyse de texture, les mesures d'exsudation et de couleur sont des technologies abordables en ce qui concerne leur coût mais consommatrices de temps.

D'un point de vue global, un débat pourrait être ouvert sur la technique la plus pertinente pour évaluer les dommages causés par la congélation. Deux paramètres clés peuvent être considérés, à savoir : la dimension du domaine pris en compte par une technique donnée et la résolution spatiale rattachée à cette même technique. Par exemple, la RMN permet de traiter un échantillon d'environ 1 cm et fournit des informations au niveau d'une molécule d'eau (2,75 Å). La cryo-SEM examine un champ de 100 µm avec une information à 0,1 µm, même si, dans ce cas, l'observation de l'effet de la congélation est observé à l'échelle d'un cristal de glace (environ 10 µm). Le ratio entre la dimension du domaine pris en compte dans l'échantillon et la résolution spatiale de la technique pourrait être considéré comme une sorte d'indice de pertinence de l'évaluation des dommages causés par la congélation (indice FD-RI pour Freeze Damage Relevance Index) pour évaluer la pertinence de chaque technique. Plus cet indice de FD-RI sera élevé, plus la technique sera *a priori* discriminate. De ce point de vue, la RMN semble être la meilleure technique, même si l'interprétation et la quantification des dommages dus à la congélation basés sur les valeurs T_1 et T_2 sont assez subjectives et n'ont pas permis, dans nos conditions, de distinguer avec une grande pertinence les écarts entre les différents modes de congélation. Une des principales préoccupations est liée à la dimension du domaine couvert par une technique donnée. L'observation des dommages causés par la congélation sur une seule cellule peut être très informative et détaillée, mais sur un plan statistique, on pourrait estimer qu'une centaine de cellules doivent être analysées pour obtenir une information moyenne représentative, ce qui est hors de portée pour des raisons de temps. Un autre aspect repose sur la possibilité de répéter l'analyse et sur le temps nécessaire pour une mesure unique. Prenant en compte l'ensemble de ces critères, il est presque impossible de conclure sur la meilleure technique. La CLSM et la cryo-SEM apportent des images informatives visuelles qui peuvent aider à imager les défauts et qui peuvent conforter des observations faites avec d'autres techniques dans un champ plus large comme la RMN, la texture, l'exsudation…. L'évaluation correcte des dommages causés par la congélation demeure un défi et nécessite une quantité importante de travail expérimental avant de tirer des conclusions. L'impact de la durée et de la température de stockage ajoute une "dimension" supplémentaire au problème, rendant le travail expérimental rapidement très important.

Impact des différents protocoles de congélation sur les caractéristiques de congélation et la qualité des pommes et des pommes de terre.

Afin d'étudier l'effet de la cinétique de congélation sur la qualité de la pomme, différents protocoles de congélation ont été appliqués : à − 18 ºC (congélation lente ou SF), à − 40 ºC et une vitesse d'air de 2 m/s (congélation intermédiaire ou IF = Intermediate Freezing) et à − 72 ºC et 1 m/s (congélation rapide ou FF = Fast Freezing). Le procédé de congélation lente a donné des courbes de congélation comportant trois étapes, à savoir la surfusion, la nucléation et le changement de phase. Dans les cas de la congélation intermédiaire et la congélation rapide, les courbes de température ne présentaient aucune caractéristique évidente pour les trois étapes ci-dessus. Comme attendu, des cristaux de glace plus fins se sont formés lorsque la vitesse de congélation a été augmentée. La différence de taille dans les cristaux de glace entre les trois protocoles de congélation a été clairement mise en évidence par les mesures de cryo-SEM. Les données sur l'exsudation, la texture et le gain de matière sèche révèlent qu'une amélioration significative se produit uniquement lorsque la différence de taux de congélation est très importante (congélation avec température ambiante de – 18 °C vs. – 72 °C).

Les pommes de terre ont également été congelées par des protocoles de congélation et leur qualité a été évaluée, de manière similaire aux essais effectués sur la pomme. Les échantillons ont été congelés à − 18 ℃ (processus de congélation lente), − 30 ℃ (processus de congélation intermédiaire) et − 74 ℃ (processus de congélation rapide) et l'évaluation des dommages dus au gel a été réalisée à l'aide de plusieurs techniques d'analyse classiques et nouvelles. Les pommes de terre congelées lentement ont présenté une surfusion pendant la congélation, alors qu'aucune surfusion n'a été observée pour les autres conditions de congélation. Le point de congélation initial pouvait être détecté pour des conditions de congélation lente et intermédiaire, alors qu'il était difficile de détecter le point de congélation initial pour la congélation rapide. Les données initiales sur la température du point de congélation pour les conditions de congélation lente et de congélation intermédiaire ont révélé qu'une dépression du point de congélation s'est produite lorsque la vitesse de congélation a augmenté. Le procédé de congélation lente a entraîné la formation de cristaux de glace plus gros et a également causé des dommages plus importants à la structure cellulaire. Les cellules étaient fortement déformées (avec une structure de paroi cellulaire pliée et déformée) lorsque la condition de congélation lente était utilisée. La congélation intermédiaire conduit à des cristaux de glace relativement petits par rapport à la congélation lente et maintient également l'intégrité de la structure de la paroi cellulaire, mais elle ne préserve pas la forme de la cellule. Le procédé de congélation

rapide a non seulement favorisé la formation de cristaux de glace très fins, mais a également préservé la morphologie des cellules. Les paramètres analytiques tels que la RMN bas champ, la texture et l'exsudation ont montré que le procédé de congélation pouvait avoir un effet significatif lorsque la différence de taux de congélation utilisée au cours du procédé de congélation est plus élevée. En revanche, aucun des protocoles de congélation étudiés n'a préservé les paramètres de couleur de la pomme de terre fraîche.

Comme conclusion globale de cette section, le procédé de congélation rapide (à − 72 °C et − 74 °C pour la pomme et la pomme de terre respectivement) pourrait être considéré comme le meilleur choix parmi les conditions de congélation étudiées pour la congélation de produits de petite taille puisqu'il conduit à la formation de cristaux de glace de petite taille dans les produits et confère également des dommages plus faibles.

Impact de la congélation assistée par micro-ondes sur les paramètres de congélation et la qualité de la pomme et de la pomme de terre

La MAF des pommes et des pommes de terre a été obtenue en appliquant une puissance micro-onde constante (CMAF = 167 W/kg) et une puissance micro-ondes pulsée (P1MAF et P2MAF = 500 et 667 W/kg avec une largeur d'impulsion de 10 s et un intervalle de 20 s entre les pulses soit une puissance moyenne de 166 à 222 W/kg)). Un congélateur à micro-ondes construit sur mesure consistant en une cavité à micro-ondes domestique installée dans un congélateur à air comprimé a été utilisé pour le procédé MAF. À notre connaissance, c'est la première fois que le procédé MAF est utilisé pour congeler des produits végétaux. Dans cette étude, l'impact des conditions du procédé MAF sur les paramètres de congélation et les attributs de qualité (par exemple microstructure, texture, exsudation, etc.) des pommes et des pommes de terre a été étudié à l'aide de plusieurs techniques analytiques.

POMME : Dans le cas des pommes, l'utilisation des micro-ondes pendant la congélation n'a pas affecté les paramètres de congélation. Par exemple, la forme de la courbe de congélation obtenue lors de la congélation conventionnelle et de la congélation « MAF » des pommes était identique. Aucune surfusion n'a été observée pour aucune des conditions de congélation. Le temps de congélation caractéristique et les valeurs globales du temps de congélation et du taux de congélation se sont révélés similaires pour toutes les conditions. En ce qui concerne les paramètres de qualité, l'application de micro-ondes pendant le processus de congélation a produit une microstructure supérieure (distribution homogène de la taille des pores avec une

plus grande population de petits pores ; les pores correspondant aux fantômes des cristaux de glace) que l'échantillon témoin. De plus, le procédé MAF de la pomme entraînait une exsudation inférieure, alors que, par rapport à l'échantillon de référence, la diminution de la fermeté et de la dureté était plus faible. La forme des micro-ondes appliquées (mode constant ou mode pulsé) et le niveau de puissance ont été trouvés comme étant des paramètres critiques qui contrôlent la qualité des échantillons de pomme. Par exemple, la taille moyenne des pores, la perte de texture et l'exsudation ont diminué de manière significative ($p < 0,05$) avec l'introduction de micro-ondes pulsées et avec l'augmentation du niveau de puissance des micro-ondes. La condition P2MAF (procédé MAF avec mode d'émulsion pulsé « P2 ») a donné le meilleur résultat en termes de microstructure et d'autres attributs de qualité tels que l'exsudation et la texture.

➔ Il semble donc que, dans le cas de la pomme et dans le contexte et modalités de nos essais, l'hypothèse avancée par Xanthakis et al. (2014b) sur un possible effet de pompage thermique induisant un effet de cristallisation secondaire en cours de congélation soit confirmée, l'hypothèse d'une perturbation des clusters de molécules d'eau sous l'effet d'une puissance constante semblant aussi avoir un effet sur le phénomène de cristallisation.

POMME DE TERRE : À l'instar de la pomme, la courbe de congélation et les paramètres de congélation (temps de congélation, temps de congélation global et taux de congélation) n'ont pas été affectés par l'introduction des micro-ondes pendant la congélation de la pomme de terre. Les échantillons produits par le procédé MAF présentaient une microstructure avec davantage de pores de petite taille qui étaient distribués uniformément dans tout l'échantillon. Aucune condition de procédé MAF ne donnait un produit ayant des pores relativement plus grands et une gamme de distribution de taille de pores plus large. La perte de texture et l'exsudation étaient plus faibles pour l'échantillon MAF que pour l'échantillon témoin. Aucun effet significatif des conditions de congélation sur les paramètres de couleur n'a été observé. La préservation de la qualité était plus grande lorsque l'intensité des micro-ondes était augmentée. Parmi toutes les conditions de congélation, la condition P2MAF a donné le meilleur résultat en termes de microstructure et d'autres attributs de qualité tels que l'exsudation et la texture.

➔ Il semble donc que, dans le cas de la pomme de terre et dans le contexte et modalités de nos essais, l'hypothèse avancée par Xanthakis et al. (2014b) sur un possible effet de pompage

thermique induisant un effet de cristallisation secondaire en cours de congélation soit confirmée, l'hypothèse d'une perturbation des clusters de molécules d'eau sous l'effet d'une puissance constante semblant aussi avoir un effet sur le phénomène de cristallisation.

En conséquence, les objectifs clés de ce projet de doctorat ont été globalement atteints. L'étude des fruits et des légumes en cours de congélation compte parmi les sujets les plus difficiles, en comparaison de la viande par exemple, pour laquelle il est relativement plus facile d'évaluer les dommages causés par la congélation. L'impact précis des micro-ondes sur la congélation est encore en débat. Xanthakis et al. (2014b) ont proposé deux hypothèses concernant l'effet possible des MW pendant la congélation, soit la rupture des cristaux de glace avec une émission de puissance MW continue (CMAF), soit la nucléation induite par le rapport de puissance MW (PMAF). D'après nos résultats, il semble donc que l'hypothèse du PMAF soit la bonne. Cependant, des investigations supplémentaires sont alors nécessaires car des combinaisons optimales de niveau de puissance et de rapport de puissance peuvent exister pour un aliment donné avec une géométrie donnée. Le deuxième point est le niveau de puissance nécessaire. Notre système expérimental était une petite cavité domestique avec des conditions multimodales ; dans une telle configuration, il est presque impossible de garantir que toute l'énergie émise était piégée par l'échantillon, une partie de celle-ci pouvant en effet être réfléchie vers l'émetteur. En outre, l'émetteur utilisé était exploité avec une très faible puissance (quelques watts pour un équipement pouvant atteindre 180 watts). Par conséquent, la valeur de l'énergie spécifique à prendre en compte pour ces procédés PMAF et CMAF devrait être considérée comme indicative à cette étape de la recherche.

Malgré ces problèmes mineurs, la conclusion finale de cette étude est que la congélation assistée par MW a un effet évident sur la réduction de la taille des cristaux de glace dans le cas de la congélation des fruits et des légumes. La réduction de la taille n'est pas énorme, mais elle est significative. D'autres études complémentaires pourraient par exemple aborder les aspects suivants :

- appliquer la congélation assistée par micro-ondes à plus grande échelle dans un système continu
- évaluer l'évolution de la qualité pendant le stockage à l'état congelé pour vérifier à quel point l'avantage initial de la congélation assistée par MW est préservé pendant le stockage par rapport à un contrôle.

- rechercher différentes longueurs d'onde MW ou RF ; en particulier, les ondes radiofréquences sont beaucoup moins énergétiques que les micro-ondes. Les résultats obtenus en RF par différentes études (Anese et al., 2012; Hafezparast-Moadab et al., 2018) semblent très encourageantes. Cependant, la manière dont ces auteurs ont procédé et les valeurs d'énergie spécifique utilisée ne sont pas totalement claires et des études supplémentaires sont évidemment nécessaires.

Tableau 1. Analyse comparative des différentes méthodes d'évaluation des dommages causés par le gel.

Méthodes d'évaluation des dommages causés par le gel pour les fruits et légumes	Méthodes ciblées		Méthodes globales						
	Cryo-SEM	CLSM	Analyse de texture		RMN	perte d'exsudat	Couleur	Diffusivité de masse	Tomographie à rayons X
			Conventionnel	Laser-Puff					
La préparation des échantillons	Difficult	Difficult	Easy	Easy	Easy	Easy	Easy	Easy	Easy
Capacité à détecter les différences entre les échantillons frais et congelé / décongelé	×	++++	++++	++++	++++	++++	++++	++++	×
Possibilité de distinguer différents protocoles de congélation	++++	++++	++	++	+	++	-	+++	++++
Temps d'analyse (préparations d'échantillons + acquisition et traitement des données)	++	++	+	+	+++	+	+	++++	++++
Interprétation des paramètres analytiques mesurés	Facile	Facile	Facile	Facile	Difficile	Facile	Facile	Facile * & Difficile**	Facile
Nature de l'échantillon	C	C/D	C/D	C/D	C & C/D	C/D	C/D	C/D	L
Coût d'exploitation	Cher	Cher	Abordable	Abordable	Cher	Abordable	Abordable	Abordable	Cher
Statut de la méthode	SU	PSU	TC	NM	PSU	TC	TC	NM	PSU

+ = Valeur la plus basse; ++++ = Valeur la plus élevée; × = Non applicable; = Aucun effet;* = Immédiatement après la congélation/décongélation; ** = Diffusion de masse pendant la période d'essai de 3h (les lectures ont été effectuées à un intervalle de temps de 0,5h pendant le test)

Abréviations des mots: C = Congelé; C/D = Congelé/Décongelé; L = Lyophilisé; OU = Souvent utilisé; NUO = Pas souvent utilisé; TC = Très commun; NM = Nouvelle méthode.

Titre : Etude de l'effet des perturbations électromagnétiques sur la cristallisation

Mots clés : Congélation, taille des cristaux de glace, qualité des aliments, analyse des images

Résumé : L'objectif de cette étude était d'étudier l'effet d'un procédé innovant de congélation assistée par micro-ondes (CAPMO) à faible énergie sur le temps de congélation, la qualité (microstructure, texture, perte de masse, et couleur) de la pomme et de la pomme de terre. La CAPMO des pommes et des pommes de terre a été effectuée à une puissance micro-onde constante (167 W/kg) et une puissance micro-ondes appliquée par créneaux (500 et 667 W/kg avec 10 s de micro-ondes sur une période de 30 s). Les températures ont été mesurées pendant le processus de congélation et la microstructure a été examinée en utilisant la tomographie à rayons X et les techniques de cryo-SEM. D'autres paramètres de qualité tels que la texture, la perte de masse et la couleur ont été évalués après décongélation de l'échantillon à température ambiante. Les résultats ont montré que le processus de CAPMO n'affectait pas le temps de congélation. L'application de micro-ondes pendant le processus de congélation a produit une microstructure de qualité supérieure à celle de l'échantillon témoin ; La CAPMO a réduit de manière significative la taille moyenne des cristaux de glace dans les échantillons de pommes et de pommes de terre. De plus, la CAPMO de la pomme et de la pomme de terre a entrainé une perte de masse moindre. La réduction de la fermeté / dureté et du module de Young a également été diminué par rapport à l'échantillon témoin. La couleur n'a pas été significativement influencée par la CAPMO. Parmi toutes les conditions de congélation testées, la condition micro-onde pulsée de 667 W/kg a donné le meilleur résultat en termes de réduction de la taille des cristaux de glace et de qualité. Ces résultats prometteurs indiquent donc que l'application de micro-ondes pendant la congélation permettrait d'obtenir des produits congelés de meilleure qualité.

Title : Study on the effects of electromagnetic disturbances on crystallization

Keywords : Freezing, ice crystal size, food quality, image analysis

Abstract: The objective of this study was to investigate the effect of innovative low energy microwave assisted freezing (MAF) on freezing time, quality attributes (microstructure, texture, drip loss and colour) of apple and potato. MAF of apples and potatoes was performed by applying constant microwave power (167 W/kg) and pulsed microwave power (500 and 667 W/kg with 10 s pulse width and 20 s pulse interval) during the freezing process. The temperature profile was monitored during the freezing process, and the microstructure was examined using X-ray tomography and cryo-SEM techniques. Other quality parameters such as texture, drip loss and colour were evaluated after thawing frozen sample at room temperature. Results showed that the freezing time was not affected by the MAF process. The application of microwaves during freezing process produced superior microstructure than the control sample; MAF significantly reduced the mean ice crystal size in apple and potato sample. Moreover, MAF of apple and potato resulted in a lower drip loss, meanwhile, it also led to a lower reduction in firmness/hardness and Young's modulus value if compared to control sample. The colour was not significantly influenced by MAF. Among all the tested freezing conditions, the 667 W/kg pulsed microwave condition yielded the best result in terms of reduction in ice crystals size and retention of other quality parameters. Lastly, these results indicate that the application of microwave during freezing would result in higher quality frozen products.